

การพิสูจน์เอกลักษณ์ของยีนและโปรตีนที่เกี่ยวข้องกับการพัฒนารังไข่ของกิ้งกูดดำ

Penaeus monodon



นางสาว วิชชุดา ตาลาคูณ

ศูนย์วิทยทรัพยากร
จุฬาลงกรณ์มหาวิทยาลัย

วิทยานิพนธ์นี้เป็นส่วนหนึ่งของการศึกษาตามหลักสูตรปริญญาวิทยาศาสตรมหาบัณฑิต

สาขาวิชาเทคโนโลยีชีวภาพ

คณะวิทยาศาสตร์ จุฬาลงกรณ์มหาวิทยาลัย

ปีการศึกษา 2551

ลิขสิทธิ์ของจุฬาลงกรณ์มหาวิทยาลัย

IDENTIFICATION OF GENES AND PROTEINS RELATED TO OVARIAN DEVELOPMENT
OF THE GIANT TIGER SHRIMP *Penaeus monodon*



Miss Witchulada Talakhun


ศูนย์วิทยทรัพยากร
จุฬาลงกรณ์มหาวิทยาลัย

A Thesis Submitted in Partial Fulfillment of the Requirements
for the Degree of Master of Science Program in Biotechnology

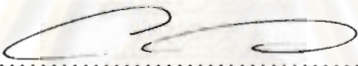
Faculty of Science
Chulalongkorn University
Academic Year 2008


Thesis Title Identification of Genes and Proteins Related to Ovarian
Development of the Giant Tiger Shrimp *Penaeus monodon*
By Miss Witchulada Talakhun
Field of Study Biotechnology
Advisor Professor Piamsak Menasveta, Ph.D.
Co-Advisor Sirawut Klinbunga, Ph.D.


Accepted by the Faculty of Science, Chulalongkorn University in Partial
Fulfillment of the Requirements for the Master's Degree

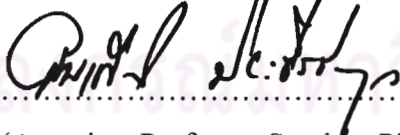

..... Dean of the Faculty of Science
(Professor Supot Hannongbua, Dr. rer .nat.)

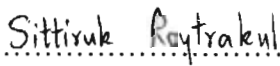
THESIS COMMITTEE


..... Chairman
(Associate Professor Charoen Nitithamyong, Ph.D.)


..... Advisor
(Professor Piamsak Menasveta, Ph.D.)


..... Co-Advisor
(Sirawut Klinbunga, Ph.D.)


..... Examiner
(Associate Professor Somkrat Piyatiratitivorakul, Ph.D.)


..... External Examiner
(Sittiruk Roytrakul, Ph.D.)

นางสาววิชุดดา ตาลาคุณ : การพิสูจน์เอกลักษณ์ของยีนและ โปรตีนที่เกี่ยวข้องกับการพัฒนารังไข่ของ กุ้งกุลาดำ *Penaeus monodon*. (Identification of genes and proteins related to ovarian development of the giant Tiger Shrimp *Penaeus monodon*) อ.ที่ปรึกษาวิทยานิพนธ์หลัก : ศ.ดร. เปี่ยมศักดิ์ เมนะเสวต, อ.ที่ปรึกษาวิทยานิพนธ์ร่วม : ดร.ศิวารุช กลิ่นบุหงา 231 หน้า.

ศึกษารูปแบบการแสดงออกของโปรตีนในรังไข่ของแม่พันธุ์กุ้งกุลาดำปกติและแม่พันธุ์กุ้งที่ตัดก้านตาจากธรรมชาติด้วย วิธี 2D-Gel Electrophoresis โดยใช้โปรตีนจากส่วน organic phase ที่เหลือจากการสกัดอาร์เอ็นเอด้วย TRI-Reagent และ โปรตีน ทั้งหมดในรังไข่ที่สกัดด้วยกรดไตรคลอโร อะซิติก/อะซิโตน พบว่าโปรตีนที่ได้จาก TRI-Reagent มีจำนวนจุดโปรตีนน้อยกว่า โปรตีนที่ได้จากการตกตะกอนด้วยกรดไตรคลอโร อะซิติก/อะซิโตน จึงทำการแยกวิเคราะห์จุดโปรตีนของรังไข่ระยะต่างๆ ของ กุ้งกุลาดำปกติและกุ้งที่ตัดก้านตาโดยเทคนิค MALDI-TOF จำนวน 35 จุด และ MALDI-TOF/TOF จำนวน 90 จุด พบว่ามีเพียง 4 จุด โปรตีน (protein disulfide isomerase, transketolase, calreticulin และ allergen pen m2) จาก MALDI-TOF/TOF ที่ตรงกับ โปรตีนใน ฐานข้อมูล จึงได้เปลี่ยนมาใช้เทคนิค nanoLC-MS/MS สำหรับวิเคราะห์จุดโปรตีนในรังไข่ระยะที่ 2 และระยะที่ 4 ของกุ้งกุลาดำ ปกติและกุ้งกุลาดำที่ตัดก้านตา โดยวิเคราะห์โปรตีนจากรังไข่ปกติ และรังไข่กุ้งที่ตัดก้านตา จำนวนทั้งสิ้น 375 และ 300 จุด โปรตีน ตามลำดับ โดยโปรตีนจากรังไข่ระยะที่ 2 และ 4 ของกุ้งกุลาดำปกติจำนวน 90 (41.86%) และ 102 (63.75%) จุดโปรตีน เหมือนกับลำดับโปรตีนในฐานข้อมูล ในขณะที่โปรตีนจากรังไข่ระยะที่ 2 และ 4 ของกุ้งที่ตัดก้านตาจำนวน 85 (47.22%) และ 41 (34.16%) จุดโปรตีน เหมือนกับลำดับโปรตีนในฐานข้อมูล ผลจากการทดลองบ่งชี้ว่าการตัดก้านตาส่งผลให้มีการแสดงออกของ unknown proteins จำนวนมาก โดยสามารถแบ่งกลุ่มของโปรตีนที่เหมือนกับโปรตีนในฐานข้อมูล ได้เป็น 4 กลุ่ม ประกอบด้วย 1) โปรตีนที่มีการแสดงออกในรังไข่ระยะที่ 2 ของกุ้งปกติและกุ้งที่ตัดก้านตา 2) โปรตีนที่มีการแสดงออกในรังไข่ระยะที่ 4 ของกุ้ง ปกติและกุ้งที่ตัดก้านตา 3) โปรตีนที่มีการแสดงออกในรังไข่ทั้งระยะที่ 2 และ 4 ของกุ้งปกติและกุ้งที่ตัดก้านตา 4) โปรตีนที่มีการ แสดงออกในรังไข่ของกุ้งที่ตัดก้านตาเท่านั้น

จากการหาลำดับนิวคลีโอไทด์ที่สมบูรณ์ของยีนต่างๆโดยเทคนิค RACE-PCR พบว่า *DEAD box 52*, *DEAD box ATP-dependent RNA helicase*, *ATP-dependent RNA helicase*, *L-3-hydroxyacyl coenzyme A dehydrogenase* และ *PDI* มี open reading frame (ORF) ยาว 1824, 1209, 1206, 933 และ 1293 คู่เบส แปลรหัสได้ 607, 402, 401 310 และ 430 กรดอะมิโน ตามลำดับ เมื่อ ตรวจสอบการแสดงออกของยีนต่างๆใน ก้านตา, ขาวายน้ำ, เหงือก, หัวใจ, รังไข่, อัมชะ, ภาวะอาหาร, ลำไส้, เลือด, ปม ประสาทส่วนอก, ตับอ่อน, ลิมฟอค์ ออร์แกน และ อีพิทิวคิล ของกุ้งกุลาดำเต็มวัย พบว่า ยีนต่างๆมีการแสดงออกในทุกเนื้อเยื่อที่ ทำการศึกษา โดยไม่พบการแสดงออกของ *ATP-dependent RNA helicase* และ *L-3-hydroxyacyl coenzyme A dehydrogenase* ในก้าน ตาและลำไส้ ตามลำดับ และไม่พบการแสดงออกของ *PDI* และ *helicase lymphoid-specific isoform 2* ในก้านตาและปมประสาท ส่วนอก

ศึกษาการแสดงออกของยีนต่างๆด้วยวิธี semiquantitative RT-PCR พบว่า *DEAD box ATP-dependent RNA helicase*, *ATP-dependent RNA helicase*, *helicase lymphoid specific isoform 2* และ *PDI* มีการแสดงออกของ mRNA ในรังไข่ระยะต่างๆที่ แตกต่างกันอย่างมีนัยสำคัญในกุ้งปกติ ($P < 0.05$) ในขณะที่ยีน *DEAD box 52* มีการแสดงออกที่ไม่แตกต่างกันในรังไข่ของกุ้ง กุลาดำทั้งสองกลุ่ม ($P > 0.05$) ทำการขึ้นชั้นการแสดงออกของยีน *DEAD box ATP-dependent RNA helicase* และ *PDI* โดยวิธี quantitative real-time PCR พบว่า *DEAD box ATP-dependent RNA helicase* มีการแสดงออกเพิ่มขึ้นในรังไข่ ระยะที่ 3 และ 4 ในกุ้ง ปกติ และระยะที่ 4 ของกุ้งที่ตัดก้านตา ($P < 0.05$) ในขณะที่ *PDI* มีการแสดงออกเพิ่มขึ้นในรังไข่ระยะที่ 3 ของกุ้งเต็มวัยปกติ ($P < 0.05$) แต่มีการแสดงออกที่ไม่แตกต่างกันในกุ้งที่ตัดก้านตา ($P > 0.05$) นอกจากนี้ยังได้ศึกษาการแสดงออกของยีน *valosin containing protein* ด้วยวิธีดังกล่าว ซึ่งพบว่า *VCP* มีการแสดงออกที่ไม่ต่างกันในรังไข่ของกุ้งปกติ ($P > 0.05$) แต่มีการแสดงออกที่ เพิ่มขึ้นในรังไข่ระยะที่ 4 ของกุ้งเต็มวัยที่ตัดก้านตา ($P < 0.05$)

สาขาวิชา.....เทคโนโลยีชีวภาพ.....

ปีการศึกษา.....2551.....

ลายมือชื่อ นิสิต วิชุดดา ตาลาคุณ
ลายมือชื่อ อ.ที่ปรึกษาวิทยานิพนธ์หลัก
ลายมือชื่อ อ.ที่ปรึกษาวิทยานิพนธ์ร่วม

4972482623 : MAJOR BIOTECHNOLOGY

KEYWORDS : *Penaeus monodon* / GIANT TIGER SHRIMP / TWO-DIMENSIONAL GEL ELECTROPHORESIS / MASS SPECTROMETRY

WITCHULADA TALAKHUN: IDENTIFICATION OF GENES AND PROTEINES RELATED TO OVARAIN DEVELOPMENT OF THE GIANT TIGER SHRIMP *Penaeus monodon* ADVISOR: PROF. PIAMSAK MENASVETA, Ph.D, CO-ADVISOR: SIRAWUT KLINBUNGA, Ph.D, 231 pp.

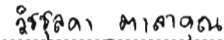
Two dimensional gel electrophoresis (2-DE) of proteins in different ovarian stages (I, II, III and IV ovaries, respectively) of normal and eyestalk-ablated giant tiger shrimp (*Penaeus monodon*) broodstock was carried out. Proteomic patterns between different stages of ovaries were clearly different. Protein spots after 2-DE were further analyzed by mass spectrometry. Initially, 35 protein spots from various ovarian stages were selected and analyzed by peptide mass fingerprinting (PMF) using MALDI-TOF. All protein spots did not match any protein in the database. Additionally, 90 protein spots were analyzed by peptide fragmentation using MALDI-TOF/TOF and only 4 protein spots significantly matched calreticulin, protein disulfide isomerase, transketolase and allergen pen m2. Afterwards, nanoLC-MS/MS was used for identification of ovarian proteins separated by 2-DE. A total of 375 protein spots (215 spots from stage II and 160 spots from stage IV) from ovaries of normal *P. monodon* broodstock were examined. Of which, 90 (41.86%) and 102 (63.75%) spots of respective ovarian stages were significantly homologous to known proteins. The remaining 183 (125 and 58 from stages II and IV, 58.14 and 36.25%, respectively) protein spots did not match any protein and were regarded as novel uncharacterized proteins of *P. monodon*. In addition, 300 protein spots (180 and 120 spots from stages II and IV) from ovaries of eyestalk-ablated *P. monodon* broodstock were also characterized. A total of 85 (47.22%) and 41 (34.16%) proteins matched proteins in the databases, respectively. A large number of unknown protein; 95 and 79 protein spots accounting for 52.77 and 65.83%, were observed. Results clearly indicated that additional unknown proteins expressed at stage IV ovaries were induced by eyestalk ablation. Comparative analysis using MW and pI of protein spots can classify proteins in ovaries of *P. monodon* to 4 categories; those expressed in stages II, IV, both stages II and IV ovaries of normal and eyestalk-ablated broodstock and those expressed only in ovaries of eyestalk-ablated broodstock.

The full length cDNA of *DEAD box 52* (ORF of 1824 bp deduced to a polypeptide of 607 amino acids), *DEAD box ATP-dependent RNA helicase* (1209 bp, 402 aa), *ATP-dependent RNA helicase* (1206 bp, 401 aa) and *L-3-hydroxyacyl coenzyme A dehydrogenase* (933 bp, 301 aa) and *protein disulfide isomerase (PDI)*, 1293 bp, 430 aa) and the partial sequence of *valosin containing protein (VCP)* were successfully characterized. Tissues distribution analysis of various genes was examined. Generally, these genes were constitutively expressed in all examined tissues of *P. monodon* broodstock. Nevertheless, *ATP-dependent RNA helicase* was not expressed in eyestalk whereas *L-3-hydroxyacyl coenzyme A dehydrogenase* was expressed in intestine. *PDI* and *helicase lymphoid-specific isoform 2* were not expressed in both eyestalk and thoracic ganglion.

Semiquantitative RT-PCR of *DEAD box 52*, *DEAD box ATP-dependent RNA helicase*, *ATP-dependent RNA helicase*, *helicase lymphoid specific isoform 2* and *PDI* in ovaries of normal and eyestalk-ablated were carried out. *DEAD box ATP-dependent RNA helicase*, *ATP-dependent RNA helicase* and *PDI* were differentially expressed during ovarian development of normal broodstock ($P < 0.05$). However, expression of *helicase lymphoid-specific isoform 2* was comparable during ovarian development of both normal and eyestalk-ablated *P. monodon* broodstock ($P > 0.05$). In addition, expression of *DEAD box ATP-dependent RNA helicase*, *VCP* and *PDI* were examined by quantitative real-time PCR. *DEAD box ATP-dependent RNA helicase* were up-regulated at stage III and IV ovaries of normal shrimp and at stage IV ovaries of eyestalk-ablated shrimp ($P < 0.05$). *VCP* was comparably expressed during ovarian development of normal *P. monodon* but was up-regulated at the final stage of ovarian development in eyestalk-ablated *P. monodon* broodstock. Considering expression levels of *PDI* in both normal and eyestalk-ablated *P. monodon* simultaneously, *PDI* was up-regulated at stage III ovaries of normal shrimp ($P < 0.05$) but its levels were not significant different during ovarian development of eyestalk-ablated broodstock ($P > 0.05$).

Field of Study :.....Biotechnology.....

Academic Year :.....2008.....

Student's Signature 

Advisor's Signature 

Co-Advisor's Signature 

ACKNOWLEDGMENTS

I would like to express my deepest sense of gratitude to my advisor Professor Dr. Piamsak Menasveta and my co-advisor, Dr. Sirawut Klinbunga and Dr. Sittiruk Roytrakul for their great helps, guidance, encouragement, valuable suggestion and supports throughout my study.

My gratitude is also extended to Associate Professor Dr. Charoen Nitithamyong and Dr. Somkiat Piyatiratitivorakul who serve as the committee of my thesis.

I would particularly like to thank the Center of Excellence for Marine Biotechnology, National Center for Genetic Engineering and Biotechnology (BIOTEC), Faculty of Science, Chulalongkorn University and National Science and Technology Development Agency (NSTDA) for providing facilities.

I would like to extend my special thank to all of every one in the Proteomic laboratory, Genome Institute for valuable suggestions. In addition, many thanks are also expressed to all of every one in our laboratory for best friendship, their help and friendly assistance.

Finally, I would like to express my deepest gratitude to my parents and members of my family for their love, understanding and encouragement extended throughout my study.

CONTENS

	Page
ABSTRACT (THAI)	iv
ABSTRACT (ENGLISH)	v
ACKNOWLEDMENTS	vi
CONTENTS	vii
LIST OF TABLES	xi
LIST OF FIGURES	xiii
LIST OF ABBREVIATION	xx
CHAPTER I INTRODUCTION	1
1.1 Background and objective of this thesis.....	1
1.2 General introduction.....	4
1.2.1 Taxonomy of <i>Penaeus monodon</i>	4
1.2.2 Farming of <i>P. monodon</i> in Thailand.....	5
1.2.3 Ovarian development of <i>Penaeus monodon</i> and hormonal control in reproductive manipulation in shrimp.....	8
1.2.4 Hormonal studies in shrimp.....	11
1.3 Molecular techniques uses in this thesis.....	19
1.3.1 Two dimensional gel electrophoresis.....	19
1.3.2 Mass spectrometry.....	20
1.3.3 PCR.....	23
1.3.4 Reverse transcription-polymerase chain reaction (RT-PCR).....	24
1.3.5 Rapid amplification of cDNA ends-polymerase chain reaction (RACE-PCR).....	26
1.3.6 Real-time PCR.....	27
1.4 Proteomics studies for isolation and characterization of functionally important proteins in various organisms.....	29

	Page
1.4.1 Immune-related proteins in shrimp.....	29
1.4.2 Reproduction-related proteins in various organisms.....	30
CHAPTER II MATERAILS AND METHODS.....	35
2.1 Experimental samples.....	35
2.2 Protein extraction.....	35
2.2.1 Phenol-based extraction.....	35
2.2.2 Total protein extraction.....	36
2.3 RNA extraction.....	36
2.4 Genomic DNA extraction.....	37
2.5 Estimate of extracted total protein, total RNA and DNA concentration	38
2.6 Two dimensional gel electrophoresis.....	38
2.6.1 Sample preparation.....	38
2.6.2 Isoelectric focusing.....	39
2.6.3 SDS-polyacrylamide gel electrophoresis.....	39
2.6.4 Silver staining.....	39
2.7 Mass spectrometry analysis.....	40
2.7.1 In-gel digestion for protein identification.....	40
2.7.2 MALDI-TOF MS and MALDI-TOF/TOF MS.....	40
2.7.3 nanoLC-MS/MS.....	41
2.7.4 Database searches.....	41
2.8 Synthesis of the first strand cDNA.....	42
2.9 Reverse transcription (RT-PCR) of gene homologues in <i>P. monodon</i>	42
2.9.1 Design of primer from EST of <i>P. monodon</i>	42
2.9.2 RT-PCR	42
2.9.3 Agarose gel electrophoresis	43

	Page
2.10 Tissues distribution analysis of interesting genes or differential expression pattern	44
2.10.1 Total RNA extraction and the first strand cDNA synthesis ...	44
2.10.2 Tissues distribution analysis by RT-PCR	45
2.11 Isolation and characterization of the full length cDNA of functionally important gene homologues of <i>P. monodon</i> using Rapid amplification of cDNA ends-Polymerase chain reaction....	45
2.11.1 Preparation of the 5' and 3' RACE template	45
2.11.2 Primer designed for RACE-PCR primer walking	46
2.11.3 RACE-PCR	46
2.11.4 Elution DNA fragments from agarose gels	50
2.12 Cloning of the PCR product	50
2.12.1 Ligation of the PCR product to the pGEM-T easy vector	50
2.12.2 Transformation of the ligation product to <i>E. coli</i> host cell	51
2.12.2.1 Preparation of competent cell	51
2.12.2.2 Transformation	51
2.13 Colony PCR and digestion of the amplification inserts by restriction endonucleases	52
2.14 Extraction of recombinant plasmid DNA	52
2.15 Semiquantitative RT-PCR in ovaries of femals broodstock of of normal and unilateral eyestalk ablation of <i>P. monodon</i>	53
2.15.1 Experimental animal	53
2.15.2 Total RNA extraction and first strand cDNA synthesis	54
2.15.3 Optimization of semiquantitative RT-PCR conditions	54
2.15.3.1 Optimization of primer concentration	54
2.15.3.2 Optimization of MgCl ₂ concentration	54
2.15.3.3 Optimization of number of amplification cycles	55
2.15.3.4 Gel electrophoresis, quantitative and data analysis	55

	Page
2.16 Examination of expression levels of interesting genes in ovaries of <i>P. monodon</i> by real-time PCR	55
2.16.1 Experimental animals.....	55
2.16.2 Primers and the construction of the standard curve	56
2.16.3 Quantitative real-time PCR	56
CHAPTER III RESULTS.....	57
CHAPTER IV DISCUSSION	185
CHAPTER V CONCLUSION	192
REFERENCES	194
APPENDICS	202
APPENDIX A	203
APPENDIX B	207
APPENDIX C	209
APPENDIX D	219
APPENDIX E	228
APPENDIX F	230
BIOGRAPHY	231

LIST OF TABLES

	Page
Table 1.1 Total shrimp production (metric tons) from the aquaculture sector during 2000-2005 in the region.....	6
Table 1.2 Giant tiger shrimp export from Thailand during 2002-2007.....	7
Table 2.1 Gene homologue, primer sequences and expected sizes of the PCR product designed from EST of <i>P. monodon</i>	44
Table 2.2 Primer sequence for the first strand cDNA synthesis and RACE-PCR.....	47
Table 2.3 Gene-Specific Primers (GSPs) and nested GSP used for isolation of the full length cDNA of functionally important genes in <i>P. monodon</i>	47
Table 2.4 Compositions for amplification of 5' end of gene homologues using 5' RACE-PCR.....	48
Table 2.5 Compositions for amplification of 3' end of gene homologues using 3' RACE-PCR.....	48
Table 2.6 The amplification conditions for RACE-PCR of various gene homologues of <i>P.monodon</i>	49
Table 3.1 Protein spots identified by MALDI -TOF/TOF.....	71
Table 3.2 Characterized protein spots in stage II and IV ovaries of normal <i>P. monodon</i> broodstock.....	87
Table 3.3 Characterized protein spots found in stage II and IV ovaries of eyestalk-ablated <i>P. monodon</i> broodstock.....	98
Table 3.4 Characterized protein spots in stage II ovaries of normal and eyestalk-ablated <i>P. monodon</i> broodstock.....	108
Table 3.5 Characterized protein spots in stage IV ovaries of normal and eyestalk-ablated <i>P. monodon</i> broodstock.....	121

	Page
Table 3.6	A summary of ovarian proteins of normal and eyestalk-ablated <i>P. monodon</i> broodstock identified by nanoLC-MS/MS
	130
Table 3.7	Expression of functionally important genes in different tissues of <i>P. monodon</i>
	165
Table 3.8	Expression profiles of gene homologues in various tissues of a female and testes of a male <i>P. monodon</i> broodstock
	166
Table 3.9	Primer and MgCl ₂ concentration and the number of PCR cycles for semiquantitative RT-PCR analysis of gene homologues in <i>P. monodon</i>
	170
Table 3.10	Analysis of relative expression levels of various genes during ovarian development of normal and eyestalk-ablated <i>P. monodon</i> broodstock using semiquantitative RT-PCR.....
	178

LIST OF FIGURES

		Page
Figure 1.1	External morphology of <i>P. monodon</i>	4
Figure 1.2	A diagram of production of <i>P. monodon</i> and <i>P. vanami</i> during 2001-2006 in Thailand.....	8
Figure 1.3	Different ovarian development stages of <i>P. monodon</i>	9
Figure 1.4	Reproductive cycle of the close-thelycum penaeid shrimp.....	11
Figure 1.5	Diagram illustrating the hormonal controls of physiological processes of penaeid shrimp.....	12
Figure 1.6	A schematic diagram illustrating the major endocrine organs in shrimp.....	14
Figure 1.7	Localization and hormones that control several systems from the sinus gland/X-organ complex of <i>P. monodon</i>	14
Figure 1.8	Schematic diagram of the endocrine control of vitellogenesis in shrimp	17
Figure 1.9	Partial ESI mass spectrum with two signals from doubly peptides	21
Figure 1.10	Schematic view representation of MALDI-TOF mass spectrometry	22
Figure 1.11	Schematic view of an electrospray ion source	23
Figure 1.12	General illustration of the polymerase chain reaction (PCR) for amplification of the target DNA.....	24
Figure 1.13	Overall concepts of RT-PCR.....	25
Figure 1.14	Overview of the SMART TM RACE cDNA Amplification Kit.....	27
Figure 1.15	An overall concept of the Real-time PCR procedure.....	28
Figure 3.1	Protein profiles of ovaries of wild <i>P. monodon</i> broodstock	58
Figure 3.2	Protein profiles of ovaries of eyestalk-ablated wild <i>P. monodon</i> broodstock.....	58
Figure 3.3	Protein profiles of ovaries of wild <i>P. monodon</i> broodstock.....	59
Figure 3.4	Protein profiles of ovaries of eyestalk-ablated wild <i>P. monodon</i> broodstock.....	59

	Page
Figure 3.5 Protein profiles of stage I ovaries of wild <i>P. monodon</i> broodstock	61
Figure 3.6 Protein profiles of stage II ovaries of wild <i>P. monodon</i> broodstock	62
Figure 3.7 Protein profiles of stage III ovaries of wild <i>P. monodon</i> broodstock analyzed by 2D gel electrophoresis.....	63
Figure 3.8 Protein profiles of stage IV ovaries of wild <i>P. monodon</i> broodstock analyzed by 2D gel electrophoresis.....	64
Figure 3.9 Protein profiles of stage I ovaries of eyestalk-ablated wild <i>P. monodon</i> broodstock analyzed by 2D gel electrophoresis	65
Figure 3.10 Protein profiles of stage II ovaries of eyestalk-ablated wild <i>P. monodon</i> broodstock analyzed by 2D gel electrophoresis	66
Figure 3.11 Protein profiles of stage III ovaries of eyestalk-ablated wild <i>P. monodon</i> broodstock analyzed by 2D gel electrophoresis	67
Figure 3.12 Protein profiles of stage IV ovaries of eyestalk-ablated wild <i>P. monodon</i> broodstock analyzed by 2D gel electrophoresis.....	68
Figure 3.13 Protein profiles of stage I (A), II (B), III (C) and IV (D) ovaries of unilaterally eyestalk-ablated <i>P. monodon</i> broodstock analyzed by two-dimensional gel electrophoresis (IEF of pH 4-7 followed by 12.5% SDS-PAGE).....	70
Figure 3.14 Protein profiles of stage I (A) and IV (B) ovaries of wild <i>P. monodon</i> broodstock analyzed by two-dimensional gel electrophoresis (IEF of pH 4-7 followed by 12.5% SDS-PAGE).	71
Figure 3.15 Protein profiles of stage II ovaries of wild <i>P. monodon</i> broodstock analyzed by two-dimensional gel electrophoresis (IEF of pH 4-7 followed by 12.5% SDS-PAGE). Numbers indicate protein spots that were identified by nanoLC-MS/MS.....	74
Figure 3.16 Protein profiles of stage II ovaries of eyestalk-ablated <i>P. monodon</i> broodstock analyzed by two-dimensional gel electrophoresis (IEF of pH 4-7 followed by 12.5% SDS-PAGE). Numbers indicate protein spots that were identified by nanoLC-MS/MS.....	75

	Page
Figure 3.17 Protein profiles of stage IV ovaries of wild <i>P. monodon</i> broodstock analyzed by two-dimensional gel electrophoresis (IEF of pH 4-7 followed by 12.5% SDS-PAGE). Numbers indicate protein spots that were identified by nanoLC-MS/MS.....	76
Figure 3.18 Protein profiles of stage IV ovaries of eyestalk-ablated <i>P. monodon</i> broodstock analyzed by two-dimensional gel electrophoresis (IEF of pH 4-7 followed by 12.5% SDS-PAGE). Numbers indicate protein spots that were identified by nanoLC-MS/MS.....	77
Figure 3.19 Intracellular transport of long-chain fatty acids.....	79
Figure 3.20 The categories of biological function of known protein spots.....	136
Figure 3.21 The primary 5' (A) and 3' (B) RACE-PCR product of <i>DEAD box 52 P. monodon</i>	137
Figure 3.22 Nucleotide sequences of 5' RACE-PCR , EST and 3' RACE-PCR of <i>DEAD box 52 of P.monodon</i>	138
Figure 3.23 The full length cDNA sequences of <i>DEAD box 52 of P. monodon</i>	139
Figure 3.24 Diagram illustrating <i>DEAD box 52 cDNA of P. monodon</i>	140
Figure 3.25 The primary 5' and 3' RACE-PCR product of <i>DEAD box ATP-dependent RNA helicase</i>	141
Figure 3.26 Nucleotide sequence of 5' RACE-PCR, EST and 3' RACE-PCR of <i>DEAD box ATP-dependent RNA helicase of P. monodon</i>	142
Figure 3.27 The full length cDNA and deduced protein sequences of <i>DEAD box ATP-dependent RNA helicase of P. monodon</i>	143
Figure 3.28 Diagram illustrating the full length cDNA of <i>DEAD box ATP-dependent RNA helicase of P. monodon</i>	144
Figure 3.29 Semi-nested 5' and 3' RACE-PCR product of <i>ATP-dependent RNA helicase</i>	144
Figure 3.30 Nucleotide sequence of 5' RACE-PCR, EST and 3' RACE-PCR of <i>ATP-dependent RNA helicase of P. monodon</i>	145

	Page
Figure 3.31 The full length cDNA and deduced protein sequences of <i>ATP-dependent RNA helicase</i> of <i>P. monodon</i>	146
Figure 3.32 Diagram illustrating the full length cDNA of <i>ATP-dependent RNA helicase</i> of <i>P. monodon</i>	147
Figure 3.33 The primary 3' RACE-PCR product of <i>L-3-hydroxyacyl coenzyme A dehydrogenase</i>	147
Figure 3.34 Nucleotide sequence of EST (A) and 3' RACE-PCR (B) of <i>L-3-hydroxyacyl coenzyme A dehydrogenase</i> of <i>P. monodon</i>	148
Figure 3.35 The full length cDNA and deduced protein sequences of <i>L-3-hydroxyacyl coenzyme A dehydrogenase</i> of <i>P. monodon</i>	149
Figure 3.36 Diagram illustrating the full length cDNA of <i>L-3-hydroxyacyl coenzyme A dehydrogenase</i> of <i>P. monodon</i>	150
Figure 3.37 Repeating nested 5' and 3' RACE-PCR product of <i>protein disulfide isomerase</i>	150
Figure 3.38 The sequence of primary , repeat-nested , RACE-PCR, EST and 3' RACE-PCR (C) of <i>protein disulfide isomerase</i> of <i>P. monodon</i>	152
Figure 3.39 Similarity analysis based on BlastX of <i>protein disulfide isomerase</i> of <i>P. monodon</i> with previously deposited sequences in the GenBank.....	153
Figure 3.40 Partial cDNA and deduced amino sequences of <i>protein disulfide isomerase</i> of <i>P. monodon</i>	154
Figure 3.41 The primary 5' RACE-PCR product of <i>valosin-containing protein</i>	154
Figure 3.42 Nucleotide sequence of 5' RACE-PCR and EST of <i>valosine containing protein</i> of <i>P. monodon</i>	155
Figure 3.43 Partial nucleotide and deduced amino sequences of <i>valosine containing protein</i> of <i>P. monodon</i>	156
Figure 3.44 A 1.0% ethidium bromide-stained agarose gel showing the quality of total RNA extracted from female broodstock of <i>P. monodon</i>	157

	Page
Figure 3.45 A 1.0% ethidium bromide-stained agarose gel showing the first strand cDNA synthesized from ovaries of <i>P. monodon</i>	157
Figure 3.46 A 1.5% ethidium bromide-stained agarose gel showing results from RT-PCR and tissue distribution analysis <i>DEAD box 52</i>	158
Figure 3.47 A 1.5% ethidium bromide-stained agarose gel showing results from RT-PCR and tissue distribution analysis of <i>DEAD box ATP-dependent RNA helicase</i>	160
Figure 3.48 A 1.5% ethidium bromide-stained agarose gel showing results from RT-PCR and tissue distribution analysis of <i>ATP-dependent RNA helicase</i>	160
Figure 3.49 A 1.5% ethidium bromide-stained agarose gel showing results from RT-PCR and tissue distribution analysis of <i>helicase lymphoid specific isoform 2</i>	161
Figure 3.50 A 1.5% ethidium bromide-stained agarose gel showing results from RT-PCR and tissue distribution analysis of <i>heterogeneous nuclear ribonucleo protein</i>	161
Figure 3.51 A 1.5% ethidium bromide-stained agarose gel showing results from RT-PCR and tissue distribution analysis of <i>protein disulfide isomerase</i>	162
Figure 3.52 A 1.5% ethidium bromide-stained agarose gel showing results from RT-PCR and tissue distribution analysis) of <i>valosin-containing protein</i>	162
Figure 3.53 A 1.5% ethidium bromide-stained agarose gel showing results from RT-PCR (A) and tissue distribution analysis (B) of <i>L-3-hydroxyacyl coenzyme dehydrogenase</i>	163
Figure 3.54 A 1.6% ethidium bromide-stained agarose gel showing results from RT-PCR (A) and <i>EF-1α</i> (B) of <i>beta-thymosin</i>	163
Figure 3.55 A 1.6% ethidium bromide-stained agarose gel showing results from RT-PCR and <i>EF-1α</i> of <i>p68 RNA helicase</i>	164

	Page
Figure 3.56 Optimization of primer concentration ,MgCl ₂ concentration and number of cycles of <i>P. monodon</i> <i>DEAD box 52</i>	168
Figure 3.57 Optimization of primer concentration (A), MgCl ₂ concentration (B) and number of cycles of <i>DEAD box ATP-dependent RNA helicase</i>	168
Figure 3.58 Optimization of primer concentration , MgCl ₂ concentration and number of cycles of <i>ATP-dependent RNA helicase</i>	169
Figure 3.59 Optimization of primer concentration , MgCl ₂ concentration and number of cycles of <i>helicase lymphoid specific isoform 2</i>	169
Figure 3.60 Optimization of primer concentration , MgCl ₂ concentration and number of cycles of <i>protein disulfide isomerase</i>	170
Figure 3.61 A 1.6% ethidium bromide-stained agarose gel showing the expression levels of <i>DEAD box 52</i>	172
Figure 3.62 Histograms showing relative expression levels of <i>DEAD box protein 52</i> during ovarian development of normal.....	172
Figure 3.63 A 1.6% ethidium bromide-stained agarose gel showing the expression levels of <i>DEAD box ATP-dependent RNA helicase</i>	173
Figure 3.64 Histograms showing relative expression levels of <i>DEAD box ATP-dependent RNA helicase</i> during ovarian development of normal and unilateral eyestalk-ablated <i>P. monodon</i> broodstock.....	173
Figure 3.65 A 1.6% ethidium bromide-stained agarose gel showing the expression levels of <i>ATP-dependent RNA helicase</i>	174
Figure 3.66 Histograms showing relative expression levels of <i>ATP-dependent RNA helicase</i> during ovarian development of normal and unilateral eyestalk-ablated <i>P. monodon</i> broodstock.....	174
Figure 3.67 A 1.6% ethidium bromide-stained agarose gel showing the expression levels of <i>helicase lymphoid specific isoform 2</i>	176

	Page
Figure 3.68 Histograms showing relative expression levels of <i>helicase lymphoid specific isoform 2</i> during ovarian development of normal and unilateral eyestalk-ablated <i>P. monodon</i> broodstock.....	176
Figure 3.69 A 1.6% ethidium bromide-stained agarose gel showing the expression levels of <i>protein disulfide isomerase</i>	177
Figure 3.70 Histograms showing relative expression levels of <i>protein disulfide isomerase</i> during ovarian development of normal and unilateral eyestalk-ablated <i>P. monodon</i> broodstock.....	177
Figure 3.71 The standard amplification curve of various genes examine by real-time PCR.....	180
Figure 3.72 Histograms showing relative expression levels of <i>DEAD box ATP-dependent RNA helicase</i> during ovarian development of normal , unilateral eyestalk-ablated and both shrimp analyzed by 2D gel electrophoresis.....	181
Figure 3.73 Histograms showing relative expression levels of <i>valosin containing protein</i> during ovarian development of normal , unilateral eyestalk-ablated and both shrimp of <i>P. monodon</i> broodstock.....	183
Figure 3.74 Histograms showing relative expression levels of <i>protein disulfide isomerase</i> during ovarian development of normal , unilateral eyestalk-ablated and both shrimp of <i>P. monodon</i> broodstock.....	184

LIST OF ABBREVIATIONS

bp	base pair
°C	degree celcius
DEPC	diethylpyrocarbonate
DTT	dithiothreitol
dATP	deoxyadenosine triphosphate
dCTP	deoxycytosine triphosphate
dGTP	deoxyguanosine triphosphate
dTTP	deoxythymidine triphosphate
DNA	deoxyribonucleic acid
HCl	hydrochloric acid
IPTG	isopropyl-thiogalactoside
Kb	kilobase
kDa	kilo daltan
M	molar
MgCl ₂	magnesium chloride
mg	mlligram
ml	mlilitre
mM	mllimolar
ng	nanogram

OD	optical density
PCR	polymerase chain reaction
pI	isoelectric point
RNA	ribonucleic acid
RNase A	ribonuclease A
rpm	revolution per minute
RT	reverse transcription
SDS	sodium dodecyl sulfate
Tris	tris (hydroxyl methyl) aminomethane
μg	microgram
μl	microlitre
μM	micromolar
UV	ultraviolet

ศูนย์วิทยทรัพยากร
จุฬาลงกรณ์มหาวิทยาลัย

CHAPTER I

INTRODUCTION

1.1 Background information and objectives of this thesis

Farming of the giant tiger shrimp (*Penaeus monodon*) in Thailand relies almost entirely on wild-caught broodstock for supply of juveniles because of poor reproductive maturation of cultured *P. monodon* females (Withyachumnarnkul et al., 1998; Preechaphol et al., 2007). As a result, breeding of pond-reared *P. monodon* is extremely difficult and rarely produced enough quality of larvae required by the industry.

The high demand on wild female broodstock leads to overexploitation of the natural populations of *P. monodon* in Thai waters (Klinbunga et al., 1999; Khamnamtong et al., 2005). The lack of high quality wild and/or domesticated broodstock of *P. monodon* has caused a significant decrease in its farmed production since the last few years (Limsuwan, 2004). Reduced degrees of reproductive maturation in captive *P. monodon* females have limited the potential of genetic improvement resulted in remarkably slow domestication and selective breeding programs of *P. monodon* in Thailand (Withyachumnarnkul et al., 1998; Clifford and Preston, 2006; Preechaphol et al., 2007).

Progress in genetic and biotechnology researches in penaeid shrimps have been slow because a lack of knowledge on fundamental aspects of their biology (Benzie, 1998). The domestication and selective breeding programs of penaeid shrimp would provide a more reliable supply of seed stock and the improvement of their production efficiency (Makinouchi and Hirata, 1995; Clifford and Preston, 2006; Coman *et al.*, 2006). The use of selectively bred stocks having improved culture performance, disease resistance and/or other commercially desired traits rather than the reliance on wild-caught stocks is a major determinant of sustainability of the shrimp industry (Clifford and Preston, 2006).

Eyestalk ablation is used commercially to induce ovarian maturation of penaeid shrimp but the technique leads to an eventual loss in egg quality and death of the spawner (Benzie, 1998). Therefore, predictable maturation and spawning of captive penaeid shrimp without the use of eyestalk ablation is a long-term goal for the industry (Quackenbush, 2001).

A research concerning domestication of *P. monodon* is being carried out in Thailand by production of high quality pond-reared *P. monodon* broodstock. Subsequently, it is expected that selective breeding programmes of *P. monodon* will be the key to provide shrimps having commercially desired phenotypes (e.g. high growth rate and/or disease resistance) and to produce *P. monodon* stocks with the ability to induce high quality egg development in domesticated females without the irreversible side-effects caused by a typical eyestalk ablation technique (Lyons and Li, 2002). Applications of the knowledge for genetic selection and biotechnology of *P. monodon* should also be studied and practically implemented to fulfill that purpose. Despite the potential benefits, the domestication of *P. monodon* has been remarkably slow in Thailand (Withyachumnarnkul *et al.*, 1998) and is still at the initial stage.

The development of oocytes consists of a series of complex cellular events, in which specific gene classes were expressed to ensure the proper development of oocytes and to store transcripts and proteins as maternal factors for early embryogenesis (Qiu and Yamano, 2005; Qiu *et al.*, 2005). An understanding of sex determination and gonad development is necessary to manipulate the sex ratio and to control reproductive maturation of this economically important species (Benzie *et al.*, 1998; Leelatanawit *et al.*, 2009). Accordingly, the identification, characterization and expression analysis of genes and proteins involving ovary/oocyte development is an initial step toward understanding the molecular mechanism governing reproductive maturation in *P. monodon* (Khamnamtong *et al.*, 2006; Preechaphol *et al.*, 2007).

To identify sex-related genes expressed in vitellogenic ovaries of *P. monodon*, 1051 cDNAs (expressed sequence tags, EST) were unidirectionally sequenced from the 5' terminus. Nucleotide sequences of 743 EST (70.7%) significantly matched known genes previously deposited in the GenBank (E-value $<10^{-4}$) whereas 308 ESTs

(29.3%) were regarded as newly unidentified transcripts (E-value $>10^{-4}$). A total of 559 transcripts (87 contigs and 472 singletons) were obtained. Several full length transcripts (e.g. *cyclophilin*, *profilin* and *thioredoxin peroxidase*) were also isolated. Expression patterns of 14 gene homologues in ovaries and testes of *P. monodon* broodstock were examined by RT-PCR. *Polehole* and *ovarian lipoprotein receptor* homologues were only expressed in ovaries. Almost all transcripts (*thioredoxin peroxidase*, *phosphatidylinositol 4 kinase*, *Rab-protein 10 CG17060-PA*, *ubiquitin specific protease 9*, *agCP13148*, *nuclear autoantigenic sperm protein*, *adenine nucleotide translocator 2*, *chromobox protein*, *small androgen receptor interacting protein*, *Y-box protein Ct-p0*, and *Zonadhesin precursor*) were higher expressed in ovaries than testes of *P. monodon* broodstock. A homologue of *ubiquitin-specific proteinase 9, X chromosome (Usp9X)* revealed a preferential expression level in ovaries than testes of broodstock-sized *P. monodon* ($N = 13$ and 11 , $P < 0.05$) but was only expressed in ovaries of 4-month-old shrimp ($N = 5$ for each sex) (Preechaphol et al., 2007).

Understanding mechanisms and functions of genes and proteins in different stages of ovarian development would provide a new tool applicable for understanding of their important biological and molecular processes and finally, for improving reproductive maturation *P. monodon*. Nevertheless, identification of proteins in ovaries during ovarian development of penaeid shrimp have not been performed and reported in any species.

Proteomic technique is a powerful and widely used method for analysis of protein mapping and expression of interesting expressed proteins in various cells and tissues of organisms. Proteomic techniques provide the basic information on protein expression profiles and post-translational modification of interesting proteins. Molecular mechanisms and expression patterns of proteins controlling each step of oocyte maturation and formation of CRs could be further carried out for better understanding the reproductive maturation of *P. monodon* in captivity.

Objective of this thesis

The objectives of this thesis were determination of protein profiles in different ovarian stages of normal and eyestalk-ablated wild female *P. monodon* broodstock by two-dimensional gel electrophoresis and identification of electrophoresed protein spots by mass spectrometry. In addition, the full length cDNA and expression of reproduction-related genes from EST and proteomic analyses were also analyzed.

1.2 General introduction

1.2.1 Taxonomy of *P. monodon*

The giant tiger shrimp is taxonomically classified as a member of Phylum Arthropoda; Subphylum Crustacea; Class Malacostraca; Subclass Eumalacostraca; Order Decapoda; Suborder Natantia; Infraorder Penaeidea; Superfamily Penaeoidea; Family Penaeidae, Rafinesque, 1985; Genus *Penaeus*, Fabricius, 1798 and Subgenus *Penaeus*. The scientific name of shrimp is *Penaeus monodon* (Fabricius, 1798) where the English common name is giant tiger shrimp or black tiger prawn (Bailey-Brook and Moss, 1992).

The external morphology of *P. monodon* and sex characteristics of male (petasma) and female (thelycum) are illustrated in Figure 1.1.

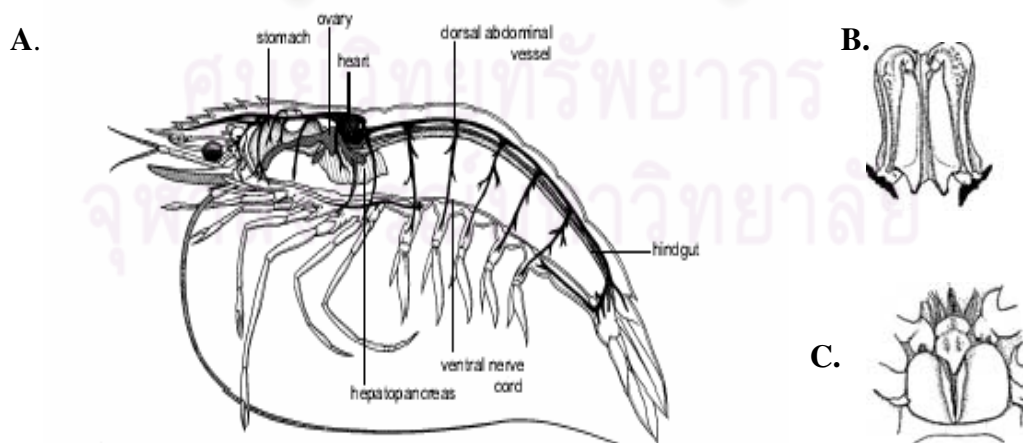


Figure. 1.1 External morphology of *P. monodon* (A). Sexes of juveniles and broodstock of penaeid shrimp can be externally differentiated by petasma of male (B) and thelycum of female (C).

1.2.2 Farming of *P. monodon* in Thailand

The giant tiger shrimp, *P. monodon* has dominated production of farmed shrimp along with the Pacific white shrimp (*Litopenaeus vannamei*) and is one of the most economically important penaeid species in South East Asia. Farming of *P. monodon* has achieved a considerable economic and social importance, constituting a significant source of income and employment in this region.

In Thailand, *P. monodon* had been intensively cultured for more than two decades and had contributed approximately 60% of the total cultivated shrimp production. The reasons for this are supported by several factors including the appropriate farming areas without serious disturbing from typhoons or cyclone, small variable of seawater during seasons, and ideal soils for pond construction. Culture of *P. monodon* had increased the national revenue, therefore *P. monodon* was, until recently, the most economically important cultured species in Thailand.

Marine shrimp farms and hatcheries are located along the coastal areas of Thailand where Nakorn Sri Thammarat and Surat Thani located in peninsular Thailand are the major parts of shrimp cultivation. In addition, Chanthaburi (eastern Thailand), Samut Sakhon and Samut Songkhran (central region) also significantly contribute on the country production. The intensive farming system has resulted in consistent production of marine shrimp of Thailand. Thailand has been regarded as the leading shrimp producer of cultivated shrimp for over a decade (Table 1.1).

Farming of *P. monodon* in Thailand relies almost entirely on wild-caught broodstock for supply of juveniles because reproductive maturation of cultured *P. monodon* female is extremely low. As a result, breeding of pond-reared *P. monodon* is extremely difficult and rarely produced enough quality of larvae required by the industry. The high demand on wild female broodstock leads to overexploitation of the natural populations of *P. monodon* in Thai waters (Klinbunga *et al.*, 1999).

Despite the success of the farmed production, the shrimp industry has encountered problems outbreaks of diseases and environmental degradation. Besides these, the lack of high quality wild and/or domesticated broodstock of *P. monodo*

has possibly caused an occurrence of a large portion of stunted shrimp at the harvest time. The farmed production of *P. monodon* has significantly decreased since the last few years (Table 1.2). As a result, domesticated Pacific white shrimp, *Litopenaeus vannamei*, has recently been introduced to Thailand as a new cultured species (Khamnamtong *et al.*, 2005) and initially contributed approximately 20000 MT (7.4%) of the cultured production in 2002 and dramatically increased to 220000 MT (73.3%) in 2004, respectively (Figure 1.2) (Limsuwan, 2004).

However, the price of *L. vannamei* is quite low and broodstock used relies almost entirely on genetic improved stocks brought from different sources. In addition, the labor costs in Thailand are higher than other countries (e.g. Vietnam and China) preventing the advantage of competition for the world market. In contrast, the market of premium-sized *P. monodon* is still open for Thailand because *L. vannamei* is not suitable for that market. Accordingly, *P. monodon* culture is currently promoted for increasing the production of this species.

Table 1.1 Total shrimp production (metric tons) from the aquaculture sector during 2000 – 2005 in Southeast Asia

Country	2000	2001	2002	2003	2004	2005
Thailand	290,000	280,000	250,000	350,000	360,000	360,000
Indonesia	110,000	90,000	102,000	168,000	180,000	230,000
China	200,000	300,000	280,000	400,000	350,000	280,000
India	85,000	80,000	125,000	100,250	100,000	100,000
Vietnam	75,000	95,000	85,000	110,000	160,000	115,000
Malaysia	17,000	20,000	24,000	280,000	280,000	320,000
Philippines	30,000	20,000	30,000	30,000	35,000	35,000
Total	807,000	885,000	896,000	1,186,250	1,213,000	1,152,000

(Source: World shrimp farming, 2004)

Table 1.2 Export of the giant tiger shrimp from Thailand during 2002-2007

Country	2002		2003		2004		2005		2006		2007	
	Quantity (MT)	Value (MB)	Quantity (MT)	Value (MB)	Quantity (MT)	Value (MB)	Quantity (MT)	Value (MB)	Quantity (MT)	Value (MB)	Quantity (MT)	Value (MB)
USA	97681.81	36,011.4 1	89115.28	29,032.8 7	58365.2	17,206.7 5	29116.62	17,206.7 5	34537.23	8,847.42	7979.91	1,909.64
Japan	16644.6	13,813.3 3	33235.52	11,916.8 7	27977.27	9,586.59	20182.85	9,586.59	15,709.39	3,832.31	3711.32	1,067.25
Canada	6455.76	3,890.48	11216.47	3,412.09	6490.03	2,072.25	3249.37	2,072.25	2798.61	744.95	1762.16	462.68
Singapore	5251.66	3,138.86	3317.14	1,258.13	3383.18	537.88	1933.5	537.88	1580.11	236.31	401.47	63.53
Taiwan	4917.65	1,276.86	3051.77	799.44	2964.62	564.58	1673.65	564.58	607.7	170.12	692.69	194.78
Australia	4481.25	1,326.06	4817.5	1,252.31	2418.19	1,042.02	2097.76	1,042.02	1418.36	445.05	658.54	225.13
Hong Kong	1365.12	533.26	1437.54	340.42	1396.98	409.93	1026.84	409.93	921.88	256.91	1569	365.91
Chaina	1649.23	352.68	992.91	214.54	833.1	162.66	1003	162.66	710.7	85.65	1629.74	235.57
U. Kingdom	661.07	210.81	184.23	64.11	505.76	181.63	161.79	181.63	241.91	70.54	242.4	73.46
Total	180,615.8 1	63,822.7 3	160,986.48	51,524.1 0	118,343.12	16,629.0 5	69,168.96	16,629.0 5	64,565.41	16,178.8 5	23,933.1	5,922.11

Source: http://www.fisheries.go.th/foreign/doc/excel/export_backtiger.xls

ศูนย์วิจัยทรัพยากร
จุฬาลงกรณ์มหาวิทยาลัย

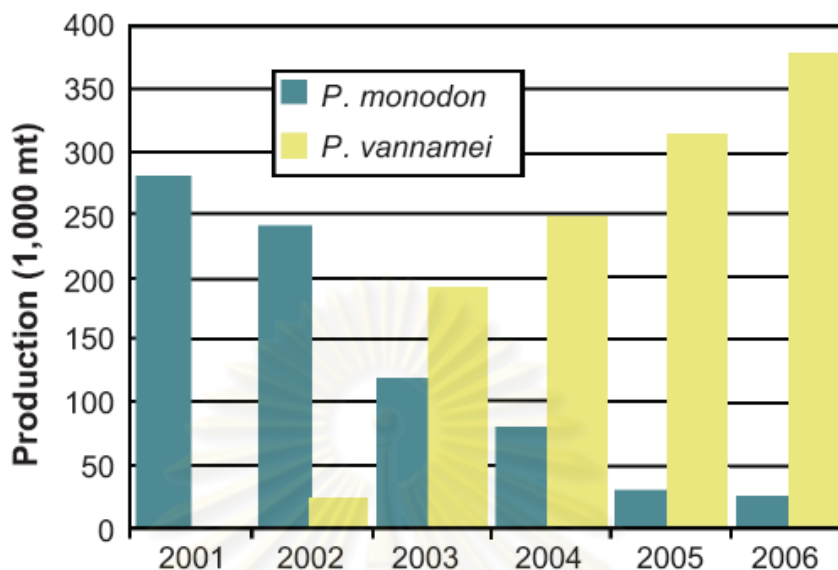


Figure. 1.2 A diagram of production of *P. monodon* and *P. vanami* during 2001-2006 in Thailand

1.2.3 Ovarian development of *Penaeus monodon* and hormonal control in reproductive manipulation in shrimp

In penaeid shrimp, the major part of ovaries is found within the cephalothorax area. Ovaries are paired, but partially fused in the cephalothoracic region, and consist of a number of lateral lobes. The intensity of the ovarian shadow is due to the different density of the ovaries and the pigmentation of the egg mass. The ovarian development of penaeid shrimp are generally classified to four different stages; underdeveloped stage (Stage I), developing or early vitellogenic stage (Stage II), nearly ripe or late vitellogenic stage (Stage III) and ripe or mature stage (Stage IV; Figure 1.3).

In an undeveloped stage, the ovaries either do not cast any shadow or a thin opaque line is seen along the length of the tail. At this point the ovaries are composed of a connective tissue capsule surrounding a soft vascular area containing oogonia, and accessory cells (called follicle or nurse cells, Figure 1.3A). The internal wall of the ovary capsule is lined with epithelial cells (called the germinal epithelium). Once

the female is sexually mature, the germinal epithelium will produce oogonia by mitosis division throughout the reproductive life of the females.

The eggs develop from oogonia in an area known as the zone of proliferation. As the oogonia develop they increase in size and enter the first stage of meiotic division and henceforth are irreversibly destined to become haploid, with only one set of maternal chromosomes. At this point, although the developing eggs are increasing in size (Figure 1.3B), they are not as yet producing yolk, and are known as previtellogenic oocytes. At this stage the ovaries can be visualized with a light beam as a large centrally located opaque rope-like structure, and classified as the stage 2.

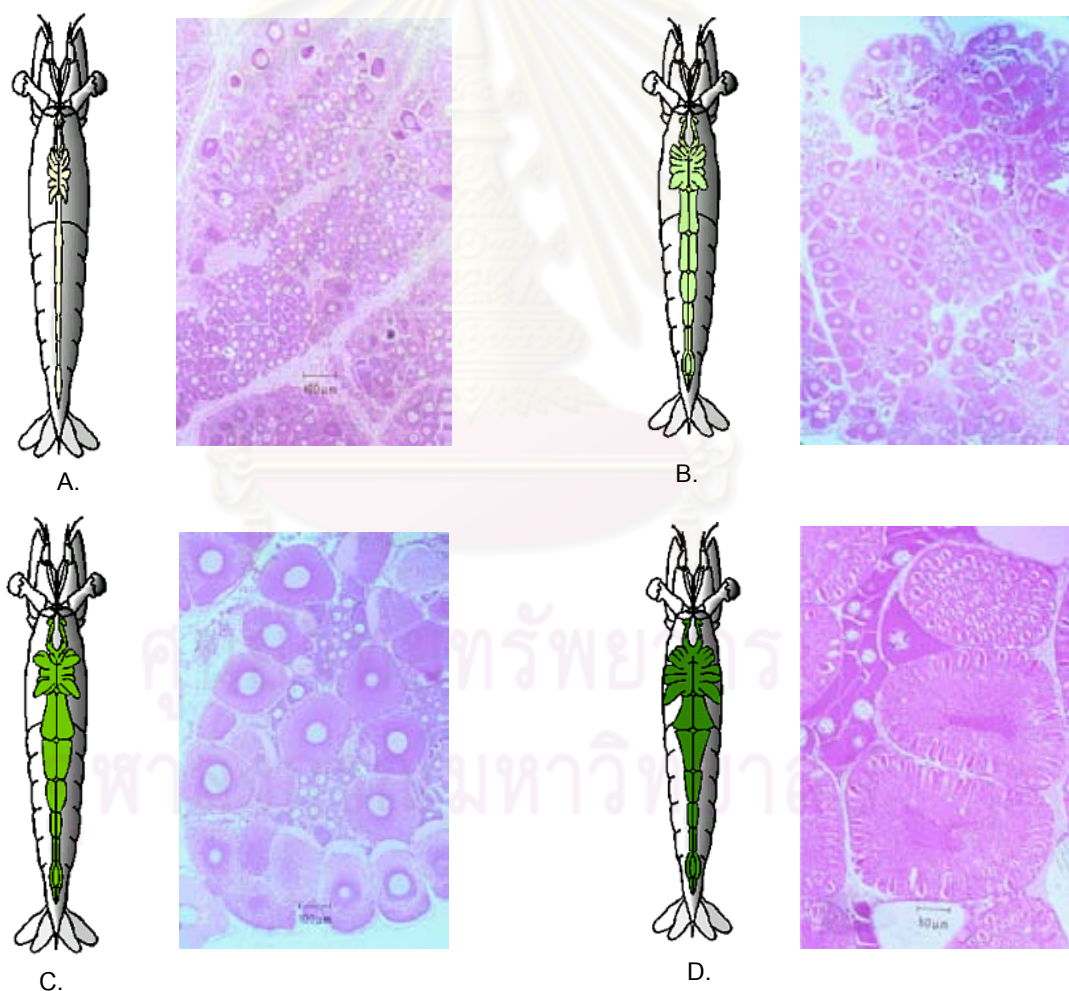


Figure 1.3 Different ovarian development stages of *P. monodon*. **Panel A.**, the underdeveloped ovaries (Stage I), **B.**, the developing stage (Stage II), **C.**, the nearly ripe stage (Stage III) and **D.**, the ripe stage (Stage IV) (www.aims.gov.au/.../mdef/images/fig01-4a.gif).

As the oocytes develop, they migrate towards the margins of the ovarian lobes in preparation for ovulation. During this migration, follicle cells are attached to the periphery of each oocyte. It is believed that the follicle cells produce the yolk that is internal in the oocytes in a process called vitellogenesis. As vitellogenesis proceeds, oocytes mature synchronously as yolk accumulates and develop a characteristic dark green colour as a result of deposition of carotenoid pigments. It is the carotenoid pigmentation that mainly causes the dark ovarian shadow during illumination of the female by the torchlight. The female is now in the stage 3 (Figure 1.3C).

By the end of vitellogenesis, the eggs develop cortical granules filled with a jelly-like substance destined to form part of the egg shell membrane after ovulation. At this time the shadow cast by the ovaries is large, resulting in a very distinct dark thick region extending the length of the abdomen, with an enlarged bulbous region directly behind the carapace, called the saddle. The saddle may not be as apparent in some broodstock. The female is now in a pre-spawning state and is regarded as in the stage 4.

Penaeid shrimp are divided into two groups: open-thelycum and closed-thelycum species. In the life history of penaeid shrimps, final maturation, spawning and mating behaviour presage successful reproduction. The final phase of maturation, spawning, mating and their interrelationships differ significantly between the groups. The giant tiger shrimp is one of the closed-thelycum species. Typically, mature males insert their spermatophore into the soft thelycum of newly moulted immature females. Final maturation with germinal vesicle breakdown (GVBD) immediately precedes spawning in a closed thelycum species (Yano, 1988). Two phases are involved: the appearance of ripe ova. and germinal vesicle breakdown (GVBD) in preparation for fertilization after spawning (Figure 1.4).

Ovulation occurs when nuclei, shrunken during the late pre-maturation phase, have migrated to the peripheral cytoplasm of the oocytes. In the late phase of the maturation cycle, meiotic metaphase is arrested and remains visible just beneath the cytoplasmic membrane of the oocyte, indicating that GVBD is completed after ovulation.

Immediately after release from the female gonopore, the mature eggs, still in metaphase (for example in *Marsupenaeus japonicus*), are fertilized by sperm released into the seawater from the spermatophore held in the thelycum. Once begun, spawning is continuous, females releasing batches of eggs from the ripe ovaries and sperm from the spermatophore into the seawater, where fertilization takes place. Therefore, female shrimp have to repeat the process of molting, mating, and sexual maturation in order to achieve several spawning during their life.

Prematuration accumulation of egg-yolk protein (vitellin) in developing oocytes at the yolk-granule stage, occurs approximately 1 month after spawning without mating in spent shrimps (for example in *M. japonicus*). Female shrimp (closed thelycum), do not mature for several months, even after mating with spermatophore transfer in the season from late autumn to early spring (Yano, 1995). These observations indicate that mating does not directly accelerate vitellogenesis in closed-thelycum species.

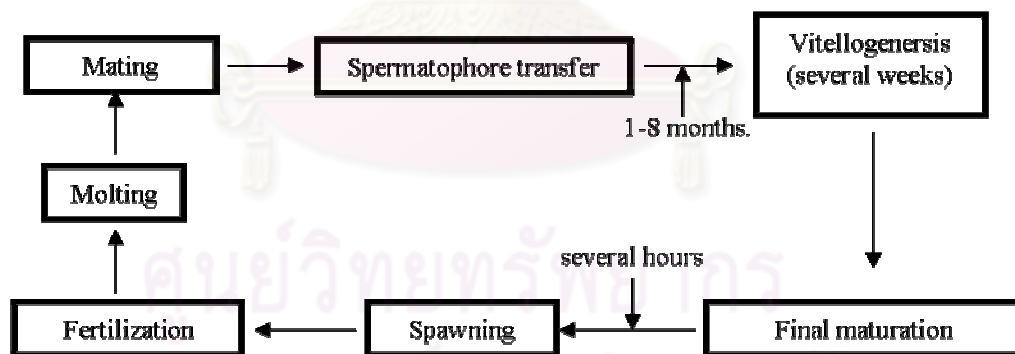


Figure 1.4 Reproductive cycle of the close-thelycum penaeid shrimp.

1.2.4 Hormonal studies in shrimp

Biological and physiological processes (growth, reproduction, body color, and metabolism etc.) are hormonal controlled (Figure 1.5). Knowledge from shrimp

endocrinology is necessary to develop the hormonal manipulation techniques in shrimp

Eyestalk hormones play the important role for regulating several physiological mechanisms and unilateral eyestalk ablation is practically used for induction of ovarian development and oviposition. The technique gives predictable peaks of

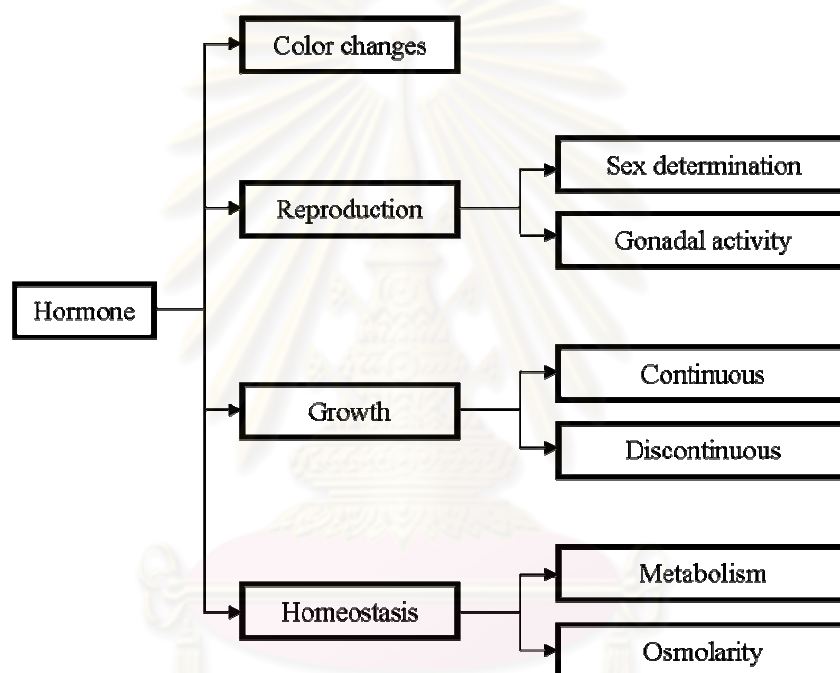


Figure 1.5 Diagram illustrating the hormonal controls of physiological processes of penaeid shrimp.

maturation and spawning but many associated problems, which leads to an eventual loss in egg quality and causes high mortality and death (Benzie, 1998). Predictable maturation and spawning in captive shrimp without the use of eyestalk ablation is a long-term goal for the industry (Quackenbush, 1991).

Crustacean hyperglycemic hormone (CHH) is a member of a structurally related peptide family, which also includes molt-inhibiting hormone (MIH), gonad-inhibiting hormone (GIH) and mandibular organ-inhibiting hormone (MOIH). It is the

most abundant peptide in the eyestalk of crustaceans (Chang et al., 1990) This hormone not only plays its major role in controlling the glucose level in the hemolymph, but is also significantly contributed to other processes such as ecdysteroid synthesis and ovarian maturation. Multiple forms of CHH have been reported. CHH has been isolated from several crustaceans such as crabs, (Kegel et al., 1989; Chung et al., 1998), lobster (Tensen et al., 1991), crayfishes (Kegel et al., 1991; Huberman et al., 1993), shrimp (Sithigorngul et al., 1999) as well as isopod (Martin et al., 1984).

The growth in crustaceans is not continuous because of the rigid exoskeleton. It is often shed to allow periodic growth. Molting is controlled by a complex interplay of hormones (Figure 1.6), in particular, the negative regulation of molt-inhibiting hormone (MIH) from the X-organ/sinus gland (XO/SG) complex which suppresses the synthesis or secretion of molting hormones (ecdysteroids) from the Y-organ (Fig 1.7).

MIH is classified as a member of the crustacean hyperglycemic hormone (CHH) family and has been shown to inhibit the synthesis of the molting hormone, ecdysone, which release from the Y-organ of decapod crustaceans keeps the animal in the intermolt stage that dominates its molting cycle. MIH is thus one of the major keys in mediating growth and reproduction.

Udomkit et al. (2004) cloned and characterized *P. monodon* CHH transcripts and produced recombinant Pem-CHH2 and Pem-CHH3 peptides, a member of a structurally related CHH/MIH/GIM/MO-IH peptide family. Both cDNAs contained 381-bp open reading frame encoding 127 amino acids. Amino acid sequence analysis revealed that Pem-CHH2 and Pem-CHH3 shared 95% identity in their amino acid sequence to that of Pem-CHH1 (Udomkit et al., 2000). Both recombinant Pem-CHH2 and Pem-CHH3 expressed as secreted proteins in *Pichia pastoris* exhibited the hyperglycemic activity at the comparable level to that of Pem-CHH1. The *Pem-CHH* transcript in several tissues of *P. monodon* was examined by RT-PCR. Expression of Pem-CHH1, Pem-CHH2, Pem-CHH3 was not restricted only to the eyestalk but also

detectable in heart. In addition, the transcript of Pem-CHH1 was also present in gills. CHHs from various origins may play different physiological roles.

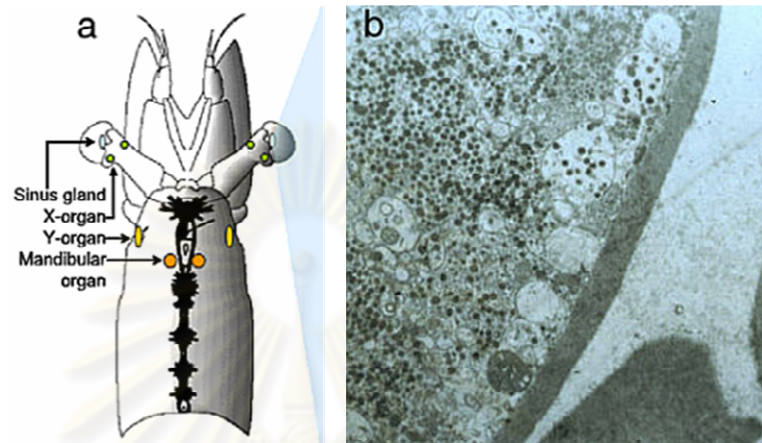


Figure 1.6. (a) A schematic diagram illustrating the major endocrine organs in shrimp. The sinus gland is composed of the terminals from neurons which have their cell bodies in the X-organ and brain. (b) Electron microscopy section (8500X) of the sinus gland demonstrating hormone filled vesicles (dark circles) which are fused and released their contents into the blood. (www.aims.gov.au/.../mdef/images/fig01-4a.gif).

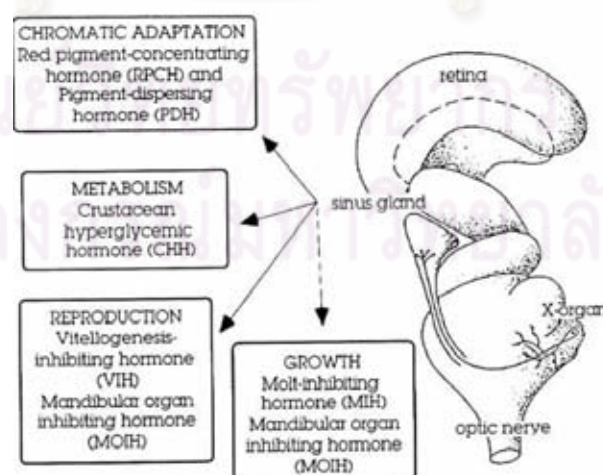


Figure 1.7 Localization of hormones that control several physiological systems from the sinus gland/X-organ complex of *P. monodon*. (Okumura, 2004)

Yodmuang et al. (2004) isolated cDNA encoding two types of *MIH*, *Pem-MIH1* and *Pem-MIH2* of *P. monodon* by direct PCR amplification and PCR-based genome walking strategies. *Pem-MIH1* cDNA contained a 318 bp ORF encoded for a translated product containing 28 amino acids of the signal peptide and a putative mature *Pem-MIH* of 77 amino acids. *Pem-MIH1* and *Pem-MIH2* genes have the same structures. The interruption of the three exons by the two introns occurs at the same positions in both genes. RT-PCR was used to detect the expression of *Pem-MIH1* and *Pem-MIH2* in several tissues of *P. monodon* and found that *Pem-MIH1* was abundantly detected in eyestalk and thoracic ganglia, whereas no transcript was present in heart. A lower expression level was detected in gill and muscle, *Pem-MIH2* was detected only in eyestalk but not in other tissues. The recombinant *Pem-MIH1* was expressed in *Pichia pastoris* as a secreted protein. *Pem-MIH1* exhibited the ability to extend molting duration of *P. monodon* from 11.8 days to 16.3 days suggesting that *Pem-MIH1* played the molt-inhibiting function in this shrimp.

In crustacean females, the late phase of gonadal maturation to form mature oocytes is named vitellogenesis. This process comprises the synthesis or deposition, or both, of yolk or vitellus. The major component of this nutritive material is the lipoprotein vitellin, derived from a precursor called vitellogenin that can be synthesized in extraovarian tissues or in the ovaries.

Penhouse (1943 and 1944 cited in Huberman, 2000) described that unilateral eyestalk ablation has been used to accelerate ovarian maturation and spawning in different shrimp species used as broodstock in aquaculture. The effect has been attributed to the presence of gonad inhibiting hormone, GIH (or vitellogenin inhibiting hormone, VIH) in the X-organ-sinus gland complex.

Gonad inhibiting hormone (GIH or vitellogenin inhibiting hormone, VIH) is a member of the CHH/MIH/GIH family. It plays an important role on inhibition of ovarian development. The removal of GIH by unilateral eyestalk ablation is practically used for stimulation of ovarian development in shrimp but identification of GIH was only reported in lobsters. Two isoforms of the GIH were isolated and

sequenced by Soyez et al. (1991) from the sinus gland of the lobster *H. americanus*. Both consisted of 77 residues and MWs of 9.135 Kda.

Treerattrakoo et al. (2007) characterized a cDNA encoding a GIH (Pem-GIH) from the eyestalk of *Penaeus monodon*. *Pem-GIH* cDNA is 861 bp in size with an ORF of 288 bp. The deduced Pem-GIH consists of a 17-residue signal peptide and a mature peptide region of 79 amino acids with features typical of type II peptide hormones from the CHH family. Pem-GIH transcript was detected in eyestalk, brain, thoracic and abdominal nerve cords of *P. monodon* adults. The gonad-inhibiting activity of Pem-GIH was investigated using the RNA interference technique. Double-stranded RNA, corresponding to the mature Pem-GIH sequence, triggered a decrease in *Pem-GIH* transcript levels both *in vitro* (eyestalk ganglia and abdominal nerve cord culture) and *in vivo* (female *P. monodon* broodstock). The conspicuous increase in *Vg* transcript level in the ovary of GIH-knockdown shrimp suggests a negative influence for Pem-GIH on *Vg* gene expression, and thus implies its role as the gonad-inhibiting hormone.

Recombinant peptides related to vitellogenesis-inhibiting hormone (VIH) of the American lobster (*Homarus americanus*) were expressed in bacterial cells, and then purified after being allowed to refold. Biological activities of the recombinant VIHs having an amidated C-terminus (rHoa-VIH-amide) and a free carboxyl-terminus (rHoa-VIH-OH) were examined using an ovarian fragment incubation system derived from the kuruma prawn, *Marsupenaeus japonicus*. The rHoa-VIH-amide significantly reduced vitellogenin mRNA levels, while rHoa-VIH-OH had no effect on vitellogenin mRNA levels in ovaries (Ohira et al., 2006).

Gonad stimulating hormones, GSH (or vitellogenin stimulating hormone, VSH), believed to be secreted by the supraesophageal and thoracic ganglia has been proposed to have the opposite effects of GIH (stimulates the gonadal maturation) of shrimp. However, this hormone has not been identified and characterized in any shrimp.

Ecdysteroids are known as the molting hormones in crustacean and insects. In crustacean, the inactive forms are secreted and converted to 20-hydroxyecdysone by the Y-organ. Ecdysteroids stimulate vitellogenesis in some insects. However, the levels of ecdysteroids in hemolymph of the giant freshwater shrimp (*Macrobrachium rosenbergii*) were not related to vitellogenesis and showed no distinct relation to the molt cycle suggesting that ecdysteroids are not involved in vitellogenesis in *M. rosenbergii* (Okumura and Aida, 2000).

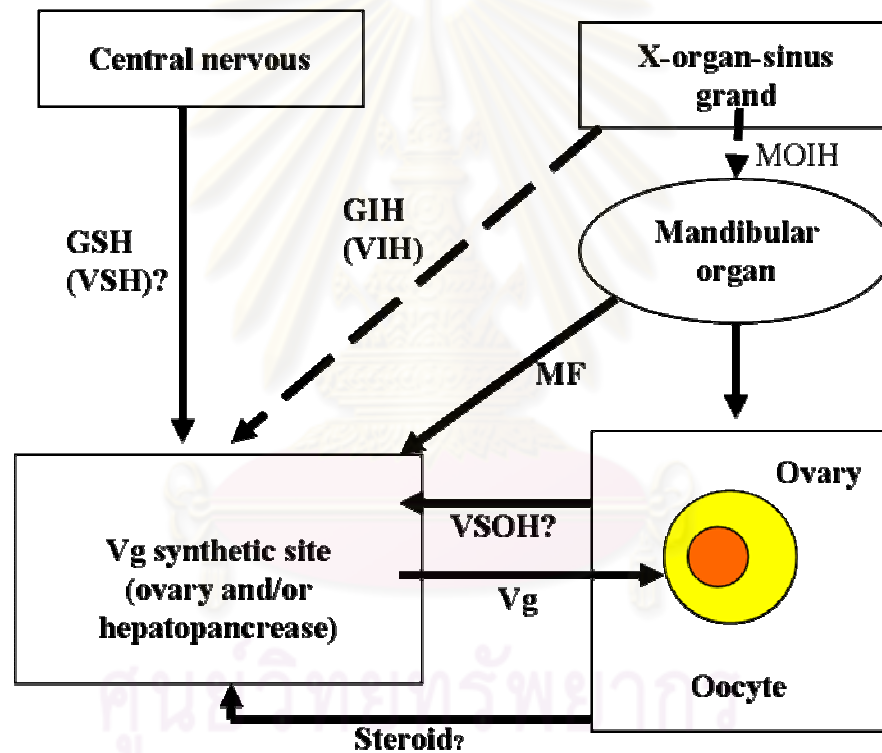


Figure 1.8 Schematic diagram of the endocrine control of vitellogenesis in shrimp (Okumura, 2004) GIH: gonad inhibiting hormone, GSH: gonad stimulating hormone, MF: methyl farnesoate, MOIH: mandibular organ inhibiting hormone, Vg: vitellogenin, VIH: vitellogenesis-inhibiting hormone, VSH: vitellogenesis stimulating hormone.

MF is structurally related to the juvenile hormone and synthesized by mandibular organ (MO). MF has been implicated in the regulation of crustacean development and reproduction in conjunction with eyestalk molt inhibiting hormones and ecdysteroids. The presence of MF in the medium for culturing of ovarian tissue *in vitro* of *L. vannamei* resulted in a significant increase in sizes of oocytes. In contrast, MF inhibits ovarian development in the tadpole shrimp, *Troops longicaudatus* (Tsukimura et al. 2006).

Farnesoic acid O-methyltransferase (FAMeT) catalyzes the methylation of farnesoic acid (FA) in the terminal step of MF synthesis. A schematic diagram of regulatory mechanism of vitellogenesis in shrimp is shown in (Figure 1.8).

Laufer et al. (1998) reported stimulating effects of MF on ovarian maturation in the red swamp crayfish *Procambarus clarkii* in three different trials of MF administration. After 30 days of treatment, ovaries of pre-reproductive females were 2- to 10-fold larger and were in the later stages of vitellogenesis than those of the controls. Similar and statistically significant results were observed in a second 30-day trial, which was begun during the middle of the vitellogenic cycle. The control ovaries were white or yellowish colored but ovaries from the MF-fed groups were larger and showed a dose response for which the 1- μ g MF group had tan colored ovaries. A group receiving the higher dose of 2 μ g MF had dark brown to black colored ovaries.

Lam Hui et al (2008) studies functions of *L. vannamei FAMeT (LvFAMeT)* in molting using the RNA interference (RNAi) technique. Injection of double stranded RNA (dsRNA) of *LvFAMeT* successfully knocked down the expression of *LvFAMeT* in juvenile shrimp for at least 3 days and shrimp did not proceed to the final stage of molt cycle. Furthermore, the expression of molt-related genes encoding *cathepsin-L* and *hemocyanin* gene was disturbed. Subsequently, 100% mortality of shrimp was observed in *LvFAMeT* dsRNA-injected shrimp. In contrast, control shrimp completed their molt and proceeded to the next molt cycle. Therefore, RNAi injection knocked down the expression of *LvFAMeT* which could potentially result in a decrease in the production of MF and subsequently, could affect the molting process.

1.3 Molecular techniques used in this thesis

1.3.1 Two-dimensional electrophoresis

Two-dimensional electrophoresis is a powerful and widely used method for the analysis of complex protein mixture extracted from cells, tissues, or other biological samples. This technique sorts proteins according to two independent properties in two steps. Initially, samples are prepared by extraction of proteins in the appropriate buffer. The extracted proteins are then electrophoretically analyzed.

The first dimension step, isoelectric focusing (IEF), separates proteins according to their isoelectric points (pI). Proteins are amphoteric molecules; they carry either positive, negative or zero net charges, depending on the pH of their surroundings. The net charge of a protein is the sum of all the negative and positive charges of its amino acid side chain and amino and carboxyl-termini. The isoelectric point (pI) is the specific pH at which the net charge of the protein is zero. Proteins are positively charged at pH values below their pI and negatively charged at pH values above their pI .

The IEF step is the most critical step for 2-DE process. During IEF, protein mixtures must be solubilized in denaturing buffer without non-ionic detergents, usually in chaotrophs [high concentrate urea solution (8M urea or 7M urea with 2M thiourea)] together with surfactant (CHAPS) and reducing agents (DTT). To obtain high quality separation, samples protein should be optimized to select a suitable range of isoelectric focusing pH gradients due to different types of interesting proteins.

The second dimension step, SDS-polyacrylamide gel electrophoresis (SDS-PAGE), separates proteins according to their molecular weights. Each spot on the resulting two-dimensional array corresponds to a single (or mixed) protein in the sample. Thousands of different proteins can thus be separated, and information such as the protein pI , the apparent molecular weight, and the amount of each protein is obtained. The resolution of the secondary separation can be optimized by varying the percentage of crosslink of the acrylamide gel.

After electrophoresis, the separated proteins must be visualized in the gel. Most commonly, this is achieved with dyes that firmly bind protein. Individual dyes differ in sensitivity and the ability to stain all types of proteins equally. The most frequently used dye is Coomassie Blue R-250 (with a detection limit of about 1 μg of a protein). Alternatively, Coomassie Blue G-250, Amido black, and Nigrosine are also used.

Silver staining is more sensitive than Coomassie Blue staining for about 10 - 20 fold. Silver staining leads to a non-stoichiometric binding of silver ions to proteins. After reduction, these complexes become visible as black to brownish bands. Unfortunately, silver stains are inconsistent as some proteins are hardly stained by silver ions. Therefore, quantity of stained proteins is not proportionally indicated from intensity of the protein spots. Fluorescent staining has been recently developed as an alternative choice for high sensitivity of staining. Dyes including SyproRuby™, Deep Purple™ and 5-hexadecanoylamino-fluorescein are commercially available. However, the fluorescent staining is more expensive than conventional Coomassie Blue and silver staining and requires a specific gel documentation for visualization of electrophoresed proteins.

1.3.2 Mass spectrometry

Mass spectrometry is a highly sensitive technique of instrumental analysis of molecules invented about 90 years ago. In the 1950s, mass spectrometry expanded into organic chemistry. Today, a wide range of mass spectrometry types that are specialized for the analysis of elements, small gaseous molecules, or biomolecules and biopolymer, exists. Protein identification by this analysis used proteomically digested protein to give higher accuracy of identification than the intact proteins. Proteolysis is achieved using common enzymes such as trypsin prior to MS analysis. This enzyme hydrolyzes peptide bonds on the C terminal side of lysine (Lys) and arginine (Arg) residues, except when they are immediately followed by proline (Pro). Other enzymes such as pepsin, proteinase K and even chemical digestion using reagent such as cyanogenbromide (CNBr) can also be used for the protein digestion.

However, the use of CNBr yields large peptide fragments that may not be useful for peptide sequencing by MS.

Mass spectrometers are made up of three functional units: an ion source, a mass analyzer, and a detector. For mass spectrometric analyses, free gaseous ions are generated from the sample in the ion source and then focused into an ion beam in vacuum. The mass analyzer separates ions in this beam according to their mass/charge (m/z)-ratio; these ions are then registered by detector. Individual measurements are plotted in a mass spectrum with m/z (x-axis) and intensity (y-axis) as shown in (Fig 1.9).

Two techniques of mass spectrometry have established in biomolecular analysis; matrix-assisted laser desorption/ionization (MALDI) and electrospray ionization (ESI).

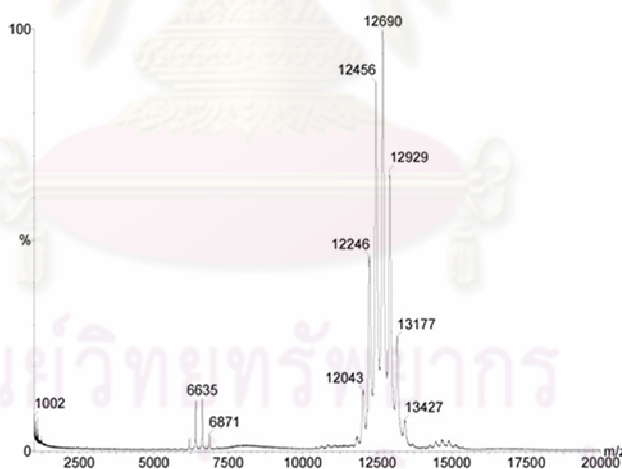


Figure 1.9 Partial ESI mass spectrum with two signals from doubly charged peptides. The registered ion m/z -values (mass-to-charge ratio) are plotted on the x-axis, their intensity on y-axis. [www.waters.com/.../LCT Premier detail 3.jpg](http://www.waters.com/.../LCT_Premier_detail_3.jpg).

Matrix-assisted laser desorption/ionization (MALDI) is a soft method of ionization. It can transfer large biomolecules like proteins, which are fragile and are fragmented when ionized by this conventional ionization method. It is most similar in

character to electrospray ionization both in relative softness and the ions produced. The ionization is triggered by a laser beam. A matrix is used to protect the biomolecules from being destroyed by direct laser beam and to facilitate vaporization and ionization. Known peptides can quickly be identified with MALDI-MS. The technique is therefore routinely used for analysis of trypsin-digested fragments from two-dimensional gel electrophoresis. The working schematic of MALDI is show in (Fig. 1.10).

Electrospray ionization involves spraying the analyte solution from a microcapillary that carries a high (negative or positive) potential in reference to the mass spectrometer. When the electrostatic force of the applied current exceeds the surface tension of the analyte solution, a *Taylor cone* forms at the tip of the microcapillary. Highly charged droplets form and solvent evaporation disintegrates them further to a fine spray. This analyte spray is then sucked into the evacuated mass. analyzer through a microorifice. In the interface area, the droplets are dried and ion formation occurs. The working schematic of an ESI ion source is show in (Fig. 1.11).

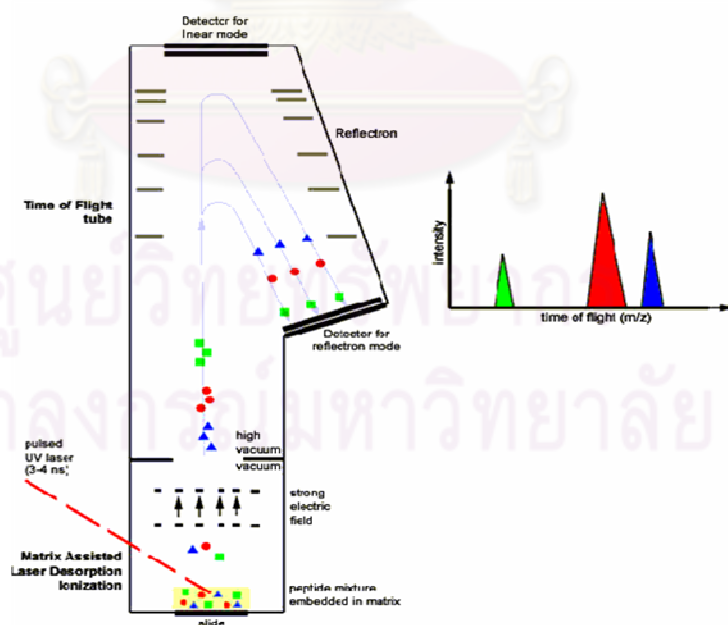


Figure 1.10. Schematic view representing MALDI-TOF mass spectrometry.
http://www.proteomicsnijmegen.nl/Maldi_pages/Images/NPF_MALDI_Fig21.gif .

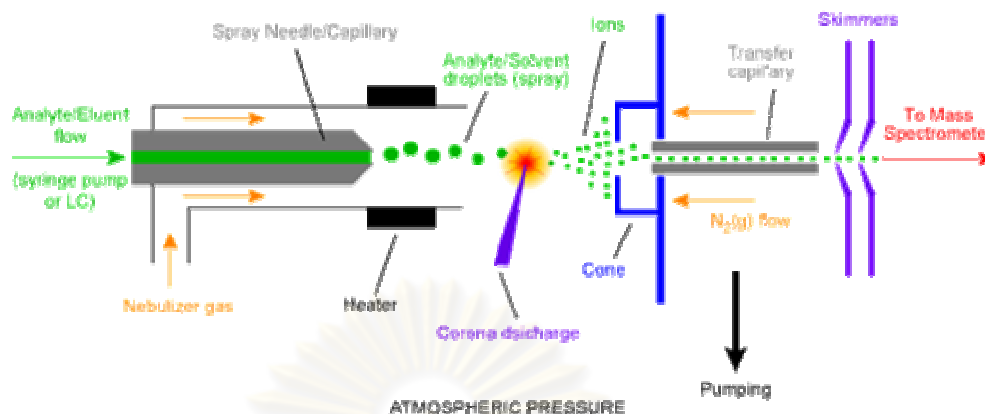


Figure 1.11. Schematic view of an electrospray ion source. Analyte solution is sprayed at atmospheric pressure, droplets enter the evacuated analyzer area through a microorifice and anion beam is formed.

(www.bris.ac.uk/nerclsmsf/techniques/hplcms.html)

1.3.3 PCR

The introduction of the polymerase chain reaction (PCR) by Mullis et al. (1987) has opened a new approach for molecular genetic studies. This method is technique for enzymatically replicating DNA without using a living organism, such as *E. coli* or yeast and is a method using specific DNA sequences by the two oligonucleotide primers, usually 18-25 nucleotides in length. Million copies of the target DNA sequence can be synthesized from the low a mount of starting the DNA template within a few hours.

The PCR components are composed of DNA template, a pair of primers for the target sequence, dNTPs (dATP, dCTP, dGTP and dTTP), PCR buffer and heat-stable DNA polymerase (usually *Taq* polymerase). The amplification reaction typically consists of three steps; denaturation of double stranded DNA at high temperature, annealing to allow primers to form hybrid molecules at thr optimal temperature, and extension of the annealed primers by heat-stable DNA polymerase. The cycles is repeated for 30-40 times (Figure 1.13). The amplification product is determined by agarose or polyacrylamide gel electrophoresis.

1.3.4 Reverse transcription-polymerase chain reaction (RT-PCR)

RT-PCR is a comparable method of conventional PCR but the first strand cDNA template rather than genomic DNA was used as the template in the amplification reaction. (Figure 1.13). It is a direct method for examination of gene expression of known sequence transcripts in the target species. The template for RT-PCR can be the first stranded cDNA synthesized from total RNA or poly A⁺ RNA. Reverse transcription of total RNA can be performed with oligo(dT) or random primers using a reverse transcriptase. The product is then subjected to the second strand synthesis using a gene-specific forward primer.

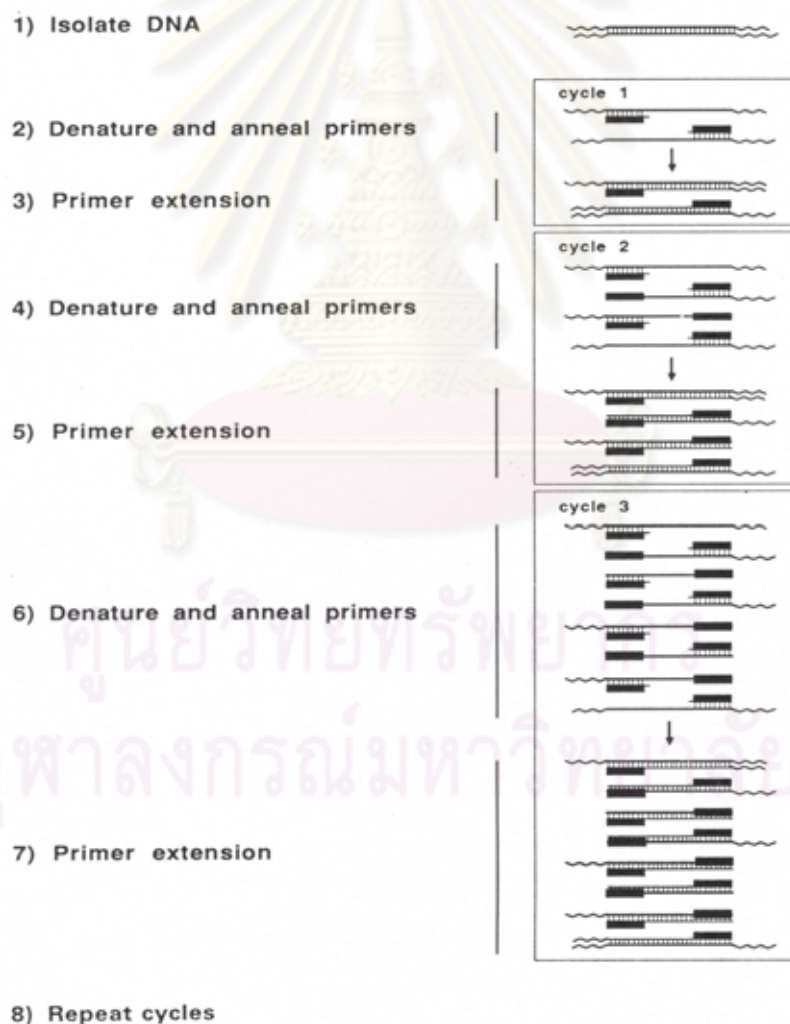


Figure 1.12 General illustration of the polymerase chain reaction (PCR) for amplification of the target DNA.

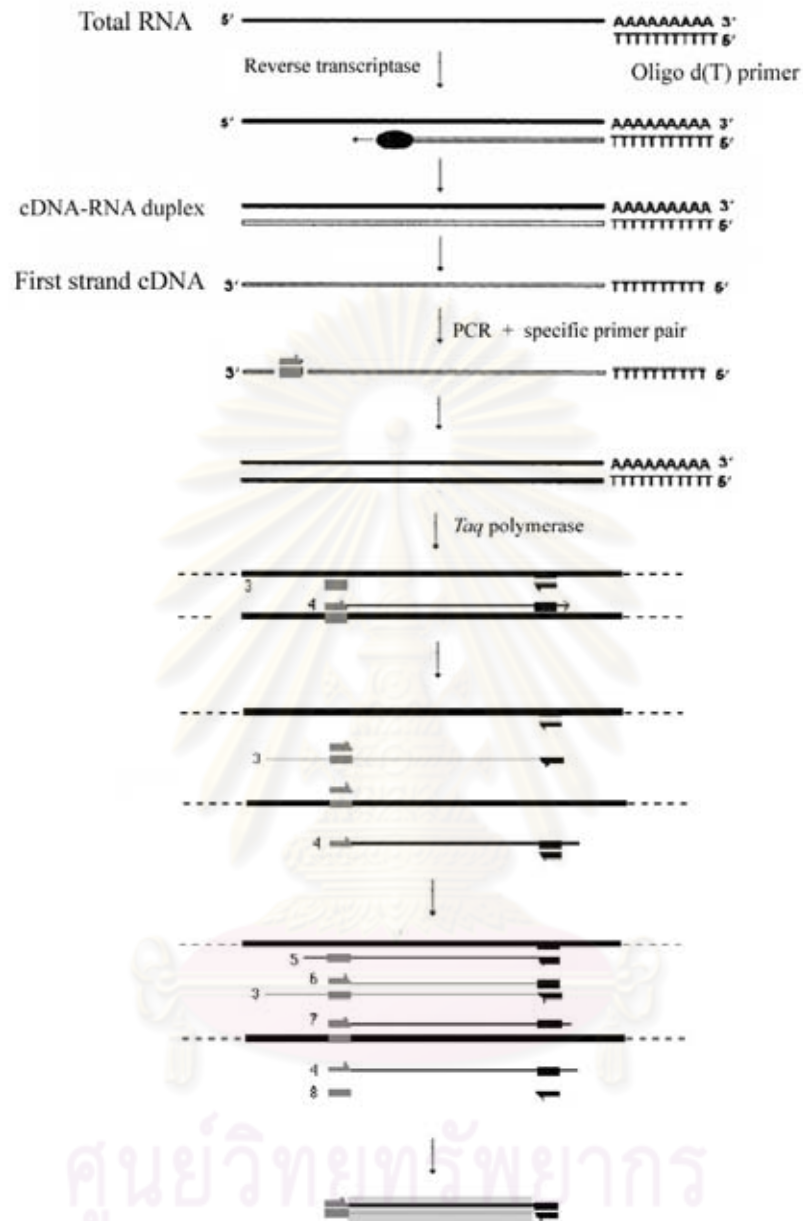


Figure 1.13 Overall concepts of RT-PCR. During the first strand cDNA synthesis, an oligo d(T) (or random primers) primer anneals and extends from sites present within mRNA. The second strand cDNA synthesis primed by the 18 – 25 base specific primer proceeds during a single round of DNA synthesis catalyzed by thermostable DNA polymerase (e.g. *Taq* polymerase).

RT-PCR can also be used to identify homologues of interesting genes by using degenerate primers and/or conserved gene-specific primers from the original species

and the first strand cDNA of the interesting species is used as the template. The amplified product is further characterized by cloning and sequencing.

Semi-quantitative RT-PCR is a relatively quantitative approach where the target genes and the internal control (e.g. a housekeeping gene) were separately or simultaneously amplified using the same template. The internal control (such as *β -actin*; *elongation factor*, *EF-1 α* or *G3PDH*) is used under the assumption that those coding genes are transcribed constantly and independently from the extracellular environment stimuli and that their transcripts are reverse transcribed with the same efficiency as the product of interesting transcript.

1.3.5 Rapid amplification of cDNA ends-polymerase chain reaction (RACE-PCR)

RACE-PCR is the common approach used for isolation of the full length of characterized cDNA. Using SMART (Switching Mechanism At 5' end of RNA Transcript) technology, terminal transferase activity of Powerscript Reverse Transcriptase (RT) adds 3 - 5 nucleotides (predominantly dC) to the 3' end of the first-strand cDNA. This activity is harnessed by the SMART oligonucleotides whose terminal stretch of dG can anneal to the dC-rich cDNA tail and serve as an extended template for reverse transcriptase. A complete cDNA copy of original mRNA is synthesized with the additional SMART sequence at the end (Fig. 1.15).

The first strand cDNA of 5' and 3' RACE is synthesized using a modified oligo (dT) primers and serve as the template for RACE PCR reactions. Gene specific primers (GSPs) are designed from interested gene for 5'- RACE PCR (antisense primer) and 3'-RACE PCR (sense primer) and used with the universal primer (UPM) that recognize the SMART sequence. RACE products are characterized. Finally, the full length cDNA is constructed.

1.3.6 Real-time PCR

Real Time PCR is a kinetic approach based on the polymerase chain reaction, which is used to amplify and simultaneously quantify a target DNA molecule. It

enables both detection and quantification (as absolute number of copies or relative amount when the expression level of the target gene is normalized by that of the reference gene) of a specific sequence in the sample.

The real-time PCR procedure follows the general principle of PCR. Its key feature is that the amplification DNA is quantified as it accumulates in the reaction in the real time situation after each amplification cycle. Two common methods of quantification are the use of fluorescent dyes that intercalate with double-stranded DNA such as SYBR green and modified DNA oligonucleotide probes that are fluorescent when hybridized with a complementary DNA.

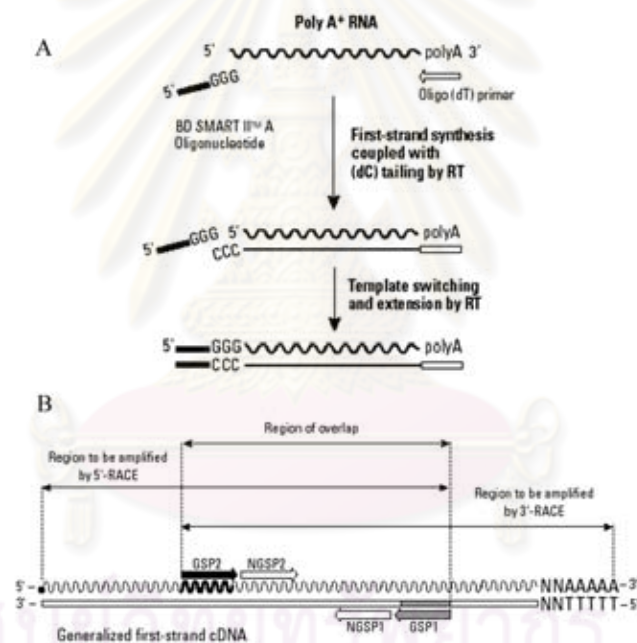


Figure 1.14 Overview of the SMARTTM RACE cDNA Amplification Kit.

A. Mechanism of SMART cDNA synthesis. First strand synthesis is primed using a modified oligo (dT) primer. After reverse transcriptase reaches the end of the mRNA template, it added several dC residues. The SMART II A Oligonucleotide anneals to the tail of the cDNA and serves as an extended template for PowerScriptRT.

B. Relationships of gene-specific primers to the cDNA template. This diagram shows a generalized first strand cDNA template.

The general principle of SYBR green polymerase chain reaction is composed of the first step, denaturation: at the beginning of amplification, the unbound dye molecules are weakly fluorescent, the second step, annealing: after annealing of the primer, a few dye molecules bind to the double strand. The last step, extension: during elongation, more dye molecules bind to the newly synthesized DNA. Fluorescence measurement at the end of the elongation step of every PCR cycle is performed to monitor the increasing the amount of quantified DNA (Fig. 1.16).

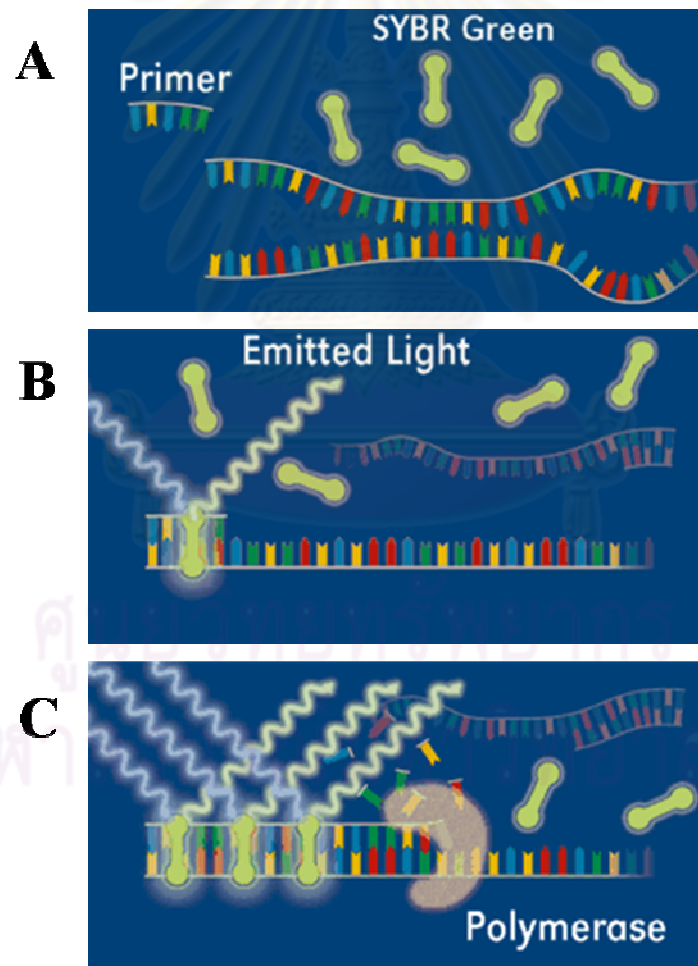


Figure 1.15 An overall concept of the Real-time PCR procedure (www.thaiscience.com/lab_vol/p23/Real-time PCR.asp).

Real-time PCR in the laboratory can be applied to numerous applications. It is common use for both diagnostic and research applications. Diagnostic real-time PCR is applied to rapidly detect the presence of genes involved in infection diseases, cancer and genetic abnormalities. In the research setting, real-time PCR is mainly use to provide highly sensitive quantitative measurement of gene transcription. The technology is commonly used in determining expression levels of a particular gene changes over time.

1.4 Proteomics studies for isolation and characterization of functionally important proteins in various organisms

1.4.1 Immune-related proteins in shrimp

To identify the structural and functional proteins of white spot syndrome virus (WSSV), the purified virions were separated by SDS-PAGE and characterized by mass spectrometry. Eighteen proteins matching the open reading frames of WSSV genome were identified. Except for three known structural proteins and collagen, the functions of the remaining 14 proteins were unknown. Temporal analysis revealed that all the genes were transcribed in the late stage of WSSV infection except for VP121. Of the newly identified proteins, VP466 was further characterized. The cDNA encoding VP466 was expressed in *E. coli* as a glutathione S-transferase (GST) fusion protein. Specific antibody was generated with the purified GST-VP466 fusion protein. Western blot showed that the mouse anti-GST-VP466 antibody bound specifically to a 51-kDa protein of WSSV. Immunogold labeling revealed that VP466 protein is a component of the viral envelope (Huang et al., 2002).

Two-dimensional gel electrophoresis (2-DE) was used to illustrate protein expression profiles of stomach of normal and 48 h post-infected with white spot syndrome virus (WSSV) of specific pathogen free *Litopenaeus vannamei*. Seventy-five protein spots that consistently showed either a marked change (50%) in accumulated levels or a highly expressed level throughout the course of WSSV infection were selected for further study. A total of 53 proteins with functionally involved in energy production, calcium homeostasis, nucleic acid synthesis,

signaling/communication, oxygen carrier/transportation, and SUMO-related modification were identified. 2-DE results were shown to be consistent with relative EST database of two *Penaeus monodon* cDNA libraries. Expression profiles of seven selected genes analyzed from time-course RT-PCR were comparable with 2-DE and EST data. The results are useful both for identifying potential biomarkers and for developing antiviral measures (Wang et al., 2007).

Bourchookarn et al. (2008) identified altered proteins in the yellow head virus (YHV) infected lymphoid organ (LO) of *Penaeus monodon*. At 24 h post-infection, the infected shrimps showed obvious signs of infection, while the control shrimps remained healthy. 2-DE of proteins extracted from the LO revealed significant alterations in abundance of several proteins in the infected group. Protein identification by MALDI-TOF MS and nanoLC-ESI-MS/MS revealed significant increase of transglutaminase, protein disulfide isomerase, ATP synthase beta subunit, V-ATPase subunit A, and hemocyanin fragments. A significant decrease was also identified for Rab GDP-dissociation inhibitor, 6-phosphogluconate dehydrogenase, actin, fast tropomyosin isoform, and hemolymph clottable protein. Some of these altered proteins were further investigated at the mRNA level using real-time PCR and results confirmed proteomic data. Identification of these altered proteins in the YHV-infected shrimps may provide novel insights into the molecular responses of *P. monodon* to YHV infection.

14.2 Reproduction-related proteins in various organisms

In sturgeon aquaculture, the fish are sexed by an invasive surgical examination of the gonads. Development of a non-invasive procedure for sexing fish based on a molecular method is of special interest. Keyvanshokoo et al. (2008) applied a proteomics approach to analyze a differential protein expression between mature male and female gonads of the Persian sturgeon (*Acipenser persicus*). When comparing protein patterns on the 2-DE gels of the testis and ovary, 48 unique spots were distinguished in testis while only two spots were matchless in ovary. The largest group of sturgeon testis proteins (31.8%) was related to metabolism and energy production. Proteins related to translational and transcriptional regulation or DNA-

and RNA-binding protein, such as aspartyl-tRNA synthetase, accounted for 20.4% of identified sturgeon testis proteins. Testicular proteins identified as chaperones, heat shock proteins and oxidative stress defense enzymes (16%) were also observed. Three protein spots identified as heat shock proteins (HSPs). The cell structure protein class (16%) was composed of cytoskeletal proteins such as tubulin and actin. The remaining 15.8% of the identified testis proteins are implicated in diverse functions such as signal transduction (6.8%), transport (6.8%), and cell division (2.2%). No ovarian and testicular proteins were directly linked to a sex-determining gene.

Ziv et al. (2008) defined the protein repertoires of different maturation stages of both gilthead seabream (GSB, *Sparus aurata*) and the zebrafish (ZF, *Danio rerio*), oocytes to identify candidate stage-specific proteins and examine comparative protein profiles between mature oocytes of ZF and GSB analyzed by 1D, 2DE and tandem mass spectrometry. More than six hundreds proteins were identified. The result indicated that VTGs accumulated to significantly higher levels in the ZF oocytes relative to GSB oocytes. Furthermore, some unprocessed vitellogenins were still detected in the ZF oocytes of all stages. These protein can be divided into three main families represented by vitellogenin 1 (vg1, 4, 5, 6 and 7), vitellogenin 2 and vitellogenin 3. The shifts in the non-VTGs protein patterns during oocytes maturation were identified and the result indicated some non-vitellogenin proteins were increased and others were decreased as the oocytes are mature. Some (member of TPC1 protein complex) were observed to peak at stage III relative to both stages I/II or IV. Examples for non-vitellogenin proteins, whose levels increase at the late stages oocytes, include Serpin A1, importin and ZP3a. Some proteins, such as Hsp90, Hsp96 and calreticulin were observed at significantly higher levels only at the early oocyte stages.

Paz et al. (2006) comparatively analyzed proteomic profiles of the soluble proteins expressed at different stages of mouse testis development (8, 18 and 45 postnatal day). After comparative analysis, 44 proteins or variant forms were further identified by MALDI-TOF. Six proteins were classified as uniform expression, the protein from this group are either involved in carbohydrate metabolism or oxidoreductase activity. Nine proteins showed significant downregulation ($P < 0.05$).

These protein expression occurs mainly in the Sertoli cells/spermatogonia (8 dpn) and spermatocytes (18 dpn), becoming reduced or even abolished in postmeiotic spermatids. However, Ran GDP-binding protein, glutathione S-transferase (GST) A4, and one of the two forms of aldo-keto reductase 1B8 showed increased accumulation at 18 dpn, suggesting their relative stronger expression in meiotic spermatocytes. These upregulated proteins were detected mainly in 45 dpn maps, and only weakly or not at all in 8 and 18 dpn protein maps. This accumulation pattern indicates a strong relationship with the presence and differentiation of round and elongation spermatids. Most of the upregulated cytosolic proteins identified were involved in oxidoreductase processes (isocitrate dehydrogenase 1, aldo-keto reductase B8, peroxiredoxin 4, hydroxyacyl glutathione hydrolase, DJ-1 and GSTM5). Sixteen identified proteins detected in testis exhibited changes of protein levels, but they did not reach the significant level ($P < 0.05$) during the testis development.

In fish, oocyte post-ovulatory ageing is associated with egg quality decrease. During this period, eggs are held in the body cavity where they bath in a semi-viscous liquid known as coelomic fluid (CF). CF components are suspected to play a role in maintaining oocyte fertility and developmental competence (egg quality). However, CF proteic composition remains poorly studied. Thus rainbow trout (*Oncorhynchus mykiss*) CF proteome was studied during the egg quality decrease associated with oocyte post-ovulatory ageing by 2-DE and MALDI-TOF. A first experiment was performed using CF pools originating from 17 females sampled at ovulation as well as 7, 14 and 21 days later. These observations were verified using a second set of CF pools originating from 22 females sampled 5 and 16 days following ovulation. Approximately 200 protein spots of 10-105 kDa molecular mass and 3–10 pI were detected in CF samples. Several protein spots, while undetected at the time of ovulation, exhibited a progressive and strong accumulation in CF during post-ovulatory ageing. After silver-staining and MALDI-TOF mass spectrometer analysis, some of these protein spots were identified as lipovitellin II fragments. These observations suggest that egg protein fragments accumulate in the CF during the post-ovulatory period and could therefore be used to detect egg quality defects associated with oocyte post-ovulatory ageing (Rime et al., 2004).

Okumura et al. (2006) reported expression of vitellogenin and cortical rod proteins during induced ovarian development by eyestalk ablation in the kuruma prawn, *Marsupenaeus japonicus*. The synthesis of vitellogenin (VTG, precursor of vitellin) and two kinds of cortical rod proteins (cortical rod protein, CRP; and thrombospondin, MjTSP) was induced by bilateral eyestalk ablation in immature females of *M. japonicus* and the synthesis process was monitored over a 7-day period after the ablation. The ovarian weight and hemolymph VTG levels increased in the ablated females. The VTG mRNA levels in ovary increased concomitantly with vitellin accumulation in the ovary after eyestalk ablation. On the other hand, the CRP and MjTSP protein levels in the ovary increased after eyestalk ablation, whereas the CRP and MjTSP mRNA levels in the ovary did not change concomitantly. Results suggested that the regulatory mechanism of gene expression by eyestalk hormone is different between VTG (transcriptional control) and CRP-MjTSP (translational control).

Tomoharu et al. (2005) isolated valosine containing protein (VCPs) from the common lumbricid earthworm (*Eisenia fetida*). Nucleotide sequence of *eVCP-1* and *eVCP-2*, display a similarity of 74%. Results from blast search against the databases demonstrated that both transcripts are closely related to each other and to VCP/P97/Cdc48, a gene family known to be involved in cell cycle regulation and meiosis. The predicted amino acid sequence reveals that *eVCP-1* contains two AAA domains and a VCP/P97/Cdc48 consensus carboxyl-terminal motif including a stretch of acidic residues and carboxyl-terminal tyrosine (DDDLY). Likewise, *eVCP-2* also contains two AAA domains, but does not have the carboxyl-terminal DDDLTY motif. The deduced amino acid sequence of *eVCP-1* is 58.9% identical to *eVCP-2*. The intron/exon organizations of *eVCP-1* and *eVCP-2* genes were deduced from fragments amplified by genomic PCR. Both contain 14 introns and 15 exons with 10 conserved intronic splice sites. Results from *in situ* hybridization demonstrated that *eVCP-2* mRNA is abundant in the enlarged cytophores surrounded by small and isodiametric nuclei.

DEAD-box (D-E-A-D is the single letter code of Asp-Glu-Ala-Asp) RNA helicase are present in almost all organisms and play important roles in RNA

metabolism, mRNA export, pre-mRNA splicing, translation initiation and ribosomal biogenesis (Matsumoto et al., 2005). Expression of rck/p54, a DEAD-box RNA helicase, in mouse gametogenesis and early embryogenesis were examined. Resulting from western blot analysis revealed that rck/p54 was highly expression in both the ovary and testis. In the ovary, maturing oocytes strongly expressed rck/p54 in their cytoplasm. In contrast, rck/p54 was highly expressed in cytoplasm of spermatogonia and primary spermatocytes, but its expression decrease in spermatids. Importantly, the expression of rck/p54 is found to be regulated in gametogenesis and in early embryogenesis. The finding indicated that rck/p54 may execute its roles in the cells in which gene expression is strictly regulated or repressed (Matsumoto et al., 2005).

Vitellin (Vt) was purified from ovary extracts of mature females of the Pacific white shrimp (*Litopenaeus vannamei*) using sepharose CL-4B and Q-Sepharose columns. Native Vt had an apparent molecular weight of 388 kDa as detected in Native-PAGE and bound the lipophilic dye Oil Red O and had a total lipid content of approximately 43.8%. Under the denaturation condition (SDS-PAGE), Vt is composed of three major subunits of 87, 78 and 46 kDa, although minor bands of 65, 61 and 31 kDa are also detected. The 87 and 78 kDa polypeptide were strongly recognized by *Penaeus semisulcatus* anti-Vt polyclonal and *Penaeus monodon* anti-Vt monoclonal antibodies. Furthermore, the N-terminal amino acid sequence of the 78-kDa polypeptide is very similar to *Marsupenaeus japonicus* vitellogenin (Vg) and *P. semisulcatus* Vt, with an identity of 76%. The β -helix content of Vt was 25% while β -sheet correspond to 37 and 14% of unordered secondary structure. These values were similar to insect microvitellogenin. *Litopenaeus vannamei* Vt has an emission fluorescence maximum at 329 nm, comparable to the shrimp high-density lipoprotein/beta-glucan binding protein (HDL/BGBP) (Karina et al., 2002).

CHAPTER II

MATERIALS AND METHODS

2.1 Experimental samples

Female broodstock were wild-caught from the Andaman Sea and acclimated under the farm conditions for 2-3 days. The post-spawning group was immediately collected after shrimp were ovulated ($N = 6$). Ovaries were dissected out from cultured juveniles ($N = 5$) and normal broodstock and weighed ($N = 34$). For the eyestalk ablation group, shrimp were acclimated for 7 days prior to unilateral eyestalk ablation. Ovaries of eyestalk-ablated shrimp were collected at 2-7 days after ablation ($N = 32$). The gonadosomatic index (GSI, ovarian weight/body weight $\times 100$) of each shrimp was calculated. Ovarian developmental stages were classified by conventional histology (Qiu et al., 2005) and divided to previtellogenic (I, $N = 10$ and 4 for normal and eyestalk-ablated broodstock, respectively), vitellogenic (II, $N = 7$ and 7), early cortical rod (III, $N = 7$ and 10) and mature (IV, $N = 10$ and 11) stages, respectively. The average body weight of *P. monodon* broodstock was 142.98 ± 28.37 g.

2.2 Protein extraction

2.2.1 Phenol-based extraction

Ovarian proteins of *P. monodon* broodstock were extracted from the organic phase after extraction of RNA by TRI-reagent. DNA was precipitated from the organic phase by an addition of absolute ethanol. The mixture was left at room temperature for 2-5 minutes before centrifuged at 2000 g for 5 minutes at 4° C. The supernatant was transferred to a new tube and proteins were precipitated by adding 3 volume of acetone and left at room temperature for 10 minutes before centrifugation at 12000 g for 10 minutes at 4° C. The pellet was washed by guanidine hydrochloride in ethanol containing 2.5 % glycerol, left at room temperature for 10 minutes and centrifuge three times at 8000 g for 5 minutes at 4° C. The pellet was air-dried and dissolved in the lysis buffer. The amount of extracted protein was measured by a dye binding assay (Bradford, 1976).

2.2.2 Total protein extraction

Approximately 0.5 gram of frozen ovaries of *P. monodon* were ground to fine power in the presence of liquid N₂ and suspended in a three fold-diluted PBS buffer containing protease inhibitor cocktail. After centrifugation at 10000 g for 10 minutes at 4 ° C. The supernatant were collected. Trichloroacetic acid in acetone (TCA; 10% w/v) was added and left at -20°C overnight. The mixture was centrifuged at 10000 g for 30 minutes at 4° C. The supernatant was discarded and the pellet was suspended in acetone containing 0.1% dithiothreitol (DTT). The sample was spun at 10000 g for 30 minutes at 4° C. The pellet was air-dried and dissolved in the lysis buffer. The amount of extracted protein was measured by a dye binding assay (Bradford, 1976).

2.3 RNA extraction

Total RNA was extracted from ovaries and testes of each the shrimp using TRI-REAGENT (Molecular Research Center). A piece of tissue was immediately placed in mortar containing liquid nitrogen and ground to the fine powder. The tissue powder was transferred to a microcentrifuge tube containing 500 µl of TRI REAGENT (1 ml/50-100 mg tissue) and homogenized. Additional 500 µl of TRI REAGENT were added. The homogenate was left at room temperature for 5 minutes before 0.2 ml of chloroform was added. The homogenate was vortexed for at least 15 seconds, left at room temperature for 2 - 15 minutes and centrifuged at 12000 g for 15 minutes at 4°C. The mixture was separated into the lower phenol-chloroform phase (red), the interphase, and the upper aqueous phase (colorless).

The aqueous phase (inclusively containing RNA) was carefully transferred to a new 1.5 ml microcentrifuge tube. RNA was precipitated by an addition of 0.5 ml of isopropanol and mixed thoroughly. The mixture were left at room temperature for 10 - 15 minutes and centrifuged at 12000 g for 10 minutes at 4 °C. The supernatant was removed. The RNA pellet was washed with 1 ml of 75% ethanol and centrifuged at 7500g for 10 minutes at 4°C. The ethanol was removed. The RNA pellet was air-dried for 5-10 minutes. RNA was dissolved in DEPC-treated H₂O for immediately used.

Alternatively, the RNA pellet was kept under absolute ethanol in a -80 °C freezer for long storage.

Total RNA was also extracted from other tissues including eyestalks, gills, heart, hemocytes, hepatopancreases, lymphoid organs, intestine, stomach, pleopods and thoracic ganglion of *P. monodon* using the same extraction procedure. The quality of extracted total RNA was examined by electrophoresed through 1.0% agarose gels.

2.4 Genomic DNA extraction

Genomic DNA was extracted from the pleopod of *P. monodon* using a phenol-chloroform-proteinase K method. The pleopod was placed in a centrifuge tube containing 2 ml of the extraction buffer (100 mM Tris-HCl, 100 mM EDTA, 250 mM NaCl; pH 8.0) and briefly homogenized with a micropestle and aliquoted into microcentrifuge tubes (500 µl). SDS (10%) and RNase A (10 mg/ml) solution were added to a final concentration of 0.1% (w/v) and 100 µg/ml, respectively. The resulting mixture was then incubated at 37 °C for 1 hour. At the end of the incubation period, a proteinase K solution (10 mg/ml) was added to the final concentration of 200 µg/ml and further incubated at 55 °C for 3 hours. An equal volume of buffer-equilibrated phenol was added and gently mixed for 15 minutes. The upper aqueous phase was transferred to a new sterile microcentrifuge tube. This extraction process was then repeated once with phenol and twice with chloroform : isoamylalcohol (24:1). The aqueous phase was transferred into a sterile microcentrifuge. One-tenth volume of 3 M sodium citrate, pH 5.2 was added. DNA was precipitated by an addition of two volume of pre-chilled absolute ethanol and mixed thoroughly. The mixture was incubated at -80 °C for 30 minutes and centrifuged at 12000 g for 10 minutes at 4 °C. The precipitated DNA was washed twice with 1 ml of 70% ethanol (10 and 5 minutes, respectively). After centrifugation, the supernatant was removed. The DNA pellet was air-dried and resuspended in 30-50 µl of TE buffer (10 mM Tris-HCl and 0.1 mM EDTA, pH 8.0). The DNA solution was incubated at 37 °C for 1-2 hours for complete solubilization and kept at 4 °C until further used.

2.5 Estimation of extracted total protein, total RNA and DNA concentration

The concentration of extracted protein sample is estimated by a dye binding assay. The binding of the dye to protein causes a shift in the absorption maximum of the dye from 465 to 595 nm. This assay is rapid, reproducible and virtually complete in approximately 2 minutes with the color stability for 1 hour. The concentration of extracted protein sample is estimated corresponding to the BSA standard.

The concentration of extracted RNA and DNA samples is estimated by measuring the optical density at 260 nm (OD_{260}). An OD_{260} of 1.0 corresponds to a concentration of 40 $\mu\text{g/ml}$ single stranded RNA, 50 $\mu\text{g/ml}$ double stranded DNA and 33 $\mu\text{g/ml}$ single stranded DNA (Sambrook and Russell, 2001). Therefore, the concentration of RNA and DNA sample was estimated in $\mu\text{g/ml}$ by using the following equation;

$$[\text{RNA of DNA}] = OD_{260} \times \text{dilution factor} \times (40, 50 \text{ or } 33 \text{ for RNA, double strand DNA and single stranded DNA})$$

The ratio between OD_{260}/OD_{280} provides an estimate on the purity of extracted DNA/RNA. For the extracted DNA, a pure preparation of DNA has OD_{260}/OD_{280} ratio of 1.8-2.0. The ratio of approximately 2.0 indicates the good quality of the extracted RNA. The ratios that much lower than those values indicate contamination of residual proteins or phenol in extracted DNA or RNA (Kirby, 1992).

2.6 Two dimensional gel electrophoresis

2.6.1 Sample preparation

One hundred micrograms of phenol-based extracted proteins or total proteins were added to rehydration buffer (7 M urea, 2 M thiourea, 4% CHAPS and 0.002% bromophenol blue) containing 2.4 mg DTT and 1% IPG buffer in a total volume of 360 μl . The sample solution was vortexed and left in the dark for 30 minutes before centrifugation at 13,000 g for 15 minutes at 4 °C.

2.6.2 Isoelectric focusing

The first dimension of 2D gel, isoelectric focusing (IEF), was performed using a 18 cm Immobiline Drystrip gel (GE Healthacres) linear pH gradient strips 3-10 and pH 4-7 in an integrated system, the Ettan IPGphor III. The sample solution was applied in the strip holder. An IPG strip was then placed on the top of the sample and covered with a dry strip cover, after rehydrated for 12 hour in the IPGphor III. IEF was performed using the following step voltage focusing protocol: pH 3-10; 500 V for 500 Vh, 1000V for 800 Vh, 8000V for 13,500 Vh, 8,000V for 12,200 Vh and pH 4-7; 500 V for 500 Vh, 1000V for 800 Vh, 8,000V for 13,500 Vh, 8,000V for 21,200 Vh. All the above processes were carried out at 20 ° C.

2.6.3 SDS-polyacrylamide gel electrophoresis (SDS-PAGE)

After the first dimension IEF, the IPG strip was equilibrated in equilibration buffer (50 mM Tris-HCl pH 8.8, 6M urea, 30% glycerol, 2% SDS and bromophenol blue 200 ml) containing 1% DTT for 15 min. The IPG strip gel was removed to another equilibration buffer containing 2.5 % iodoacetamide and equilibrated for a further 15 min. The equilibrated IPG strip was then placed on the top of 12.5% polyacrylamide gel (30 % acrylamide in Tris-HCl pH 8.8, 10% SDS). The second dimension separation was electrophoresed initially at 2.5 W per gel for 30 min followed by 20 W/gel at 20° C for 3-4 hours.

2.6.4 Silver staining

At the end of each run, the gel protein was fixed in the fixing solution (50% methanol, 12% acetic acid and 50 µl of 37% formaldehyde to 100 ml fixing solution) for 2 h. The gel was removed in the washing solution (35% ethanol) 3 times for 20 min each and sensitizing in 0.02% sodium thiosulfate for 2 min. After washing in water 3 times for 5 min each, the gel was stained with silver nitrate (2%) for 20 min. The gel was shaken in the developing solution (60% NaCO₃ w/v, 0.04% Na₂S₂O₃ v/v, 37% formaldehyde CH₂O) until regarded protein spots were visualized and stopped quickly in the stopping solution (14.6% w/v sodium EDTA C₁₀H₁₂N₂Na₄O₈) for 20 min. The gel was scanned by a Labscan (GE Healthacres). Gel image matching were

carried out using Image master 2D platinum™ (GE Healthacre) and the gel was kept in 0.1% acetic acid at 4°C.

2.7 Mass spectrometry analysis

2.7.1 In-gel digestion for protein identification

Protein spots were excised manually from silver-stained 2D gels. Gel plugs were placed in a 96 well plate and subjected to in-gel trypsin digestion, the spots were washed 3 times with 3% hydrogenperoxide and water, respectively. Acetonitrile (ACN) were added to the proteins for 5 min following by additional reduction and alkylation step using 10 mM DTT at room temperature for 1 h and 10 mM iodoacetamide in the dark at room temperature for 1 h. The gel pieces were hydrated with acetonitrile for 5 min, rehydrated with 10 mM ammonium bicarbonate for 10 min and hydrated again. Finally, the gels pieces were dried. The dried gels spots were rehydrated by addition of appropriate volume of the digestion buffer (10 ng/μL of trypsin in 10 mM ammonium bicarbonate) and incubated for 20 min on ice and 20 μl of 10 mM ammonium bicarbonate was added to cover the gel pieces. Digestion was performed overnight at 37°C. Tryptic peptide were extracted by an addition of 30 μl of 30% ACN and shaken for 30 s and transferred to a new 96 well plate followed by the addition of 30 μl of 50% ACN/0.1% TFA and incubated for 20 min, 30 μl of 60% ACN/0.1% TFA and incubated for 20 min, respectively. The digested proteins were dried at 40°C for 3-4 hours and stored in -80°C.

2.7.2 MALDI-TOF/TOF MS

The tryptic peptides were acidified with formic acid to the final concentration of 0.1% FA in ACN and α -cyano-4-hydroxycinnamic acid (CHCA) as the MALDI matrix were mixed, applied to sample target plate and air-dried. The mass spectra were recorded on a reflector Bruker Ultraflex delayed extraction MALDI-TOF/TOF mass spectrometer (Bruker Daltonics, Germany) equipped with a 2 GHz LeCroy digitizer and 337 nm N₂ laser. Instrumental parameters were set up as positive polarity, acceleration voltage of 20 kV, IS/2 17kV, focusing lens voltage of 8.90 kV,

extraction delay of 400 ns and gate detector. Two hundred laser shots were accumulated different positions within a sample spot.

2.7.3 nanoLC-MS/MS

Nano-electrospray liquid chromatography ionization tandem mass spectrometry (nanoLC-MS/MS) was performed as followed. Selected protein spots were submitted to an integrated the HCTultra ETD II system™ operated under HyStar™ (Bruker Daltonics). This system was controlled by the Chromeleon Chromatography Management system and comprised a two-pump Micromass/Loading Iontrap system with an autosampler. Injected samples were first trapped and desalted on an AccLaim PepMap C18 μ Precolumn Cartridge (5 μ m, 300- μ m inside diameter by 5 mm) for 3 min with 0.1% formic acid delivered by a loading pump at 20 μ l/min, after which the peptides were eluted from the pre-column and separated on a nano column, AccLaim PepMap 100 C18 (15 cm x 3 μ m) connected inline to the mass spectrometer, at 300 nl/min using a 30 min fast gradient of 4 to 96% solvent B (80% acetonitrile in 0.1% formic acid).

2.7.4 Database searches

After data acquisition, Peptide Mass Fingerprints from MALDI-TOF/TOF and MS/MS ion from nanoLC-MS/MS were identified using MASCOT (<http://www.matrixscience.com>) searched against data of the local shrimp database. In addition, data from nanoLC-MS/MS were searched against data of the National Central for Biotechnology Information (NCBI, nr) and SWITPROT. For peptide mass fingerprint search, mass value was MH^+ , mass tolerance was ± 1.2 Da, fragment mass tolerance ± 0.5 Da, and allowance for 1 miss cleavage. Variable modification was methionine oxidation and cysteine carbamidomethylation. For MS/MS ion search, the peptide charge was 1+, 2+ and 3+, MS/MS ion mass tolerance was ± 1 Da, fragment mass tolerance ± 0.5 Da, and allowance for 1 miss cleavage. Variable modification was methionine oxidation and cysteine carbamidomethylation. Proteins with the highest score or higher significant scores were selected. The significant hit proteins were selected according to Mascot probability analysis and regarded as positive

identification after additional conformation with molecular weight (MW)/ isoelectric point (pI) values.

2.8 First strand cDNA synthesis

One and half micrograms of total RNA from various tissues of *P. monodon* were reverse transcribed to the first strand cDNA using an ImProm-II™ Reverse Transcription System Kit (Promega). Total RNA was combined with 0.5 µg of oligo dT₁₂₋₁₈ and appropriate amount of DEPC-treated H₂O in a final volume of 5 µl. The reaction was incubated at 70 °C for 5 minutes and immediately placed on ice for 5 minutes. The 5x reaction buffer, MgCl₂, dNTP mix, RNasin were added to final concentration of 1x, 2.25 mM, 0.5 mM and 20 units, respectively. Finally, 1 µl of ImProm-II™ Reverse transcriptase was added and gently mixed by pipetting. The reaction mixture was incubated at 25 °C for 15 minutes and 42 °C for 90 minutes. The reaction was terminated by incubated at 70 °C for 15 minutes to terminate reverse transcriptase activity. Concentration and rough quality of newly synthesized first strand cDNA was spectrophotometrically examined (OD₂₆₀/OD₂₈₀) and electrophoretically analyzed by 1.2% agarose gel.

2.9 Reverse transcription (RT)-PCR of gene homologues in *P. monodon*

2.9.1 Primer design

Ten primer pairs were designed from EST sequences of gene homologues from hemocyte, ovary and testis cDNA libraries of *P. monodon* (Table 2.1).

2.9.2 RT-PCR

One hundred nanograms of the first strand cDNA of ovaries of female broodstock-sized *P. monodon* were used as the template in a 25 µl RT-PCR reaction composing of 10 mM Tris-HCl, pH 8.8, 50 mM KCl, 0.1% Triton X-100, 100 mM of each dNTP, 2 mM MgCl₂, 0.2 µM of each primer and 1 unit of Dynazyme™ DNA polymerase (FINNZYMES). RT-PCR was carried out with the temperature profile of predenaturation at 94 °C for 3 minutes followed by 25 cycles of denaturation at 94 °C

for 30 seconds, annealing at 53 °C for 45 second and extension at 72 °C for 30 seconds. The final extension was carried out at the same temperature for 7 minutes.

Fives microliters of the amplification products are electrophoresed though 1.2-2.0% agarose gel dependent on size of the amplification products. The electrophoresed band was visualized under a UV transilluminator after ethidium bromide staining (sambrook and Russell, 2001).

2.9.3 Agarose gel electrophoresis

An appropriate amount of agarose was weighed out and mixed with the desired volume of 1X TBE buffer (89 mM Tris-HCl, 89 mM boric acid and 2 mM EDTA, pH 8.3). The gel slurry was boiled in a microwave oven to complete solubilization and allowed to lower than 60 °C before poured into the gel mold. A comb was inserted. The agarose gel was left to solidify. When needed, enough amount of 1x TBE buffer covering the gel for approximately 0.5 cm. The comb was removed.

The PCR product was mixed with the one-fourth volume of the 10x loading dye (0.25% bromophenol blue and 25% ficoll in water) and loaded into the well. A 100 bp DNA ladder was used as the standard DNA marker. Electrophoresis was carried out at 5-6 volt/cm until bromophenol blue moved to approximately one-haft of gel.

The electrophoresed gel was stained with an ethidium bromide solution (25 µg/ml) for 5 minutes and destained in running tap water to remove unbound ethidium bromide from the gel. DNA fragments were visualized under a UV transluminator and photographed through a Gel Doc using a Quality One software (BioRad).

Table 2.1 Gene homologue, primer sequences and expected sizes of the PCR product designed from EST of *P. monodon*

Gene	Primer sequence	size
<i>Beta Thymosin</i>	F: 5'TATTGAAACGGAACGAACAC3' R: 5'CTTTGGCTGGTAGGGTAACTTTT3'	110
<i>DEAD box 52</i>	F: 5'CTCATTCTTTGTTCGCCTTCTTC3' R: 5'ATCAACTATGACTTCCCTCCT3'	204
<i>DEAD box ATP-dependent RNA helicase</i>	F: 5'TACCGTTACCTTCCACCAGC3' R: 5'GTCAGCCAGTCCACCTTACG3'	269
<i>ATP- dependent RNA helicase</i>	F: 5'TG TTCAGAAGGACGAAGAGACC3' R: 5'TG TTCAGCATCTTGTCGCATTC3'	153
<i>Helicase lymphoid specific isoform 2</i>	F: 5'CACATTCCCATCAGCAAACCGTC3' R: 5'TGGAGTG TTCCTATGACCTGCTTC3'	216
<i>P68 RNA helicase</i>	F: 5'GCTGGAGCAAATAACATCTG3' R: 5'TCCCACTTTGGCTTCCGTAG3'	201
<i>Protein disulfide isomerase</i>	F: 5'GAGCCTTAGATGCCACTGTTCAC3' R: 5'GCTCTGGCAGTCAAGAATGTGTG3'	275
<i>Heterogeneous nucleoprotein</i>	F: 5'CGACTTCCAGGGCAACGGTATG3' R: 5'ATCCTTTGCGCTGGTTCTTGGTC3'	482
<i>Valosin containing protein</i>	F: 5'GCAGTTGAACGAGGTGGGCTAC3' R: 5'TTGCGAAGGTTGCTCTCGCATT3'	276
<i>L-3-hydroxyacyl coA dehydrogenase</i>	F: 5'TAAGAATGTTACCGTCATCGGGAGC3' R: 5'ACGGCTAAGTGCCTCCGAGATGAAC3'	217

2.10 Tissue distribution analysis of interesting genes or differential expression pattern

2.10.1 Total RNA extraction and the first strand cDNA synthesis

Total RNA was extracted from eyestalk, gills, heart, hemocytes, hepatopancrease, lymphoid organ, intestine, ovaries, pleopods, stomach, testes, thoracic ganglion and epicuticle of broodstock of *P. monodon*. The first strand cDNA was synthesized as described previously.

2.10.2 Tissue distribution analysis

For the target genes, 150 ng of the first strand cDNA from various tissues was used as the template in 25 µl reaction volume containing 10 mM Tris-HCl, pH 8.8, 50 mM KCl and 0.1% Triton X-100, 2 mM MgCl₂, 100 µM each of dATP, dGTP, dTTP and dCTP, 0.2 µM of each primer and 1 unit of Dynazyme™ DNA polymerase (FINNZYMES). *Elongation factor-1α* (F: 5'-ATGGTTGTCAACTTTGCCCC-3' and R: 5'-TTGACCTCCTTGATCACACC-3') were also amplified from the same template and considered as the positive control. The reactions were predenaturation at 94 °C for 3 min followed by 30 cycles composing of a 94 °C denaturation step for 30 s, a 53 °C annealing step for 45 s and 72 °C extension step for 30 s. The final extension was carried out at 72 °C for 7 min. Fives microliters of the amplification product was electrophoretically analyzed though a 1.5% agarose gel.

2.11 Isolation and characterization of the full length cDNA of functionally important gene homologues of *P. monodon* using Rapid Amplification of cDNA Ends-Polymerase Chain Reaction (RACE-PCR)

2.11.1 Preparation of the 5' and 3' RACE template

Total RNA was extracted from ovaries of *P. monodon* using TRI REAGENT. The quality of extracted of total RNA was determined by agarose gel electrophoresis. Messenger (m) RNA was purified using a QuickPrep micro mRNA Purification Kit (Amercham Phamacia Biotech) according to the protocol recommended from the manufacturer. RACE cDNA template was prepared by combining 1 µg of ovarian

mRNA with 1 μ l of 5'-CDS primer and 1 μ l of 10 μ M SMART II oligonucleotide for 5' RACE-PCR or 1 μ g of ovarian mRNA with 1 μ l of 3' CDS primer A for 3' RACE-PCR (Table 2.2). The component were mixed and centrifuged briefly. The reaction was incubated at 70°C for 2 min and snap-cooled on ice for 2 minutes. The reaction tube was centrifuged briefly. After that, 2 μ l of 5x First-Strand buffer, 1 μ l of 20 mM DTT, 1 μ l of dNTP Mix (10 mM each) and 1 μ l of PowerScript Reverse Transcriptase were added. The reaction were mixed by gently pipetting and centrifuged briefly to collect the contents at the bottom of the tube. The reaction tube was incubated at 42 °C for 1.5 h in a thermocycler. The first strand reaction products were diluted with 125 μ l of TE buffer and heated at 72 °C for 7 min. The first strand cDNA template was kept at -20 °C until needed.

2.11.2 Primer designed for RACE-PCR and primer walking

Gene-specific primers (GSPs) were designed from ovary and hemocyte cDNA libraries. The antisense primer (and nested primer) for 5' and/or 3' RACE-PCR of each gene was designed (Table 2.3).

For sequencing of genes that showed the full length from the 5' direction, the product from colony PCR was considered. If the insert of a particular gene was larger than that of its homologues, the 3' direction was further sequenced. Internal primers were designed for primer walking of the inserted cDNA (Table 2.4).

2.11.3 RACE-PCR

The master mix sufficient for 5' and/or 3' RACE-PCR and the control reactions was prepared (Tables 2.4 and 2.5). For each 25 μ l amplification reaction, 14.0 μ l sterile deionized H₂O, 2.5 μ l of 10x Advantage[®] 2 PCR buffer, 0.5 μ l of 10 uM dNTP mix and 0.5 μ l of 50x Advantage[®] 2 polymerase mix were combined. The reaction was carried out for as described in Table 2.7.

The primary 5' and 3' RACE-PCR product were electrophoretically analyzed through 0.8-1.0% agarose gels. If the discrete expected bands were not obtained from the primary amplification, nested PCR was performed using the recipes illustrated in

Tables 2.5 and 2.6. The primary PCR product was 50-fold diluted. The secondary PCR was performed using 1 - 5 µl of the diluted first PCR product as a template using the conditions described in Table 2.7.

Table 2.2 Primer sequence for the first strand cDNA synthesis and RACE-PCR

Primers	Sequence
SMART II A Oligonucleotide	5'-AAGCAG TGG TATCAACGCAGAGTACGC GGG-3'
3' RACE CDS Primer A	5'-AAGCAGTGGTATCAACGCAGAGTAC(T) ₃₀ N ₁ N-3' (N=A, C, G orT; N ₁ = A,G or C)
5' RACE CDS Primer	5'-(T) ₂₅ N ₁ N-3' (N=A, C, G orT; N ₁ = A,G or C)
10X Universal PrimerA Mix (UPM)	Long : 5'-CTAATACGACTCACTATAGGGCAA GCAGTGGTATCAACGCAG AGT-3' Short : 5'-CTAATACGACTCACTATAGGG C - 3'
Nested Universal Primer A (NUP)	5 - AAG CAG TGG TAT CAA CGC AGA GT -3'

Table 2.3 Gene-specific primers (GSPs) and nested GSP used for isolation of the full length cDNA of functionally important genes in *P. monodon*

Gene specific primer	Sequence	Tm (°C)
<i>DEAD box 52</i>		
5' RACE	R: 5'CCCTTGAAGTCAATACCACGGGCCATG3'	66.56
3' RACE	F:5'ATTCACAGAGTAGGAAGGACTGGCAGAGCT3'	68.10
5'Nested	R: 5'ATCACTCTCGTCAACAACCAACCACTCC3'	66.6
<i>DEAD box ATP-dependent RNA helicase</i>		
5' RACE	R: 5'GTCAGCCAGTCCACCTTACG3'	59.40
3' RACE	F: 5'TACCGTTACCTTCCACCAGC3'	
<i>ATP-dependent RNA helicase</i>		
5' RACE	R: 5'TGTTCCAGCATCTTGTCGCATTTC3'	60.06
3' RACE	F: 5'TGTTCAGAAGGACGAAGAGACC3'	60.30
5' Nested	R: 5'AGTGGCGGAGATTGGGCTTCTTGTTGC3'	68
<i>L-3-hydroxyacyl coenzyme A dehydrogenase</i>		
3' RACE	F: 5' ACGGCTAAGTGCCTCCGAGATGAAC 3'	61.98
<i>Protein disulfide isomerase</i>		
5' RACE	R: 5' GCTCTGGCAGTCAAGAATGTGTG 3'	62.40
3' RACE	F: 5' GAGCCTTAGATGCCACTGTTTAC 3'	62.40
5' Nested	R: 5' TGGAGGTTGGATGGAATAAGGTCACA3'	61.60
3' Nested	F: 5' TGGTGGATTTGGATACCCTGCTCTTG 3'	64.80
<i>Valosin containing protein</i>		
5' RACE	R: 5' TTGCGAAGGTTGCTCTCGCATT 3'	60.07
3' RACE	F: 5' GCAGTTGAACGAGGTGGGCTAC 3'	63.80

Table 2.4 Compositions for amplification of the 5' end of gene homologues using 5' RACE-PCR

Component	5' RACE-PCR	UPM only (Control)	GSP1 only (Control)
5' RACE-Ready cDNA template	1.5 µl	1.5 µl	1.5 µl
UPM (10x)	5.0 µl	5.0 µl	-
GSP1 (10 uM)	1.0 µl	-	1.0 µl
GSP2 (10 uM)	-	-	-
H ₂ O	-	1.0 µl	5.0 µl
Master Mix	17.5 µl	17.5 µl	17.5 µl
Final volume	25 µl	25 µl	25 µl

Table 2.5 Compositions for amplification of the 3' end of gene homologues using 3' RACE-PCR

Component	3' RACE-PCR	UPM only (Control)	GSP1 only (Control)
5' RACE-Ready cDNA template	1.5 µl	1.5 µl	1.5 µl
UPM (10x)	5.0 µl	5.0 µl	-
GSP1 (10 uM)	1.0 µl	-	1.0 µl
GSP2 (10 uM)	-	-	-
H ₂ O	-	1.0 µl	5.0 µl
Master Mix	17.5 µl	17.5 µl	17.5 µl
Final volume	25 µl	25 µl	25 µl

Table 2.6 The amplification conditions for RACE-PCR of various gene homologues of *P. Monodon*

Gene homologue	Amplification condition
<i>DEAD box 52</i>	
5' RACE-PCR	5 cycles of 94 °C for 30 s and 72 °C for 2 min 5 cycles of 94 °C for 30 s, 70 °C for 30 s and 72 °C for 2 min 20 cycles of 94 °C for 30 s, 68 °C for 30 s and 72 °C for 2 min and the final extension at 72 °C for 7 min
3' RACE-PCR	5 cycles of 94 °C for 30 s and 72 °C for 2 min 5 cycles of 94 °C for 30 s, 70 °C for 30 s and 72 °C for 2 min 20 cycles of 94 °C for 30 s, 68 °C for 30 s and 72 °C for 2 min and the final extension at 72 °C for 7 min
5' Nested RACE-PCR	20 cycles of 94 °C for 30 s, 66 °C for 30 s, 72 °C for 2 min and the final extension at 72 °C for 7 min
<i>DEAD box ATP-dependent RNA helicase</i>	
5' RACE-PCR	20 cycles of 94 °C for 30 s, 66 °C for 45 s, 72 °C for 3 min and the final extension at 72 °C for 7 min
3' RACE-PCR	20 cycles of 94 °C for 30 s, 66 °C for 45 s, 72 °C for 3 min and the final extension at 72 °C for 7 min
<i>ATP-dependent RNA helicase</i>	
5' RACE-PCR	20 cycles of 94 °C for 30 s, 66 °C for 45 s, 72 °C for 3 min and the final extension at 72 °C for 7 min
3' RACE-PCR	20 cycles of 94 °C for 30 s, 66 °C for 45 s, 72 °C for 3 min and the final extension at 72 °C for 7 min
5' Nested RACE-PCR	20 cycles of 94 °C for 30 s, 66 °C for 45 s, 72 °C for 3 min and the final extension at 72 °C for 7 min
<i>L-3-hydroxyacyl coenzyme A dehydrogenase</i>	
3' RACE-PCR	20 cycles of 94 °C for 30 s, 66 °C for 45 s, 72 °C for 3 min and the final extension at 72 °C for 7 min
<i>Protein disulfide isomerase</i>	
5' RACE-PCR	20 cycles of 94 °C for 30 s, 66 °C for 45 s, 72 °C for 3 min and the final extension at 72 °C for 7 min
3' RACE-PCR	20 cycles of 94 °C for 30 s, 66 °C for 45 s, 72 °C for 3 min and the final extension at 72 °C for 7 min
5' Nested RACE-PCR	20 cycles of 94 °C for 30 s, 66 °C for 45 s, 72 °C for 3 min and the final extension at 72 °C for 7 min
3' Nested RACE-PCR	20 cycles of 94 °C for 30 s, 66 °C for 45 s, 72 °C for 3 min and the final extension at 72 °C for 7 min
<i>Valosin containing protein</i>	
5' RACE-PCR	20 cycles of 94 °C for 30 s, 66 °C for 45 s, 72 °C for 3 min and the final extension at 72 °C for 7 min
3' RACE-PCR	20 cycles of 94 °C for 30 s, 66 °C for 45 s, 72 °C for 3 min and the final extension at 72 °C for 7 min

2.11.4 Elution DNA fragments from agarose gels

After electrophoresis, the desired DNA fragment was excised from the agarose gel using a sterile scalpel and placed in a pre-weighed microcentrifuge tube. DNA was eluted out from the gel using a HiYield™ Gel Elution Kit (RBC). Five hundred microlitres of the DF buffer was added to the sample and mixed by vortexing. The mixture was incubated at 55 °C for 10 - 15 min until the gel slice was completely dissolved. During the incubation period, the tube was inverted every 2-3 min. A DF column was placed in a collection tube and 800 µl of the sample mixture was applied into the DF column and centrifuged at 6,000 g (8,000 rpm) for 30s. The flow-through was discarded. The DF column was placed back in the collection tube. The column was washed by the addition of 500 µl of the ethanol-added Wash Buffer and centrifuged at 6,000 g for 30s. After discarding the flow-through, the DF column was centrifuged for 2 min at the full speed (14,000 rpm) to dry the column matrix. The dried column was placed in a new microcentrifuge tube and 15 µl of the Elution Buffer or water was added to the center of the column matrix. The column was left at room temperature for 2 min before centrifuged for 2 minutes at the full speed to recover the gel-eluted DNA.

2.12 Cloning of the PCR product

2.12.1 Ligation of the PCR product to the pGEM®-T Easy vector

DNA fragments was ligated to the pGEM®-T Easy vector in a 10 µl reaction volume containing 5 µl of 2x Rapid Ligation Buffer (60 mM Tris-HCl, pH 7.8, 20 mM MgCl₂, 20 mM DDT, 2 mM ATP and 10% PEG8000), 3 Weiss unit of T4 DNA ligase, 25 ng of the pGEM®-T Easy vector and approximately 50 ng of the DNA insert. The reaction mixture was incubated overnight at 4 - 8 °C before transformed to *E.coli* JM 109 (or XL1-Blue).

2.12.2 Transformation of the ligation product to *E.coli* host cells

2.12.2.1 Preparation of competent cell

A single colony of *E. coli* JM109 (or XL1-Blue) was inoculated in 10 ml of LB broth (1% Bacto tryptone, 0.5% Bacto yeast extract and 0.5% NaCl, pH 7.0) with vigorous shaking at 37 °C overnight. The starting culture was then inoculated into 50 ml of LB broth and continued culture at 37 °C with vigorous shaking to OD₆₀₀ of 0.5 to 0.8. The cells were briefly chilled on ice for 10 minutes and recovered by centrifugation at 2700 g for 10 minutes at 4 °C. The pellets were resuspended in 30 ml of ice-cold MgCl₂/CaCl₂ solution (80 mM MgCl₂ and 20 mM CaCl₂) and centrifuged as above. The cell pellet was resuspended with 2 ml of ice-cold 0.1 M CaCl₂ and the cell suspension was divided into 100 or 200 µl aliquots. These competent cells were used immediately or stored at -80°C for subsequently used.

2.12.2.2 Transformation

The competent cells were thawed on ice for 5 min. Two to four microlitres of the ligation mixture were added and gently mixed by pipetting. The mixture was left on ice for 30 min. During the incubation period, the ice box was gently moved forward and backward a few times every 5 min. The transformation reaction was heat-shocked in a 42 °C water bath (without shaking) for exactly 45 seconds. The reaction tube was immediately placed on ice for 2 - 3 min. The mixture was removed from the tubes and added to a new tube containing 1 ml of pre-warmed SOC (2% Bacto tryptone, 0.5 % Bacto yeast extract, 10 mM NaCl, 2.5 mM KCl, 10 mM MgCl₂, 10 mM MgSO₄ and 20 mM glucose). The cell suspension was incubated with shaking at 37 °C for 90 min. The mixture was centrifuged for 20 seconds at room temperature, and resuspended in 100 µl of the SOC medium and spread onto a selective LB agar plates (containing 50 µg/ml of ampicillin and spread with 20 µl of 25 µg/ml of X-gal and 25 µl of 25 µg/ml of IPTG for approximately 1 hr before using) and further incubated at 37 °C overnight. The recombinant clones containing inserted DNA are white whereas those without inserted DNA are blue (Sambrook and Russell, 2001).

2.13 Colony PCR and digestion of the amplified inserts by restriction endonucleases

Colony PCR was performed in a 25 µl reaction mixture containing 10 mM Tris-HCl, pH 8.8, 50 mM (NH₄)₂SO₄, 0.1% Triton X-100, 100 mM of each dNTP, 2 mM MgCl₂, 0.1 µM each of pUC1 (5'-CCG GCT CGT ATG TTG TGT GGA-3') and pUC2 (5'-GTG GTG CAA GGC GAT TAA GTT GG-3'), 0.5 unit of *Taq* DNA polymerase (Fermentas). A colony was picked by a pipette tip, placed in the culture tube and served as the template in the reaction. PCR was carried out in a thermocycler consisting of predenaturation at 94°C for 3 min followed by 35 cycles of denaturation at 94°C for 30s, annealing at 50°C for 1 min and extension at 72°C for 1.5 min. The final extension was carried out at the same temperature for 7 min. The colony PCR products were electrophoresed through a 1.2 % agarose gel and visualized after ethidium bromide staining.

The colony PCR products containing the insert were separately digested with *Alu* I and *Rsa* I (Promega) in a 15 µl reaction volume containing 1x buffer (6 mM Tris-HCl, 6 mM MgCl₂, 50 mM NaCl and 1 mM DDT, pH 7.5 for *Alu* I and 10 mM Tris-HCl, 10 mM MgCl₂, 50 mM NaCl and 1 mM DDT, pH 7.9 for *Rsa* I), 0.1 mg/ml BSA, 2 units of each enzyme and 4 µl of the colony PCR product. The reaction mixture was incubated at 37°C overnight. The reaction was analyzed by 1.2% agarose gel electrophoresis.

2.14 Extraction of recombinant plasmid DNA

Plasmid DNA was isolated using a HiYieldTM Plasmid Mini Kit (RBC). A discrete white colony was inoculated into a sterile culture tube containing 3 ml of LB broth supplemented with 50 µg/ml of ampicillin and incubated with shaking (200 rpm) at 37 °C overnight. The culture was transferred into a sterile 1.5 ml microcentrifuge tube and centrifuged at 14,000 rpm for 1 min. The supernatant was discarded. The bacterial pellet was resuspended in 200 µl of the PD1 buffer containing RNase A and thoroughly mixed by vortexed. The resuspended cells were lysed by the addition of 200 µl of the PD 2 buffer and mixed gently by inverting the

tube for 10 times. The mixture was left for 2 minutes at room temperature. After that, 300 μl of the PD3 buffer was added to neutralize the alkaline lysis step and mixed immediately by inverting the tube for 10 times. The mixture was then centrifuged at 14,000 rpm for 15 min.

A PD column was placed in a collection tube and the clear lysate was applied into the PD column and centrifuged at 6,000 g (8,000 rpm) for 30s. The flow-through was discarded. The PD column was placed back in the collection tube. The column was washed by the addition of 400 μl of the W1 buffer and centrifuged at 6,000 g for 30s. After discarding the flow-through, 600 μl of the ethanol-added Wash buffer was added and centrifuged as above. The PD column was further centrifuged for 2 min at the full speed (14,000 rpm) to dry the column matrix. The dried column was placed in a new microcentrifuge tube and 50 μl of the elution buffer or water was added at the center of the column matrix. The column was left at room temperature for 2 min before centrifuged for 2 min at the full speed to recover the purified plasmid DNA. The concentration of extracted plasmid DNA was spectrophotometrically measured.

2.15 Semiquantitative RT-PCR of genes in ovaries of female broodstock of normal and unilateral eyestalk ablated *P. monodon* broodstock

2.15.1 Experimental animals

Female broodstock were caught alive from the Andaman Sea and acclimated under the farm conditions for 2-3 days. Ovaries were dissected out from normal broodstock and weighed. For the eyestalk ablation group, shrimp were acclimated for 7 days prior to unilateral eyestalk ablation. Ovaries of ablated shrimp were collected at 2-7 days after ablation. The gonadosomatic index (GSI, ovarian weight/body weight \times 100) of each shrimp was calculated. Ovaries of each shrimp were kept at -70°C until needed. Stages of ovarian development were classified according to the GSI values (<2% for stages I, >2 – 4% for stage II, >4 – 6% for stage III and >6% for stage IV).

2.15.2 Total RNA extraction and first strand cDNA synthesis

Ovaries were dissected from each shrimp immediately after specimens were collected and placed in liquid N₂. Total RNA was extracted from ovaries of *P. monodon* ($N = 5$ for each treatment) and 1.5 µg of total RNA was reverse-transcribed using an ImProm- IITM Reverse Transcription System Kit (Promega) as described previously.

2.15.3 Optimization of semiquantitative RT-PCR conditions

Initially, RT-PCR of the target genes (Table 2.1) and *elongation factor-1α* (F:5'-ATG GTT GTC AAC TTT GCC CC-3' and R:5'-TTG ACC TCC TTG ATC ACA CC-3') were amplified in a 25 µl reaction volume following the non-quantitative RT-PCR for initial screening of gene expression profiles described previously. The reaction contained 10 mM Tris - HCl pH 8.8 at 25°C, 50 mM KCl and 0.1 % Triton X-100, 2 mM MgCl₂, 100 mM each of dATP, dCTP, dGTP and dTTP, 0.2 µM of each primer, 1 µl of 10-fold diluted first strand cDNA and 1 unit of DynazymeTM DNA polymerase (FINNZYMES). For semiquantitative RT-PCR analysis, primer and MgCl₂ concentrations and the cycle numbers used for amplification were further optimized.

2.15.3.1 Optimization of primer concentration

The optimal primer concentration for each primer pair (between 0, 0.02, 0.04, 0.07, 0.1, 0.15, 0.2, 0.25 and 0.3 µM) was examined using the standard PCR conditions. The resulting product was electrophoretically analyzed. The primer concentration that gave product specificity and clear results were selected for further optimization of the PCR conditions.

2.15.3.2. Optimization of MgCl₂ concentration

The optimal MgCl₂ concentration of each primer pair (0, 0.5, 1.0, 1.5 and 2.0 mM of MgCl₂) was examined using the standard PCR conditions with the optimized primer concentration. The concentration of MgCl₂ that gave the highest yields and specificity for each PCR product was chosen.

2.15.3.3 Optimization of the number of amplification cycles

The PCR amplifications were carried out at different cycles (e.g. 20, 23, 25, 28 and 30 cycles) using the optimized concentration of primers and MgCl₂. The number of cycles that gave the highest yield before the product reached a plateau phase of amplification was chosen.

2.15.3.4 Gel electrophoresis, semiquantitative RT-PCR and data analysis

The amplification product of genes under investigation and *EF-1 α* were electrophoretically analyzed by the same gel and photographed by a gel documentation machine (BioRad). The intensity of the amplified target genes and that of *EF-1 α* was quantified from the photograph of the gels using the Quantity One programme (BioRad).

The expression level of each gene was normalized by that of *EF-1 α* . Expression levels between different groups of *P. monodon* were statistically tested using one way analysis of variance (ANOVA) followed by a Duncan's new multiple range test. Significant comparisons were considered when the *P* value was < 0.05.

2.16. Examination of expression levels of interesting genes in ovaries of *P. monodon* by quantitative real-time PCR

Expression levels of several transcripts including *DEAD box ATP-dependent RNA helicase*, *protein disulfide isomerase* and *valosin containing protein* were examined using quantitative real-time PCR analysis.

2.16.1 Experimental animals

Normal and eyestalk-ablated wild broodstock of *P. monodon* (ABW = 142.98 \pm 28.37) possessing different stages of ovarian development (GSI <2% for stages I; *N* = 10, >2 – 4% for stage II; *N* = 7, >4 – 6% for stage III ; *N* = 7, >6% for stage IV ; *N* = 10, post spawn ; *N* = 6 and juvenile ; *N* = 6) were used for estimating expression levels of various genes in their ovaries.

2.16.2 Primers and construction of the standard curve

Primers for *DEAD box ATP-dependent RNA helicase*, *protein disulfide isomerase* and *valosin containing protein* (Table 2.1) were applied for real-time PCR analysis. For construction of the standard curve of each gene, the PCR product of the target gene and *EF-1 α* was amplified, electrophoresed through agarose gel and eluted out. The gel eluted product was cloned into pGEM-Teasy vector and transformed into *E. coli* JM109. Plasmid DNA were extracted and used as the template for construction of the standard curve. Templates of each gene homologues and *EF-1 α* were ten fold diluted covering $10^3 - 10^8$ copy numbers. Real-time RT-PCR was carried out (see below) and each standard point was run in duplicate.

2.16.3 Quantitative real-time PCR

The first strand cDNA was reverse-transcribed. The target transcript (*DEAD box ATP-dependent RNA helicase*, *protein disulfide isomerase* and *valosine containing protein*) and internal control (*EF-1 α*) of each shrimp were amplified in reaction volume 10 μ l containing 5 μ l of 2x SYBR Green Master Mix (Roch). The specific primer pairs were used at a final concentration of 0.1, 0.15, 0.2 and 0.3 μ M, respectively. The thermal profile for quantitative real-time RT-PCR was 95°C for 10 min followed by 40 cycles of denaturation at 95 °C for 15 s, annealing at 53 °C, 55 °C or 56 °C for 30 s and extension at 72 °C for 20 s. Continually, cycles for the melting curve analysis was carried out at 95 °C for 15 s, 65 °C for 1 min and at 98°C for continue and cooling 40 °C for 30 s. Real-time RT-PCR assay was carried out in 96 well plate and each sample was run in duplicate. Relative expression levels of different group of samples were statistically test by one way ANOVA followed by Duncan's new multiple rang test ($P < 0.05$).

CHAPTER III

RESULTS

3.1 Protein profiles of *P. monodon* ovaries examined by two dimensional gel electrophoresis

Two-dimensional gel electrophoresis (2-DE) was carried out to examine protein profiles during ovarian development of both normal (non-ablated) and eyestalk-ablated wild *P. monodon* broodstock. Initially, residual proteins after extraction of total RNA were isolated and subjected to two-dimensional gel electrophoresis. The conditions were further optimized and total proteins extracted from different stages of *P. monodon* ovarian development were eventually used to identify and characterize ovarian protein profiles of this economically important species.

3.1.1 Protein profiles during ovarian development using TRI-REAGENT-extracted proteins

Initially, TRI-REAGENT-extracted proteins from different stages of *P. monodon* ovaries were electrophoretically analyzed using the pH gradient of pH 3-10 followed by 12.5% SDS-PAGE. In normal broodstock, the number of protein spots in stage I ovaries were greater than that of other stages (Figure 3.1). In contrast, the number of protein spots was comparable in different stages of ovaries in eyestalk-ablated broodstock (Figure 3.2).

Two-dimensional gel electrophoresis of TRI-REAGENT-extracted proteins at the broad pH gradient revealed that almost all of the expressed ovarian proteins were acidic proteins. Therefore, proteins extracted from different stages of ovarian development were re-analyzed using a narrower pH gradient of 4-7.

As can be seen from Figure 3.3, a better resolution of ovarian protein profiles in normal shrimp broodstock was observed at an acidic pH gradient than a broad pH gradient. Results were consistent when applied to eyestalk-ablated *P. monodon* broodstock (Figure 3.4).

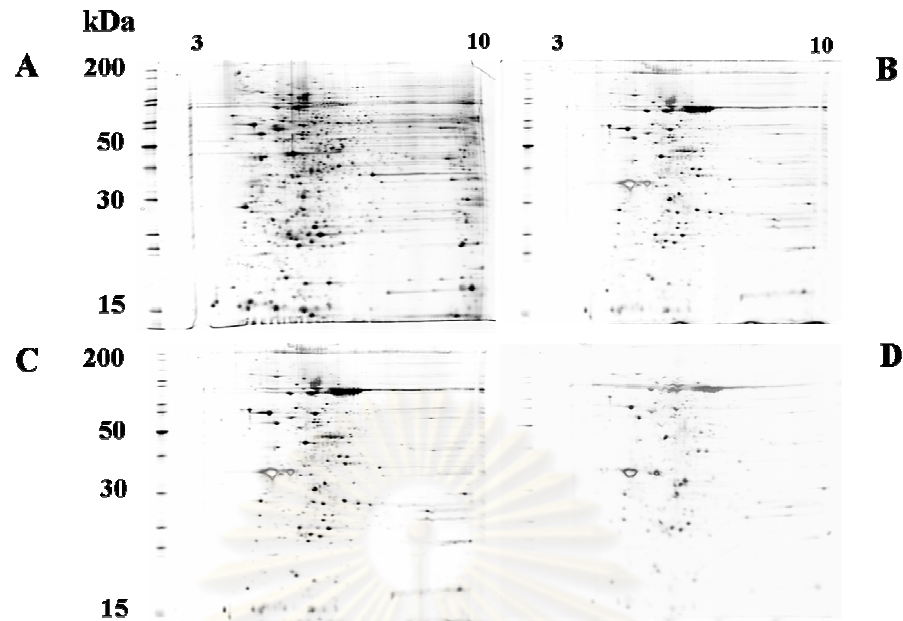


Figure 3.1 Protein profiles of ovaries of wild *P. monodon* broodstock (stages I, II, III and IV corresponding to panels A-D, respectively) analyzed by 2D gel electrophoresis. Residual proteins from RNA extraction of different stages of ovaries using TRI-REAGENT were electrophoretically analyzed in Immobiline Drystrip gels (pH 3-10) followed by 12.5% SDS PAGE and silver-stained .

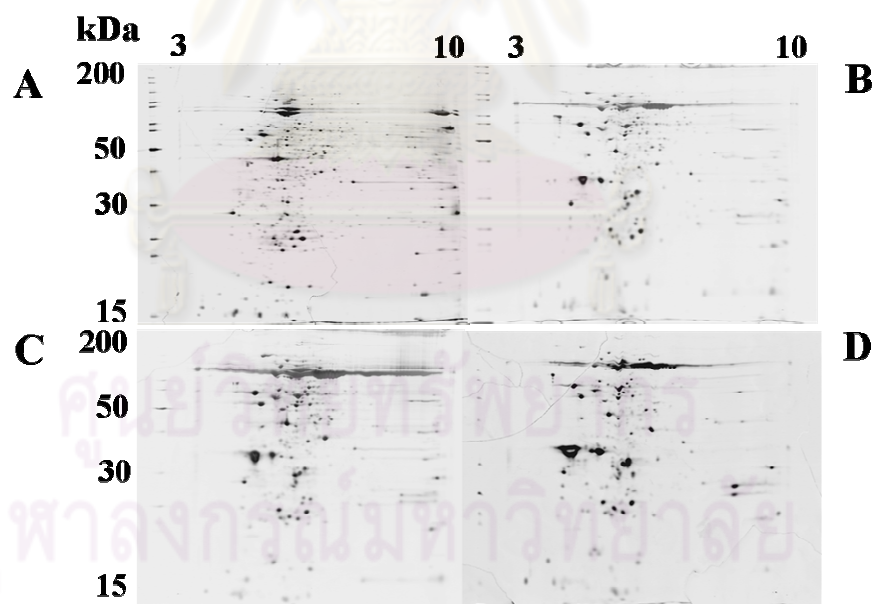


Figure 3.2 Protein profiles of ovaries of eyestalk-ablated wild *P. monodon* broodstock (stages I-IV, panels A-D, respectively) analyzed by 2D gel electrophoresis. Residual proteins from RNA extraction of different stages of ovaries using TRI-REAGENT were electrophoretically analyzed in Immobiline Drystrip gels (pH 3-10) followed by 12.5% SDS-PAGE and silver-stained.

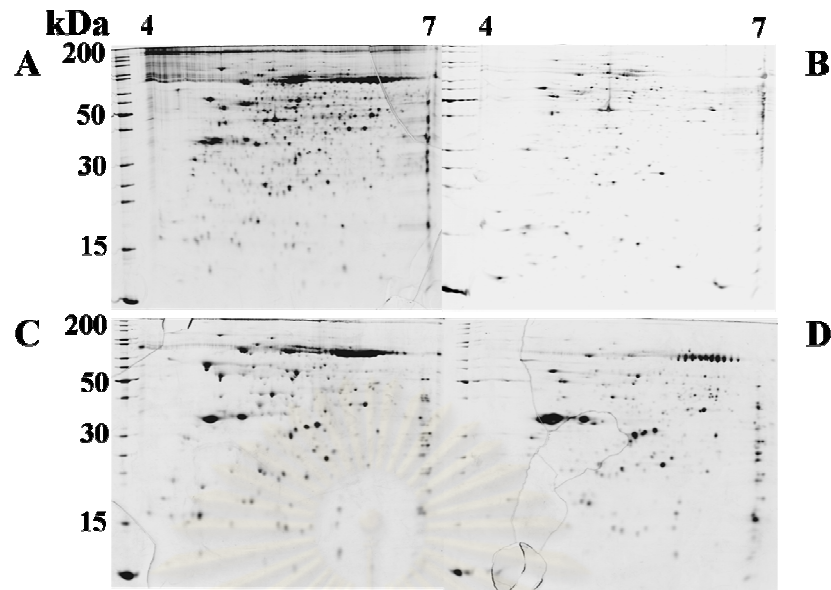


Figure 3.3 Protein profiles of ovaries of wild *P. monodon* broodstock (stages I-IV corresponding to panels A-D, respectively) analyzed by 2D gel electrophoresis. Residual proteins from RNA extraction of different stages of ovaries using TRI-REAGENT were electrophoretically analyzed in Immobiline Drystrip gels (pH 4-7) followed by 12.5% SDS-PAGE and silver-stained.

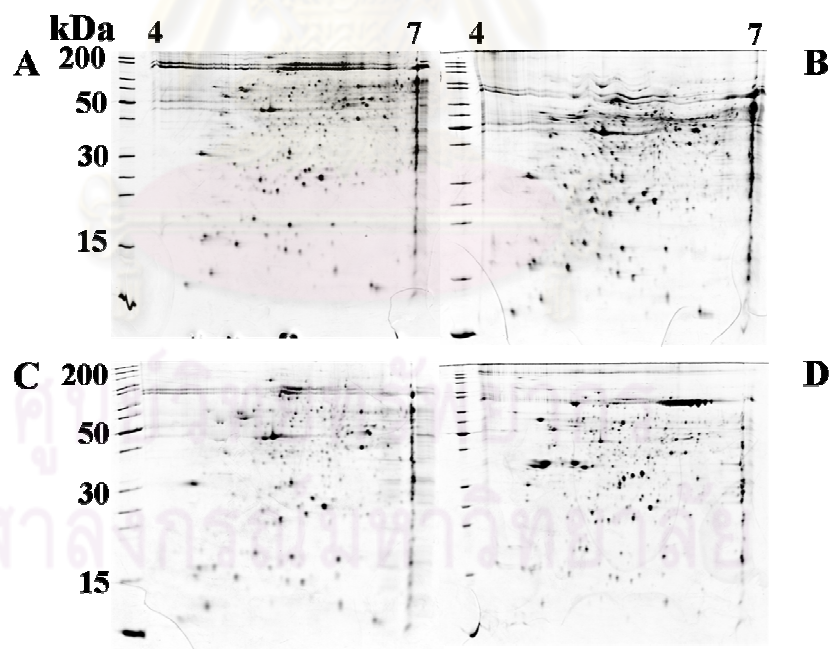


Figure 3.4 Protein profiles of ovaries of eyestalk-ablated wild *P. monodon* broodstock (stages I-IV, panels A-D, respectively) analyzed by 2D gel electrophoresis. Residual proteins from RNA extraction of different stages of ovaries using TRI-REAGENT were electrophoretically analyzed in Immobiline Drystrip gels (pH 4-7) followed by 12.5% SDS-PAGE and silver-stained.

TRI-REAGENT-extracted proteins are a by-product of phenol-based RNA extraction. Phenol is one of the strongest dissociating agents that can modify the protein nature. In addition, extraction of the residual proteins from RNA extraction requires the precipitation step. Small proteins may not be recovered effectively. At this stage, conditions for two-dimensional gel electrophoresis were successfully optimized. Therefore, total proteins extracted from ovarian tissues were used instead.

3.1.2 Protein profiles during ovarian development using total ovarian proteins

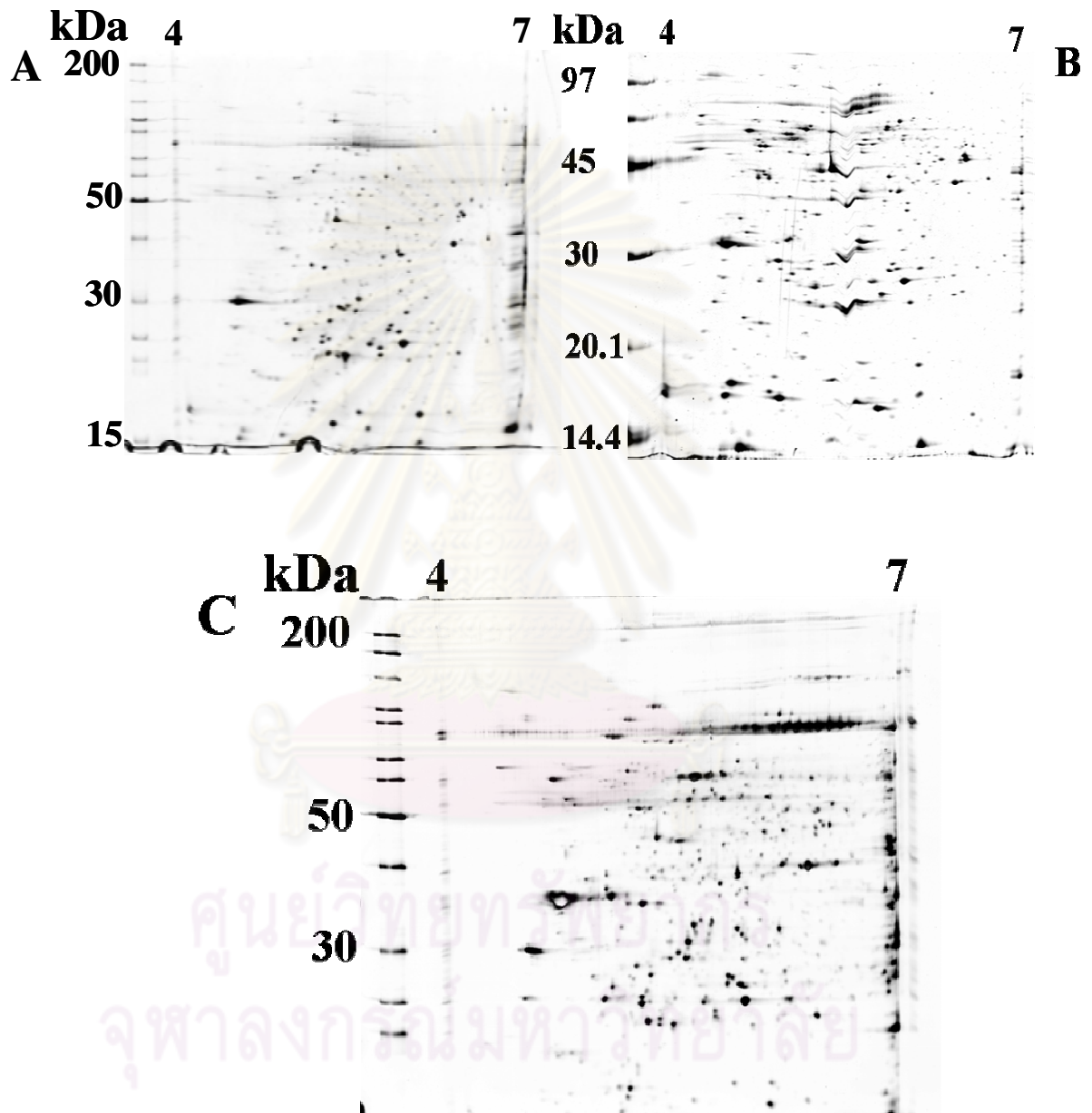
Relatively large amount of total protein were consistently obtained (200 – 300 µg/ 500 mg of starting tissue). Total proteins from the same stage of ovaries were carried out in triplicate; one from the same individual and the other from different individual.

Generally, the number of protein spots from total ovarian proteins was obviously greater than that of TRI-REAGENT extracted proteins. For the normal broodstock, the number of protein spots found in stages I, II, III and IV was (585,751 and 568), (1074, 286 and 581), (409, 237 and 754) and (596, 281 and 195), respectively (Figures 3.5-3.8). Large numbers of protein spots were also observed in eyestalk-ablated broodstock [(538,384 and 928), (604, 454 and 352), (346, 311 and 465) and (220, 336 and 380) for the respective stages] (Figures 3.9-3.12).

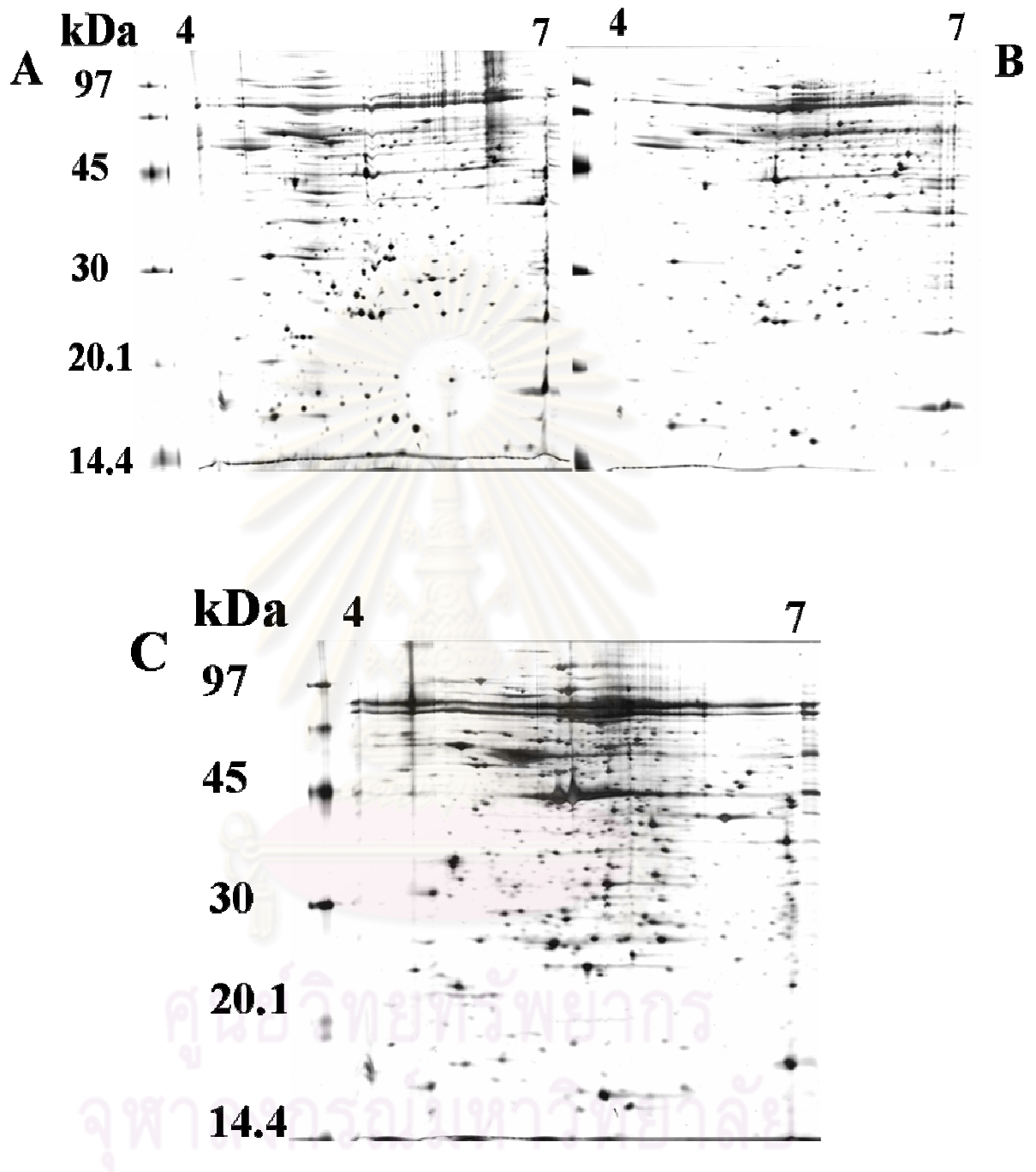
In addition, profiles of basic ovarian proteins were also examined using the Immobiline Drystrip of pH 7-10. However, those proteins were not electrophoretically separated and dense streaks of analyzed proteins were observed at the top of the 2-DE gels indicating their highly basic molecular masses. Therefore, basic ovarian proteins were not further studied.

Protein profiles were matched by Imagemaster 2D Platinum™ (GE Healthcare). Comparison of *pI* and MW between protein spots of different individuals carrying the same stages of ovaries was initially carried out in both normal and eyestalk-ablated groups. Subsequently, those parameters of protein spots among different ovarian stages within each group and among the same stages of different

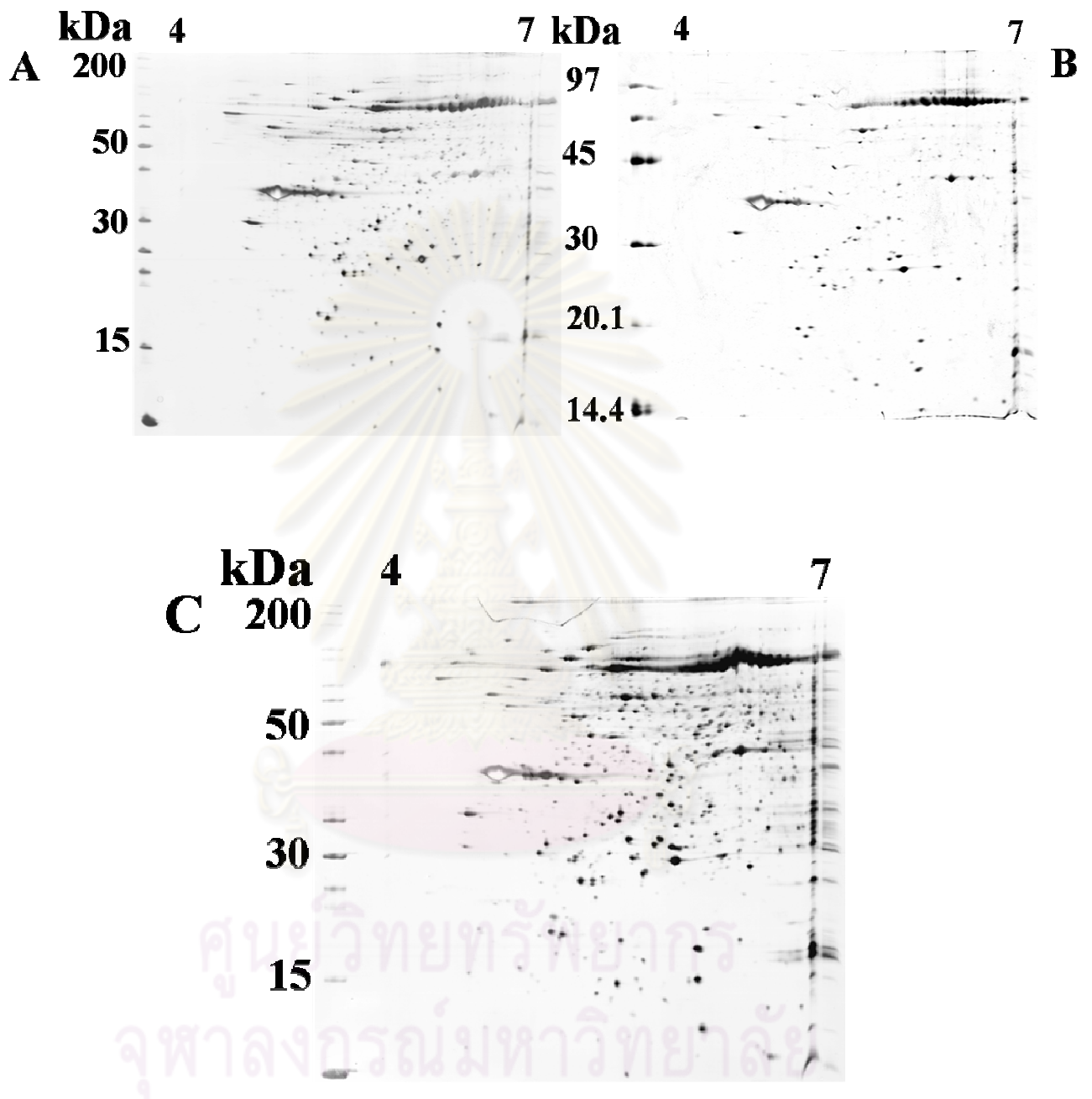
shrimp groups were carried out. Only a single spot of a protein representing identical *pI* and MW was further characterized by mass spectrometry.



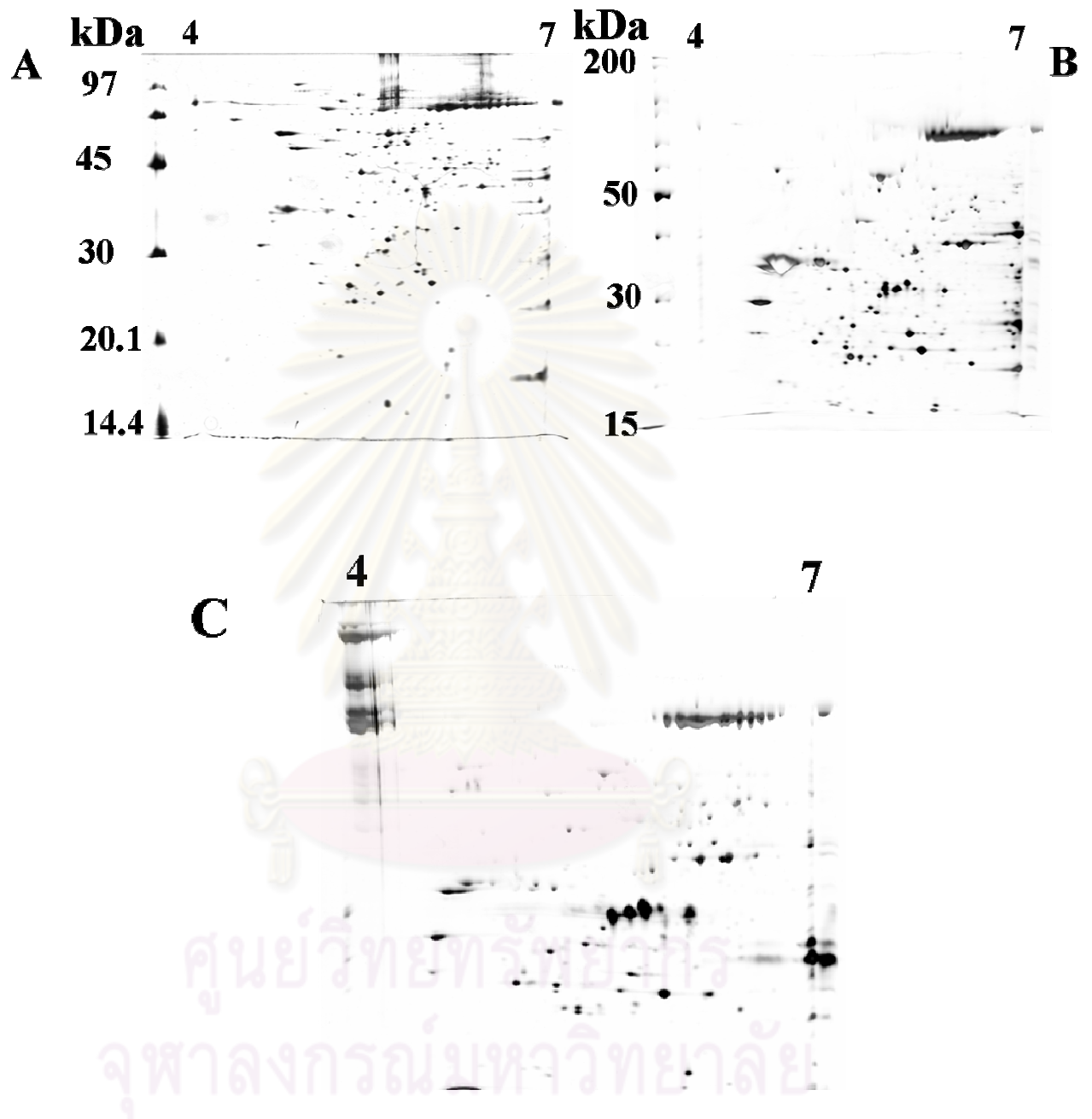
Figures 3.5 Protein profiles of stage I ovaries of wild *P. monodon* broodstock analyzed by 2D gel electrophoresis. Total proteins from two individuals (panels A and B, GSI = 0.57% and panel C, GSI = 0.66%) were electrophoretically analyzed in Immobiline Drystrip gels (pH 4-7) followed by 12.5% SDS-PAGE and silver-stained.



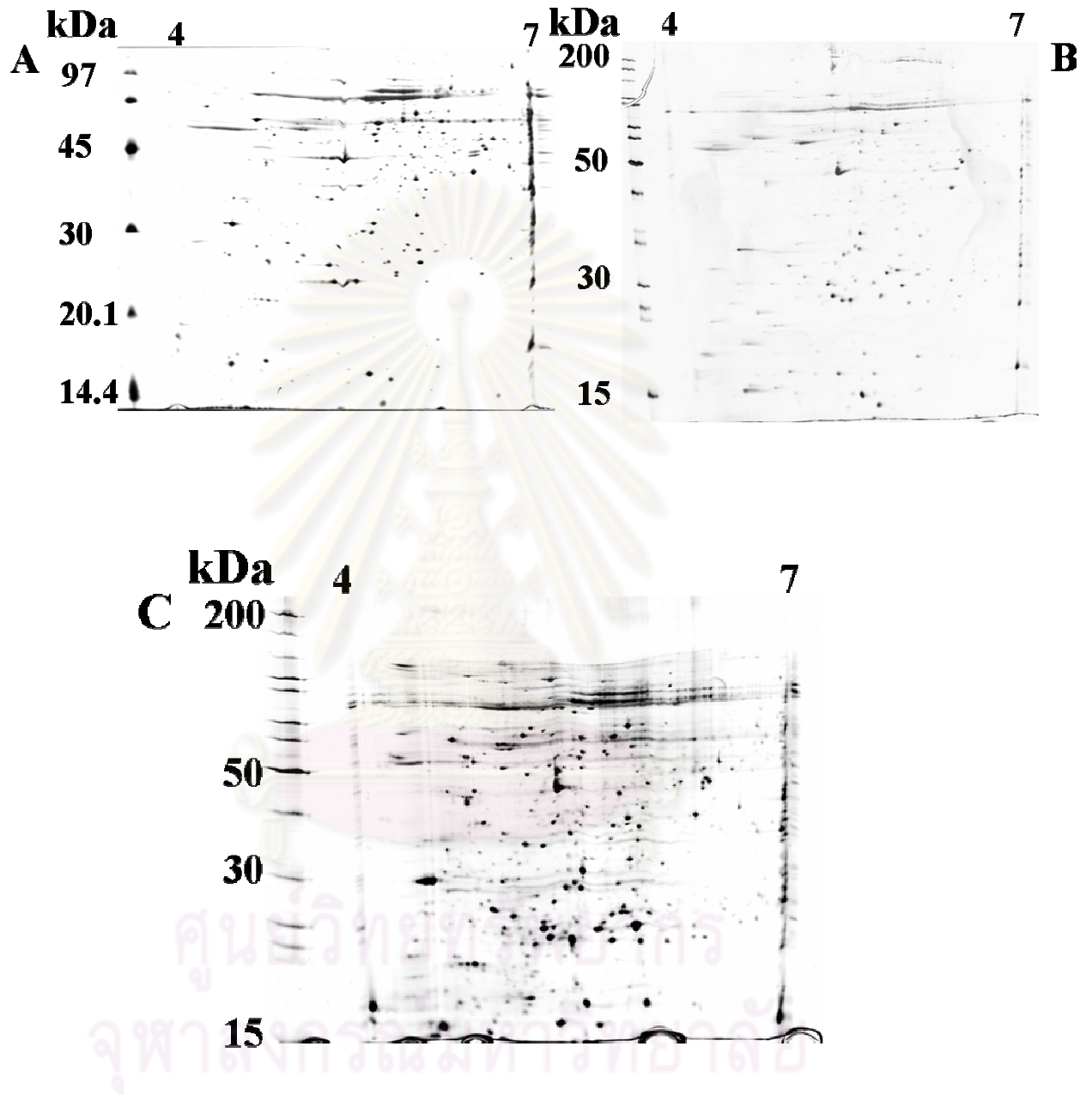
Figures 3.6 Protein profiles of stage II ovaries of wild *P. monodon* broodstock analyzed by 2D gel electrophoresis. Total proteins from two individuals (panels A and B, GSI = > 1.44% and panel C, GSI = > 1.33%) were electrophoretically analyzed in Immobiline Drystrip gels (pH 4-7) followed by 12.5% SDS-PAGE and silver-stained.



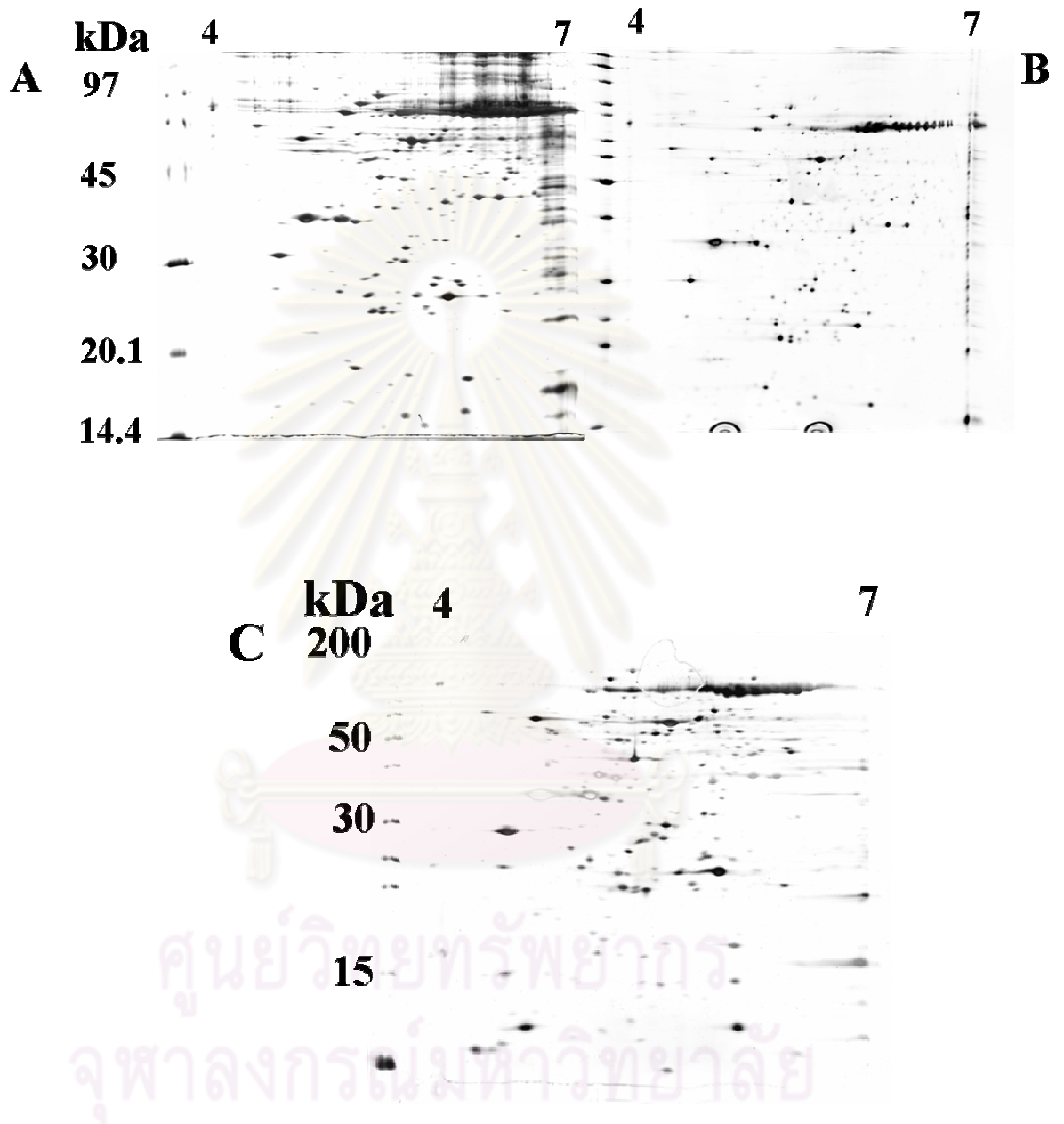
Figures 3.7 Protein profiles of stage III ovaries of wild *P. monodon* broodstock analyzed by 2D gel electrophoresis. Total proteins from two individuals (panels A and B, GSI = 5.75% and panel C, GSI = 5.91%) were electrophoretically analyzed in Immobiline Drystrip gels (pH 4-7) followed by 12.5% SDS-PAGE and silver-stained.



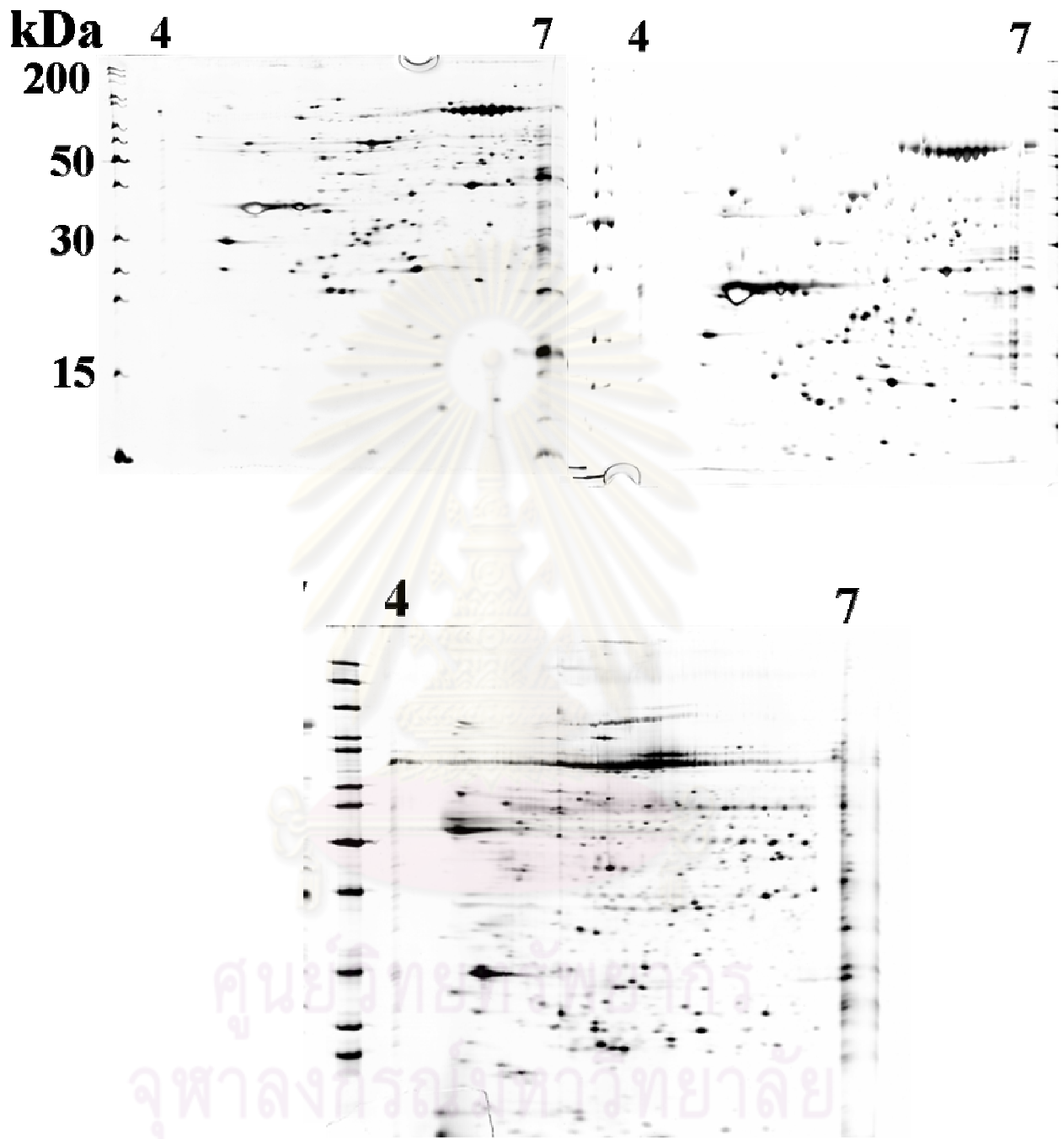
Figures 3.8 Protein profiles of stage IV ovaries of wild *P. monodon* broodstock analyzed by 2D gel electrophoresis. Total proteins from two individuals (panels A and B, GSI = 7.32% and panel C, GSI = 11.66%) were electrophoretically analyzed in Immobiline Drystrip gels (pH 4-7) followed by 12.5% SDS-PAGE and silver-stained.



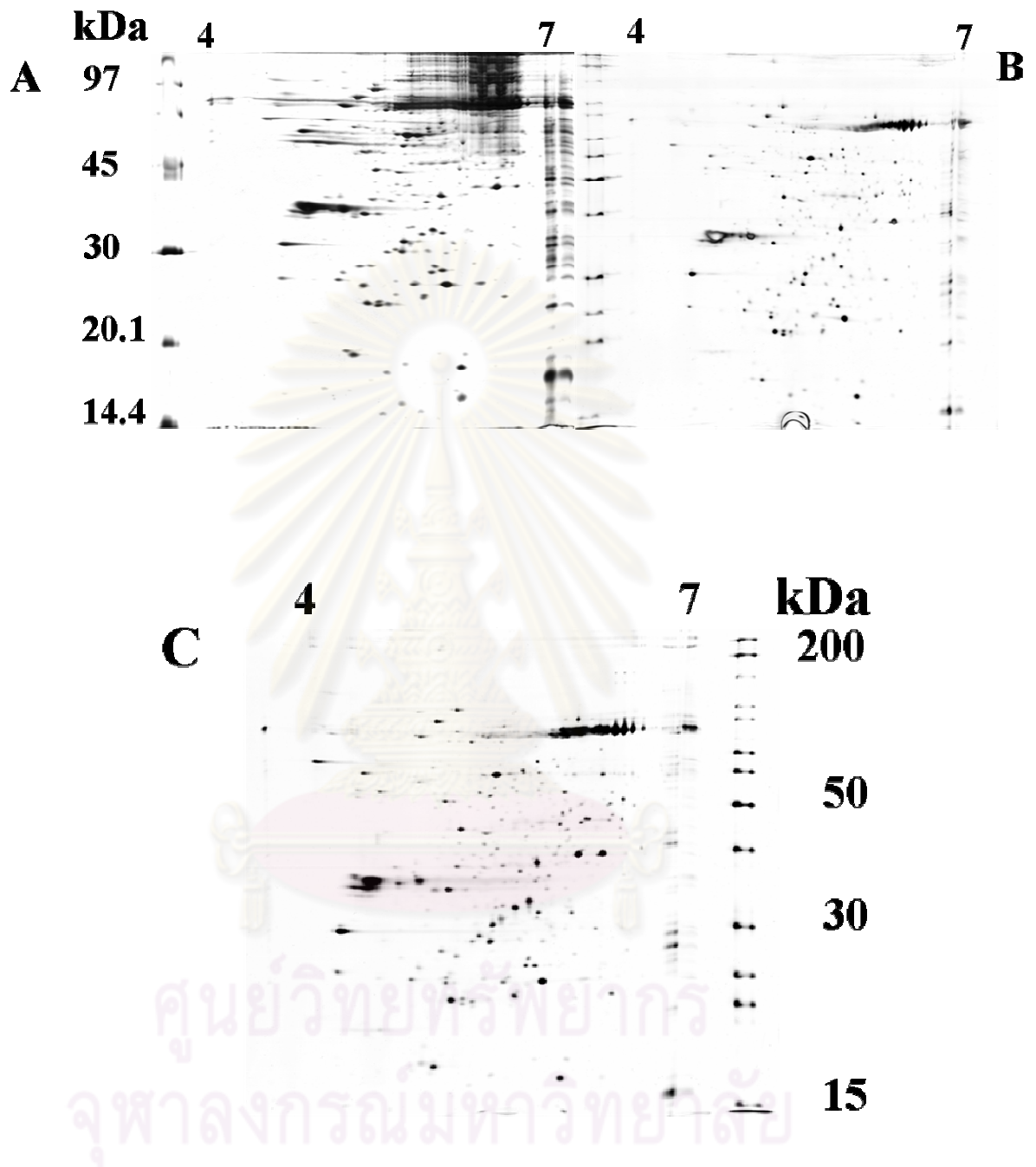
Figures 3.9 Protein profiles of stage I ovaries of eyestalk-ablated wild *P. monodon* broodstock analyzed by 2D gel electrophoresis. Total proteins from two individuals (panels A and B, GSI = 0.76% and panel C, GSI = 0.90%) were electrophoretically analyzed in Immobiline Drystrip gels (pH 4-7) followed by 12.5% SDS-PAGE and silver-stained.



Figures 3.10 Protein profiles of stage II ovaries of eyestalk-ablated wild *P. monodon* broodstock analyzed by 2D gel electrophoresis. Total proteins from two individuals (panels A and B, GSI = 1.69% and panel C, GSI = 1.23%) were electrophoretically analyzed in Immobiline Drystrip gels (pH 4-7) followed by 12.5% SDS-PAGE and silver-stained.



Figures 3.11 Protein profiles of stage III ovaries of eyestalk-ablated wild *P. monodon* broodstock analyzed by 2D gel electrophoresis. Total proteins from two individuals (panels A, GSI = 5.75%, B, GSI = 5.08% and panel C, GSI = 4.85%) were electrophoretically analyzed in Immobiline Drystrip gels (pH 4-7) followed by 12.5% SDS-PAGE and silver-stained.



Figures 3.12 Protein profiles of stage IV ovaries of eyestalk-ablated wild *P. monodon* broodstock analyzed by 2D gel electrophoresis. Total proteins from two individuals (panels A and B, GSI = 6.87% and panel C, GSI = 6.92%) were electrophoretically analyzed in Immobiline Drystrip gels (pH 4-7) followed by 12.5% SDS-PAGE and silver-stained.

3.2 Characterization of ovarian proteins of *P. monodon* by mass spectrometry

3.2.1 MALDI-TOF/TOF

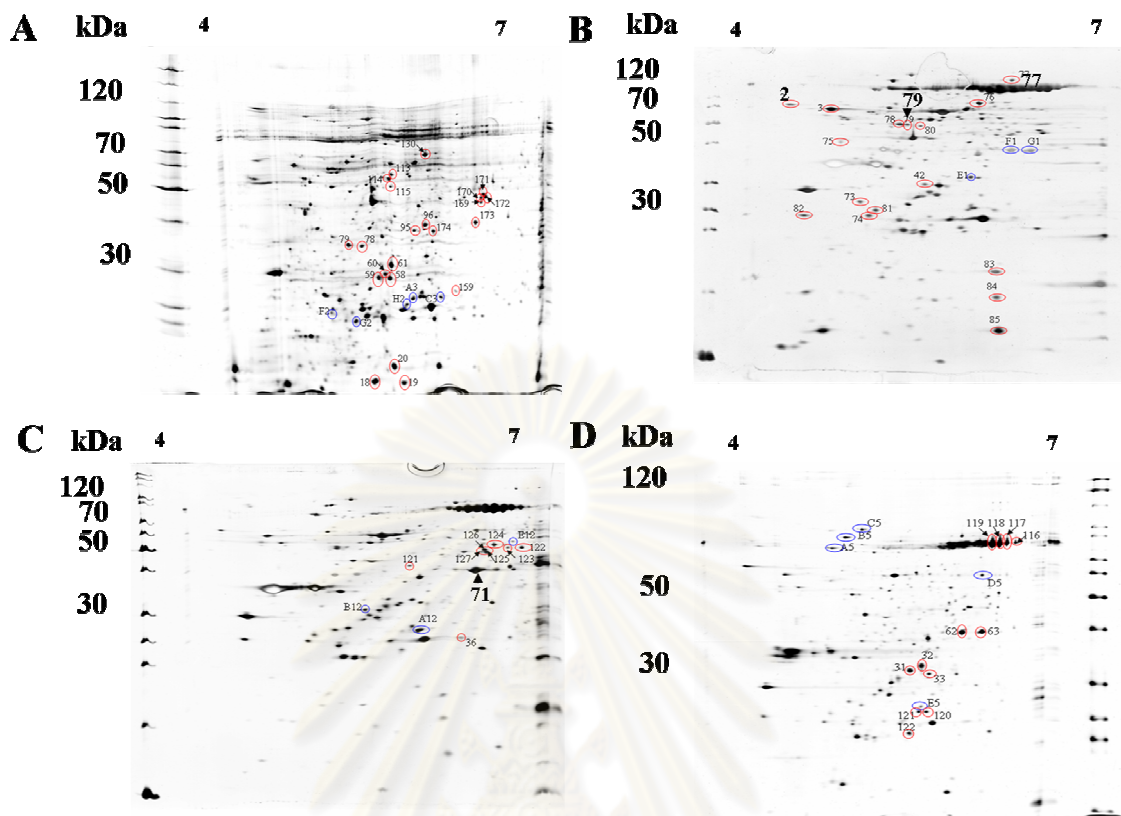
Understanding mechanisms and functions of genes and proteins in ovaries would provide a new tool for breeding programmes and for understanding of the important biological and molecular processes in *P. monodon*.

Initially, protein spots in different ovarian stages of normal and eyestalk-ablated broodstock were characterized MALDI-TOF/TOF (Figures 3.13 and 3.14). Quantitative analysis between proteins showing identical *pI* and MW cannot be precisely estimated from silver-stained protein electrophoresis. Therefore, proteins that were present or absence in the same ovarian stages of normal and eye-stalk-ablated broodstock were analyzed for peptide mass fingerprint (PMF) using MALDI-TOF. Protein spots that exhibit a parent ion with molecular mass greater than 1000 dalton were further analyzed for peptide fragmentation by MALDI-TOF/TOF

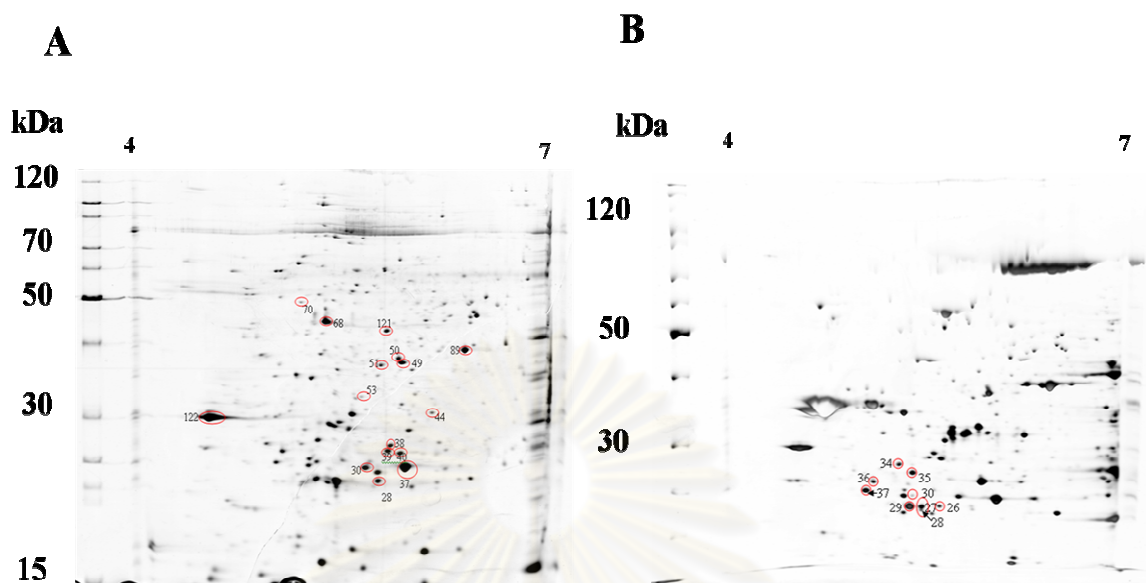
In total, 35 protein spots were used to analyzed the PMF and 90 protein spots were analyzed for peptide fragmentation. All proteins analyzed by PMF did not match previously deposited sequences in the database. Only peptide spectrum of 4 protein spots significantly matched deposited sequences (Table 3.1). Results of peptide mass fingerprints on examined protein spots are shown in Appendix A.

The protein spot numbers 2, 76 and 79 found in stage II ovaries of eyestalk-ablated broodstock was significant similarity to calreticulin of *Galleria mellonella* (score = 69), transketolase of *Apis mellifera* (score = 77) and protein disulfide isomerase A6 of *Tribolium castaneum* (score = 135). In addition, the protein spot no. 71 found in stage III ovaries of eyestalk-ablated broodstock significantly match allergen pen m2 of *Peneaus monodon* (score = 57) (Table 3.1).

Changes in cytosolic calcium (Ca^{2+}) concentration affect many essential cellular responses. Calreticulin (CRT) plays the crucial role in many cellular processes including Ca^{2+} storage and release, protein synthesis, and molecular chaperone activity (Michalak et.al., 1999).



Figures 3.13 Protein profiles of stage I (A), II (B), III (C) and IV (D) ovaries of unilaterally eyestalk-ablated *P. monodon* broodstock analyzed by two-dimensional gel electrophoresis (IEF of pH 4-7 followed by 12.5% SDS-PAGE). Protein spots that were further analyzed by mass spectrometry MALDI-TOF/TOF) are illustrated by red open circles for those exhibited a trend of differential expression and by blue open circles for those present in eyestalk-ablated shrimp but not in normal shrimp.



Figures 3.14 Protein profiles of stage I (A) and IV (B) ovaries of wild *P. monodon* broodstock analyzed by two-dimensional gel electrophoresis (IEF of pH 4-7 followed by 12.5% SDS-PAGE). Protein spots that were further analyzed by MALDI-TOF/TOF mass spectrometry (PMF and/or peptide fragmentation) are illustrated by red open circles for those exhibited a trend of differential expression and by blue open circles for those present in eyestalk-ablated shrimp but not in normal shrimp.

Table 3.1 Protein spots identified by MALDI -TOF/TOF

stage	Spot no.	Protein name	% coverage	score	Species matched	Dif (fold)/ Present
II	2	Calreticulin	9	69	<i>Galleria mellonella</i>	Absent
	76	Transketolase	7	77	<i>Apis mellifera</i>	-
	79	Protein disulfide isomerase	6	62	<i>Tribolium castaneum</i>	-
III	71	Allergen pen m 2	5	57	<i>Peneaus monodon</i>	-

Dif (fold) = differential expression and the fold change >1.5 is regarded as upregulation, < 0.67 = down regulation, - = comparable protein levels, Absent = proteins that were found in stage II ovaries of eyestalk-ablated broodstock but not in same stage of normal broodstock.

Protein disulfide isomerase A6 (also called PDI P5 or CaBP1) plays an important role in rearrangement of both intra-chain and inter-chain disulfide bonds, where it catalytically acts to both initiate and reduce disulfide bonds. It has been proposed that the cell surface PDI acts as a reductase cleaving the disulfide bound of proteins attached to the cell surface. It may also control function of certain extracellular proteins by regulating their redox states (Goplen et al., 2006).

Transketolase (TKT) is an enzyme in the nonoxidative branch of the pentose phosphate pathway. TKT catalyzes the reversible transfer of a two-carbon ketol unit from a ketose to aldose, and, together with transaldolase, provides a link between the pentose phosphate and the glycolytic pathway (Langbein et al., 2006 and Salamon et al., 1998).

Allergen pen m 2 (also called arginine kinase, AK) is a phosphotransferase that plays a critical role in energy metabolism in invertebrates. It catalyzes the reversible phosphorylation of arginine by Mg-ATP to form phosphoarginine and Mg-ADP. Phosphoarginine functions as ATP buffers, permitting maintenance of high ATP values during periods of cellular activity in invertebrates (Cui-Luan et al., 2009).

Basically, peptides mass fingerprinting was more suitable for species that a large number of known protein sequences is available. Nevertheless, results from mass spectrometry in this study were compared to the local shrimp EST database (<http://www.matrixscience.com>) and this database contained translated 40,001 deduced proteins. MALDI-TOF/TOF indicated only 4 matched proteins. This indicated that more sensitive techniques and/or more numbers of ESTs are required. It is rather difficult to increase a larger number of *P. monodon* ESTs because additional cost on library construction and sequencing are needed. Accordingly, a more sensitive technique like nanoLC-MS/MS was applied for sequencing of ovarian proteins of *P. monodon*. Sequence similarity search was then carried out using the local shrimp EST database, MASCOT software, SWIT-PROT and NCBI databases

3.2.2 NanoLC-MS/MS

Total proteins extracted from stages II and IV of normal and eyestalk-ablated broodstock were analyzed by 2-DE. A total of 675 protein spots were characterized including 215 and 160 spots from stages II and IV of normal broodstock and 180 and 120 spots from those of eyestalk-ablated broodstock, respectively (Figures 3.15-3.18).

Of these, 90 and 58 protein spots accounting for 41.86 and 36.25% of the respective ovarian stages of normal broodstock significantly matched previously deposited sequences in the databases. In the eyestalk-ablated broodstock, 95 and 79 protein spots accounting for 52.77 and 65.83% of the respective ovarian stages were regarded on homologues of known proteins (Tables 3.2 and 3.3).

Large numbers of unknown proteins were found in ovaries of both normal (125 and 102 accounting for 58.14 and 63.75% for stages II and IV ovaries) and eyestalk-ablated (85 and 41 accounting for 47.27 and 34.17%) *P. monodon* broodstock (Tables 3.2 and 3.3).

Several different protein families were characterized. Protein associated with cellular function such as protein disulfide isomerase, Rab3 GTPase-activating protein, valosin containing protein, Ubiquitin carboxyl-terminal hydrolase L5-like protein, transketolase, transaldolase. Triose-phosphate isomerase, G3PDH, F1-ATP synthase and isocitrate dehydrogenase 2 (NADP⁺) which play an important role on energy production and catabolism were identified. Moreover, several cellular structure proteins such as β -actin and β -tubulin-1 were also characterized. Sacroplasmic reticulum-calcium binding protein and hemocyanin functionally involved in Ca²⁺ homeostasis and oxygen transportation were also identified, respectively.

3.3 Comparative analysis of protein from different stages of *P. monodon* ovaries

Proteome profiles of different ovarian stages of normal and eyestalk-ablated broodstock were compared in order to identify proteins that play an important role on ovarian development of *P. monodon*. A trend of expression levels was also considered

from the intensity of homologous protein spots from the same developmental stages among different 2-DE gels.

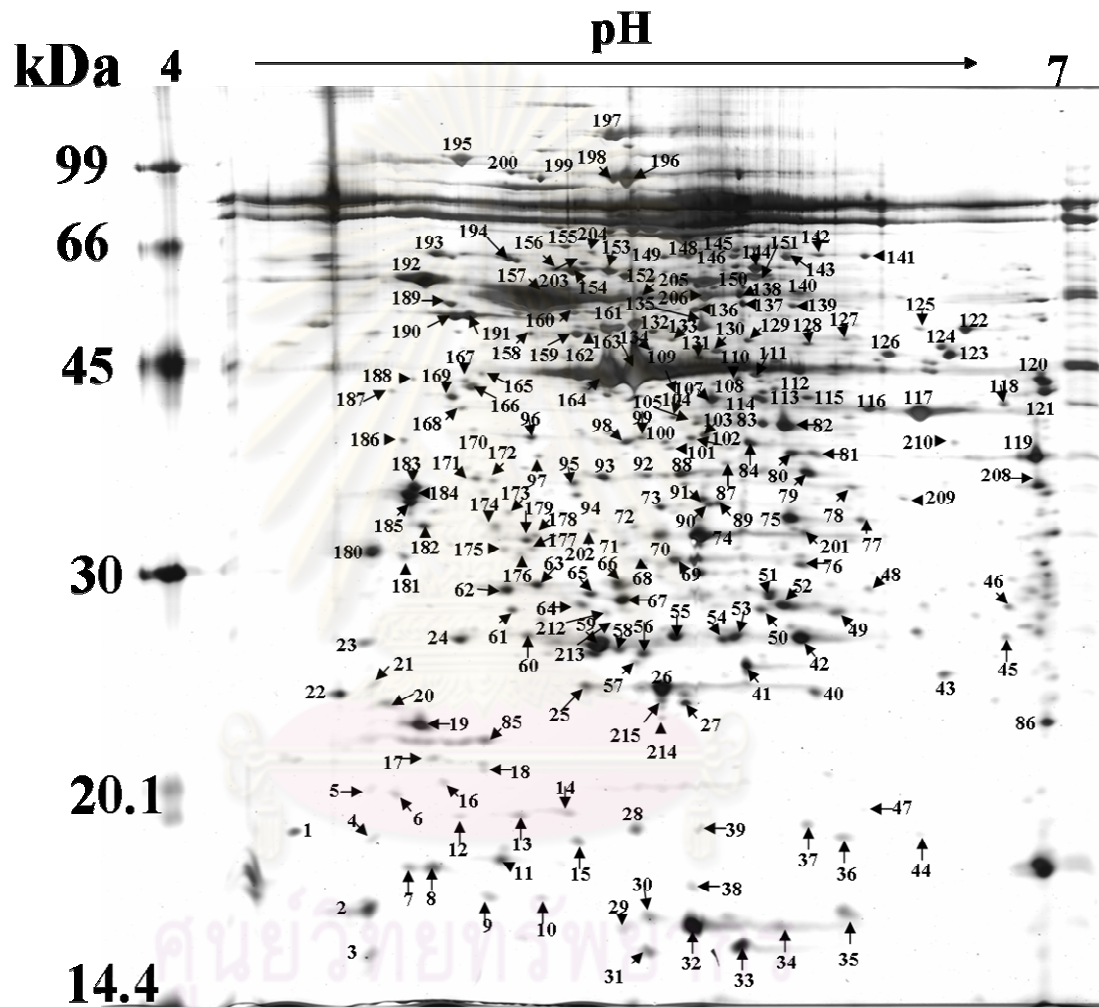


Figure 3.15 Protein profiles of stage II ovaries of wild *P. monodon* broodstock analyzed by two-dimensional gel electrophoresis (IEF of pH 4-7 followed by 12.5% SDS-PAGE). Numbers indicate protein spots that were identified by nanoLC-MS/MS.

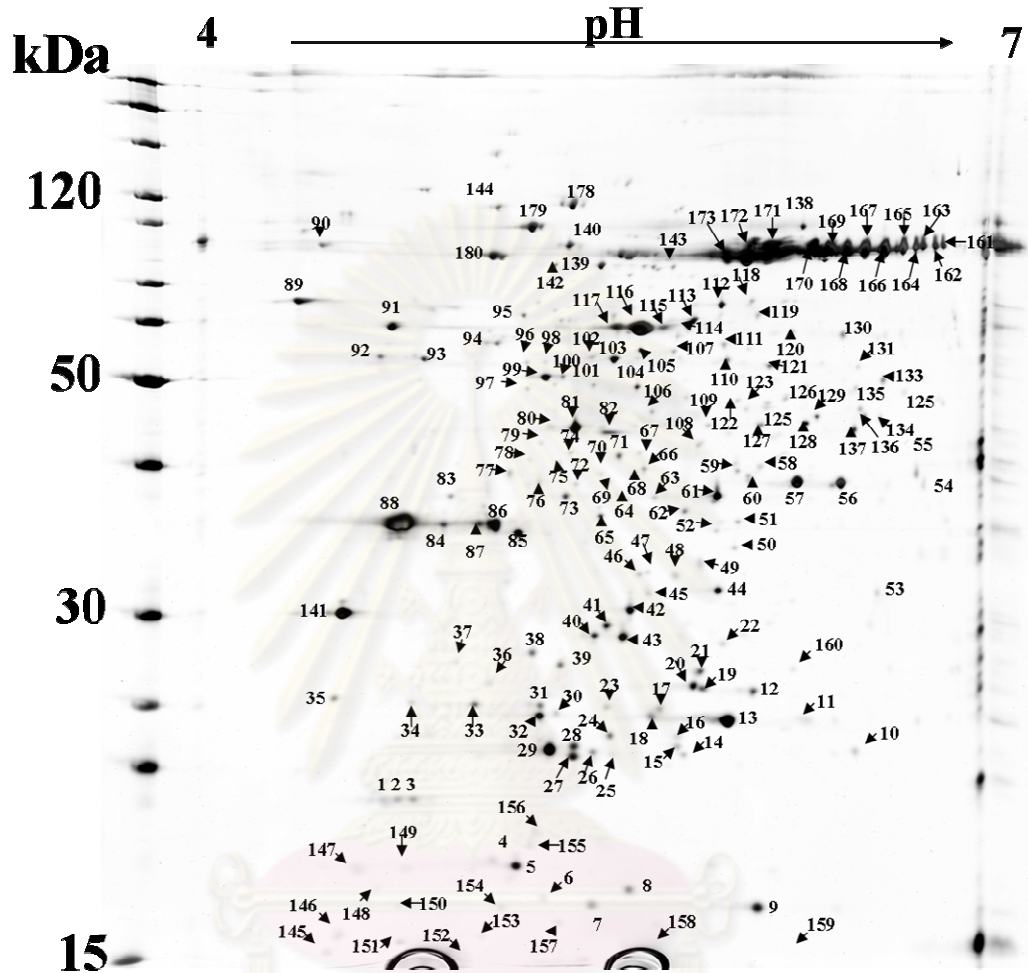
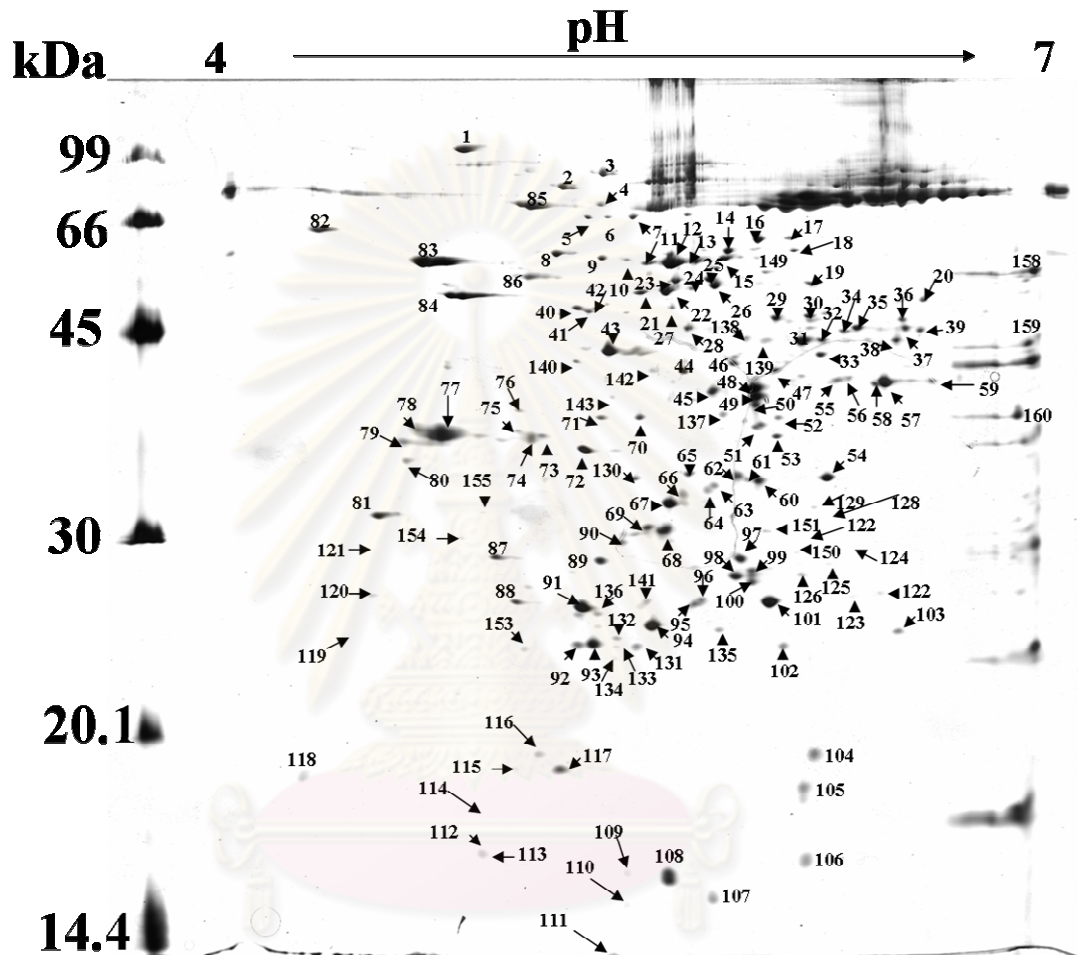


Figure 3.16 Protein profiles of stage II ovaries of eyestalk-ablated *P. monodon* broodstock analyzed by two-dimensional gel electrophoresis (IEF of pH 4-7 followed by 12.5% SDS-PAGE). Numbers indicate protein spots that were identified by nanoLC-MS/MS.



ศูนย์วิทยทรัพยากร
จุฬาลงกรณ์มหาวิทยาลัย

Figure 3.17 Protein profiles of stage IV ovaries of wild *P. monodon* broodstock analyzed by two-dimensional gel electrophoresis (IEF of pH 4-7 followed by 12.5% SDS-PAGE). Numbers indicate protein spots that were identified by nanoLC-MS/MS.

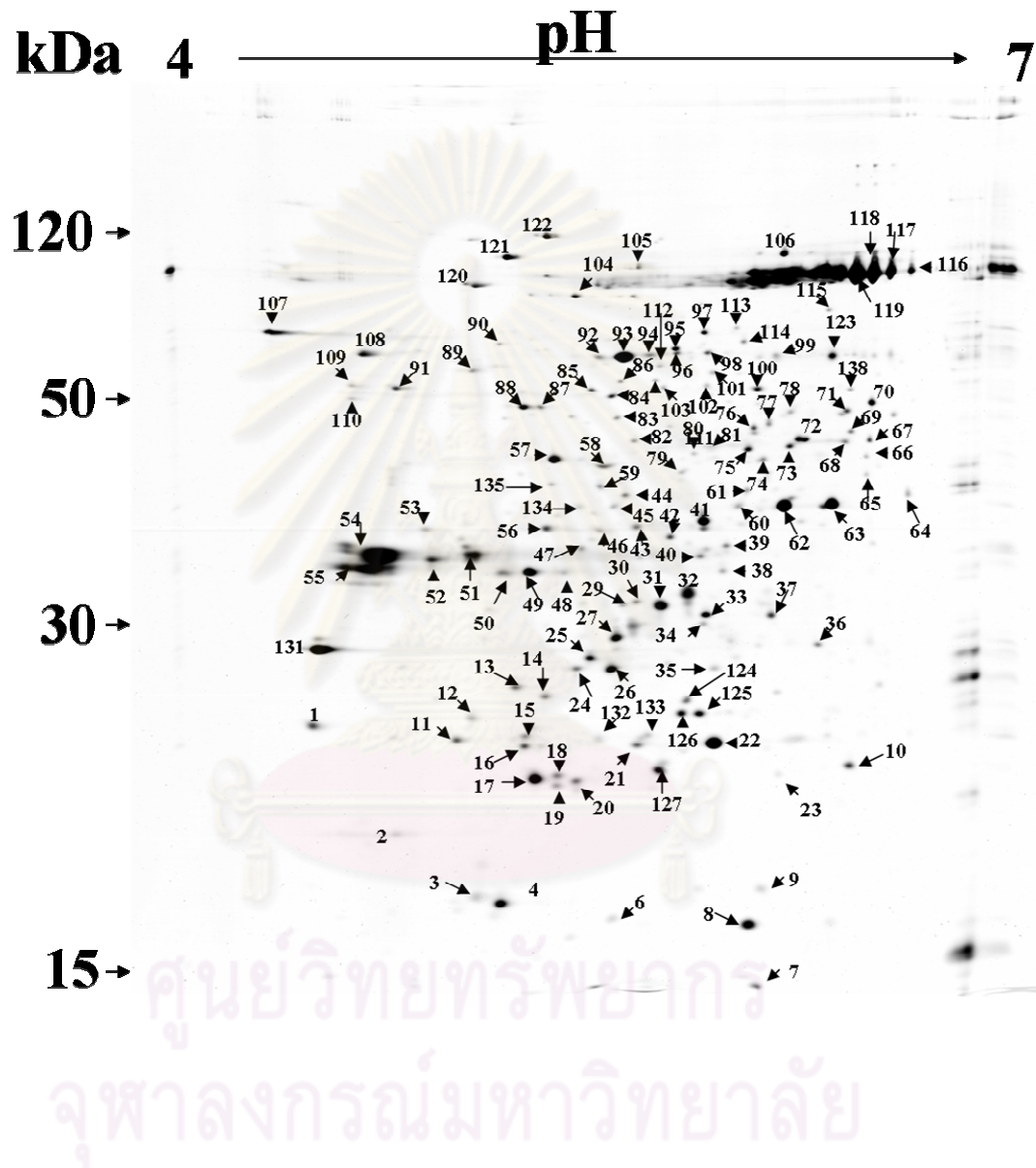


Figure 3.18 Protein profiles of stage IV ovaries of eyestalk-ablated *P. monodon* broodstock analyzed by two-dimensional gel electrophoresis (IEF of pH 4-7 followed by 12.5% SDS-PAGE). Numbers indicate protein spots that were identified by nanoLC-MS/MS.

3.3.1 Stages II and IV ovaries of normal broodstock

Proteins expressed stages II and IV ovaries of normal broodstock were compared. No protein showed upregulation patterns during ovarian development. However, 21 known proteins were down-regulated. These included several unknown proteins and cyclic AMP-regulated protein like protein, cofilin/actin-depolymerizing factor, CG10527-like-methyltransferase, glutathione-*s*-transferase, glutathione peroxidase, 2-cys thioredoxin peroxidase, proteasome subunit α type 5, cytosolic manganese superoxide dismutase, alcohol dehydrogenase, β -actin, chaperonin containing TCP1 subunit 2, tubulin beta-1 chain (Table 3.2)

Cofilin/actin-depolymerizing factor is a member of an actin dynamizing protein (ADF) family. Proteins of this family play a critical role in rapid adaptation of the actin cytoskeleton to localized cellular function. The activation of ADF/cofilin is essential for cell motility and polarized cell migration. ADF/cofilin plays an essential role in both the actin polymerization and depolymerization processes during cell movement (Zhao et al., 2008).

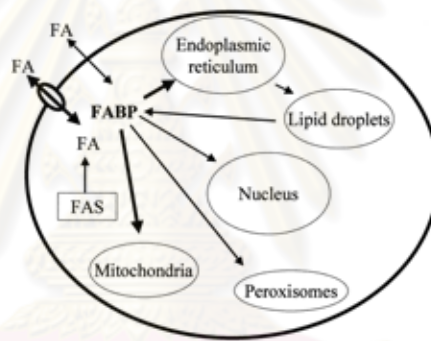
Superoxide dismutases (SODs) are metalloproteins that catalyse the dismutation of superoxide radicals to oxygen and hydrogen peroxide. The enzyme has been found in all aerobic organisms examined, where it plays a major role in the defense against toxic reduced oxygen species which are generated in many biological oxidations (Brouwer et al., 2003).

A total of 57 proteins, for example; translocation protein TolB, translationally controlled tumor, intracellular fatty acid (LP-N-S01-0246-LF), glutathione peroxidase, 2-cys thioredoxin, arginine kinase, phosphoglycerate kinase and NADH-specific isocitrate dehydrogenase did not expressed differentially during ovarian development of normal *P. monodon*.

Phosphoglycerate kinase (PGK) is an enzyme in the Embden-Meyerhof-Parnas pathway of glycolysis, PGK catalyzes the reversible conversion of 1,3-bisphosphoglycerate to 3-phosphoglycerate coupled to phosphorylation of ADP to ATP (Eikmanns et al., 1992).

NAD-dependent isocitrate dehydrogenase in eukaryotic organisms is a key enzyme in the cellular energy metabolism. The oxidative decarboxylation of isocitrate is an important control point for flux through the tricarboxylic acid cycle (Zhao et al., 1996).

Several classes of functions have been proposed for the fatty acid binding proteins. These are broadly described as modulation of specific enzymes for lipid metabolic pathway (either anabolic or catabolic), maintenance of cellular membrane fatty acid level and regulation of expression of fatty acid responsive genes. Intracellular transport of long chain fatty acid illustrated in Figures 3.19 (Storch et al., 2000).



Figures 3.19 Diagram illustrating intracellular transportation of long-chain fatty acids. Influx and/or efflux of fatty acids across the plasma membrane takes place by either protein-mediated or diffusive processes. Cytosolic transport to, or from, various intracellular organelles, including mitochondria, endoplasmic reticulum, peroxisomes, nucleus and lipid droplets, may be mediated by the FABPs. Abbreviations: FA: fatty acid; FABP: fatty acid-binding protein; FAS: fatty acid synthetase (Storch et al., 2000).

A large number of proteins (111 proteins), for example; sarcoplasmic Ca^{2+} binding protein, α B and A chain, intracellular fatty acid (LP-N-N01-0788-LF), beta actin, beta thymosin, adenosine kinase, phosphopyruvate hydratase, methylmalonate semialdehyde dehydrogenase and F1-ATP synthase beta subunit (52500/4.90), were

present in stage II ovaries but not in mature ovaries (stage IV). On the other hand, 64 proteins, for example; protein disulfide isomerase (55000/5.5), mitochondrial aldehyde dehydrogenase, L-3-hydroxyacyl coenzyme A dehydrogenase, trios-phosphate isomerase, secreted inorganic pyrophosphatase, HAD family hydrolase, vitellogenin and putative conjugal transfer protein, were observed in mature ovaries but not at the stage II

An example of protein successfully identified in eyestalk-ablated shrimp is trios-phosphate isomerase (TPI) which is an enzyme in the Embden-Meyerhof-Parnas pathway of glycolysis. TPI is responsible for the reversible isomerization of dihydroxyacetone-phosphate and glyceraldehydes-3-phosphate.

Additionally, secreted inorganic pyrophosphatase involved in one or more steps in a wide variety of biochemical pathways that lead to most of the biosynthesis of proteins, lipids, phospholipids, nucleotides and nucleic acids, urea, steroid, structural polysaccharides and glycogen was detected.

3.3.2 Stages II and IV ovaries of eyestalk-ablated broodstock

Unlike normal broodstock, 8 proteins including glutathione peroxidase, protein disulfide isomerase (60000/5.70), histidine-rich glycoprotein precursor, PDI (60000/4.8), hypothetical protein, unnamed protein product and two unknown proteins were up-regulated during ovarian development of eyestalk-ablated broodstock. Sixteen protein spots including nucleoplasmin isoform 1-like protein, eukaryotic initiation factor 5A, CG10527-like methyltransferase, Rab3 GTPase-activating protein, hydroxyacyl glutathione hydrolase, beta thymosin (22000/5.4), arginine kinase, 26s proteasome regulatory subunit 7, isocitrate dehydrogenase 2 (NADP⁺, peroxiredoxin 4, es1 protien, proteasome subunit α type, unknown protein, D-lactate dehydrogenase, rab gdp-dissociation inhibitor and PDI (60000/5.75) revealed a trend of differential expression during ovarian development of *P. monodon* (Table 3.3).

Rab3 GTPase-activating protein is a member of the Rab protein family (which belong to the Ras family of small G proteins). Rab proteins are prime regulators of

vesicular membrane transport in both the exocytic and endocytic pathways. The active form of Rab proteins have multiple functions in cargo selection and as scaffolds for the sequential assembly of effectors required for vesicle budding, cytoskeletal transport, and target membrane fusion (Irene et al., 2006). The four members of Rab3 subfamily (Rab3A, Rab3B, Rab3C and Rab3D) have been implicated in regulated exocytosis of neurotransmitters and hormones (Takai et al., 1996; Schluter et al., 2002; Li and Chain 2003; Sudhof. 2004). The activity of Rab3 protein is tightly regulated by RabGDI (GDP dissociation inhibitor), Rab3GEP, and Rab3GAP. The latter two determine the balance of active (GTP) to inactive (GDP) forms and Rab3GAP specifically converts active Rab3-GTP to the inactive-GDP form (Fukui et al., 1997).

D-lactate dehydrogenase (d-LDH) is an enzyme catalyzing the oxidation of d-lactate to pyruvate, which is coupled to transmembrane transport of amino acids and sugars. D-lactate dehydrogenase (d-LDH) of *E. coli* is a peripheral membrane respiratory enzyme involved in electrontransfer, located on cytoplasmic side of the inner cell membrane (Dym et al., 2000).

Examples of proteins that were downregulated during ovarian development were hydroxyacyl glutathione hydrolase and beta thymosin. These proteins involved in the multiple aspects of cellular events including neuritogenesis, angiogenesis, migration, metastasis and apoptosis.

Hydroxyacyl glutathione hydrolase (glyoxalase II) hydrolases *S*-D-lactoylglutathione to D-lactate and hence generates glutathione-*s*-transferase (GSH). Glyoxalase II is a member of the zinc metallohydrolase family having a β -lactamase fold. It has broad substrate specificity for glutathione thiol ester, hydrolyzing a member of these species (beside *S*-D-lactoylglutathione) to their corresponding carboxylic acids and reduced glutathione (Cordell et al., 2004).

A total of 69 proteins, for example; glutathione peroxidase, trios-phosphate isomerase, proteasome subunit beta type I, glutathione-*s*-transferase, cytosolic

superoxide dismutase, aldo-keto reductase, beta actin and careticulin were comparably expressed during ovarian development of normal *P. monodon*.

Aldo-keto reductase enzymes comprise a functionally diverse gene family which catalyzes the NADH-dependent reduction of a variety of carbonyl compounds such as sugars, glucuronate, curtain aldehyde metabolites derived from the biogenetic amines and corticosteroid hormones as well as xenobiotic aldehydes and ketones (Bohren et al., 1989).

Proteasome subunit beta type I was characterized by proteomic studies. Proteasome are highly complex protease responsible for selective protein degradation in eukaryotic cells. The 26S proteasome consists of two regulatory 19S cap complexes and 20S proteasome, which acts as the proteolytic or module subunit. The 26S proteasome degrades ubiquitinated proteins in an ATP-dependent reaction, whereas 20S proteasome alone does not exhibit that activity. It is thought that the 19s cap complexes of the 26S proteasome, which consist of ATPase, are associated with various cellular activities and non-ATPase subunits are recognition, unfolding and transport of a substrate protein to the proteolytically active 20S core (Gueckel et al., 1998).

Seventy-nine proteins, for example; beta NAC-like protein, alcohol dehydrogenase, heterogeneous nuclear ribonucleoprotein, Epa4p, ovarian peritrophin, cysteine protease, L-3-hydroxyacyl-coenzyme A dehydrogenase and heat shock protein 21.4, were present in stage II ovaries but not in mature ovaries (stage IV). In contrast, 34 proteins, for example; glyoxylase 1, transaldolase, RAN binding protein, phosphoglycerase kinase, cytosolic NADP-dependent isocitrate dehydrogenase, Tat-binding protein 7, Fah-prov protein and vitellogenin, were observed in mature ovaries but not at the stage II ovaries.

Beta-NAC-like protein involves metabolism of N-acetyl-L-cysteine (NAC). The free radical scavenger, NAC, is used clinically for a broad spectrum of indications including mucolysis, detoxification after acetaminophen poisoning, adult respiratory distress syndrome (ARDS), hyperoxia-induced pulmonary damage, HIV

infection, cancer, and heart disease (Pajonk et al., 2001). Free radicals are critical in the determination of protein structure, regulation of enzyme activity, protein phosphorylation, and control of transcription factor activity (Pajonk et al., 2001).

The nuclear accumulation of proteins containing nuclear localization signals requires the Ran GTPase and a complex of proteins assembled at the nuclear pore. RanBP1 is a cytosolic Ran-binding protein that inhibits RCC1-stimulated release of GTP from Ran GTPase. RanBP1 also promotes the binding of Ran GTPase to karyopherin β (also called importin β and p97) and is a co-stimulator of RanGAP activity. RanBP1 and karyopherin β interact with distinct sites of Ran GTPase suggesting that RanBP1 plays an essential role in nuclear transport by permitting RanGAP-mediated hydrolysis of GTP on Ran complexes to karyopherin β (Lounsbury et al., 1997).

Heterogeneous nuclear ribonucleoprotein (hnRNPs) is RNA-binding proteins involved in RNA processing, an essential step for control of mammalian gene expression (Shin, K. et al., 2008). Glutathione peroxidase is antioxidant enzyme plays an important role in scavenging H_2O_2 and lipid hydroperoxide function in detoxifying lipid by-product.

Generally, protein successfully identified in eyestalk-ablated shrimp included enzymes in the glycolytic pathway and amino acid metabolism, protein involved in cellular structure and functions. Stress-related proteins were also identified and characterized. Some proteins such as glutathione peroxidase, trios-phosphate isomerase, β -actin and protein disulfide isomerase were existent in multiple spots. This may resulted from more posttranslational modification of these proteins.

3.3.3 Stages II ovaries of normal and eyestalk-ablated *P. monodon* broodstock

Protein profiles of stage II ovaries of normal and eyestalk-ablated *P. monodon* were compared to identify key proteins that responded to induction of ovarian development by eyestalk ablation.

Twelve proteins including trios-phosphate isomerase, unnamed protein product, unknown protein, ubiquitin carboxyl terminal hydrolase L5-like protein, 26s proteasome non ATPase-regulatory isoform A subunit, allergen pen m2, phosphopyruvate hydratase, phosphoglycerate kinase, adenosylhomocysteinase, beta actin, unknown protein and F1-ATP synthase beta subunit were up-regulated. Trios-phosphate isomerase and phosphopyruvate hydratase functionally involved energy production and catabolism (Table 3.4).

In contrast, 26 proteins for example, chaperonin containing TCP1 subunit 5, arginine kinase, carbonic anhydrase, hypothetical protein, beta NAC-like protein and peroxiredoxin 4 were down-regulated.

Chaperonin containing TCP1 subunit 5, a member of the chaperonin family of molecular chaperones, binds to newly synthesized or denatured proteins and facilitates folding in an ATP-dependent reaction cycle (Hynes et al., 1996).

Carbonic anhydrase (or carbonate dehydrogenase) catalyze the rapid conversion of carbon dioxide to bicarbonate and proteins, a reaction that occurs rather slowly in the absence of a catalyst. The active site of most carbonic anhydrase contains a zinc ion; they are therefore classified as one of the metalloenzymes. The primary function of this enzyme in animal is to interconvert carbon dioxide and bicarbonate to maintain acid-base balance in blood and other tissues, and to facilitate transport carbon dioxide out of tissues (Khalifah et al., 1970).

Peroxiredoxin 4 has recently been regarded as a new family of thiol-specific antioxidant protein. Peroxiredoxins perform their protective antioxidant role in cells through their peroxidase activity whereby hydrogen peroxide, peroxynitrite and wide range of organic hydroperoxides are reduced and detoxified (Giguere et al., 2007).

Expression of 29 proteins, for example, beta thymosin, adenosine kinase, spermatogonial stem cell renewal factor, vitellogenin precursor, NADH-specific isocitrate dehydrogenase, cytosolic manganese superoxide dismutase, proteasome subunit α type, glutathione peroxidase, glutathione-s-transferase and aldo-keto reductase, were comparable expressed during ovarian development of *P. monodon*.

Interestingly, 120 proteins were present in stage II ovaries of normal shrimp but not in those of eyestalk-ablated shrimp and 106 proteins were present in the opposite direction (Table 3.4).

Adenosine kinase (adenosine 5'-phosphotransferase) catalyzes the phosphorylation of adenosine to its monophosphate form. Purified adenosine kinase enzymes from several sources have been shown to possess broad substrate specificities. Because of this important property the enzyme has been implicated in the phosphorylation of many potentially pharmacologically active purine nucleotide analogs (Datta et al., 1986).

The reactive oxygen species (ROS) and reactive oxygen intermediates (ROI) are produced during normal aerobic metabolism and increased in physiological conditions that resulted in oxidative stress and during defense reactions. ROI and ROS are rapidly eliminated by antioxidant enzymes, such as superoxide dismutase (SOD), catalase, glutathione peroxidase, glutathione reductase, glutaredoxin, thioredoxin reductase, etc. SOD detoxifies superoxide radical by converting the substrate to hydrogen peroxide and oxygen. Hydrogen peroxide is then transformed to water and oxygen by catalase, resulting in innocuous compounds to cells (Gomez-Anduro et al., 2006).

3.3.4 Stages IV ovaries of normal and eyestalk-ablated *P. monodon* broodstock

Characterization of proteins expressed in mature ovaries of normal and eyestalk-ablated *P. monodon* broodstock revealed that 11 protein spots were upregulated. They are carbonic anhydrase, electron transfer flavoprotein, Epa4p, es1 protein, glutathione peroxidase, Rab3 GTPase-activating protein, CG10527-like methyltransferase, unnamed protein product and hypothetical protein and two unknown proteins.

Electron transfer flavoprotein (ETF), a soluble protein located in the mitochondrial matrix, plays a crucial role in the β -oxidation of fatty acids and the oxidative demethylation reaction of mitochondrial 'one-carbon cycle' by coupling

several flavoprotein dehydrogenase to the electron transport system (Husain et al., 1982).

Methyltransferase is a transferase enzyme which transfers a methyl group from a donor to an acceptor. Often methylation occurs on nucleic bases in DNA or amino acids in protein structures. DNA methylation may be necessary for normal growth from embryonic stages in mammals. Site-specific methyltransferases have the same DNA target sequences as certain restriction enzymes. Methylation can also serve to protect DNA from enzymatic cleavage, since restriction enzymes are unable to bind and recognize externally modified sequences (<http://en.wikipedia.org/wiki/Methyltransferase>).

Six protein spots including protein disulfide isomerase (6500/5.6), cytosolic manganese superoxide dismutase, mitochondrial aldehyde dehydrogenase, protein disulfide isomerase (53500/5.7), acyl coenzyme A dehydrogenase and glutathione-*s*-transferase were downregulated (Table 3.5).

The glutathione-*s*-transferase (GST) enzymes are the best known for their role in detoxification of various exogenous compounds. These enzymes catalyze the nucleophilic attack of the thiol group of GSH, γ -glutamylcysteinylglycine, at an electrophilic site of the second substrate. This reaction most frequently results in the covalent linkage of GSH to the second substrate, yielding a GSH conjugate, which generally less toxic than the parent compound (Irzyk et al., 1993).

Acyl-coA dehydrogenases are a class of enzymes which function to catalyze the initial step in each cycle of fatty acid α , β -dehydrogenation in the mitochondria of cells and transfer electron to electron transfer flavoprotein (Nagao et al., 1993). Their action results in the introduction of a trans double-bond between C2 and C3 of the acyl-coA thioester substrate. FAD is a required co-factor in the mechanism in order for the enzyme to bind to its appropriate substrate.

Table 3.2 Characterized protein spots in stage II and IV ovaries of normal *P. monodon* broodstock**Table 3.2** Characterized protein spots in stage II and IV ovaries of normal *P. monodon* broodstock (cont.)

Spot no.		Protein name II/IV	Clone no.	gi II/IV	Observed Mr (Da)/pI II/IV	Calculated Mr (Da)/pI II/IV	Masscot Score II/IV	Dif(fold) / Present
Stages II	Stages IV							
1	118	Unknown/ unknown						0.1
2	114	Unknown/ unknown						-
3	113	unknown/ unknown						0.02
4		Polymerase (RNA) II(DNA direct) polypeptide	LP-V-S01- 0409-LF	000199976	18000/4.5	20600/8.48	85	Present
5		Unknown						Present
6		Unknown						Present
7	115	Unknown/ Translocation protein Tol B		13473330	18500/5.0	47651/6.69	71	-
8		Unknown						Present
9		Unknown						Present
10		Unknown						Present
11	117	Cyclic AMP-regulated protein like protein/ unknown	AG-N-N01- 0644-W	0000002809	18000/5.0	27711/6.15	286	0.13
12		Unknown						Present
13		Unknown						Present
14		Unknown						Present
15		Unknown						Present
16		Unknown						Present
17		Unknown						Present
18		Unknown						Present
19		Unknown						Present
20		Sarcoplasmic Ca ²⁺ binding protein, alpha B and A chain	AG-N-N01- 0210-W	000000897	23500/4.6	27761/5.55		Present
21		Unknown						Present
22	119	Translationally controlled tumor protein/ unknown	AG-N-N01- 0078-W	000000307	24000/4.4	26667/4.52		-
23	120	Unknown/ unknown						-
24		Unknown						Present
25	92	Unknown/ unknown						0.18

Spot no.		Protein name II/IV	Clone no.	gi II/IV	Observed Mr (Da)/pI II/IV	Calculated Mr (Da)/pI II/IV	Masscot Score II/IV	Dif(fold) / Present
Stages II	Stages IV							
26	132	Unknown/ Unknown						0.15
27		Unknown						Present
28		Beta actin	HC-N-N01- 10367-LF		19000/5.5	27359/6.59	51	Present
29		Intracellular fatty acid binding protein	LP-N-N01- 0788-LF	000192873	16500/5.5	21988/7.75	62	Present
30	109	Unknown/ Unknown						-
31	110	Unknown/ Unknown						-
32	108	Unknown/Intracellular fatty acid binding protein	LP-N-N01- 0938-LF	000193375	16800/5.6	25439/8.84	403	0.02
33		Unknown						Present
34	107	Intracellular fatty acid binding protein/ Unknown	LP-N-S01- 0246-LF	000196483	16000/6.0	28247/9.05	251	-
35	106	Unknown/ Unknown						-
36	105	Cofilin/actin-depolymerizing factor/ Unknown	HC-H-S01- 0582-LF	000072104	19000/6.2	27806/7.25	185	0.07
37		Unknown						Present
38		Unknown						Present
39		Unknown						Present
40	102	Unknown/Proteasome subunit type 6 precursor	HC-N-N01- 3953-LF	000108639	24000/6.0	26674/5.38	98	0.04
41	135	Unknown/ Unknown						-
42	101	Unknown/Glutathione peroxidase	GlEp-N-S01- 1793-LF	000061515	25500/5.95	27384/7.53	254	-
43	103	Unknown/ Unknown						-
44		Unknown						Present
45		Unknown						Present
46		Unknown						Present
47	104	Unknown/CG10527-like- methyltransferase	IN-N-S01- 0718-LF	000186525	19000/6.10	22764/5.89	127	0.1
48		Unknown						Present

Table 3.2 Characterized protein spots in stage II and IV ovaries of normal *P. monodon* broodstock (cont.)

Spot no.		Protein name II/IV	Clone no.	gi II/IV	Observed Mr (Da)/pI II/IV	Calculated Mr (Da)/pI II/IV	Masscot Score II/IV	Dif(fold) / Present
Stages II	Stages IV							
49	126	unknown/ Glutathione -s-transferase	AG-N-N01-0855-W	0000003782	28000/6.15	29371/6.12	60	-
50	98	Glutathione-s-transferase/ Glutathione-s-transferase	HPa-N-N04-1530-LF AG-N-N01-0855-W	000177675/ 000177675	(26000/5.98) /	(28485/6.27) /	246/77	0.1
51	97	Unknown/DN						-
52	99	Trios-phosphate isomerase/ DN	HC-N-N01-11301- LF	000085996	29000/6.0	26634/6.22	88	-
53	96	Hypothetical peptide transporter ATP- binding protein/unknown			37000/5.85	35701/9.59	54	-
54	95	Unknown/unknown						0.06
55	141	Unknown/Glutathione peroxidase	GL-H-S01-1009-LF	000023037	25500/5.5	27221/6.59	52	0.01
56		Unknown						Present
57		Beta thymosin	HC-N-N01-7394-LF	000127904	26000/5.95	27660/6.65	109	Present
58	136	2-cys thioredoxin peroxidase/2-cys thioredoxin peroxidase	OV-N-S01-0212-W OV-N-N01-0360-W	000217496/ 000207902	(26500/5.93) /	(25235/6.41) /	171/66	-
59	91	Unknown/2-cys thioredoxin peroxidase	OV-N-S01-1662-W	000225393	25500/5.30	27726/5.3	251	0.01
60	88	Unknown/ unknown						0.12
61		Unknown						Present
62	87	Unknown/ Proteasome subunit α type 5	HC-N-N01-12735- LF	000093024	29000/5.0	28421/8.80	105	0.05
63		Unknown						Present
64		Unknown						Present
65		Unknown						Present
66		Unknown						Present
67	89	Unknown/unknown						-
68		Unknown						Present
69	68	Unknown/unknown						-
70	156	ND/unknown						-
74	67	Unknown/Cytosolic manganese superoxide dismutase	HC-V-S01-0153-LF	000145497	32500/5.6	34293/6.19	98	0.10

Table 3.2 Characterized protein spots in stage II and IV ovaries of normal *P. monodon* broodstock (cont.)

Spot no.		Protein name II/IV	Clone no.	gi II/IV)	Observed Mr (Da)/pI II/IV	Calculated Mr (Da)/pI II/IV	Masscot Score II/IV	Dif(fold) / Present
Stages II	Stages IV							
75	60	Unknown/unknown						-
79	53	Unknown/unknown						-
80	51	Unknown/DN						-
81	52	Unknown/unknown						-
82	49	Unknown/unknown						-
84	137	Unknown/ unknown						-
89		Unknown						Present
90		Unknown						Present
93	71	Unknown/Hypothetical protein	TT-N-S01-0372-W	000234403	38500/5.35	24360/9.32	61	-
97		Unknown						Present
99		Unknown						Present
100		Unknown						Present
101		Unknown						Present
102		Unknown						Present
103		Unknown						Present
104		Unknown						Present
105		Transaldolase	HC-N-N01-5537-LF	000117451	41000/5.65	25248/5.92	181	Present
107	44	Unknown/Alcohol dehydrogenase	OV-N-S01-0682-W	000220107	42500/5.65	26981/5.41	261	0.15
108		Hypothetical protein	GIep-N-N01-0985-LF	000040682	40000/5.75	29498/8.61	54/91	Present
109		Actin D	HC-N-N01-5201-LF		44000/5.65	27053/5.54	124	Present
110		Actin 2	AG-N-N01-0779-W		44500/5.80	26914/4.85	135	Present
111		Unknown						Present
112		Unknown						Present
113	46	Unknown/ unknown						0.07
114		Adenosine kinase	HPA-N-N01-0792-LF		43000/5.90	24514/9.72	54	Present
115	47	Unknown/unknown						0.57
116	55	Arginine kinase/ unknown	GIep-N-N01-0368-LF	000037477	41500/6.3	28557/7.83	351	-

Table 3.2 Characterized protein spots in stage II and IV ovaries of normal *P. monodon* broodstock (cont.)

Spot no.		Protein name II/IV	Clone no.	gi II/IV	Observed Mr (Da)/pI II/IV	Calculated Mr (Da)/pI II/IV	Masscot Score II/IV	Dif(fold) / Present
Stages II	Stages IV							
117	57	Arginine kinase/Arginine kinase	AG-N-N01-1003-W AG-N-N01-0619-W	0000004411/ 0000002692	(42000/6.55)/ (42000/6.55)	(28557/7.83)/ (28261/8.80)	939/255	-
118	59	Allergen pen m 2/unknown	HC-N-N01-9647-LF	000139652	42000/6.75	27877/7.84	357	-
119	60	Glyceraldehyde 3 phosphate dehydrogenase/unknown	GL-H-S01-0663-LF	000021673	33500/6.90	25544/6.38	250	-
120	159	Putative fructose 1,6-bisphosphate aldolase/unknown	HC-H-S01-0323-LF	000070615	44000/6.90	28601/6.67	80	-
121		Phosphopyruvate hydratase		3885968	51000/6.2	47805/6.18	696	Present
122	20	Phosphopyruvate hydratase/ Phosphopyruvate hydratase	HC-H-S01-0713-LF HC-H-S01-0713-LF	000072865/ 000072865	(50000/6.60) (50000/6.5)	(28432/5.26)/ (28432/5.26)	405/235	-
123	37	Spermatogonial stem cell renewal factor/unknown	HC-H-S01-0581-LF	000072097	45000/6.55	26986/6.02	256	-
124	36	Phosphoglycerate kinase/unknown	HC-N-N01-12748- LF	000093100	45000/6.50	272874/9.45	172	-
125		Phosphopyruvate hydratase	HC-H-S01-0713-LF	000072865	50000/6.45	28432/5.26	110	Present
126	35	NADH-specific isocitrate dehydrogenase/ unknown	OV-N-S01-1780-W	000225962	(45000/6.45)	(27118/5.37)	264	-
127	30	unknown/ unknown						-
128	29	Adenosyl homocysteine/ unknown		72110134	44000/6.35	48061/5.89	78	-
129		Adenosylhomocysteinase	OV-N-S01-1595-W	000225037	45000/5.85	27118/5.37	249	Present
130	28	Beta actin/unknown	HC-N-N01-1004-LF	000079292	45000/5.75	30042/5.14	101	0.13
131		Beta actin	HC-N-N01-1092-LF	000083835	45000/5.70	30042/5.14	322	Present
132		Beta actin	HC-N-S01-0525-LF	000143936	50000/5.50	34171/5.81	67	Present
133		Beta actin	HC-N-N01-1092-LF	000083835	48000/5.60	30042/5.14	56	Present
134		Unknown						Present
135		rab gdp-dissociation inhibitor	HC-N-N01-4554-LF	000111854	50000/5.75	23862/6.62	129	Present
136	22	Unknown/Mitochondrial aldehyde dehydrogenase 2	OV-N-S01-1601-W	000225074	50000/5.6	26678/5.63	96	-
137		Methylmalomate-semialdehyde dehydrogenase	OV-N-S01-0565-W	000219471	54000/5.85	27233/5.14	88	Present

Table 3.2 Characterized protein spots in stage II and IV ovaries of normal *P. monodon* broodstock (cont.)

Spot no.		Protein name II/IV	Clone no.	gi II/IV	Observed Mr (Da)/pI II/IV	Calculated Mr (Da)/pI II/IV	Masscot Score II/IV	Dif(fold) / Present
Stages II	Stages IV							
138		Tubulin beta-1 chain	HC-N-S01-0037-LF	000141337	55000/5.85	33568/6.44	83	Present
140		Unknown						Present
141		Unknown						Present
142	17	Unknown/unknown						-
143	16	Unknown/DN						-
144	14	chaperonin containing TCP1 subunit 5/unknown	HC-N-N01-7872-LF	000130592	60000/5.95	26006/4.94	60	-
145		Unknown						Present
146		Unknown						Present
148		Hemocyanin		854403	65000/5.60	74992/5.27	118	Present
149		Hemocyanin	HPa-N-S01-0106-LF	000179787	65000/5.55	28981/5.77	112	Present
150	12	Protein disulfide isomerase/ Protein disulfide isomerase	OV-N-S01-0764-W OV-N-S01-0764-W	000220555/ 000220555	(59000/5.70)/ (59000/5.70)	(29075/5.60)/ (29075/5.60)	418/435	-
151	15	Unknown/Pyrroline-5-carboxylate dehydrogenase	GIEp-N-N01-2568- W	000050030	59500/5.95	26690/8.0	65	-
152	9	chaperonin containing TCP1, subunit 2/unknown		5453603	60000/5.45	57794/6.01	82	0.08
153		chaperonin containing TCP1, subunit 2	LP-N-S01-0061-LF	000195548	60000/5.4	27691/9.22	245	Present
154	8	Hsp60 protein, putative/unknown	TT-N-S01-0846-W	000236557	60000/5.25	26532/5.11	336	-
155		Cytochrome b	HPa-N-N03-1765-LF	00016702	66000/5.2	23867/10.39	52	Present
156		Tubulin beta-2 chain		3915093		51354/4.85	1018	Present
157	86	Tubulin beta-1 chain/ Tubulin beta-1 chain	HC-N-S01-0037-LF HC-N-S01-0037-LF	000141337/ 000141337	(52000/5.1)/ (52000/5.1)	(33568/6.44)/ (33568/6.44)	722/76	0.07
158		beta Tubulin	HC-N-S01-0150-LF	000141985	49000/5.08	28808/8.25	72	Present
159		Tat-binding protein 1	OV-N-S01-1291-W	000223407	49000/5.25	27220/4.58	354	Present
160	40	Unknown/Protein disulfide isomerase	LP-N-N01-1193-LF	000194648	29000/5.6	27345/6.11	104	-
161	42	Unknown/ Tat binding protein 7		263099	46000/5.28	51635/5.52	63	-
163		Beta actin	HC-N-N01-1092-LF	000083835	44000/5.4	30042/5.14	535	Present
164	43	Beta actin/ Beta actin	HC-N-N01-1092-LF HC-N-N01-1092-LF	000083835/ 000083835	(44000/5.50)/ (44000/5.50)	(30042/5.14)/ (30042/5.14)	809/408	-

Table 3.2 Characterized protein spots in stage II and IV ovaries of normal *P. monodon* broodstock (cont.)

Spot no.		Protein name II/IV	Clone no.	gi II/IV	Observed Mr (Da)/pI II/IV	Calculated Mr (Da)/pI II/IV	Masscot Score II/IV	Dif(fold) / Present
Stages II	Stages IV							
165		Unknown						Present
166		Putative 40S ribosomal protein	HC-N-N01-13854-LF	000098347	43500/4.90	27102/6.51	159	Present
167		Putative 40S ribosomal protein	AG-N-N01-0263-W	0000001143	44000/4.85	27096/9.82	159	Present
168		Unknown						Present
169		Unknown						Present
170		Unknown						Present
171	75	Unknown/unknown						-
172	73	Unknown/unknown						-
173		Unknown						Present
174		Unknown						Present
175		Unknown						Present
176		Beta actin	HC-N-S01-0525-LF	000143936	31000/5.05	34171/5.81	67	Present
177		Unknown						Present
178		Unknown						Present
179		Unknown						Present
180	81	Chromobox protein homolog1/Chromobox protein homolog1	OV-N-S01-1463-W	000224391/ 000224391	(31000/4.55)/ (31000/4.55)	(27869/5.17)/ (27869/5.17)	70/73	-
181		Unknown						Present
182	80	Unknown/unknown						-
183	78	Unknown/Ovarian peritrophin 2 precursor	OV-N-S01-0396-W	000218515	36500/4.7	29164/5.17	121	-
184		Proliferating cell nuclear antigen	OV-N-N01-0805-W	000210488	36000/4.70	27144/5.0	472	Present
185	79	Unknown/Peritrophin 3 precursor	OV-N-N01-0689-W	000209805	37000/4.65	27869/5.17	127	-
186		Unknown						Present
187		Unknown						Present
188		Unknown						Present
189		Retinoblastoma binding protein 4	OV-N-S01-2043-W	000227384	54000/4.80	27401/5.43	60	Present

Table 3.2 Characterized protein spots in stage II and IV ovaries of normal *P. monodon* broodstock (cont.)

Spot no.		Protein name II/IV	Clone no.	gi II/IV	Observed Mr (Da)/pI II/IV	Calculated Mr (Da)/pI II/IV	Masscot Score II/IV	Dif(fold) / Present
Stages II	Stages IV							
190	84	F1-ATP synthase beta subunit/ F1-ATP synthase beta subunit	OV-N-S01-1723-W	000225709/ 000225709	(49000/4.85)/ (490000/4.85)	(26036/4.81)/ (26036/4.71)	446/246	-
191		F1-ATP synthase beta subunit	OV-N-S01-1723-W	000223015	52500/4.90	26036/4.81	454	Present
192	83	Protein disulfid isomerase/ Protein disulfid isomerase	OV-N-S01-1221-W	000223015/ 000223015	(56500/4.70)/ (56500/4.70)	(28064/4.66)/ (28060/4.66)	563/343	-
193		Unknown						Present
194		Unknown						Present
195	1	Glycoprotein 93 CG5520-PA/DN	OV-N-N01-0023-W	000205923	97000/4.85	28011/4.70	466	-
196	3	Valosin containing protein-1/DN	HC-N-N01-5012-LF	000114465	75000/5.45	27017/5.30	85	-
198		Valosin containing protein-1	HC-N-N01-5012-LF	000114465	75000/5.40	27017/5.30	85	Present
199		Unknown						Present
200		Unknown						Present
201		Unknown						Present
202		Unknown						Present
203		Unknown						Present
204		Unknown						Present
205		Unknown						Present
206		Beta tubulin	HC-N-S01-0150-LF	000141985	56500/5.70	36348/9.97	69	Present
207		Unknown						Present
210		Unknown						Present
211		Unknown						Present
212		Unknown						Present
213		Unknown						Present
215		Unknown						Present
	10	Unknown						Absent

Table 3.2 Characterized protein spots in stage II and IV ovaries of normal *P. monodon* broodstock (cont.)

Spot no.		Protein name N/EA	Clone no.	gi II/IV	Observed Mr (Da)/pI II/IV	Calculated Mr (Da)/pI II/IV	Masscot Score II/IV	Dif(fold) / Present
Stages II	Stages IV							
	11	Protein disulfide isomerase	IN-N-S01-0691-LF	000186374	55000/5.5	27052/5.10	61	Absent
	13	Protein disulfide isomerase	OV-N-S01-0764-W	000220555	65000/5.6	29075/5.6	712	Absent
	18	Unknown						Absent
	19	Unknown						Absent
	21	Mitochondrial aldehyde dehydrogenase 2	OV-N-S01-1601-W	000225074	50000/5.1	26678/5.63	59	Absent
	23	Hypothetical protein	GlEp-N-N01-2817- LF	000051477	52000/5.6	26517/8.67	48	Absent
	24	Unknown						Absent
	25	Unknown						Absent
	26	Methyl malonate semialdehyde dehydrogenase	OV-N-S01-0565-W	000219471	52000/5.7	27233/5.41	79	Absent
	27	Unknown						Absent
	31	Putative conjugal transfer protein		116250544	44000/6.05	170011/6.29	74	Absent
	33	Unknown						Absent
	34	Unknown						Absent
	38	Unknown						Absent
	39	Unknown						Absent
	41	Unknown						Absent
	45	Hypothetical protein	LP-V-S01-0528-LF	000200635	41000/5.75	27243/9.85	206	Absent
	48	Unknown						Absent
	50	Unknown						Absent
	54	L-3-hydroxyacyl-Co A dehydrogenase	OV-N-N01-1642-W	00021537	34000/6.25	26197/9.3	59	Absent
	56	Unknown						Absent
	58	Arginine kinase	AG-N-N01-1003-W	0000004411	41000/6.29	28557/7.83	50	Absent
	61	Unknown						Absent
	62	Unknown						Absent
	63	Unknown						Absent
	64	Unknown						Absent
	65	Unknown						Absent

Table 3.2 Characterized protein spots in stage II and IV ovaries of normal *P. monodon* broodstock (cont.)

Spot no.		Protein name II/IV	Clone no.	gi II/IV	Observed Mr (Da)/pI II/IV	Calculated Mr (Da)/pI II/IV	Masscot Score II/IV	Dif(fold) / Present
Stage II	Stages IV							
	66	Unknown						Absent
	69	Unknown						Absent
	70	Unknown						Absent
	72	Secreted inorganic pyrophosphatase	OV-N-N01-0542-W	000208952	36000/5.3	26955/6.42	96	Absent
	74	Unknown						Absent
	76	Unknown						Absent
	77	Ovarian peritrophin 2 precursor	OV-N-S01-0389-W	000218474	36000/4.85	31441/5.0	216	Absent
	82	Unknown						Absent
	85	Heat shock like protein	OV-N-N01-0015-W	000205873	70000/5.10	27824/4.71	128	Absent
	90	Unknown						Absent
	93	Unknown						Absent
	94	Unknown						Absent
	100	Triose-phosphate isomerase	OV-N-N01-0364-W	000207925	27000/5.95	16635/6.66	240	Absent
	111	Translocation protein Tol B		13473330	14000/5.48	47651/6.69	78	Absent
	116	Unknown						Absent
	122	Unknown						Absent
	123	HAD family hydrolase		145590757	27500/6.30	145590757	51	Absent
	124	Unknown						Absent
	125	Unknown						Absent
	127	HAD family hydrolase		145590757	28500/6.05	145590757	64	Absent
	128	Unknown		223947443	30000/6.10	70395/5.47	67	Absent
	129	Unknown						Absent
	130	Unknown						Absent
	131	Unknown		223947443	24000/5.42	70395/5.47	74	Absent
	133	Unknown						Absent
	134	Unknown						Absent
	138	Unknown		223947443	43000/5.85	70395/5.47	65	Absent
	140	NLI interacting factor like phosphatase family protein		118354395	43000/5.25	64193/8.92	63	Absent

Table 3.2 Characterized protein spots in stage II and IV ovaries of normal *P. monodon* broodstock (cont.)

Spot no.		Protein name II/IV	Clone no.	gi II/IV	Observed Mr (Da)/pI II/IV	Calculated Mr (Da)/pI II/IV	Masscot Score II/IV	Dif(fold) / Present
Stages II	Stages IV							
	142	Hypothetical protein		123477668	43000/5.50	20547/9.73	63	Absent
	143	Hypothetical protein		123477668	40000/5.40	20547/9.73	67	Absent
	144	Unknown						Absent
	145	Albumin		30962111	67000/6.75	67862/5.23	165	Absent
	148	Vitellogenin		45774386	67000/6.50	285335/6.55	368	Absent
	149	Unknown		223947443	54000/5.90	70395/5.47	62	Absent
	150	Unknown		223947443	28500/5.90	70395/5.47	66	Absent
	151	Unknown		223947443	30000/5.9	70395/5.47	63	Absent
	157	Vitellogenin		45774386	72000/6.50	285335/6.55	114	Absent
	160	Unknown						

DN = chromatogram was not observed during mass spectrometrical analysis

ND = not determined by nanoESI-LC-MS/MS

Dif (fold) = differential expression and the fold change >1.5 is regarded as upregulation, < 0.67 = down regulation, - = comparable protein levels,

Present = proteins that were found in stage II ovaries of normal broodstock but not in the stage IV of normal broodstock.

Absent = proteins that were not found in stage IV ovaries of normal broodstock but not in the the stage II of normal broodstock.

ศูนย์วิทยทรัพยากร
จุฬาลงกรณ์มหาวิทยาลัย

Table 3.3 Characterized protein spots found in stage II and IV ovaries of eyestalk-ablated *P. monodon* broodstock

Spot no.		Protein name II/IV	Clone no.	gi II/IV	Observed Mr (Da)/pI II/IV	Calculated Mr (Da)/pI II/IV	Mass cot Score II/IV	Dif(fold) / Present
Stages II	Stages IV							
1		DN						Present
2	2	DN/ nucleoplasmin isoform 1-like protein	GL-H-S01-0626-LF	000021469	23000/4.5	21693/4.77	72	0.7
3		DN						Present
4	3	DN/unknown			17000/5.2	29064/9.24	55	-
5	4	DN/Eukaryotic initiation factor 5A	HC-H-S01-1060-LF	000074845	17000/5.3	17488/5.71	113	2.18
6		DN						Present
7		DN						Present
8	6	DN/unknown						-
9	8	Unknown/CG10527-like methyltransferase	LP-V-S01-0093-LF	000198230	17000/6.0	22764/5.89	111	0.1
10	10	Unknown/Rab3 GTPase-activating protein	HC-H-S01-0575-LF	000072064	22000/6.5	21511/11.29	70	0.42
11		Glutathione peroxidase	IN-N-S01-1245-LF	000189297	24000/6.4	25178/5.78	94	Present
12		Glutathione-s-transferase	AG-N-N01-0855-W	000177675	26000/6.2	29371/6.27	234	Present
13	22	Glutathione peroxidase / Glutathione peroxidase	GL-H-S01-1009-LF IN-N-S01-1245-LF	000023037/ 000189297	(24000/6.20)/ (24000/6.20)	(27221/6.59)/ (25178/6.59)	555/7 9	-
14		Glutathione peroxidase	IN-N-S01-1245-LF	000189297	20000/6.0	25178/5.78	271	Present
15	127	Unknown/ND						
16		Unknown						Present
17	133	proteasome subunit beta type I/ND	TT-N-S01-0369-W	000234396	25000/5.85	19494/5.09	66	-
18	21	Glutathione peroxidase/ Glutathione peroxidase	IN-N-S01-1245-LF GL-H-S01-1009-LF	000189297/ 000023037	(24500/5.95)/ (24500/5.95)	(25178/5.78)/ (27221/6.59)	226/1 42	5.40
19	125	Triose-phosphate isomerase/ND	HC-N-N01-9543-LF	000139250	26000/6.0	26449/6.30	256	-
20	126	Glutathione-s-transferase/ND	HPa-N-N04-1530-LF	000177675	26000/5.98	26521/6.22	481	-
21	124	Peroxioredoxin 4/ND	OV-N-S01-0549-W	000219380	27000/6.0	24378/5.96	58	0..36
22	35	Hydroxyacyl glutathione hydrolase/ Hydroxyacyl glutathione hydrolase	HC-H-S01-0325	000070627/ 000070627	(27000/6.10)/ (27000/5.9)	(21088/6.13)/ (21088/6.13)	67/88	0.40
23		Unnamed protein product	OV-N-S01-1944-W	000226831	25000/5.7	28884/11.88	67	Present
24		Unknown						Present

Table 3.3 Characterized protein spots found in stage II and IV ovaries of eyestalk-ablated *P. monodon* broodstock (cont.)

Spot no.		Protein name II/IV	Clone no.	gi II/IV	Observed Mr (Da)/pI II/IV	Calculated Mr (Da)/pI II/IV	Massco t Score II/IV	Dif(fold) / Present
Stages II	Stages IV							
25		Beta thymosin	OV-N-S01-1085-W	000222248	20500/5.85	14784/5.35	59	Present
26		Glutathione peroxidase	IN-N-S01-1245-LF	000189297	22000/5.6	25178/5.78	115	Present
27	19	Beta thymosin/DN	GIep-N-S01-1318-LF	000058975	20000/5.5	26091/6.09	188	-
28	18	Beta thymosin/ Beta thymosin	HC-W-S01-0050-LF	000147620/	(22000/5.4)/	(26519/5.45)/	289/56	0.25
			GIep-N-S01-1318-LF	000058975	(22000/5.4)	(26091/6.09)		
29	17	Glyoxylase 1/DN	OV-N-S01-1440-W	000224263	(21000/5.5)/	(28333/6.51)/	139/71	-
					(22000/5.6)	(21511/11.09)		
30		Scavenger receptor cysteine protein precursor	IN-N-S01-1294-LF	000189569	24000/5.48	22358/10.30	51	Present
31	15	2-cys thioredoxin peroxidase/2-cys thioredoxin peroxidase	HC-H-S01-0335-LF	000070688/	(25000/5.35)/	(23660/5.49)/	340/288	-
				000070688	(25000/5.35)	(23660/5.49)		
32		Heat shock protein 21.4	OV-N-N01-0298-LF	000207530	24000/5.4	25851/7.16	126	Present
33	11	Unknown/unknown						-
34		Unknown						Present
35	1	Unknown/ unknown						-
36	12	Unknown/unnamed protein product	HC-N-N01-10980-LF	000084186	26000/5.2	27150/4.66	73	3.11
37		Proteasome subunit alpha type	HC-H-S01-0111-LF	000141763	35000/6.0	27226/7.7	107	Present
38		beta-Nac-like protein	HC-N-N01-13561-LF		28000/5.4	26425/4.58	68	Present
39	14	es1 protein/es1 protein	OV-N-N01-0895-W	000211011/	(27000/5.5)/	(25409/6.23)/	71/288	0.5
			HC-H-S01-0335-LF	000070688	(27000/5.5)	(23660/5.49)		
40	24	Beta thymosin/ Beta thymosin	GIep-N-N01-2428-LF	000049202/	(29000/5.6)/	(27345/6.11)/	342/126	0.44
			LF AG-N-N01-0805-W	0000003585	(29000/5.6)	(26392/5.22)		
41	25	Proteasome subunit α type/ Proteasome subunit α type	LP-N-N01-0262-LF	000190425/	(29500/5.5)/	(20323/6.06)/	98/95	0.51
			LP-N-N01-0262-LF	000190425	(29500/5.5)	(20323/6.06)		
42	27	Cytosolic manganese superoxide dismutase/ Cytosolic manganese superoxide dismutase	OV-N-S01-0378-W	000218419/	(30000/5.6)/	(26967/5.79)/	225/98	-
			HC-V-S01-0153-LF	000145497	(30000/5.6)	(34293/6.19)		
43	26	Carbonic anhydrase/ Carbonic anhydrase	OV-N-N01-1186-W	000212702/	(29000/5.75)/	(26424/5.76)/	111/50	-
			GL-H-S01-0060-LF	000018685	(29000/5.75)	(24565/6.19)		

Table 3.3 Characterized protein spots found in stage II and IV ovaries of eyestalk-ablated *P. monodon* broodstock(cont.)

Spot no.		Protein name II/IV	Clone no.	Gi II/IV	Observed Mr (Da)/pI II/IV	Calculated Mr (Da)/pI II/IV	Masscot Score II/IV	Dif(fold) / Present
Stages II	Stages IV							
44	33	Hypothetical protein/ND	HC-V-S01-0348-LF	000146544	31500/6.05	27238/9.65	50	28.55
45	28	Unknown/unknown						-
46	29	Unknown/unknown						4.28
47	30	Unknown/ electron transfer flavoprotein	HC-N-N01-0997-LF	000079053	32500/5.70	27958/8.4	217	-
48	31	Unknown/ Rab3 GTPase-activating protein	ES-N-S03-0709-W	000015846	32000/5.80	27302/9.85	68	-
49	32	Unknown/ND						-
50	38	Unknown/Protein henna	GIep-N-S01-0628-LF	000055195	35000/5.95	27992/11.69	51	-
51	39	26s proteasome non-ATPase regulatory isoform A subunit 14/ 26s proteasome non-ATPase regulatory isoform A subunit 14	GIep-N-N01-1900-LF	000046617/ 000046617	(36500/6.15)/ (36500/6.15)	(27226/7.7)/ (28104/9.5)	189/70	-
52	40	Ubiquitin carboxyl terminal transferase/ Ubiquitin carboxyl terminal transferase	GIep-N-N01-0730-LF	000039213/ 000039213	(36000/6.05)/ (36000/6.05)	(28104/9.55) / (28104/9.55)	157/70	-
53		L-3-hydroxyacyl-co A dehydrogenase	OV-N-N01-1642-W	000215317	31500/6.65	26197/9.30	119	Present
54		unknown						Present
55	64	Unknown/unknown						0.08
56	63	Allergen pen m 2/ND	HC-N-N01-9647-LF	000139652	40000/6.5	28024/8.72	653	-
57	62	Arginine kinase/unknown	AG-N-N01-1003-W GIep-N-N01-1166-LF	0000004411 / 000041760	(40000/6.20)/ (40000/6.20)	(28557/7.83) / (29885/6.20)	460/146	0.49
58	61	Arginine kinase/ Arginine kinase	AG-N-N01-1003-W AG- N-N01-0154-W	0000004411 / 000000634	(40000/6.0)/ (40000/6.0)	(28250/7.83) / (28250/8.50)	47/112	-
59		unknown						Present
60		Alcohol dehydrogenase	OV-N-S01-0682-W	000220107	40000/6.15	26981/5.41	55	Present

Table 3.3 Characterized protein spots found in stage II and IV ovaries of eyestalk-ablated *P. monodon* broodstock(cont.)

Spot no.		Protein name II/IV	Clone no. Stages II	gi II/IV	Observed Mr (Da)/pI II/IV	Calculated Mr (Da)/pI II/IV	Masscot Score II/IV	Dif(fold) / Present
Stages II	Stages IV							
61	41	Hypothetical protein/ Hypothetical protein	GlEp-N-N01-0073-LF	000035965/ 000035965	(38500/6.05)/ (38500/6.05)	(27401/7.70)/ (27401/7.70)	138/133	-
62	42	aldo-keto-reductase/ aldo-keto-reductase	HC-N-S01-0103-LF	000141719/ 000141719	(37000/5.9)/ (37000/5.9)	(28487/8.94)/ (27302/9.85)	75/70	-
63	43	Heterogeneous nucleare ribonucleoprotein / Heterogeneous nucleare ribonucleoprotein	HC-H-S01-0995-LF OV-N-S01-2373-W	000074481/ 000229029	(38000/5.75)/ (38000/5.75)	(26095/5.28)/ (23374/9.34)	82/133	-
64	46	Heterogeneous nucleare ribonucleoprotein/ Heterogeneous nucleare ribonucleoprotein	HC-N-S01-0995-LF	000074481/ 000074481	(38500/5.7)/ (38000/5.7)	(26095/5.28)/ (26095/5.28)	71/68	-
65	47	Transaldolase/DN	HC-N-N01-5537-LF	000117451	37000/5.63	25248/5.92	234	-
66	44	Alcohol dehydrogenase/ Alcohol dehydrogenase	OV-N-S01-0682-W	000220107/ 000220107	(40000/5.8)/ (40000/5.8)	(26981/5.14)/ (26981/5.14)	105/54	-
67		Hypothetical protein	HC-N-N01-8339-LF	000133175	40000/5.75	29234/8.75	91	Present
68		Heterogeneous nuclear ribonucleoprotein	HC-H-S01-0995-LF	000074481	39500/5.75	26095/5.28	71	Present
69		unknown						Present
70	134	Heterogeneous nuclear ribonucleoprotein/ND	HC-H-S01-0995-LF	000074481	32000/5.5	26095/5.28	60	-
71		Cysteine proteinase	LP-N-S01-0217-LF	000196323	32500/5.4	28940/6.08	186	Present
72		unknown						Present
73		DN						Present
74		unknown						Present
75		Vitellogenin precursor	OV-N-S01-0317-W	000218095	40000/5.45	27438/9.02	57	Present
76		Ovarian peritrophin	OV-N-S01-0206-W	000217459	39000/5.35	29830/6.82	177	Present
77		Ovarian peritrophin	OV-N-S01-0206-W	000217459	39000/5.28	29830/6.82	192	Present
78		unknown						Present
79		unknown						Present
80		Beta actin	HC-N-N01-1092-LF	000083835	43000/5.4	30042/5.14	567	Present

Table 3.3 Characterized protein spots found in stage II and IV ovaries of eyestalk-ablated *P. monodon* broodstock(cont.)

Spot no.		Protein name II/IV	Clone no. Stages II	Gi II/IV	Observed Mr (Da)/pI II/IV	Calculated Mr (Da)/pI II/IV	Masscot Score II/IV	Dif(fold) / Present
Stages II	Stages IV							
81	57	Beta actin/unknown	HC-N-N01-1092-LF	000083835	44000/5.55	30042/5.14	567	-
82	58	Beta actin/beta actin	HC-N-S01-0525-LF	000083835/ 000083835	(44000/5.50)/ (44000/5.50)	(34171/5.81)/ (34171/5.81)	98/282	-
83		RAN binding protein	GIEp-N-N01-0595-LF	000038517	38000/5.5	27523/4.75	128	Present
84		Epa4p	OV-N-N01-0835-W	0000210671	36000/5.05	28834/4.78	271	Present
85	50	Histidine-rich glycoprotein precursor/DN	HC-N-N01-8689-LF	000135068	35500/5.29	27499/9.39	48	2.44
86		Ovarian peritrophin	OV-N-S01-0329-W	000218168	36000/5.2	31222/5.15	155	Present
87		Epa4p	OV-N-N01-0835-W	000210671	36000/5.15	28834/4.78	374	Present
88	55	Ovarian peritrophin 2 precursor/ Ovarian peritrophin 2 precursor	OV-N-S01-0396-W OV-N-N01-0786-W	000218515/ 000210374	(36000/4.85)/ (36000/4.85)	(31792/5.70)/ (28726/4.92)	149/93	-
89	107	Calreticulin/unknown	OV-N-N01-1274-W	000213225	65000/4.4	27852/4.91	67	-
90	136	Unknown/ND						-
91	108	Protein disulfide isomerase/unknown	OV-N-N01-2641-W	000230209	60000/4.8	26214/4.7	602	2.74
92	109	DN/unknown						-
93	91	unknown/unknown						1.57
94	89	Tubullin beta-1 chain/ unknown	HC-W-S01-0062-W HC-H-S01-1014-LF	000147681/ 000074595	(57000/5.21)/ (57000/5.21)	(28353/5.06)/ (17179/7.97)	202/78	-
95	90	60 kDa heat shock protein/unknown	OV-N-N01-0358-W	000207891	60000/5.3	26264/5.28	95	-
97		unknown						Present
98		Tat-binding protein-1	HC-N-N01-4075-LF	000109328	52000/5.39	27220/5.03	125	Present
99		Protein disulfide isomerase	OV-N-S01-0893-W	000221197	50000/5.39	28808/8.25	669	Present
100	87	Protein disulfide isomerase/unknown	LP-N-N01-1193-LF	000194648	51000/5.5	22261/8.61	155	-
101		Dynactin subunit 2	HPa-N-N04-1190-LF	000175801	50000.5.6	26646/5.9	58	Present

Table 3.3 Characterized protein spots found in stage II and IV ovaries of eyestalk-ablated *P. monodon* broodstock(cont.)

Spot no.		Protein name II/IV	Clone no.	Gi II/IV	Observed Mr (Da)/pI II/IV	Calculated Mr (Da)/pI II/IV	Masscot Score II/IV	Dif(fold) / Present
Stages II	Stages IV							
102		Mitochondrial aldehyde dehydrogenase 2	OV-N-S01-1601-W	000225074	54000/5.6	26678/5.63	66	Present
103	85	D-lactate dehydrogenase/unknown	HC-N-N01-11562	000087493	45000/5.7	30042/5.14	51	0.08
104	83	Rab gdp-dissociation inhibitor/unknown	HC-N-N01-8951- LF	000136496	50000/5.75	27346/6.50	86	0.22
105	86	Unknown/unknown						-
106		Acyl-co A dehydrogenase long chain	GIep-N-S01-0329- LF	000053546	47000/5.80	26118/9.10	52	Present
107	103	Unknown/unknown						-
108	79	Unknown/unknown						-
109	80	Unknown/unknown						-
110		Methylmalonate-semialdehyde dehydrogenase	AG-N-N01-0860	000227631	54000/6.05	26937/6.18	83	Present
111	101	Unknown/unknown						-
112	97	Transketolase/unknown	OV-N-S01-0294-W	000227631	65000/6.05	26683/5.35	193	-
113	96	Chaperonin containing TPC1 subunit 5/ Chaperonin containing TPC1 subunit 5	HC-N-N01-7872- LF	000130592/ 000130592	(60000/5.95)/ (60000/5.85)	(20006/4.94)/ (20006/4.94)	85/53	-
114		Pyrroline-5-carboxylate dehydrogenase	GIep-N-N01-2568- W	000050030	59500/5.95	26690/8.0	97	Present
115	94	Protein disulfide isomerase/ Protein disulfide isomerase	OV-N-S01-0764-W	000220555/ 000220555	(60000/5.85)/ (60000/5.85)	(29075/5.6)/ (29075/5.6)	274/491	-
116	93	Protein disulfide isomerase/ Protein disulfide isomerase	OV-N-S01-0764-W IN-N-S01-0691-LF	000220555/ 000186374	(60000/5.75)/ (60000/5.75)	(29075/5.6)/ (27052/5.10)	435/180	0.7
117	92	Protein disulfide isomerase/DN	OV-N-S01-0764-W	000220555	60000/5.70	29075/5.6	495	1.70
118	113	Unknown/unknown						-
119	114	Unknown/unknown						-
120	99	Unknown/unknown						-
121	100	DN/unknown						-
122		Unknown						Present
123		Unknown						Present

Table 3.3 Characterized protein spots found in stage II and IV ovaries of eyestalk-ablated *P. monodon* broodstock(cont.)

Spot no.		Protein name II/IV	Clone no. Stages II	Gi II/IV	Observed Mr (Da)/pI II/IV	Calculated Mr (Da)/pI II/IV	Masscot Score II/IV	Dif(fold) / Present
Stages II	Stages IV							
124	76	Unknown/Elongation factor 2	GIep-N-S01-1165-LF	000058229	45000/6.3	29380/10.32	56	-
125	77	Unknown/DN						-
126	78	Unknown/26s protease regulatory subunit 7	HC-N-N01-7411-LF	000127992	48000/6.0	27698/9.06	97	0.38
127	75	Unknown/acyl coenzyme A dehydrogenase	OV-N-N01-0061-W	000206138	42000/6.0	26682/5.44	128	-
128		2-keto-4-pentenoate hydrolase		67643902	47000/6.40	47355/5.70	80	Present
129	72	NADPH-specific isocitrate dehydrogenase/unknown	OV-N-S01-1780-W	000225962	46000/6.45	27909/8.29	223	-
130	123	RAB, member of RAS oncogene family-like 5/ND	GL-N-S01-1414-LF	000029541	60000/6.5	26652/6.06	105	-
131	138	Glutamate carboxypeptidase/ND	OV-N-S01-0878-W	000221132	54000/6.55	27740/6.82	98	-
132	71	Unknown/Phosphopyruvate hydratase	HC-H-S01-0713-LF	000072865	50000/6.50	28432/5.26	235	-
133		Phosphopyruvate hydratase	HC-N-N01-10611-LF	000082116	50000/6.65	28453/9.07	69	-
134		unknown						Present
135		unknown					435/180	Present
136	69	Unknown/unknown			60000/5.70	29075/5.6	495	-
137	68	Unknown/Isocitrate dehydrogenase 2 (NADP+)	OV-N-N01-1170-W	000212605	42000/6.50	28050/9.17	144	0.52
138	106	Unknown/ Hemocyanin	HPa-N-N03-0431-LF	000159985	85000/5.90	26527/5.49	100	-
139	104	Unknown/unknown						-
140	128	Unknown/ND						-
141	131	Unknown/ND						-
142	129	Unknown/ND						-
143		unknown						Present
144		unknown						Present
145		unknown						Present

Table 3.3 Characterized protein spots found in stage II and IV ovaries of eyestalk-ablated *P. monodon* broodstock(cont.)

Spot no.		Protein name II/IV	Clone no.	gi II/IV	Observed Mr (Da)/pI II/IV	Calculated Mr (Da)/pI II/IV	Masscot Score II/IV	Dif(fold) / Present
Stages II	Stages IV							
146		Unknown						Present
147		Unknown						Present
148		Unknown						Present
149		Unknown						Present
150		Unknown						Present
151		Unknown						Present
152		Unknown						Present
153		Unknown						Present
154		Unknown						Present
155		Unknown						Present
156		Unknown						Present
157		Unknown						Present
158		Unknown						Present
159	7	Unknown/ similar to Cofilin/actin-depolymerizing factor	IN-N-S01-0021-LF	000182905	15000/6.15	15080/5.71	150	-
160	36	Unknown/DN						-
161	116	Unknown/ND						-
162	117	Unknown/ND						-
163	118	Unknown/ND						-
164	119	Unknown/ND						-
165		Vitellogenin		82754312	67000/6.70	285804/6.91	231	Present
166		Unknown	HC-N-N01-12416-LF	000091071	90000/6.65	27458/10.09	60	Present
167		Vitellogenin		45774386	67000/6.60	285335/6.55	382	Present
168		elongation factor 2	GIEp-N-S01-1165-LF	000058229	90000/6.55	29380/10.32	51	Present
169		Unknown	ES-N-S02-0106-W	000010178	90000/6.50	244437/9.95	72	Present
170		elongation factor 2	GIEp-N-S01-1165-LF	000058229	90000/6.40	29380/10.32	56	Present
171		Vitellogenin		23955944	67000/6.4	289032/5.42	64	Present
172		Thrombospondin	OV-N-ST01-0130-W	000230801	90000/6.28	24111/10.02	78	Present

Table 3.3 Characterized protein spots found in stage II and IV ovaries of eyestalk-ablated *P. monodon* broodstock(cont.)

Spot no.		Protein name II/IV	Clone no.	Gi II/IV	Observed Mr (Da)/pI II/IV	Calculated Mr (Da)/pI II/IV	Masscot Score II/IV	Dif(fold) / Present
Stages II	Stages IV							
172		Thrombospondin	OV-N-ST01-0130-W	000230801	90000/6.28	24111/10.02	78	Present
173		Thrombospondin	OV-N-ST01-0130-W	000230801	90000/6.10	24111/10.02	60	Present
174		Unknown						Present
175		Unknown						Present
180	120	Heat shock 70 kD protein cognate/ND	HC-N-N01-1119-LF	000085430	80000/5.20	28504/5.11	164	-
	9	Unknown						Absent
	13	Rab3 GTPase-activating protein	ES-N-S01-0575-LF	000015846	27500/5.40	27302/9.85	62	Absent
	16	Glyoxylase 1	OV-N-S01-1440-W	000224263	24000/5.4	28333/6.51	114	Absent
	20	Hypothetical protein	HC-N-N01-11847- LF	000088650	20000/5.6	15986/6.96	61	Absent
	23	Glutathione peroxidase	GL-H-S01-1009-LF	000023037	20000/6.20	27221/6.59	69	Absent
	37	L-3-hydroxyacyl-co A dehydrogenase	OV-N-N01-1642-W	000215317	28000/6.5	26197/9.30	202	Absent
	45	Heterogeneous nuclear ribonucleoprotein	OV-N-S01-2373-W	000229029	41000/5.55	23374/9.34	112	Absent
	48	Transaldolase	HC-N-N01-5537-LF	000117451	33000/5.0	25248/5.92	110	Absent
	49	Hypothetical protein	OV-N-S01-2630-W	000230155	33000/5.05	25402/9.92	58	Absent
	51	Rab3 GTPase-activating protein	ES-N-S03-0709-W	000015846	36000/5.22	27302/9.85	74	Absent
	52	Rab3 GTPase-activating protein	ES-N-S03-0709-W	000015846	36000/5.05	27302/9.85	66	Absent
	53	Epa4p	IN-N-S01-0852-LF	000187270	38000/5.05	28834/4.78	281	Absent
	54	RAN binding protein 2	GlEp-N-N01-0595- LF	000038517	32000/4.10	27523/4.75	142	Absent
	56	Unknown						Absent
	59	Unknown						Absent
	60	Cysteine proteinase	AG-N-N01-0910-W	0000004005	39000/6.0	28940/8.73	146	Absent
	65	Unknown						Absent
	66	Unknown						Absent
	67	Hypothetical protein	HC-N-N01-12917- LF	000094112	47500/6.50	28209/8.78	197	Absent

Table 3.3 Characterized protein spots found in stage II and IV ovaries of eyestalk-ablated *P. monodon* broodstock(cont.)

Spot no.		Protein name II/IV	Clone no.	gi II/IV	Observed Mr (Da)/pI II/IV	Calculated Mr (Da)/pI II/IV	Masscot Score II/IV	Dif(fold) / Present
Stages II	Stages IV							
	70	Phosphoglycerate kinase	HC-N-N01- 12748-LF	000093100	51000/6.50	27874/9.40	74	Absent
	73	Cytosolic NADP-dependent isocitrate dehydrogenase	GL-H-S01- 1073-LF	000023350	40000/6.50	27608/5.09	105	Absent
	74	Fah-prov protein		32450404	43000/5.50	46978/6.22	97	Absent
	81	Unknown						Absent
	82	Vitellogenin		30908959	44000/5.50	20787/5.59	61	Absent
	84	Unknown						Absent
	88	Tat binding protein 7		263099	36000/5.70	51633/5.52	74	Absent
	95	Protein disulfide isomerase	IN-N-S01- 0691-LF	000186374	65000/5.60	27052/5.10	268	Absent
	98	Unknown						Absent
	102	Unknown						Absent
	105	Heat shock protein 70 kD	AG-N-N01- 0802-W	0000003572	80000/5.6	26393/5.74	236	Absent
	110	Unknown						Absent
	111	Unknown						Absent
	112	Unknown						Absent
	113	Unknown						Absent
	114	Unknown						Absent
	115	Unknown						Absent
	116	Unknown						Absent

DN = chromatogram was not observed during mass spectrometrical analysis

ND = not determined by nanoESI-LC-MS/MS

Dif (fold) = differential expression and the fold change >1.5 is regarded as upregulation, < 0.67 = down regulation, - = comparable protein levels,

Present = proteins that were found in stage II ovaries of eyestalk-ablated broodstock but not in stage IV of ovaries of eyestalk-ablated broodstock.

Absent = proteins that were not found in stage IV ovaries of of eyestalk-ablated broodstock but not in stage II of ovaries of eyestalk-ablated broodstock.

Table 3.4 Characterized protein spots in stage II ovaries of normal and eyestalk-ablated *P. monodon* broodstock.

Spot no.		Protein name N/EA	Clone no.	Gi (N)/(EA)	Observed Mr (Da)/pI (N)/(EA)	Calculated Mr (Da)/pI (N)/(EA)	Masscot Score (N)/(EA)	Dif(fold) / Present
Normal	Eyestalk- ablated							
1		unknown						Present
2		unknown						Present
3		unknown						Present
4		Polymerase (RNA) II(DNA direct) polypeptide	LP-V-S01- 0409-LF	000199976	18000/4.5	20600/8.48	85	Present
5		unknown						Present
6		unknown						Present
7	1	unknown/ unknown						0.35
8	2	unknown/ unknown						-
9		unknown						Present
10	5	Unknown/ unknown						-
11		Cyclic AMP-regulated protein like protein	AG-N-N01- 0644-W	0000002809	18000/5.0	27711/6.15	286	Present
12		unknown						Present
13		unknown						Present
14		unknown						Present
15		unknown						Present
16		unknown						Present
17		unknown						Present
18		unknown						Present
19		unknown						Present
20		Sarcoplasmic Ca ²⁺ binding protein,alpha B and A chain	AG-N-N01- 0210-W	000000897	23500/4.6	27761/5.55	226	Present
21		unknown						Present
22		Translationally controlled tumor protein	AG-N-N01- 0078-W	000000307	24000/4.4	26667/4.52	117	Present
23	35	Unknown/ unknown						-
24	34	Unknown/ unknown						0.5
25		Unknown						Present
26	28	Unknown/Beta thymosin	HC-W-S01- 0050-LF	000147620	22000/5.40	26519/5.45	289	-
27		unknown						Present

Table 3.4 Characterized protein spots in stage II ovaries of normal and eyestalk-ablated *P. monodon* broodstock (cont.)

Spot no.		Protein name N/EA	Clone no.	gi (N)/(EA)	Observed Mr (Da)/pI (N)/(EA)	Calculated Mr (Da)/pI (N)/(EA)	Masscot Score (N)/(EA)	Dif(fold) / Present
Normal	Eyestalk- ablated							
28		Beta actin	HC-N-N01-10367-LF		19000/5.5	27359/6.59	51	Present
29		Intracellular fatty acid binding protein	LP-N-N01-0788-LF	000192873	16500/5.5	21988/7.75	62	Present
30		unknown						Present
31	7	Unknown/ unknown						0.35
32	8	Unknown/ unknown						-
33		unknown						Present
34		Intracellular fatty acid binding protein	LP-N-S01-0246-LF	000196483	16000/6.0	28247/9.05	251	Present
35		unknown						Present
36		Cofilin/actin-depolymerizing factor	HC-H-S01-0582-LF	000072104	19000/6.2	27806/7.25	185	Present
37		unknown						Present
38		unknown						Present
39		unknown						Present
40		unknown						Present
41	15	Unknown/unknown						-
42	13	Unknown/Glutathione peroxidase	GL-H-S01-1009-LF	000023037	24000/6.20	27221/6.59	555	-
43	10	Unknown/unknown						0.44
44		unknown						Present
45		unknown						Present
46		unknown						Present
47		unknown						Present
48	160	Unknown/ unknown						-
49	12	unknown/ Glutathione s-transferase	HPa-N-N04-1530-LF	000177675	26000/6.2	28485/6.27	234	-
50	20	Glutathione-s-transferase/ Glutathione-s-transferase	HPa-N-N04-1530-LF	000177675/ 000177675	(26000/5.98)/ (26000/5.98)	(28485/6.27)/ (28485/6.22)	246/273	0.55
51	21	Unknown/Peroxiredoxin 4	OV-N-S01-0549-W	00021938	27000/6.0	24378/5.96	58	0.36
52	19	Triose-phosphate isomerase/ Triose-phosphate isomerase	HC-N-N01-11301-LF HC-N-N01-9543-LF	000085996/ 000139250	(26000/6.0)/ (26000/6.0)	(26634/6.22)/ (26449/6.30)	88/256	2.35
53		Hypothetical peptide transporter ATP- binding protein			37000/5.85	35701/9.59	54	Present

Table 3.4 Characterized protein spots in stage II ovaries of normal and eyestalk-ablated *P. monodon* broodstock (cont.)

Spot no.		Protein name N/EA	Clone no.	gi (N)/(EA)	Observed Mr (Da)/pI (N)/(EA)	Calculated Mr (Da)/pI (N)/(EA)	Masscot Score (N)/(EA)	Dif(fold) / Present
Normal	Eyestalk- ablated							
54	18	Unknown/Glutathione peroxidase	IN-N-S01-1245-LF	000189297	24500/5.85	25178/5.78	226	0.52
55	23	Unknown/unname protein product	OV-N-S01-1944-W	000226831	25000/5.7	28884/11.88	67	1.54
56		Unknown						Present
57		Beta thymosin	HC-N-N01-7394-LF	000127904	26000/5.95	27660/6.65	109	Present
58		2-cys thioredoxin peroxidase	OV-N-S01-0212-W	000217496	26500/5.93	25235/6.41	171	Present
59	31	Unknown/2-cys thioredoxin peroxidase	OV-N-S01-0212-W	000217496	25000/5.35	23660/5.49	340	0.66
60	33	Unknown/ unknown						0.24
61		unknown						Present
62	37	Unknown/ similar to Proteasome subunit α type 5	HC-N-S01-0111-LF	000141763	27500/5.1	27887/7.18	54	-
63		unknown						Present
64		unknown						Present
65	38	Unknown/beta-NAC-like protein	HC-N-N01-13561-LF	000097041	28000/5.4	26425/4.58	68	0.3
66		unknown						Present
67	39	Unknown/es1 protein	OV-N-N01-0895-W	000211011	27000/5.5	25409/6.23	71	0.3
68	40	Unknown/beta thymosin	GIEp-N-N01-2428-LF	000049202	29000/5.6	27345/6.11	342	-
69	43	Unknown/Carbonic anhydrase	OV-N-N01-1186-W	000212702	29000/5.75	26967/5.79	111	0.28
70	41	Unknown/Proteasome subunit α type	LP-N-N01-0262-LF	000190425	29500/5.70	20323/6.06	98	-
74	42	Unknown/Cytosolic manganese superoxide dismutase	OV-N-S01-0378-W	000218419	30000/5.75	26967/5.79	225	-
75	44	Unknown/Hypothetical protein	HC-V-S01-0348-LF	000146544	31500/6.05	27238/9.65	50	-
79	50	Unknown/unknown						5.42
80	52	Unknown/Ubiquitin carboxyl-terminal hydrolase L5-like protein	GIEp-N-N01-0730- LF	000039213	36000/6.05	28104/9.55	157	2.36
81	51	Unknown/26S proteasome non ATPase regulatory isoform A subunit 14	GIEp-N-N01-1990- LF	000046617	36500/6.15	27226/7.77	189	5.14
82	61	Unknown/Hypothetical protein	GIEp-N-N01-0073- LF	000035965	38500/6.05	27401/7.7	138	-
84	62	unknown/ similar to aldo-keto reductase	HC-N-S01-0103-LF	000141719	37000/5.9	28487/8.94	75	-

Table 3.4 Characterized protein spots in stage II ovaries of normal and eyestalk-ablated *P. monodon* broodstock (cont.)

Spot no.		Protein name N/EA	Clone no.	gi (N)/(EA)	Observed Mr (Da)/pI (N)/(EA)	Calculated Mr (Da)/pI (N)/(EA)	Masscot Score (N)/(EA)	Dif(fold) / Present
Normal	Eyestalk- ablated							
89	47	Unknown/unknown						-
90	46	Unknown/ unknown						2.09
93	72	Unknown/unknown						-
97	75	Unknown/Vitellogenin precursor unknown	OV-N-S01-0317-W	000218095	40000/5.45	27438/9.02	57	-
99								Present
100	65	Unknown/ transaldolase unknown	HC-N-N01-5537-LF	000117451	37000/5.63	25248/5.92	234	0.57
101		unknown						Present
102		unknown						Present
103		unknown						Present
104		unknown						Present
105		Transaldolase	HC-N-N01-5537-LF	000117451	41000/5.65	25248/5.92	181	Present
107		Alcoholdehydrogenase	OV-N-S01-0682-W	000220107	43000/5.70	26981/5.41	261	Present
108	67	Hypothetical protein/ Hypothetical protein	GIEp-N-N01-0985-LF HC-N-N01-8339-LF	000040682/ 000133175	(40000/5.75)/ (40000/5.75)	(29498/8.61)/ (29234/8.75)	54/91	0.27
109		Actin D	HC-N-N01-5201-LF		44000/5.65	27053/5.54	124	Present
110		Actin 2	AG-N-N01-0779-W		44500/5.80	26914/4.85	135	Present
111		unknown						Present
112	109	Unknown/unknown						-
113		unknown						Present
114	108	Adenosine kinase/unknown	HPA-N-N01-0792-LF		43000/5.90	24514/9.72	54	-
115	59	Unknown/unknown						-
116	57	Arginine kinase/Arginine kinase	GIEp-N-N01-0368-LF AG-N-N01-1003-W	000037477/ 0000004411	(40000/6.4)/ (40000/6.4)	(28024/8.72)/ (28557/7.83)	519/460	0.51
117	56	Arginine kinase/Allergen pen m 2	AG-N-N01-1003-W HC-N-N01-9647-LF	0000004411/ 000139652	(42000/6.55)/ (42000/6.55)	(28557/7.83)/ (27877/7.84)	939/685	-
118	55	Allergen pen m 2/unknown	HC-N-N01-9647-LF	000139652	42000/6.75	27877/7.84	357	9.49
119		Glyceraldehyde 3 phosphate dehydrogenase	GL-H-S01-0663-LF	000021673	33500/6.90	25544/6.38	250	Present

Table 3.4 Characterized protein spots in stage II ovaries of normal and eyestalk-ablated *P. monodon* broodstock (cont.)

Spot no.		Protein name N/EA	Clone no.	gi (N)/(EA)	Observed Mr (Da)/pI (N)/(EA)	Calculated Mr (Da)/pI (N)/(EA)	Masscot Score (N)/(EA)	Dif(fold) / Present
Normal	Eyestalk- ablated							
119		Glyceraldehyde 3 phosphate dehydrogenase	GL-H-S01-0663-LF	000021673	33500/6.90	25544/6.38	250	Present
120		Putative fructose 1,6-bisphosphate aldolase	HC-H-S01-0323-LF	000070615	44000/6.90	28601/6.67	80	Present
121		Phosphopyruvate hydratase		3885968	51000/6.2	47805/6.18	696	Present
122	133	Phosphopyruvate hydratase/ Phosphopyruvate hydratase	HC-H-S01-0713-LF HC-N-N01-10611- LF	000072865/ 000082116	(50000/6.60) (50000/6.65)	(28432/5.26)/ (28453/9.07)	405/69	3.13
123	136	Spermatogonial stem cell renewal factor/unknown	HC-H-S01-0581-LF	000072097	45000/6.55	26986/6.02	256	-
124	135	Phosphoglycerate kinase/unknown	HC-N-N01-12748- LF	000093100	45000/6.50	272874/9.45	172	2.52
125	132	Phosphopyruvate hydratase/unknown	HC-H-S01-0713-LF	000072865	50000/6.45	28432/5.26	110	0.5
126	129	NADH-specific isocitrate dehydrogenase/ NADH-specific isocitrate dehydrogenase	OV-N-S01-1780-W OV-N-S01-1780-W	000225962/ 000225962	(45000/6.45)/ (45000/6.45)	(27118/5.37)/ (27909/8.09)	264/223	-
127	126	unknown/ unknown						-
128	125	Adenosylhomocysteinase / unknown		72110134	44000/6.35	48061/5.89	78	5.82
129		Adenosylhomocysteinase	OV-N-S01-1595-W	000225037	45000/5.85	27118/5.37	249	Present
130		Beta actin	HC-N-N01-1004-LF	000079292	45000/5.75	30042/5.14	101	Present
131		Beta actin	HC-N-N01-1092-LF	000083835	45000/5.70	30042/5.14	322	Present
132		Beta actin	HC-N-S01-0525-LF	000143936	50000/5.50	34171/5.81	67	0.65
133		Beta actin	HC-N-N01-1092-LF	000083835	48000/5.60	30042/5.14	56	Present
134		unknown						Present
135	104	rab gdp-dissociation inhibitor/ rab gdp-dissociation inhibitor	HC-N-N01-4554-LF HC-N-N01-8951-LF	000111854	(50000/5.75)/ (50000/5.75)	(23862/6.62)/ (27346/6.50)	129/86	0.63
136		Unknown						Present
137	110	Methylmalomate-semialdehyde dehydrogenase/ Methylmalomate- semialdehyde dehydrogenase	OV-N-S01-0565-W AG-N-N01-0077-W	00021947	(54000/5.85)/ (54000/5.85)	(27233/5.14)/ (26937/6.18)	88/83	0.63

Table 3.4 Characterized protein spots in stage II ovaries of normal and eyestalk-ablated *P. monodon* broodstock (cont.).

Spot no.		Protein name N/EA	Clone no.	gi (N)/(EA)	Observed Mr (Da)/pI (N)/(EA)	Calculated Mr (Da)/pI (N)/(EA)	Masscot Score (N)/(EA)	Dif(fold) / Present
Normal	Eyestalk- ablated							
138	111	Tubulin beta-1 chain /unknown	HC-N-S01-0037-LF	000141337	55000/5.85	33568/6.44	83	0.38
140		unknown						Present
141		unknown						Present
142		Unknown						Present
143		chaperonin containing TCP1 subunit 5		72007609	65000/5.95	60145/5.88	89	Present
144	113	chaperonin containing TCP1 subunit 5/chaperonin containing TPC1 subunit 5	HC-N-N01-7872-LF HC-N-N01-7872-LF	000130592/ 000130592	(60000/5.95)/ (60000/5.95)	(26006/4.94)/ (26006/4.94)	60/85	0.3
145		unknown						Present
146		unknown						Present
148		Hemocyanin		854403	65000/5.65	74992/5.27	118	Present
149	139	Hemocyanin/ unknown	HPa-N-S01-0106-LF	000179787	65000/5.55	28981/5.77	112	0.45
150	116	Protein disulfide isomerase/ Protein disulfide isomerase	OV-N-S01-0764-W OV-N-S01-0764-W	000220555/ 000220555	(59000/5.70)/ (60000/5.80)	(29075/5.60)/ (29075/5.60)	418/435	0.54
151	114	Unknown/Pyrroline-5-carboxylate dehydrogenase	GIEp-N-N01-2568-W	000050030	59500/5.95	26690/8.0	97	0.30
152		chaperonin containing TCP1, subunit 2		5453603	60000/5.45	57794/6.01	82	Present
153		chaperonin containing TCP1, subunit 2	LP-N-S01-0061-LF	000195548	60000/5.4	27691/9.22	245	Present
154		Hsp60 protein, putative	TT-N-S01-0846-W	000236557	60000/5.25	26532/5.11	336	Present
155		Cytochrome b	HPa-N-N03-1765-LF	000167002	66000/5.2	23867/10.39	52	Present
156		Tubulin beta-2 chain		3915093	60000/5.19	51354/4.85	1018	Present
157		Tubulin beta-1 chain	HC-N-S01-0037-LF	000141337	54000/5.1	33568/6.44	722	Present
158	97	unknown/unknown						0.37
159		Tat-binding protein-1	OV-N-S01-1291-W	000223407	49000/5.25	27220/4.58	354	Present
160		unknown						Present
161	101	Unknown/ Dynactin subunit 2	HPa-N-N04-1190-LF	000175801	50000/5.60	26646/5.90	58	0.5
163	81	Beta actin/ Beta actin	HC-N-N01-1092-LF	000083835/ 000083835	(44000/5.4)/ (44000/5.55)	(30042/5.14)/ (30042/5.14)	535/567	1.63

Table 3.4 Characterized protein spots in stage II ovaries of normal and eyestalk-ablated *P. monodon* broodstock (cont.)

Spot no.		Protein name N/EA	Clone no.	gi (N)/(EA)	Observed Mr (Da)/pI (N)/(EA)	Calculated Mr (Da)/pI (N)/(EA)	Masscot Score (N)/(EA)	Dif(fold) / Present
Normal	Eyestalk- ablated							
164	82	Beta actin/ Beta actin	HC-N-N01-1092-LF HC-N-S01-0525-LF	000083835/ 000143936	(44000/5.50) / (44000/5.50)	(30042/5.14)/ (34171/5.81)	809/98	-
165		unknown						Present
166		Putative 40S ribosomal protein	HC-N-N01-13854-LF	000098347	43500/4.90	27102/6.51	159	Present
167		Putative 40S ribosomal protein	AG-N-N01-0263-W	0000001143	44000/4.85	27096/9.82	159	Present
168		Unknown						Present
169		unknown						Present
170		unknown						Present
171		Unknown						Present
172		unknown						Present
173		Unknown						Present
174		unknown						Present
175		unknown						Present
176		Beta actin	HC-N-S01-0525-LF	000143936	31000/5.05	34171/5.81	67	Present
177		unknown						Present
178		unknown						Present
179		unknown						Present
180	141	Chromobox protein homolog 1/unknown	OV-N-S01-1463-W	000224391	31000/4.55	27869/5.17	70	-
181		unknown						Present
182		unknown						Present
183		unknown						Present
184		Proliferating cell nuclear antigen	OV-N-N01-0805-W	000210488	36000/4.70	27144/5.0	472	Present
185		unknown						Present
186		unknown						Present
187		unknown						Present
188		unknown						Present
189		Retinoblastoma binding protein 4	OV-N-S01-2043-W	000227384	54000/4.80	27401/5.43	60	Present

Table 3.4 Characterized protein spots in stage II ovaries of normal and eyestalk-ablated *P. monodon* broodstock (cont.)

Spot no.		Protein name N/EA	Clone no.	Accession no. (N)/(EA)	Observed Mr (Da)/pI (N)/(EA)	Calculated Mr (Da)/pI (N)/(EA)	Masscot Score (N)/(EA)	Dif(fold) / Present
Normal	Eyestalk- ablated							
190	92	F1-ATP synthase beta subunit/DN	OV-N-S01- 1723-W	000225709	52500/4.80	26036/4.81	446	3.43
191	93	F1-ATP synthase beta subunit/unknown	OV-N-S01- 1723-W	000225709	52500/4.90	26036/4.81	454	0.62
192		Protein disulfid isomerase	OV-N-S01- 1221-W	000223015	53500/4.70	28064/4.66	563	Present
193		unknown						Present
194		unknown						Present
195		Glycoprotein 93 CG5520-PA	OV-N-N01- 0023-W	000205923	97000/4.85	28011/4.70	466	Present
196		Valosin containing protein-1	HC-N-N01- 5012-LF	000114465	75000/5.40	27017/5.30	85	Present
198		Valosin containing protein-1	HC-N-N01- 5012-LF	000114465	75000/5.40	27017/5.30	85	Present
199		unknown						Present
200	144	Unknown/ unknown						-
201		unknown						Present
202		unknown						Present
203		unknown						Present
204		unknown						-
205		unknown						Present
206		Beta tubulin	HC-N-S01- 0150-LF	000141985	56500/5.70	36348/9.97	69	Present
207		unknown						Present
210		unknown						Present
211		unknown						Present
212		unknown						Present
213		unknown						Present
215		unknown						Present

Table 3.4 Characterized protein spots in stage II ovaries of normal and eyestalk-ablated *P. monodon* broodstock (cont.)

Spot no.		Protein name N/EA	Clone no.	gi (N)/(EA)	Observed Mr (Da)/pI (N)/(EA)	Calculated Mr (Da)/pI (N)/(EA)	Masscot Score (N)/(EA)	Dif(fold) / Present
Normal	Eyestalk- ablated							
	11	Glutathione peroxidase	IN-N-S01-1245-LF	000189297	24000/6.4	25178/5.78	94	Absent
	14	Glutathione peroxidase	IN-N-S01-1245-LF	000189297	20000/6.0	25178/5.78	271	Absent
	16	unknown						Absent
	17	Proteasome subunit beta type I	TT-N-S01-0369-W	000234396	25000/5.85	19494/5.09	66	Absent
	22	hydroxyacylglutathione hydrolase	HC-H-S01-0325-LF	000070627	27000/6.10	21088/6.13	67	Absent
	24	unknown						Absent
	25	Beta thymosin	OV-N-S01-1085-W	000222248	20500/5.85	14784/5.35	59	Absent
	26	Glutathione peroxidase	IN-N-S01-1245-LF	000189297	22000/5.6	25178/5.78	115	Absent
	27	Beta thymosin	GIEp-N-S01-1318-LF	000058975	20000/5.5	26091/6.09	188	Absent
	29	Glyoxylase 1	OV-N-S01-1440-W	000224263	21000/5.48	28333/6.51	139	Absent
	30	Scavenger receptor cysteine protein precursor	IN-N-S01-1294-LF	000189569	24000/5.48	22358/10.30	51	Absent
	32	Heat shock protein 21.4	OV-N-N01-0298-LF	000207530	24000/5.4	25851/7.16	126	Absent
	36	unknown						Absent
	45	unknown						Absent
	48	unknown						Absent
	49	unknown						Absent
	53	L-3-Hydroxyacyl-coenzyme A dehydrogenase	OV-N-N01-1642-W	000215317	31500/6.65	26197/9.30	119	Absent
	54	unknown						Absent
	58	Arginine kinase	AG-N-N01-1003-W	000000441	40000/6.2	28250/7.83	47	Absent
	60	Alcohol dehydrogenase	OV-N-S01-0682-W	000220107	40000/6.15	26981/5.41	55	Absent

Table 3.4 Characterized protein spots in stage II ovaries of normal and eyestalk-ablated *P. monodon* broodstock (cont.)

Spot no.		Protein name N/EA	Clone no.	gi (N)/(EA)	Observed Mr (Da)/pI (N)/(EA)	Calculated Mr (Da)/pI (N)/(EA)	Masscot Score (N)/(EA)	Dif(fold) / Present
Normal	Eyestalk- ablated							
	63	Heterogeneous nuclear ribonucleoprotein	HC-H-S01-0995-LF	000074481	38000/5.8	26095/5.28	82	Absent
	64	Heterogeneous nucleare ribonucleoprotein	HC-H-S01-0995-LF	000074481	38500/5.70	26095/5.26	71	Absent
	66	Alcohol dehydrogenase	OV-N-S01-0682-W	000220107	40000/5.8	26981/5.41	105	Absent
	68	Heterogeneous nucleare ribonucleoprotein	HC-H-S01-0995-LF	000074481	39500/5.75	26095/5.28	71	Absent
	69	unknown						Absent
	70	heterogeneous nuclear ribonucleoprotein	HC-H-S01-0995-LF	000074481	32000/5.5	26095/5.28	60	Absent
	71	Cystein proteinase	LP-N-S01-0217-LF	000196323	32500/5.4	28940/6.08	185	Absent
	74	unknown						Absent
	76	Ovarian peritrophin	OV-N-S01-0206-W	000217459	39000/5.35	29830/6.82	177	Absent
	77	Ovarian peritrophin	OV-N-S01-0206-W	000074481	39000/5.28	29830/6.82	192	Absent
	78	unknown						Absent
	79	unknown						Absent
	80	Beta actin	HC-N-N01-1092-LF	000083835	43000/5.4	30042/5.14	137	Absent
	83	RAN-binding protein	GIEp-N-N01-0595- LF	000038517	38000/5.5	27523/4.75	128	Absent
	84	Epa4p	OV-N-N01-0835-W	000210671	36000/5.05	28834/4.78	271	Absent
	85	Histidine-rich glycoprotein precursor	HC-N-N01-8689-LF	000135068	35500/5.29	27499/9.39	48	Absent
	86	Ovarian peritrophin	OV-N-S01-0329-W	000218168	36000/5.2	31222/5.15	155	Absent
	87	Epa4p	OV-N-N01-0835-W	000210671	36000/5.15	28834/4.78	374	Absent
	88	Ovarian peritrophin 2 precursor	OV-N-S01-0396-W	000218515	36000/4.85	31792/5.70	149	Absent
	89	Calreticulin	OV-N-N01-1274-W	000213225	65000/4.40	27853/4.91	67	Absent
	90	unknown						Absent
	91	Protein disulfide isomerase	OV-N-S01-2641-W	000230209	60000/4.8	26214/4.7	602	Absent
	94	Tubulin beta-1 chain	HC-W-S01-0062-W	000147681	57000/5.39	28353/5.06	202	Absent
	95	60 kDa heat shock protein	OV-N-N01-0358-W	000207891	60000/5.3	26264/5.28	95	Absent
	98	Tat-binding protein-1	HC-N-N01-4075-LF	000109328	52000/5.39	27220/5.03	125	Absent
	99	Protein disulfide isomerase	OV-N-S01-0893-W	000221197	50000/5.39	28808/8.25	669	Absent

Table 3.4 Characterized protein spots in stage II ovaries of normal and eyestalk-ablated *P. monodon* broodstock (cont.)

Spot no.		Protein name N/EA	Clone no. Eyestalk-ablated	gi (N)/(EA)	Observed Mr (Da)/pI (N)/(EA)	Calculated Mr (Da)/pI (N)/(EA)	Masscot Score (N)/(EA)	Dif(fold) / Present
Normal	Eyestalk- ablated							
	100	Protein disulfide isomerase	LP-N-N01-1193-LF	000194648	51000/5.5	22261/8.61	155	Absent
	102	mitochondrial aldehyde dehydrogenase 2	OV-N-S01-1601-W	000225074	54000/5.6	26678/5.63	66	Absent
	103	D-lactate dehydrogenase	HC-N-N01-11562-LF	000087493	54000/5.70	30042/5.14	51	Absent
	105	unknown						Absent
	106	Acyl-co A dehydrogenase long chain	GIep-N-S01-0329-LF	000053546	47000/5.80	26118/9.10	52	Absent
	107	unknown						Absent
	112	Transketolase	OV-N-S01-2094-W	000227631	65000/6.05	26683/5.35	198	Absent
	115	Protein disulfide isomerase	OV-N-S01-0764-W	000220555	60000/5.85	29075/5.6	274	Absent
	117	Protein disulfide isomerase	OV-N-S01-0764-W	000220555	60000/5.70	29075/5.6	495	Absent
	118	unknown						Absent
	119	unknown						Absent
	120	unknown						Absent
	122	unknown						Absent
	123	unknown						Absent
	124	unknown						Absent
	127	unknown						Absent
	128	2-keto-4-pentanoate hydrolase		67643902	47000/6.40	47355/5.70	80	Absent
	130	RAB, member of RAS	GL-N-S01-1414-LF	000029541	60000/6.5	26652/6.06	105	Absent
	131	Glutamate carboxypeptidase	OV-N-S01-0878	000221132	54000/6.55	27740/6.82	98	Absent
	134	unknown						Absent
	137	unknown						Absent
	138	unknown						Absent
	140	unknown						Absent
	142	unknown						Absent
	143	unknown						Absent
	145	unknown						Absent
	146	unknown						Absent
	147	unknown						Absent
	148	unknown						Absent
	149	unknown						Absent
	150	unknown						Absent

Table 3.4 Characterized protein spots in stage II ovaries of normal and eyestalk-ablated *P. monodon* broodstock (cont.)

Spot no.		Protein name N/EA	Clone no.	gi (N)/(EA)	Observed Mr (Da)/pI (N)/(EA)	Calculated Mr (Da)/pI (N)/(EA)	Masscot Score (N)/(EA)	Dif(fold) / Present
Normal	Eyestalk- ablated							
	151	unknown						Absent
	152	unknown						Absent
	153	unknown						Absent
	154	unknown						Absent
	155	unknown						Absent
	156	unknown						Absent
	157	unknown						Absent
	158	unknown						Absent
	159	unknown						Absent
	161	unknown						Absent
	162	unknown						Absent
	163	unknown						Absent
	164	unknown						Absent
	165	Vitellogenin		82754321	67000/6.70	285804/6.91	231	Absent
	166	unknown	HC-N-N01-12416-LF	000091071			60	Absent
	167	Vitellogenin		45774386	67000/6.60	285335/6.55	382	Absent
	168	Elongation facctor	GIep-N-S01-1165-LF	000058229	90000/6.55	29380/10.32	51	Absent
	169	unknown	ES-N-S02-0160-W	000010178	90000/6.50	24437/9.95	72	Absent
	170	Elongation facctor	GIep-N-S01-1165-LF	000058229	90000/6.40	29380/10.32	56	Absent
	171	Vitellogenin		239559444	67000/6.40	289032/5.42	64	Absent
	172	Thrombospondin	OV-N-ST01-0130-W	000230801	90000/6.28	24111/10.02	78	Absent
	161	unknown						Absent
	162	unknown						Absent
	163	unknown						Absent
	164	unknown						Absent
	165	Vitellogenin		82754321	67000/6.70	285804/6.91	231	Absent
	166	unknown	HC-N-N01-12416-LF	000091071			60	Absent
	167	Vitellogenin		45774386	67000/6.60	285335/6.55	382	Absent
	168	Elongation facctor	GIep-N-S01-1165-LF	000058229	90000/6.55	29380/10.32	51	Absent
	169	unknown	ES-N-S02-0160-W	000010178	90000/6.50	24437/9.95	72	Absent
	170	Elongation facctor	GIep-N-S01-1165-LF	000058229	90000/6.40	29380/10.32	56	Absent

Table 3.4 Characterized protein spots in stage II ovaries of normal and eyestalk-ablated *P. monodon* broodstock (cont.)

Spot no.		Protein name N/EA	Clone no.	gi (N)/(EA)	Observed <i>Mr</i> (Da)/ <i>pI</i> (N)/(EA)	Calculated <i>Mr</i> (Da)/ <i>pI</i> (N)/(EA)	Masscot Score (N)/(EA)	Dif(fold) / Present
Normal	Eyestalk- ablated							
	171	Vitellogenin		239559444	67000/6.40	289032/5.42	64	Absent
	172	Thrombospondin	OV-N-ST01-0130-W	000230801	90000/6.28	24111/10.02	78	Absent
	173	Thrombospondin	OV-N-ST01-0130-W	000230801	90000/6.80	24111/10.02	60	Absent
	174	unknown						Absent
	175	unknown						Absent
	176	unknown						Absent
	177	unknown						Absent
	178	unknown						Absent
	179	unknown						Absent
	180	similar to Heat shock 70 kD protein cognate	HC-N-N01-1119-LF	000085430	90000/5.20	28504/5.11	164	Absent

DN = chromatogram was not observed during mass spectrometrical analysis; ND = not determined by nanoESI-LC-MS/MS; Dif (fold) = differential expression and the fold change >1.5 is regarded as upregulation, < 0.67 = down regulation, - = comparable protein levels; Present = proteins that were found in stage II ovaries of normal broodstock but not in the same stage of eyestalk-ablated broodstock; Absent = proteins that were found in stage II ovaries of eyestalk-ablated broodstock but not in the same stage of normal broodstock

ศูนย์วิทยทรัพยากร
จุฬาลงกรณ์มหาวิทยาลัย

Table 3.5 Characterized protein spots in stage IV ovaries of normal and eyestalk-ablated *P. monodon* broodstock.

Spot no.		Protein name N/EA	Clone no.	Gi (N)/(EA)	Observed Mr (Da)/pI (N)/(EA)	Calculated Mr (Da)/pI (N)/(EA)	Masscot Score (N)/(EA)	Dif(fold) / Present
Normal	Eyestalk- ablated							
2		unknown						Present
3		unknown						Present
4		unknown						Present
5		unknown						Present
6		unknown						Present
7		unknown						Present
8	90	Unknown/ unknown						-
9		unknown						Present
10		unknown						Present
11		Protein disulfide isomerase	IN-N-S01-0691-LF	000186374	55000/5.5	27052/5.10	61	Present
12	93	Protein disulfide isomerase / Protein disulfide isomerase	OV-N-S01-0764-W IN-N-S01-0691-LF	000220555/ 000186374	(60000/5.7)/ (60000/5.7)	(29075/5.60)/ (29705/5.60)	712/491	-
13	94	Protein disulfide isomerase / Protein disulfide isomerase	OVN-S01-0764-W IN-N-S01-0691-LF	000220555/ 000186374	(65000/5.6)/ (65000/5.6)	(29075/5.60)/ (27052/5.10)	316/268	0.23
14		unknown						Present
15		Pyrroline-5-carboxylate dehydrogenase	GlEp-N-N01-2568-LF	000050030	59000/5.8	26690/8.0	65	Present
17	113	unknown/ND						-
18	114	unknown/ ND						-
19	99	unknown/unknown						-
20	70	Unknown/Phosphoglycerate kinase	HC-N-N01-12748-LF	000093100	51000/6.50	27874/9.40	74	-
21		Mitochondrial aldehyde dehydrogenase 2	OV-N-S01-1601-W	000225074	50000/5.1	26678/5.63	59	Present
22	84	Mitochondrial aldehyde dehydrogenase 2 /unknown	OV-N-S01-1601-W	000225074	50000/5.6	26678/5.63	96	0.34
23		Hypothetical protein	GlEp-N-N01-2817-LF	000051477	52000/5.6	26517/8.67	48	Present
24		unknown						Present
25	111	unknown/unknown						Present
26		Methylmalonate-semialdehyde dehydrogenase	OV-N-S01-0565-W	000219471	52000/5.7	27233/5.41	79	Present
27	83	unknown/unknown						-
28		unknown						Present

Table 3.5 Characterized protein spots in stage IV ovaries of normal and eyestalk-ablated *P. monodon* broodstock (cont.)

Spot no.		Protein name N/EA	Clone no.	gi (N)/(EA)	Observed Mr (Da)/pI (N)/(EA)	Calculated Mr (Da)/pI (N)/(EA)	Masscot Score (N)/(EA)	Dif(fold) / Present
Normal	Eyestalk- ablated							
	29	unknown						Present
	30	unknown						Present
	31	Putative conjugal transfer protein		116250544	44000/6.05	170011/6.29	74	Present
	33	75 Unknown/ acyl coenzyme A dehydrogenase	OV-N-N01-0061-W	000206138	42000/6.0	26682/5.44	128	0.1
	34	unknown						Present
	35	78 unknown/26s protease regulatory subunit 7	HC-N-N01-7411-LF	000127992	48000/6.0	27698/9.06	97	-
	36	unknown						Present
	37	unknown						Present
	38	unknown						Present
	39	unknown						Present
	40	Protein disulfide isomerase	LP-N-N01-1193-LF	000194648	29000/5.6	27345/6.11	104	Present
	41	unknown						Present
	42	87 Tat binding protein 7/DN		263099	46000/5.28	51635/5.52	63	-
	43	57 Beta-actin/unknown	HC-N-N01-1092-LF	000083835	44000/5.50	30042/5.14	408	-
	44	Alcohol dehydrogenase	OV-N-S01-0682-W	000220107	42500/5.65	26981/5.41	56	Present
	45	Hypothetical protein	LP-V-S01-0528-LF	000200635	41000/5.75	27243/6.05	206	Present
	46	unknown						Present
	47	unknown						Present
	48	41 unknown/ Hypothetical protein	GIEp-N-N01-0073-LF	000035965	38500/6.05	27401/7.70	133	21.88
	49	unknown						Present
	50	Unknown						Present
	52	39 unknowon/26s proteasome non- ATPase regulatory isoform A subunit 14	GIEp-N-N01-1990-LF	000046617	36500/5.9	28104/9.5	70	-
	53	38 unknown/Protein henna	GIEp-N-S01-0628-LF	000055195	35000/5.95	27992/11.69	51	-
	54	L-3-hydroxyacyl-CO A dehydrogenase	OV-N-N01-1642-W	000215371	34000/6.25	26197/9.3	59	Present
	55	unknown						Present

Table 3.5 Characterized protein spots in stage IV ovaries of normal and eyestalk-ablated *P. monodon* broodstock (cont.)

Spot no.		Protein name N/EA	Clone no.	gi (N)/(EA)	Observed Mr (Da)/pI (N)/(EA)	Calculated Mr (Da)/pI (N)/(EA)	Masscot Score (N)/(EA)	Dif(fold) / Present
Normal	Eyestalk- ablated							
56		unknown			39000/6.2	29885/9.25	62	Present
57		Arginine kinase	AG-N-N01-0619-W	0000002692	42000/6.55	28261/8.80	255	Present
58		Arginine kinase	AG-N-N01-1003-W	0000004411	41000/6.29	28557/7.83	50	Present
59		unknown						Present
60		unknown						Present
61		unknown						Present
62		unknown						Present
63		unknown						Present
64		unknown						Present
65	30	unknown/ electron transfer flavoprotein	HC-N-N01-0997-LF	000079053	32500/5.70	27958/8.4	217	2.68
66	28	unknown/unknown						-
67	27	Cytosolic manganese superoxide dismutase/ Cytosolic manganese superoxide dismutase	HC-V-S01-0153-LF	000218419/ 000218419	(30000/5.6)/ (30000/5.6)	(34293/6.19) / (34293/6.19)	98/98	0.41
68	26	unknown/ Carbonic anhydrase	GL-H-S01-0060-LF	000018685	29000/5.65	24565/6.19	50	9.38
69	25	unknown/ Proteasome subunit α type	LP-N-N01-0262-LF	000190425	29500/5.5	20323/6.06	95	-
70	47	Unknown/DN						1.86
71		Hypothetical protein	TT-N-S01-0372-W	000234403	38500/5.35	24360/9.32	61	Present
72		secreted inorganic pyrophosphatase, putative	OV-N-N01-0542-W	000208952	36000/5.3	26955/6.42	96	Present
73		unknown						
74	51	Unknown/ RAB3 GTPase-activating protein	ES-N-S03-0709-W	000015846	35000/4.50	27302/9.85	66/74	-
75		unknown						Present
76	53	Unknown/Epa4p	IN-N-S01-0852-LF	000187270	38000/5.05	28834/4.78	281	1.92
77	55	Ovarianperitrophin 2 precursor/ Ovarian peritrophin 2 precursor	OV-N-S01-0389-W OV-N-S01-0786-W	000218474/ 000210374	(36000/4.85)/ (36000/4.85)	(31441/5.0)/ (28726/4.92)	216/93	-
78		Ovarianperitrophin2precursor	OV-N-S01-0396-W	000218515	36500/4.7	31792/5.70	121	Present

Table 3.5 Characterized protein spots in stage IV ovaries of normal and eyestalk-ablated *P. monodon* broodstock (cont.)

Spot no.		Protein name N/EA	Clone no.	gi (N)/(EA)	Observed Mr (Da)/pI (N)/(EA)	Calculated Mr (Da)/pI (N)/(EA)	Masscot Score (N)/(EA)	Dif(fold) / Present
Normal	Eyestalk- ablated							
78		Ovarianperitrophin2precursor	OV-N-S01-0396-W	000218515	36500/4.7	31792/5.70	121	Present
79		Peritrophin 3 precursor/unknown	OV-N-N01-0689-W	000209805	37000/4.65	29164/5.17	127	-
80		unknown						Present
81		Chromobox protein homolog1	OV-N-S01-1463-W	000224391	31000/4.55	27869/5.17	73	Present
82	107	unknown/unknown						-
83	108	Protein disulfide isomerase/ND	OV-N-S01-1221-W	000223015	53500/5.70	28060/4.66	343	0.083
84		F1-ATP-synthase beta subunit	OV-N-S01-1723-W	000225709	49000/4.9	26036/4.81	246	Present
85	120	Heat shock like protein /ND	OV-N-N01-0015-W	000205873	70000/5.1	27824/4.71	128	-
86		Tubulin beta-1 chain	HC-N-S01-0037-LF	000141337	52000/5.1	33568/6.44	76	Present
87		Proteasome subunit, α type,5	HC-N-N01-12735-LF	000093024	29000/5.0	28421/8.80	105	Present
88		unknown						Present
89	14	Unknown/ es1 protein	HC-H-S01-0335-LF	000070688	(27000/5.5)	(23660/5.49)	288	2.75
90		unknown						Present
91		2-cys-thioredoxin peroxidase	OV-N-S01-1662-W	000225393	25500/5.3	27726/5.3	251	Present
92		unknown						Present
93	17	Unknown/ DN						3.0
94		unknown						Present
95	21	Unknown/Glutathione peroxidase	GL-H-S01-1009-LF	000023037	24500/5.95	27221/6.59	142	2.14
96		Unknown						Present
98	126	Glutathione-s-trasferase/ND	AG-N-N01-0855-W	0000003782	27500/5.85	29371/6.12	77	0.57
100		Triose-phosphate isomerase	OV-N-N01-0364-W	000207925	27000/5.95	16635/6.66	240	Present
101	22	Glutathione peroxidase/ Glutathione peroxidase	GIEp-N-S01-1793-LF IN-N-S01-1245-LF	000061515/ 000189297	(24000/6.2)/ (24000/6.2)	(27384/7.52)/ (25178/6.59)	254/79	-
102		Proteasome subunit type 6 precursor	HC-N-N01-3953-LF	000108639	24000/6.0	26674/5.38	98	Present
103	10	unknown/ Rab3 GTPase-activating protein	HC-H-S01-0575-LF	000072064	22000/6.5	21511/11.29	70	2.5
104		CG10527-like-methyltransferase	IN-N-S01-0718-LF	000186525	19000/6.10	22764/5.89	127	Present
105	8	unknown/ CG10527-like methyltransferase	LP-V-S01-0093-LF	000198230	17000/6.0	22764/5.89	111	4.37
106	7	unknown/ similar to Cofilin/actin depolymerizing factor protein	IN-N-S01-0021-LF	000182905	15000/6.15	15080/5.71	150	-

Table 3.5 Characterized protein spots in stage IV ovaries of normal and eyestalk-ablated *P. monodon* broodstock (cont.)

Spot no.		Protein name N/EA	Clone no.	gi (N)/(EA)	Observed Mr (Da)/pI (N)/(EA)	Calculated Mr (Da)/pI (N)/(EA)	Masscot Score (N)/(EA)	Dif(fold) / Present
Normal	Eyestalk- ablated							
107		unknown						Present
108		Intracellular fatty acid binding protein	LP-N-N01-0938-LF	000193375	16500/5.5	25439/8.84	403	Present
109		unknown						Present
110		unknown						Present
111		Translocation protein Tol B		13473330	14000/5.48	46651/6.69	78	Present
112	3	unknown/unknown	GIep-N-N01-2239-LF	000048077	17000/5.2	29064/9.24	55	-
113		Unknown						Present
114		unknown						Present
115		Translocation protein Tol B		13473330	18500/5.0	46651/6.69	71	Present
116		unknown						Present
117		unknown						Present
118		unknown						Present
119		unknown						Present
120	1	unknown/unknown						-
121		unknown						Present
122		unknown						Present
123		HAD family hydrolase		145590757	27500/6.30	27914/9.04	51	Present
124		unknown						Present
125		unknown						Present
126		Glutathione-s-transferase	AG-N-N01-0855-W	0000003782	28000/6.15	29371/6.12	60	Present
127		HAD family hydrolase		145590757	28500/6.05	27914/9.04	67	Present
128		unknown		223947443	30000/6.10	70395/5.47	67	Present
129		unknown						Present
130		unknown						Present
131		unknown		223947443	24000/5.42	70395/5.47	74	Present
132		Unknown						Present
133		Unknown						Present
134		2-cys-thioredoxin peroxidase	OV-N-N01-0321-W	000207668	24000/5.4	27908/6.51	66	Present
135	127	Unknown/ND						-
136		2-cys-thioredoxin peroxidase	OV-N-N01-0360-W	000207902	26000/5.3	27692/7.07	66	Present
137		Unknown						Present

Table 3.5 Characterized protein spots in stage IV ovaries of normal and eyestalk-ablated *P. monodon* broodstock (cont.)

Spot no.		Protein name N/EA	Clone no.	gi (N)/(EA)	Observed Mr (Da)/pI (N)/(EA)	Calculated Mr (Da)/pI (N)/(EA)	Masscot Score (N)/(EA)	Dif(fold) / Present
Normal	Eyestalk- ablated							
138		unknown						Present
139		unknown						Present
140		NLI interacting factor like phosphatase family protein		118354395	43000/5.25	64193/8.92	63	Present
141		Glutathione peroxidase	GL-H-S01-1009-LF	000023037	25500/5.5	27221/6.59	52	Present
142		Hypothetical protein		123477668	43000/5.5	20547/9.73	63	Present
143		Hypothetical protein		123477668	40000/5.4	20547/9.73	67	Present
144		unknown						Present
145	116	Albumin/ND		30962111	67000/6.75	67862/5.23	165	-
146	117	Unknown/ND						-
148	119	Vitellogenin/ND		45774386	67000/6.50	285335/6.55	368	-
149	101	unknown/ unknown		223947443	54000/5.90	70395/5.47	62	-
150		unknown		223947443	28500/5.90	70395/5.47	66	Present
151		Unknown		223947443	30000/5.9	70395/5.47	63	Present
152	12	Unknown/ unnamed protein product	HC-N-N01-10980-LF	000084186	26000/5.2	27150/4.66	73	1.84
153		unknown						Present
154		unknown						Present
155		unknown						Present
156		unknown						Present
157		Vitellogenin		45774386	72000/6.5	285335/6.55	114	Present
158		unknown						Present
159		unknown						Present
160		unknown						Present
	2	nucleoplasmin isoform 1-like protein	GL-H-S01-0626-LF	000021469	23000/4.5	21693/4.77	72	Absent
	4	Eukaryotic translation initiation factor 5A	HC-H-S01-1060-LF	000074845	17000/5.3	17488/5.71	113	Absent
	6	unknown						Absent
	9	unknown						Absent
	11	unknown						Absent
	13	RAB3 GTPase-activating protein	ES-N-S03-0709-LF	000015846	27500/5.4	27302/9.85	62	Absent
	15	2-cys thioredoxin peroxidase	HC-H-S01-0335-LF	000070688	25000/5.35	23660/5.49	288	Absent

Table 3.5 Characterized protein spots in stage IV ovaries of normal and eyestalk-ablated *P. monodon* broodstock (cont.)

Spot no.		Protein name N/EA	Clone no.	gi. (N)/(EA)	Observed Mr (Da)/pI (N)/(EA)	Calculated Mr (Da)/pI (N)/(EA)	Masscot Score (N)/(EA)	Dif(fold) / Present
Normal	Eyestalk- ablated							
	16	Glyoxylase 1	OV-N-S01-1440-W	000224263	24000/5.4	28333/6.51	114	Absent
	18	Beta thymosin	GIEp-N-S01-1318-LF	000058975	22000/5.4	26091/6.09	56	Absent
	20	Hypothetical protein	HC-N-N01-11847-LF	000088650	20000/5.6	15986/6.96	61	Absent
	23	Glutathione peroxydase	GL-H-S01-1009-LF	000023037	20000/6.20	27221/6.59	69	Absent
	24	Beta thymosin	AG-N-N01-0805-W	0000003585	28000/5.5	26392/5.22	126	Absent
	29	unknown						Absent
	31	Rab3 GTPase-activating protein	ES-N-S03-0709-W	000015846	32000/5.80	27302/9.85	68	Absent
	35	Hydroxyacyl glutathione hydrolase	HC-H-S01-0325-LF	000070627	27000/5.9	21088/6.13	88	Absent
	37	L-3-hydroxyacyl-co A dehydrogenase	OV-N-N01-1642-W	00021537	28000/6.5	26197/9.30	202	Absent
	40	Ubiquitin carboxyl terminal L-5 like- transferase	GIEp-N-N01-0730-LF	000039213	36000/6.05	28401/7.7	70	Absent
	42	aldo-keto-reductase	HC-N-S01-0103-LF	0000141719	37000/5.9	27302/9.85	70	Absent
	43	Heterogeneous nucle- ribonucleoprotein	OV-N-S01-2373-W	000229029	38000/5.75	23374/9.34	133	Absent
	44	Alcohol dehydrogenase	OV-N-S01-0682-W	000220107	40000/5.8	26981/5.14	54	Absent
	45	Heterogeneous nuclear ribonucleoprotein	OV-N-S01-2373-W	000229029	41000/5.55	23374/9.34	112	Absent
	46	Heterogeneous nuclear ribonucleoprotein	HC-N-S01-0995-LF	000074481	(38000/5.6)	(26095/5.28)	68	Absent
	48	Transaldolase	HC-N-N01-5537-LF	000117451	33000/5.0	25248/5.92	110	Absent
	49	Hypothetical protein	OV-N-S01-2630-W	000230155	33000/5.05	25402/9.92	58	Absent
	51	RAB3 GTPase-activating protein	ES-N-S03-0709-W	000015846	36000/5.22	27302/9.85	74	Absent
	52	Rab3 GTPase-activating protein	ES-N-S03-0709-W	000015846	36000/5.05	27302/9.85	66	Absent
	54	RAN binding protein 2	GIEp-N-N01-0595-LF	000038517	32000/4.10	27523/4.75	142	Absent
	56	unknown						Absent
	58	Actin	HC-N-S01-0525-LF	000143936	44000/5.5	34171/5.81	282	Absent
	59	Unknown						Absent
	60	Cysteine proteinase	AG-N-N01-0910-W	0000004005	39000/6.0	28940/8.73	146	Absent
	61	Arginine kinase	AG-N-N01-0154-W	000000634	40000/6.0	28250/8.50	112	Absent
	62	unknown			41000/6.0	28250/8.50	112	Absent
	65	unknown						Absent
	66	unknown						Absent

Table 3.5 Characterized protein spots in stage IV ovaries of normal and eyestalk-ablated *P. monodon* broodstock (cont.)

Spot no.		Protein name N/EA	Clone no.	Gi (N)/(EA)	Observed Mr (Da)/pI (N)/(EA)	Calculated Mr (Da)/pI (N)/(EA)	Masscot Score (N)/(EA)	Dif(fold) / Present
Normal	Eyestalk- ablated							
	67	Hypothetical protein	HC-N-N01-12917-LF	000094112	47500/6.50	28209/8.78	197	Absent
	68	Isocitrate dehydrogenase 2 (NADP+)	OV-N-N01-1170-W	00021605	42000/6.50	28050/9.17	144	Absent
	69	unknown						Absent
	71	Phosphopyruvate hydratase	HC-H-S01-0713-LF	000072865	50000/6.50	28432/5.26	235	Absent
	72	Unknown						Absent
	73	Cytosolic NADP-dependent isocitrate dehydrogenase	GL-H-S01-1073-LF	000023350	40000/6.5	27608/5.09	105	Absent
	74	Fah-prov-protein		32450404	43000/5.5	46978/6.22	97	Absent
	76	elongation factor 2	GIep-N-S01-1165-LF	000058229	45000/6.30	29380/10.32	56	Absent
	79	Unknown						Absent
	80	Unknown						Absent
	81	Unknown						Absent
	82	Vitellogenin		30908959	44000/5.5	20787/5.59	61	Absent
	85	Unknown						Absent
	86	Unknown						Absent
	88	Tat binding protein 7		263099	36000/5.7	51633/5.52	74	Absent
	89	Unknown	HC-H-S01-1014-LF	000074595	57000/5.0	17179/7.97	78	Absent
	91	Unknown						Absent
	95	Protein disulfide isomerase	IN-N-S01-0691-LF	000186374	65000/5.60	27052/5.10	268	Absent
	96	Chaperonin containing TPC1 subunit 5	HC-N-N01-7872-LF	000130592	60000/5.85	20006/7.94	53	Absent
	97	Unknown						Absent
	98	Unknown						Absent
	100	Unknown						Absent
	102	Unknown						Absent
	103	Unknown						Absent
	104	Unknown						Absent
	105	Heat shock protein 70 kD	AG-N-N01-0802-W	0000003572	80000/5.6	26393/5.74	236	Absent
	106	Hemocyanin	HPa-N-N03-0431-LF	000159985	85000/5.90	26527/5.49	100	Absent
	109	Unknown						Absent

Table 3.5 Characterized protein spots in stage IV ovaries of normal and eyestalk-ablated *P. monodon* broodstock (cont.)

Spot no.		Protein name N/EA	Clone no.	Gi (N)/(EA)	Observed Mr (Da)/pI (N)/(EA)	Calculated Mr (Da)/pI (N)/(EA)	Masscot Score (N)/(EA)	Dif(fold) / Present
Normal	Eyestalk- ablated							
	111	Unknown						Absent
	112	Unknown						Absent
	113	Unknown						Absent
	115	Unknown						Absent
	116	Unknown						Absent

DN = chromatogram was not observed during mass spectrometrical analysis

ND = not determined by nanoESI-LC-MS/MS

Dif (fold) = differential expression and the fold change >1.5 is regarded as upregulation, < 0.67 = down regulation, - = comparable protein levels,

Present = proteins that were found in stage IV ovaries of normal broodstock but not in the same stage of eyestalk-ablated broodstock.

Absent = proteins that were not found in stage IV ovaries of eyestalk-ablated broodstock but not in the same stage of normal broodstock.

Table 3.6 A summary of a ovarian proteins of in different stages normal and eyestalk-ablated *P. monodon* broodstock (cont)

Protein name	Group	Total	Normal		Eyestalk-ablated		Remark and biological function
			Stage II	Stage IV	Stage II	Stage IV	
Cytochrome b	1.1	1	+				Transport, electron transport
Polymerase (RNA)II (DNA direct polypeptide)	1.1	1	+				Cellular function
Cyclic AMP-regulated protein like protein	1.1	1	+				Cellular function
Sarcoplasmic Ca ²⁺ binding protein, α B and A chain	1.1	1	+				Calcium homeostasis
Translationally controlled tumor protein	1.1	1	+				Cellular function
Intracellular fatty acid binding protein	1.1	1	+				Transport
Actin D	1.1	1	+				Cellular structure
Actin 2	1.1	1	+				Cellular structure
Adenosine kinase	1.1	1	+				Cellular function
Glyceraldehyde-3-phosphate dehydrogenase	1.1	2	++(2)				Energy production, glycolysis
Putative fructose 1,6-bisphosphate aldolase	1.1	1	+				Energy production, glycolysis
Proliferating cell nuclear antigen	1.1	1	+				Cellular function
Retinoblastoma binding protein 4	1.1	1	+				Cellular function, chromatin remodeling
Valosin containing protein-1	1.1	2	++ (2)				Ovarian development, apoptosis
Spermatogonial stemcell renewal factor	1.1	1	+				Metabolic process, transferase activity
Phosphoglycerate kinase	1.1	1	+				Energy production, glycolysis
Beta tubulin	1.1	1	+				Cellular structure
Chaperonin containing TCP1 subunit 2	1.1	2	++(2)				Chaperone
Glycoprotein 93 CG5520-PA	1.1	1	+				Cellular function
Adenosyl homocysteinase	1.1	1	+				Metabolic process, hydrolase activity
Putative 40s ribosomal protein	1.1	2	+(2)				Cellular function, translation
Allergen pen m 2	1.2	1	+		+		Environment stress, ATP buffering
Tat-binding protein-1	1.2	2	+(1)		+(1)		Catabolic process, protein and ATP binding
Transketolase	1.2	1	+		+		Metabolic process, calcium ion binding
NADH-specific isocitrate dehydrogenase	1.2	1	+		+		Energy production, tricarboxylic cycle
Rab gdp-dissociation inhibitor	1.2	1	+		+		Ovarian development, GTPase activation
Hsp60 protein putative	1.2	1	+		+		Chaperone
Cofilin/actin-depolymerizing factor	1.3	2	+(1)			+(1)	Mass decrease when unilateral ablated, ovarian development
Hemocyanin	1.3	2	+(1)			+(1)	Transport, oxygen transport

Table 3.6 A summary of a ovarian proteins of in different stages normal and eyestalk-ablated *P. monodon* broodstock (cont)

Protein name	Group	Total	Normal		Eyestalk-ablated		Remark and biological process
			Stage II	Stage IV	Stage II	Stage IV	
Chaperonin containing TCP1 subunit 5	1.4	2	+(1)		+(1)	+	Mass increase , chaperone
Transaldolase	1.4	3	+(1)		+(1)	+(1)	Mass decrease, pentose phosphate pathway
Beta thymosin	1.4	5	+(1)		+(4)	++	Mass decrease , cellular structure
HAD family hydrolase	2.1	2		++(2)			Metabolic process, hydrolase activity
NLI interacting factor like phosphatase family protein	2.1	1		+			Metabolic process, hydrolase activity
Secreted inorganic pyrophosphatase	2.1	1		+			Metabolic process, hydrolase activity
Putative conjugal transfer protein	2.1	1		+			Cellular function
Peritrophin 3 precursor	2.1	1		+			Ovarian development
D-lactate dehydrogenase	2.1	1		+			Oxidation reduction
Albumin	2.1	1		+			Transport, lipid binding
Translocation protein TolB	2.1	2		++(2)			Transport, protein transport
Proteasome subunit type 6 precursor	2.1	1		+			Catabolic process, protease activity
Heat shock like protein	2.1	1		+			Chaperone
Pyrroline-5-carboxylate dehydrogenase	2.2	1		+	+		Energy production, praline biosynthetic process
Mitochondrial aldehyde dehydrogenase 2	2.2	2		+(1)	+(1)		Mass increase, metabolic process
Tat binding protein 7	2.3	2		+(1)		+(1)	Mass decreased, ovarian development
CG10527-like-methyltransferase	2.3	1		+		+	Metabolic process, transferase activity
L-3-hydroxyacyl-coenzyme A dehydrogenase	2.4	3		+(1)	+(1)	+(1)	Metabolic process
Ovarian peritrophin 2 precursor	2.4	2		++(1)	+(1)	+	Ovarian development
Cytosolic manganese superoxide dismutase	2.4	2		+(1)	+(1)	+	Mass decrease, oxidation reduction
Glutathione peroxidase	2.4	7		++(2)	+++ (2)	+++ (3)	Mass decrease, oxidation reduction
Alcohol dehydrogenase	2.4	4		+(1)	+++ (3)	+	Mass decrease, catabolic process
proteasome subunit α type 5	2.4	2		+	+(2)	+	Catabolic process, protein ligase activity
F1-ATP synthase beta subunit	3.1	2	++(2)*	+			Energy production, ATP synthesis
Chromobox protein homologue 1	3.1	1	+	+			Cellular function, chromatin binding
Hypothetical peptide transporter ATP-binding protein	3.1	1	+	+			Transport
Glutathione-s-transferase	3.2	3	+(1)	+(1)	+(1)		Catabolic process, transferase activity
Trios-phosphate isomerase	3.2	4	+(1)	+(1)	+(2)		Mass decrease, energy production, glycolysis
Phosphopyruvate hydratase	3.2	2	+(2)	+	+		Energy production, glycolysis
Tubulin beta-1 chain	3.2	3	++(2)	+	+(1)		Mass decrease, cellular structure
Methylmalonate-semialdehyde dehydrogenase	3.2	3	+(1)	+(1)	+(1)		Mass decrease, Metabolic process
Protein disulfide isomerase	3.4	11	++	+++++(5)	++++++(6)	++	Mass decrease and increase, chaperone

Table 3.6 A summary of a ovarian proteins of in different stages normal and eyestalk-ablated *P. monodon* broodstock (cont)

Protein name	Group	Total	Normal		Eyestalk-ablated		Remark and biological function
			Stage II	Stage IV	Stage II	Stage IV	
2-cys-thioredoxin peroxidase	3.4	3	+	+(2)	+(1)	+	Mass increase, oxidation reduction
Beta actin	3.4	10	++++++(7)	+	+++ (3)	+	Mass decrease, cellular structure
Arginine Kinase	3.4	6	+(1)	+(1)	+(2)	+(1)	Mass decrease and pI chang, environment stress
Beta-Nac-like protein	4.1	1			+		Cellular function
Vitellogenin precursor	4.1	1			+		Ovarian development
Dynactin subunit 2	4.1	1			+		Ovarian development
Heterochromatin protein 1 homologue beta	4.1	1			+		Cellular function, mitosis
proteasome subunit beta type I	4.1	1			+		Catabolic process, protease activity
Ovarian peritrophin	4.1	3			+++ (3)		Ovarain development
Histidine-rich glycoprotein precursor	4.1	1			+		Cellular function
Calreticulin	4.1	1			+		Calcium homeostasis
Scavenger receptor cysteine protein precursor	4.1	1			+		Cellular function
Heat shock protein 21.4	4.1	1			+		Chaperone
Glutamate carboxypeptidase	4.1	1			+		Energy production, lysine biosynthetic process
RAB, member of RAS oncogene family-like 5	4.1	1			+		Ovarian development, GTPase activity
Thrombospondin	4.1	2			++ (2)		Ovarian development
RAN-binding protein-2	4.1	1			+		Transport, protein transport
Peroxiredoxin 4	4.1	1			+		Oxidation reduction
2-keto-4-pentanoate hydrolase	4.1	1			+		Catabolic process
Cytosolic NADP-dependent isocitrate dehydrogenase	4.2	1				+	Energy production, tricarboxylic cycle
Isocitrate dehydrogenase 2 (NADP+)	4.2	1				+	Energy production, tricarboxylic cycle
Fah-prov protein	4.2	1				+	Metabolic process
Electron transfer flavoprotein	4.2	1				+	Transport, electron transport
26s protease regulatory subunit 7	4.2	1				+	Catabolic process, ATPase activity
Nucleoplasmin isoform 1-like protein	4.2	1				+	Cellular function
Eukaryotic initiation factor 5A	4.2	1				+	Cellular function, trnaslation
Rab 3 GTPase-activating protein	4.2	4				++++ (4)	Ovarian development, GTPase activity
Protein henna	4.2	1				+	Ovarian development, serotonin biosynthetic
Heat shock protein 70 kDa	4.2	1				+	Chaperone

Table 3.6 A summary of a ovarian proteins of in different stages normal and eyestalk-ablated *P. monodon* broodstock (cont)

Protein name	Group	Total	Normal		Eyestalk-ablated		Remark and biological function
			Stage II	Stage IV	Stage II	Stage IV	
es1 protein	4.3	1			+	+	Cellular function
Carbonic anhydrase	4.3	1			+	+	Metabolic process
Ubiquitin carboxyl-terminal hydrolase L5-like protein	4.3	1			+	+	Catabolic process, ubiquitin thiolesterase activity
26s proteasome non ATPase regulatory isoform A subunit 14	4.3	1			+	+	Catabolic process, protease activity
Aldo-keto reductase	4.3	1			+	+	Oxidation reduction
Heterogeneous nuclear ribonucleoprotein	4.3	4			+++ (3)	+++ (1)	Cellular function, nuclear mRNA processing
Hydroxyacyl-glutathione hydrolase	4.3	1			+	+	Metabolic process, hydrolase activity
Glyoxylase 1	4.3	2			+(1)	+(1)	Cellular function
Cysteine protease	4.3	2			+(1)	+(1)	Catabolic process
Vitellogenin	4.3	4			+++ (3)	+(1)	Ovarian development
Heat shock protein 70 kD protein cognate	4.3	2			+(1)	+(1)	Chaperone
Epa4p	4.3	3			++ (2)	+(1)	Cellular function

*The number of + indicates the number of protein spots found in ovaries of *P. monodon*; The number in brackets indicated that number of protein spots that MW and pI were altered.

Considering expression profiles of known protein in different stages of ovaries of normal and eyestalk-ablated *P. monodon* broodstock, their expression profiles could be categorized to 4 groups; those found in stages II (Group I) and IV (Group II) and those found in both stages II and IV ovaries (Group III) of normal broodstock and those found in eyestalk-ablated broodstock (Group IV) (Table 3.6).

Group I proteins could be further divided to 4 subgroups. They were proteins that were not expressed in ovaries of eyestalk-ablated broodstock such as glycoprotein 93 CG5520-PA, proliferating cell nuclear antigen, retinoblastoma binding protein 4, spermatogonial stem cell renewal factor and phosphoglycerate kinase (subgroup I.1), proteins that also expressed in stage II ovaries of eyestalk-ablated broodstock; for example, Hsp60 protein putative and allergen pen m 2 protein (subgroup I.2), proteins that also expressed in stage IV ovaries of eyestalk-ablated broodstock; for example, Cofilin/actin-depolymerizing factor (subgroup I.3) and proteins that also expressed in both stages II and IV ovaries of eyestalk-ablated broodstock such as beta thymosin, Ovarian peritrophin 2 precursor, Chaperonin containing TCP1 subunit 5 and transaldolase (subgroup I.4).

Group II proteins could be further divided to 4 subgroups. They were proteins that were not expressed in ovaries of eyestalk-ablated broodstock; for example, peritrophin 3 precursor, secreted inorganic pyrophosphatase, putative conjugate transfer protein and proteasome subunit type 6 precursor (subgroup II.1), proteins that were also expressed in stage II ovaries of eyestalk-ablated broodstock; for example, proteasome subunit α type 5 and mitochondrial aldehyde dehydrogenase 2 (subgroup II.2), proteins that were also expressed in stage IV ovaries of eyestalk-ablated broodstock; for example, Tat-binding protein 7 and CG10527-like-methyltransferase (subgroup II.3) and proteins that were also expressed in both stages are stage II and IV ovaries of eyestalk-ablated broodstock such as cytosolic manganese superoxide dismutase, alcohol dehydrogenase and glutathione peroxidase protein involved an antioxidant (subgroup II.4).

Group III proteins could be further divided to 4 subgroups. They were proteins that were not expressed in ovaries of eyestalk-ablated broodstock; for example, chromobox protein homologue 1 and F1-ATP synthase beta subunit (subgroup III.1), proteins that were also expressed in stage II ovaries of eyestalk-ablated broodstock; for example, glutathione-s-transferase, triose-phosphate isomerase, phosphopyruvate hydratase and tubulin beta-1 chain (subgroup III.2), proteins that were also expressed in stage IV ovaries of eyestalk-ablated broodstock (subgroup III.3) were not observed in this study. The final subgroup was proteins that were also expressed in both stages are stage II and IV ovaries of eyestalk-ablated broodstock such as protein disulfide isomerase, 2-cys thioredoxin, arginine kinase and beta actin (subgroup III.4).

Group IV proteins could be further divided to 3 subgroups. They were proteins that were also expressed in stage II ovaries of eyestalk-ablated broodstock; for example, Histidine-rich glycoprotein precursor, ovarian peritrophin, careticulin, heterochromatin protein 1 homologue beta, dynactin subunit 2 and vitellogenin (subgroup III.1), proteins that were also expressed in stage IV ovaries of eyestalk-ablated broodstock cytosolic NADP-dependent isocitrate dehydrogenase, Fah-prov protein, isocitrate dehydrogenase 2 (NADP+), Rab 3 GTPase-activating protein and protein henna (subgroup III.2) and proteins that were also expressed in both stages are stage II and IV ovaries of eyestalk-ablated broodstock such as ubiquitin carboxyl-terminal hydrolase L5-like protein, es1 protein, carbonic anhydrase, 26s proteasome non ATPase regulatory isoform A subunit 14 and aldo-keto reductase (subgroup III.4).

In addition, known proteins in this study were categorized according to their biological functions (Table 3.6). Proteins involving metabolic process (13%) and ovarian development (13%) were the most abundant protein group (13%). Members of the former group, for example, were secreted inorganic pyrophosphatase and methylmalonate semialdehyde dehydrogenase whereas those of the latter group were vitellogenin and thrombospondin. Proteins functionally involved in energy production, for example, triose-phosphate isomerase and F1-ATP synthase beta subunit were also abundantly expressed (12%). Proteins involving catabolic process were found for 11% of characterized proteins. Examples of these proteins were

ubiquitin carboxyl-terminal hydrolase L5-like protein and 26s proteasome non ATPase regulatory isoform A subunit 14. In addition, proteins function in transport and chaperone were found for 8% for both groups. Members of the former group were cytochrome b and intracellular fatty acid while those of the latter group were protein disulfide isomerase and heat shock protein 70 kDa protein cognate. Oxidation-reduction proteins (e.g. glutathione peroxidase and 2-cys thioredoxin) were found for 6%. Proteins involved in cellular structure (e.g. actin D tubulin beta-1 chain) were also found for 6% of characterized proteins. Apart from highly and moderately expressed proteins, those involved calcium homeostasis (e.g. sarcoplasmic Ca²⁺ binding protein α B and A chain and calreticulin) and environmental stress (e.g. arginine kinase and allergen pen m2) were found for 2% of characterized proteins. Proteins categorized as other cellular functions were accounted for 19% of characterized proteins in the study (Figure 3.20).

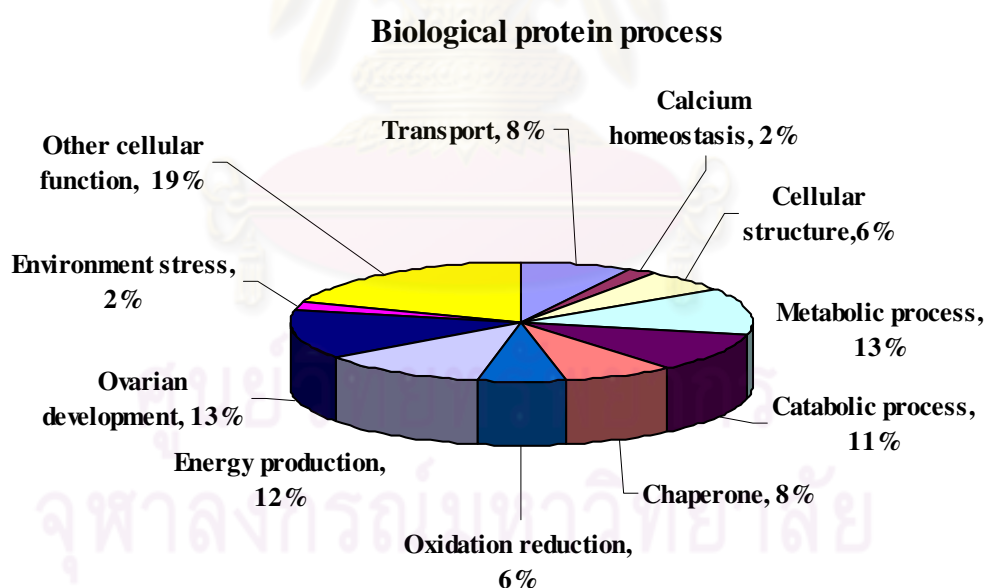


Figure 3.20 The categories of biological function of known protein spots from 2-DE gels after they were subjected to nanoLC-MS/MS followed by database searched. The 102 proteins were categorized into 11 groups according to their function within the cell.

3.4 Isolation and characterization of the full length cDNA of genes expressed in ovaries of *P. monodon*

3.4.1. *DEAD box 52*

Several discrete bands were obtained from 5' and 3' RACE-PCR of *DEAD box 52*. A 900 bp fragment generated from 3' RACE-PCR was cloned and sequenced. Nested 5' RACE-PCR was further carried out and a 1100 bp fragment was obtained (Figure 3.21). Nucleotide sequences of these fragments and EST (Figure 3.22) were assembled.

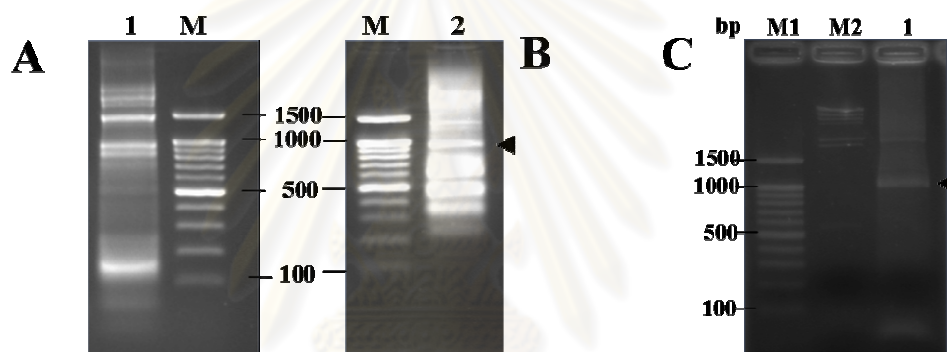


Figure 3.21 The primary 5' (A) and 3' (B) RACE-PCR product of *DEAD box 52*. Nested 5' RACE-PCR product of *DEAD box 52* was further carried out (C). Arrowheads indicate RACE-PCR products that were cloned and sequenced. Lanes M and M1 are a 100 bp DNA ladder. Lane M2 is a λ -*Hind* III DNA marker.

A.

```
CTAATACGACTCACTATAGGGCAAGCAGTGGTATCAACGCAGAGTACGCGGGAGGCAAGACAGCGGCTT
TTCTCGTGCCATTCTGAATCAGCTCGGTGGCCCTCAGAGGAAGGGTTTCCGTGCTGTAATCTAGCAC
CTACCAGAGAGTTGGCCAAACAGACTTACAGAGAGTGACAAGGCTGTCTGAGGGCCTTGGGTTACGTG
TGCACATCATTAGTAATGTGAACAAAAGCAAAAAGAAAAGTTTGGGCCAAAGTCTGCAAAAAAATTTGACG
TATTGGTGACGACCCCAAACCGCCTTGTATTTCTCCTGCGAGAGGATGATACGCCACCAATTGACTTAG
```

Nested 5' RACE-PCR

```
CCAATGTGGAGTGGTTGGTTGTTGACGAGAGTGATCGCCTCTTTGAGGGTGGAGCACGAGGATTCAGGG
ATCAGTTAGCTGCAGTATATCGTGCATGCACTGGACCCAATATCAGACGGGCTCTTTTCTCGGCTACAT
TTTCTCAGGAGTTCAACACTGGTGTAAATTGAATCTCAATAATGTTGCCATGGTTACAGTAGGCATAA
GAAATACAGCATGCGAAGATGTGAAACAAGAGTTGGTGTTTTGTGGAAATGAAACTGGAAAAATTCCTGG
CACTGCGTGATATATTCCGAAAGGGATATGAACCTCCAGTGCTAGTATTTGTGCAGACCAAAGAGCGAG
CGAAAGAAGTGTCAAGGAGCTGATTTACGACAACCTGATGGTGGATGCCATTCATGCAGATCGAACAC
AGCTGCAGCGTGATAATGTTGTACGGGCATTCAGAGAAAAGAAAAGTCTGGGTTCTGATATGCACAGAAC
TCATGGCCCGTGGTATTGACTTCAAGGGGGTGAACCTTGTTCATCAACTATGACTTCCCTCCTTCAGCAA
TC
```

B.

```
GATGGTGGATGCCATTCATGCAGATCGAACACAGCTGCAGCGTGATAATGTTGTACGGGCATTCAGAGA
5' RACE-PCR
```

AAGAAAAGTCTGGGTTCTGATATGCACAGAACTCATGGCCCGTGGTATTGACTTCAAGGGGTTGAACCT
3' RACE-PCR
 TGTCATCAACTATGACTTCCCTCCTTCAGCAATCAGTTACATTCACAGAGTAGGAAGGACTGGCAGAGC
 TCATCATCAAGGAAGAGCGGGTCACATTCTGGACAATGGCAGATAAGCCATATCTGCGGAGCATTGCCCT
 AGTAATGCATAACTCTGGCCAACATGTTCTGAATGGATGCTTGAAATGAAGAAGGCGACAAAGAATGA
 GAAAAAGAAGCTATCAGCTAAACATCCAGAGCGTGGACACGTATCTCAAGGGGTCCTGTATGAGAAGCT
 ACAAAGAGGAAGATGAAACAAATGAAAGACAAAAGCAAAAGGATGAAAATGATGAATGGAGGAGCTAT
 GCAGAAAGAGGAAGAGGAAAAGTGGTGATAATGACATAGTAGACAGTGCAGATACGCA

C.

GCAGAAAGAGGAAGAGGAAAAGTGGTGATAATGACATAGTAGACAGTGCAGATACGCAAGCCCCAAAGAA
 GAAAAAGAAGACAAAGAAAAAGAAAGTGGCAACGTAGTTGAAAAAATGCAATGTTGATCAGGGTAACGA
 ATGAGGGAAAGTCTGAATGAATGTTTTTGTGGACTGTAAGTGCACAACGGAATAGAATATGAATTTGCTA
 AACAAAAAAAAAAAAAAAAAAAA

Figure 3.22 Nucleotide sequences of 5' RACE-PCR (A), EST (B) and 3' RACE-PCR (C) of *DEAD box 52* of *P. monodon*. Primers for 5' and 3' RACE-PCR are underlined.

The full length cDNA of *DEAD box 52* of *P. monodon* was 2043 bp in length containing an ORF of 1824 bp deducing to a polypeptide of 607 amino acids and 5' and 3' UTRs of 96 and 123 bp (excluding the poly A tail), respectively (Figure 3.23). The closest species according to the best hit approach of the full length cDNA of *DEAD box 52* of *P. monodon* was closest similarity to that of *Nasonia vitripennis* (E-value = $3e-154$).

AAGCAGTGGTATCAACGCAGAGTACGCGGGGATGTGGAGGCGAAGCGAGACGCAAACACG 60
 GACTCGCGACCACGTCCTTTTTTATTCTATGGCAAGATGAATTCGTATGATATCTTTTCGA 120
M N S Y D I F R 8
 AAGCTCACGAGGGGAATGAGATTTGATCATAACAGATTTAAAGGAGATCTAAAAAAGATA 180
K L T R G M R F D H N R F K G D L K K I 28
 GGGGTCCGTAAAAACAAAAGATGATGACCAAAGCAGCGTGACAGTGAATGAGACCAAAGAA 240
G V R K T K D D D Q S S V T V N E T K E 48
 GAGGAAGAAGAGGCAGTTGACGAGCCTGAATCCAACGAAGAAGACCCAGATGAGGATGAT 300
E E E E A V D E P E S N E E D P D E D D 68
 GTTGATGCAGATGAGGAAGGCAAAGTAAGCATGCTGTCTGATATCCAGATTGGAGGATCA 360
V D A D E E G K V S M L S D I Q I G G S 88
 GAAGCAACTGAGAGGAAAAGAAAAAAGTAATCAGTAAAGAGAAACAGCTTCGA 420
E A T E R K E K K K K V I S K E K Q L R 108
 ATCCACCAACAGCAGGTTAATCATCAACGAAAATAAACTTGGCATCTCAGTATGGGGAACC 480
I H Q Q Q V N H Q R N K L G I S V W G T 128
 GACGTTCTGATCCAGTGGAGACTTTTGGATGACATGATCGTGAAGCACAAAGCTAAGTGAG 540
D V P D P V E T F D D M I V K H K L S E 148
 GTACTAGTGAGCAATCTGCTGAATCAAGGCTACTCGGAACCCACTGCAATCCAGAAGCAG 600
V L V S N L L N Q G Y S E P T A I Q K Q 168
 GCGTGGCCACTGCTGCAAGGACGGGAAATCTGGGATGTGCCCAACAGGCTCAGGC 660
A W P L M L Q G R E I L G C A P T G S G 188

```

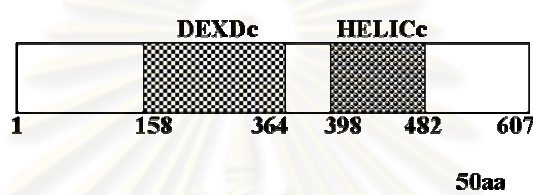
AAGACAGCGGCTTTTCTCGTGCCATTCTGAATCAGCTCGGTGGCCCTCAGAGGAAGGGT 720
K T A A F L V P I L N Q L G G P Q R K G 208
TTCCGTGCTGTAATTCTAGCACCTACCAGAGAGTTGGCCAAACAGACTTACAGAGAGTGT 780
F R A V I L A P T R E L A K Q T Y R E C 228
ACAAGGCTGTCTGAGGGCCTTGGGTACGTGTGCACATCATTAGTAATGTGAACAAAGCA 840
T R L S E G L G L R V H I I S N V N K A 248
AAAGAAAAGTTTGGGCCAAAGTCTGCAAAAAAATTTGACGTATTGGTGACGACCCCAAAC 900
K E K F G P K S A K K F D V L V T T P N 268
CGCCTTGTATTTCTCCTGCGAGAGGATGATACGCCACCAATTGACTTAGCCAATGTGGAG 960
R L V F L R E D D T T P P I D L A N V E 288
TGGTTGGTTGTTGACGAGAGTGATCGCCTCTTTGAGGGTGGAGCACGAGGATTCAGGGAT 1020
W L V V D E S D R L F E G G A R G F R D 308
CAGTTAGCTGCAGTATATCGTGCATGCACTGGACCCAATATCAGACGGGCTCTTTTCTCG 1080
Q L A A V Y R A C T G P N I R R A L F S 328
GCTACATTTTCTCACGAGGTTCAACACTGGTGAAAATTGAATCTCAATAATGTTGCCATG 1140
A T F S H E V Q H W C K L N L N N V A M 348
GTTACAGTAGGCATAAGAAAATACAGCATGCGAAGATGTGAAACAAGAGTTGGTGTTTTGT 1200
V T V G I R N T A C E D V K Q E L V F C 368
GGAAATGAAACTGGAAAAATCTGGCACTGCGTGATATATCCGAAAGGGATATGAACCT 1260
G N E T G K I L A L R D I F R K G Y E P 388
CCAGTGCTAGTATTTGTGCAGACCAAAAGAGCGAGCGAAAGAACTGTTCAAGGAGCTGATT 1320
P V L V F V Q T K E R A K E L F K E L I 408
TACGACAACCTGATGGTGGATGCCATTCATGCAGATCGAACACAGCTGCAGCGTGATAAT 1380
Y D N L M V D A I H A D R T Q L Q R D N 428
GTTGTACGGGCATTGAGAGAAAAGAAAAGTCTGGGTTCTGATATGCACAGAACTCATGGCC 1440
V V R A F R E R K V W V L I C T E L M A 448
CGTGATTGACTTCAAGGGGGTGAACCTTGTCATCAACTATGACTTCCCTCCTTCAGCA 1500
R G I D F K G V N L V I N Y D F P P S A 468
ATCAGTTACATTCACAGAGTAGGAAGGACTGGCAGAGCTCATCATCAAGGAAGAGCGGTC 1560
I S Y I H R V G R T G R A H H Q G R A V 488
ACATTCTGGACAATGGCAGATAAGCCATATCTGCGGAGCATTGCCCTAGTAATGCATAAC 1720
T F W T M A D K P Y L R S I A L V M H N 508
TCTGGCCAACATGTTTCTGAATGGATGCTTGAAAATGAAGAAGGCGACAAAGAATGAGAAA 1780
S G Q H V P E W M L E M K K A T K N E K 528
AAGAAGCTATCAGCTAAACATCCAGAGCGTGGACACGTATCTCAAGGGGTCTGTATGAG 1840
K K L S A K H P E R G H V S Q G V L Y E 548
AAGCTACAAAAGAGGAAGATGAAAACAAATGAAAAGACAAAAGCAAAAGGATGAAAATGATG 1900
K L Q K R K M K Q M K D K S K R M K M M 568
AATGGAGGAGCTATGCAGAAAAGAGGAAGAGGAAAAGTGGTGATAATGACATAGTAGACAGT 1960
N G G A M Q K E E E E S G D N D I V D S 588
GCAGATACGCAAGCCAGAAAAGAAGAAAAAGACAAAAGAAAAAGAAAGTGGCAACGTAG 2020
A D T Q A R K K K K K T K K K K V A T * 607
TTGAAAAAATGCAATGTTGATCAGGGTAACGAATGAGGGAAAGTCTGAATGAATGTTTTTG 2080
TTGACTGTAAGTGCACAACGGAATAGAATATGAATTTGCAAAAAAAAAAAAAAAAAAAAAAAA 2140
AAA 2143

```

Figure 3.23 The full length cDNA sequences of *DEAD box 52* of *P. monodon*. Start and stop codons are illustrated in boldfaced and underlined. A putative *N*-linked-glycosylation site is highlighted.

The calculated *pI* and *MW* of *P. monodon DEAD box 52* was 9.30 and 69.15 kDa, respectively. The signal peptide was not found in this putative nonsecretory

protein. The *N*-linked-glycosylation domain was found at positions 44- 46 of the deduced DEAD box 52 protein. DEXDc and HELICc domains were found in proteins functionally involved in unwinding nucleic acids of various biological processes for instance, nuclear transcription, pre-mRNA splicing, ribosomal biogenesis, nucleocytoplasmic transport, translation, RNA decay and organelle gene expression, were found at positions 158 - 364 (E-value = 1.94e-51) and 398 - 482 (E-value = 4.14e-28; Figure 3.24) of this deduced protein.



Domain	Position	E-value
DEXDc	158-364	1.94e-51
HELICc	398-482	4.14e-28

Figure 3.24 Diagram illustrating DEAD box 52 cDNA of *P. monodon*. The DEXDc and HELICc domains were found in the deduced protein of this transcript. The scale bar is 200 bp in length.

3.4.2 DEAD box ATP-dependent RNA helicase

The primary 5' and 3' RACE-PCR generated large fragments of bands (Figure 3.25A). Semi-nested PCR was carried out by amplification of the primary RACE-PCR product with the same gene-specific primer and nested adaptor primer (AP2). After electrophoresis, discrete bands of 900 bp and 1000 bp fragments were obtained from seminested 5' and 3' RACE-PCR of a *DEAD box ATP-dependent RNA helicase*, respectively (Figure 3.25B). These fragments were cloned and sequenced. Their nucleotide sequences (Figure 3.25) were assembled with the original EST sequence.

The full length cDNA of *DEAD box ATP-dependent RNA helicase* of *P. monodon* was 1680 bp in length containing an ORF of 1209 bp corresponding to a polypeptide of 402 amino acids. The 5' and 3' UTRs of *DEAD box ATP-dependent RNA helicase* were 53 and 418 bp long (excluding the poly A tail), respectively.

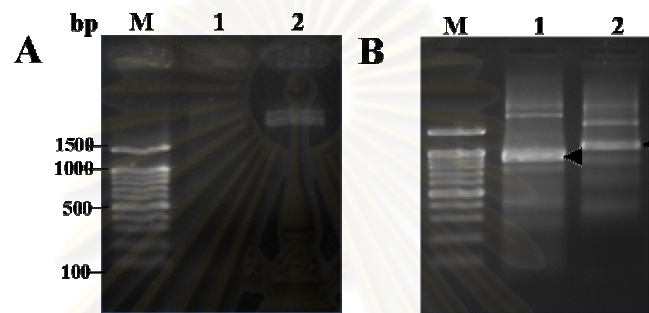


Figure 3.25 The primary 5' (lane 1, A) and 3' (lane 2, A) RACE-PCR product of *DEAD box ATP-dependent RNA helicase*. Semi-nested 5'(lane 1, B) and 3' (lane 2, B) RACE-PCR were further carried out. Arrowheads indicate RACE-PCR products that were cloned and sequenced. Lanes M are a 100 bp DNA ladder.

A.

```
GATTAAGCAGTGGTATCAACGCAGAGTACGCGGGGAGAGCGGCAGTAAACACCATGGCGGAAGGACGCG
TGAGAAGAGTGATCCCCGAGGACCTCTCCAATGTCGAGTTTGAGACCAGCGAAGAGGTGGAGGTCTGCC
CAACCTTCGATAACATGGGGCTGAGAGAGGATCTCCTTCGTGGAAATATATGCTTATGGGTTTGAAAAGC
CATCTGCTATCCAACAGCGTGCTATTCGTCCCATTGTGAAGGGTCGTGATGTCATTGCACAGGCCAGT
CTGGAACGGGTAAAACCGCCACTTTTTCCATCTCTATCCTACAAAACGCTTGACATCAATGTCCGTGAGA
CCCAGGTCCTTACACTCTCACCAACAAGGGAGTTGGCAGTGCAAATTCAAAAGGTTGTTCTGGCCTTAG
GAGATTACATGAATGTTTCAGTGTGTCATGCTTGCAATGGAGGGACCAACTGGGTGAGGACATCCGCAAGC
TTGACTATGGCCAGCATGTCGTATCTGGCACACCAGGTCGGGTGTTTGACATGATCAGACGCCGCACTC
TCAGAACCCGTTCAATTAAGATGTTGGTCCTAGATGAAGCAGATGAAATGTTGAACAAAGGCTTCAAGG
AACAGATCTACGATGTTTACCGTTACCTTCCACCAGCTACCCAGGCTGCTTGATCTCTGCCACACTTC
CCCATGAAATTCTTGAGATGACTTCAAAGTTTCATGACTGATCCAATCCGTATTCTTGTGAAACGTGATG
AACTGACACTGGAAGGGATCAACATTCTTTGTGGCAGTAGAGCGCGAAGAATGGAAATTTGATACTTTG
TGCGACTTGTACGATACACTGACCATCACACAAGCAGTAATCTTTTTGCACACGACAAGCAGTAATCTT
TTGCAACACGAAGCGTAAGGTGGACTGGCTGACAATCACTAGTGAATTCGCGGCCGCCTGCAGGTCGAC
CATATGGGAGAGCTCCCAACGCGTTGGATGCATAGCTGAGTATTCTATAGTGCACCTAAATAGCTGGC
GATAGTCATCC
```

B.

```
GGAACGGGTAAAACCGCCACTTTTTCCATCTCTATCCTACAAAACGCTTGACATCAATGTCCGTGAGACC
CAGGTCCTTACACTCTCACCAACAAGGGAGTTGGCAGTGCAAATTCAAAAGGTTGTTCTGGCCTTAGGA
GATTACATGAATGTTTCAGTGTGTCATGCTTGCAATGGAGGGACCAACTGGGTGAGGACATCCGCAAGCTT
```

GACTATGGCCAGCATGTCGTATCTGGCACACCAGGTCGAGTGTTTGACATGATCAGACGCCGCACTCTC
 AGAACCCGTTCAATTAAGATGTTGGTCCTAGATGAAGCAGATGAAATGTTGAACAAAGGCTTCAAGGAA
3' RACE-PCR
 CAGATCTACGATGTTTACCGTTACCTTCCACCAGCTACCCAGGTCCTGCTTGATCTCTGCCACACTTCCC
 CATGAAATTCCTTGAGATGACTTCAAAGTTCATGACTGATCCAATCCGTATTCTTGTGAAACGTGATGAA
 CTGACACTGGAAGGAATCAAGCAATTCCTTGTGGCAGTAGAGCGCGAAGAATGGAAATTTGATACTTTG
5' RACE-PCR
 TGCGACTTGTACGATACTGACCATCACACAAGCAGTAATCTTTTGCAACACGAAGCGTAAGGTGGAC
 TGGCTGACAGAAAAAATGCGAGAGGCCAACTTCACAGTATCTTCCATGCACGGTGACATGCCACAGAAA
 GAGCGAGATGCCATCATGAAGGAGTTCGGTTTCAGGCCAGAGTCGAGTACTAATCACTACTGATATATG
 GGCAAGAGGAATTGATGTACAGCAGGTATCCTTGGTCATTAATATGACCTGCAACA

C.

CTTTTGCAACACGAAGCGTAAGGTGGACTGGCTGACAGAAAAAATGCGGGAGGCCAACTTCACAGTATC
 TTCCATGCACGGTGACATGCCACAGAAAAGAGCGAGATGCCATCATGAAGGAGTTCGGTTCAGGCCAGAG
 TCGAGTACTAATCACTACTGATATATGGGCAAGAGGAATTGATGTACAGCAGGTATCCTTGGTCATTAA
 TTATGACCTGCCAAACAATCGTGAGTTGTACATTCATCGCATTGGTCGATCTGGTCGTTTTTGGAAAGGAA
 GGGTGTGCAATCAACTTTGTGAAGAATGATGATATTCGTATCCTGCGAGATATTGAACAGTACTACTC
 AACACAGATTGATGAAATGCCCATGAATGTTGCTGATTTAATCTAAATGGAAGTGGGACAGTACCTGAA
 ATCCATTATGATAAGATATGTATTTTCCATACATAAAAAGTATTTGTACCCAATAAGAATACCCCGTAGC
 TTTTCTTTAATATATAATATTCCTTTTTTTTTTATAGTAAATAAATGGTTTTTGATGGATCTAGGTTAT
 GTAATTTTAGAAAAGAACCTCAAATTCCTTTATGAATGTTTATATTATATTGTCTTTGTGCATACCAAAG
 CTTACATAGTTTCAAGTATGATTTTCAAGTTTGAAGACAGAAAGTATGAAGCAGATATC
 TTCACTCTTTGTTAATCACCTTTTTGTGACATGTTACACATTTTGTAGCATTTTTTGTACTGAAAGTGT
 ACAATAAAGCCCTTGACTGAAAAA

Figure 3.26 Nucleotide sequence of 5' RACE-PCR (A), EST (B) and 3' RACE-PCR (C) of *DEAD box ATP-dependent RNA helicase* of *P. monodon*. RT-PCR primers (DATPF, DATPR, underlined) were used for isolation of the full length cDNA of this gene by RACE-PCR.

The poly A additional signal (AATAAA) was located between 1632-1638 of this transcript (Figure 3.27). Its closest similarity according to the best hit approach of the full length cDNA of *DEAD box ATP-dependent RNA helicase* of *Aedes aegypti* (E-value = 0.00).

The calculated *pI* and MW of *DEAD box ATP-dependent RNA helicase* of *P. monodon* was 5.91 and 46.11 kDa, respectively. The predicted signal peptide was not found in the deduced *DEAD box ATP-dependent RNA helicase* protein. Like *DEAD box 52*, *DEXDc* and *HELICc* domains were found at positions 48 - 245 (E-value = 3.84e-55) and 282 - 363 (E-value = 1.07e-35; Figure 3.28) of the deduced protein, respectively.

```

GATTAAGCAGTGGTATCAACGCAGAGTACGCGGGGAGAGCGGCAGTAAACACCATGGCGG 60
                                     M A 2
AAGGACGCGTGAGAAGAGTGATCCCCGAGGACCTCTCCAATGTCGAGTTTGAGACCAGCG 120
E G R V R R V I P E D L S N V E F E T S 22
AAGAGGTGGAGGTCGTCCCAACCTTCGATAACATGGGGCTGAGAGAGGATCTCCTTCGTG 180
E E V E V V P T F D N M G L R E D L L R 42
GAATATATGCTTATGGGTTTGAAAAGCCATCTGCTATCCAACAGCGTGCTATTTCGTCCCA 240
G I Y A Y G F E K P S A I Q Q R A I R P 62
TTGTGAAGGGTCGTGATGTCATTGCACAGGCCAGTCTGGAACGGGTAAAACCGCCACT 300
I V K G R D V I A Q A Q A Q S G T G K T A T 82
TTTCCATCTCTATCCTACAAACGCTTGACATCAATGTCCGTGAGACCCAGGTCCTTACAC 360
F S I S I L Q T L D I N V R E T Q V L T 102
TCTCACCAACAAGGGAGTTGGCAGTGCAAATTCAAAAGTTGTTCTGGCCTTAGGAGATT 420
L S P T R E L A V Q I Q K V V L A L G D 122
ACATGAATGTTTCAGTGTTCATGCTTGCATTGGAGGGACCAACTGGGGTGAGGACATCCGCA 480
Y M N V Q C H A C I G G T N L G E D I R 142
AGCTTGACTATGGCCAGCATGTCGTATCTGGCACACCAGGTCGGGTGTTTGACATGATCA 540
K L D Y G Q H V V S G T P G R V F D M I 162
GACGCCGCACTCTCAGAACCCGTTCAATTAAGATGTTGGTCTTAGATGAAGCAGATGAAA 600
R R R T L R T R S I K M L V L D E A D E 182
TGTTGAACAAAGGCTTCAAGGAACAGATCTACGATGTTTACCGTTACCTTCCACCAGCTA 660
M L N K G F K E Q I Y D V Y R Y L P P A 202
CCCAGGTCTGCTTGATCTCTGCCACACTTCTCCATGAAATTTCTTGAGATGACTTCAAAGT 720
T Q V C L I S A T L L H E I L E M T S K 222
TCATGACTGATCCAATCCGTATTCTTGTGAAACGTGATGAACTGACACTGGAAGGAATCA 780
F M T D P I R I L V K R D E L T L E G I 242
AGCAACTCTTTGTGGCAGTAGAGCGCGAAGAAATTTGATACTTTGTGCGACTTTGT 840
K Q L F V A V E R E E W K F D T L C D L 262
ACGATACACTGACCATCACACAAGCAGTAATCTTTTGCAACACGAAGCGTAAGGTGGACT 900
Y D T L T I T Q A V I F C N T K R K V D 282
GGCTGACAGAAAAAATGCGGGAGGCCAACTTCACAGTATCTTCCATGCACGGTGACATGC 960
W L T E K M R E A N F T V S S M H G D M 302
CACAGAAAGAGCGAGATGCCATCATGAAGGAGTTCCGTTTCAGGCCAGAGTCGAGTACTAA 1020
P Q K E R D A I M K E F R S G Q S R V L 322
TCACTACTGATATATGGGCAAGAGGAATTGATGTACAGCAGGTATCCTTGGTCATTAATT 1080
I T T D I W A R G I D V Q Q V S L V I N 342
ATGACCTGCCAAACAATCGTGAGTTGTACATTCATCGCATTGGTCGATCTGGTCGTTTTG 1140
Y D L P N N R E L Y I H R I G R S G R F 362
GAAGGAAGGGTGTTCGAATCAACTTTGTGAAGAATGATGATATTCGTATCCTGCGAGATA 1200
G R K G V A I N F V K N D D I R I L R D 382
TTGAACAGTACTACTCAACACAGATTGATGAAATGCCCATGAATGTTGCTGATTTAATCT 1260
I E Q Y Y S T Q I D E M P M N V A D L I 402
AAATTGAAGTGGGACAGTACCTGAAATCCATTATGATAAGATATGTATTTTCCATACATA 1320
*
AAAGTATTTGTACACAATAAGAATACACAGTAGCTTTTTCTTTAATATATAATATTCCTTT 1380
TTTTTTATAGTGAAATAAATGGTTTCTGATGGATCTAGGTTATGTAATTTTAGAAAGAAC 1440
CTCAAATTCCTTTATGAATGTTTATATTATATTGCTTTGTGCATACCAAAGCTTACATA 1500
GTTTCAGTTCTGAAAGTATGTATTATTCAAGTTTGAAAAGACAGAAAGTATGAAGCAGATAT 1560
CTTCACTCTTTGTTAATCACCTTTTTGTGACATGTTACACATTTTTAGCATTTTTTTGTA 1620
CTGAAAGTGTACAATAAAGCCCTTACTGAAAAAAAAAAAAAAAAAAAAAAAAAAAAAAAAAAAA 1680

```

Figure 3.27 The full length cDNA and deduced protein sequences of *DEAD box ATP-dependent RNA helicase* of *P. monodon*. Start and stop codons are illustrated in boldfaced and underlined. The poly A additional signal (AATAAA is bold-faced).

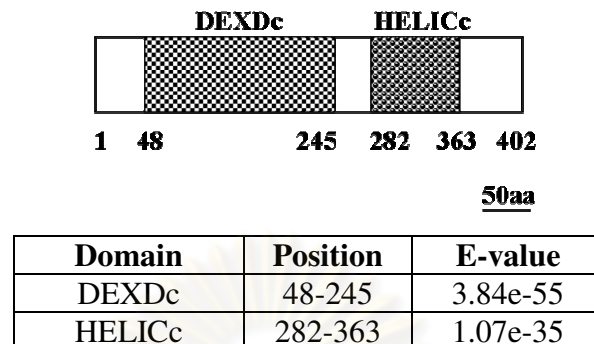


Figure 3.28 Diagram illustrating the full length cDNA of *DEAD box ATP-dependent RNA helicase* of *P. monodon*. The DEXDc and HELICc domains were found in the deduced protein of this transcript. The scale bar is 200 bp in length.

3.4.3 ATP-dependent RNA helicase

Two discrete fragments (approximately 800 and 300 bp in length) was obtained from 5' RACE-PCR whereas three discrete bands (approximately 1600, 1300 and 1000 bp in size) were generated from 3' RACE-PCR (Figure 3.29A). A 1300 bp fragment which is the most intense band among 3' RACE-PCR products was cloned and sequenced. Nested 5' RACE-PCR was further carried out and a 700 bp fragment was obtained (Figure 3.29B). Nucleotide sequences of the original EST and RACE-PCR (Figure 3.30) were assembled.

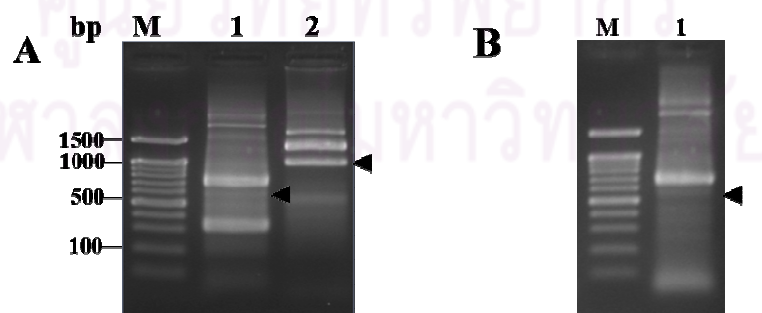


Figure 3.29 Semi-nested 5' (lane1, A) and 3' (lane 2, A) RACE-PCR product of *ATP-dependent RNA helicase*. Nested 5' (lane 1, B) RACE-PCR was further carried out. Arrowheads indicate RACE-PCR products that were cloned and sequenced. Lanes M are a 100 bp DNA ladder.

A.

AAGCAGTGGTATCAACGCAGAGTACGCGGGGGTTTAGGACGCGACACGTACAGCTTTATCCCCCCTTT
 ATTTGCTAACCAAGCAGAATGGCCGACCAGGAGACTGAACTTCTCGACTACGAGGAGGATGAGGATGCG
 GTGGAGGCAGGAGTAGGAGAAAACGACAGAGGCTGCCCCAGCCAAAAAGGATGTCAAGGGTACCTATGTG
 TCTATCCACTCCTCAGGCTTCAGGGATTTCTGCTGAAGCCAGAGATCCTGAGATCCATTGTAGACTGT
 GGCTTTGAGCATCCTTCTGAAGTGCAGCATGAGTGCATCCCTCAAGCTGTGTTGGGCATGGACATCTTG
 GGCCAGGCTAAGTCGGGTATGGGAAAAGACGGCAGTGTGTTGTGCTGGCAACACTTCAGCAGATTGATCCT
 GTTGATGGTCAGGTGTCAGTGTGTAATGTGTCATACACGAGAGTTGGCTTACCAGATAGCCAAGGAG
 TATGAAAGATTGAGCAAGTACATGCCAACACCAAAGTGGGGGTGTTTTTCGGAGGCCTAAATGTTTCAG
 AAGGACGAAGAGACCCTCAAGAACAACCTGCCCTCACATCGCTGTTGGCACCCCTGGCCGTGTTCTTGCT

Nested 5' RACE-PCR

CTGGTGCCAACAAGAAGCCCAATCTCCGCCACTAATCACTAGTGAATTCGCGGCCGCTGCAGGTCGA
CCATATGGGAGAGCTCCCAACGCGT

B.**3' RACE-PCR**

TGCCAACACCAAAGTGGGGGTGTTCTTCGGAGGCCGTGAATTGTTCAGAAGGACGAAGAGACCCTCAAGA
 ACAACTGCCCTCACATCGTTGTTGGCACCCCTGGCCGTGTTCTTGCTCTGGTGC

5' RACE-PCR

ATCTCCGCCACTTGAAACACTTTGTATTGGATGAATGCGACAAGATGCTGGAACAGCTTGACATGCGAC
GAGATGTGCAAGAAATCTTCCGCAATACTCCACATGAAAAGCAAGTGAATGATGTTTCAGCGCCACCTTGA
GCAAGGAGATCCGCCCTGTTTGCAAGAAGTTCATGCAAGATCCCATGGAAGTATATGTTGATGATGAAG
CCAAGTTGACTCTTCATGGTCTGCAGCAGCACTACGTTAAAAATCAAGGAAAATGAGAAGAATCGAAAAT
TGTTTGAATTACTCGATGCTTTAGAGTTCAACCAGGTTGTGATATTCGTTAAGTCAGT

C.

TGTTCAGAAGGACGAAGAGACCCTCAAGAACAACCTGCCCTCACATCGTTGTTGGCACCCCTGGCCGTGT
 TCTTGCTCTGGTGC

Figure 3.30 Nucleotide sequence of 5' RACE-PCR (A), EST (B) and 3' RACE-PCR (C) of *ATP-dependent RNA helicase* of *P. monodon*. RT-PCR primers (ATPF and ATPR, underlined) were initially used for the primary RACE-PCR followed by nested 5' RACE-PCR primers (underlined) for isolation of the full length cDNA of this gene.

The full length cDNA of *P. monodon ATP-dependent RNA helicase* was 1404 bp in length consisting an ORF of 1206 bp corresponding to a polypeptide of 401 amino acids and 5' and 3' UTRs of 87 and 131 bp (excluding the poly A tail) (Fig. 3.31). The closest similarity of this transcript was *ATP-dependent RNA helicase* of *Salmo salar* (E-value = 0.00).

```

AAGCAGTGGTATCAACGCAGAGTACGCGGGGGTTTAGGACGCGACACGTACAGCTTTATT 60
CCCCCTTTATTTGCTAACCAAGCAGAAATGGCCGACCAGGAGACTGAACTTCTCGACTAC 120
                                     M A D Q E T E L L D Y 11
GAGGAGGATGAGGATGCGGTGGAGGCAGGAGTAGGAGAAAACGACAGAGGCTGCCCCAGCC 180
E E D E D A V E A G V G E T T E A A P A 31
AAAAAGGATGTCAAGGGTACCTATGTGTCTATCCACTCCTCAGGCTTCAGGGATTTCTG 240
K K D V K G T Y V S I H S S G F R D F L 51
CTGAAGCCAGAGATCCTGAGATCCATTGTAGACTGTGGCTTTGAGCATCCTTCTGAAGTG 300
L K P E I L R S I V D C G F E H P S E V 71
CAGCATGAGTGCATCCCTCAAGCTGTGTTGGGCATGGACATCTTGGGCCAGGCTAAGTCG 360
Q H E C I P Q A V L G M D I L G Q A K S 91
GGTATGGGAAAGACGGCAGTGTGTTGTGCTGGCAACACTTCAGCAGATTGATCCTGTTGAT 420
G M G K T A V F V L A T L Q Q I D P V D 111
GGTCAGGTGTCTAGTGTGGTAATGTGTCTATACGAGAGTTGGCTTACCAGATAGCCAAG 480
G Q V S V L V M C H T R E L A Y Q I A K 131
GAGTATGAAAGATTAGCAAGTACATGCCCAACACCAAGTGGGGGTGTTCTTCGGAGGC 540
E Y E R F S K Y M P N T K V G V F F G G 151
CTGAATGTTTCAGAAGGACGAAGAGACCCTCAAGAACAACCTGCCCTCACATCGTTGTTGGC 600
L N V Q K D E E T L K N N C P H I V V G 171
ACCCCTGGCCGTGTTCTTGCTCTGGTGCACAACAAGAAGCCCAATCTCCGCCACTTGAAA 660
T P G R V L A L V R N K K P N L R H L K 191
CACTTTGTATTGGATGAATGCGACAAGATGCTGGAACAGCTTGACATGCGACGAGATGTG 720
H F V L D E C D K M L E Q L D M R R D V 211
CAAGAAATCTCCGCAATACTCCACATGAAAAGCAAGTGATGATGTTTCAGCGCCACTTG 780
Q E I F R N T P H E K Q V M M F S A T 231
AGCAAGGAGATCCGCCCTGTTTGCAAGAAGTTCATGCAAGATCCCATGGAAGTATATGTT 840
S K E I R P V C K K F M Q D P M E V Y V 251
GATGATGAAGCCAAGTTGACTCTTCATGGTCTGCAGCAGCACTACGTTAAAATCAAGGAA 900
D D E A K L T L H G L Q Q H Y V K I K E 271
AATGAGAAGAATCGAAAATTGTTTGAATTACTCGATGCTTTAGAGTTCAACCAGGTTGTG 960
N E K N R K L F E L L D A L E F N Q V V 291
ATATTCGTTAAGTCAGTAAGGGGAGAGACTGAGTCGTTACCAGCAGTTCAAGGACTTCCAG 1000
I F V K S V R E R L S R Y Q Q F K D F Q 311
AAGCGCATTCTGGTGGCAACAAACCTGTTTGGTAGAGGAATGGATATTGAGCGAGTGAAC 1060
K R I L V A T N L F G R G M D I E R V N 331
ATCGTGTTCAACTATGATATGCCAGAAGACAGTGACACATACCTTCACAGAGTAGCAAGA 1120
I V F N Y D M P E D S D T Y L H R V A R 351
GCTGGTCGATTCCGAACCAAGGGATTAGCTGTACATTTGTGAGTGAAGAGAGTGTGCA 1180
A G R F G T K G L A V T F V S E E S D A 371
AAGATTTTGAATGAGGTTTCAGGAGAGATTTCGATGTAAACATCACAGAGCTACCCGATGAG 1240
K I L N E V Q E R F D V N I T E L P D E 391
ATTGAGCTCAGCTCATACTTGAAGGTCGTTTGAAATGGGAGAGAGAAGGAGTAATTGTAG 1300
I E L S S Y I E G R * 401
GGTCCAGATGAGGCACTGGTGTAGTGTGAATGGTATAAGAAATGTTAATGTAAATGATTC 1360
TTGTGTGTTTCATGTTGAGATTGATATTTGAATGATCCTTTA 1404

```

Figure 3.31 The full length cDNA and deduced protein sequences of *ATP-dependent RNA helicase* of *P. monodon*. Start and stop codons are illustrated in boldfaced and underlined. The putative *N*-linked-glycosylation site is highlighted.

The calculated *pI* and MW of the deduced ATP-dependent RNA helicase protein was 5.39 and 45.96 kDa, respectively. Like other helicases described above, ATP-dependent RNA helicase protein did not contain the signal peptide. Two

domains (DEXDc and HELICc) were found at the amino acid positions 64 - 265 ($7.34e-52$) and 276 - 356 ($2.76e-15$; Figure 3.32) of the deduced protein, respectively. The *N*-linked-glycosylation domain was found at positions 383-385.

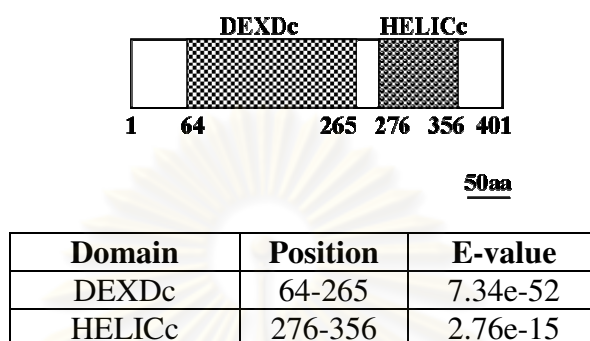


Figure 3.32 Diagram illustrating the full length cDNA of *ATP-dependent RNA helicase* of *P. monodon*. The DEXDc and HELICc domains were found in the deduced protein of this transcript. The scale bar is 200 bp in length.

3.4.4. *L*-3-hydroxyacyl coenzyme A dehydrogenase

A 1200 bp fragment was obtained from the primary 3' RACE-PCR of a *L*-3-hydroxyacyl coenzyme A dehydrogenase primer (Figure 3.33). This fragment was cloned and characterized. Nucleotide sequences of the original EST and 3' RACE-PCR were assembled (Figure 3.33).

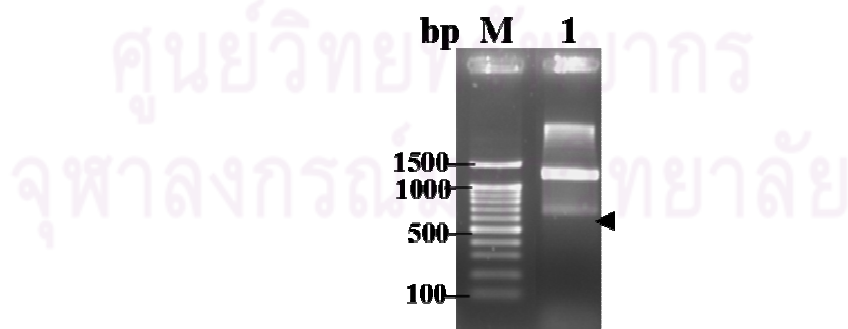


Figure 3.33 The primary 3' RACE-PCR product of *L*-3-hydroxyacyl coenzyme A dehydrogenase. An arrowhead indicates a RACE-PCR product that was cloned and sequenced. Lane M is a 100 bp DNA ladder.

The full length cDNA *P. monodon L-3-hydroxyacyl coenzyme A dehydrogenase* was 1238 bp in length with the ORF of 933 bp deducing to a polypeptide of 310 amino acids and the 5' and 3' UTRs of 57 and 268 bp (excluding the poly A tail), respectively (Figure 3.35). The closest match to this transcript was *L-3-hydroxyacyl coenzyme A dehydrogenase of Ciona intestinalis* (E-value = 1e-110).

A.

GCGCTGTTGGCAACACTTGACTCCTTTGCTCTCCTCGTTAAATAGCGCTAAAAAAAAATGTCTTTCTTC

3' RACE-PCR

ACGGCTCTCACCACTAGGACTTTCTCCAGCTCGGCTAGGATGGCAGCTGCGATTAAGAATGTTACCGTC
 ATCGGGAGCGGGTTAATGGGCGCAGGTATTGCTCAGGTGGCAGCCCAGACTGGCCACACAGTGACCATG
 GTTGATATTGACAAGGCAGCTGTGGAGAAGGCTGAAAAGAGAATTGCTGCATCAATTCAAAGGGTTGCT
 AAGAAGAAATTTAGCAGCGATGAAGGGGAGGCAACCAAGTTCATCTCGGAGGCACTTAGCCGCTCTGAAC
 ACTTCCACAGATGCAGTTGCCTCTGTGGGCTCGGCTGACTTGGTTGTGGAGGCTATTGTGGAGAACATT
 GGGGTCAAGCAGAAGTTGTTCAAGGAAGTAGATCAGGCTGCTCCAGAGCACACCATTTTTGCATCCAAT
 ACCTCATCCCTTCTATTGGCAAGATTGCTGAGGTTACAGATAGGAAGGACAGGTTTGGAGGCCTGCAT
 TTCTTCAACCCTGTGCCAGTGATGAAGCTCTTAGAGGTGGTGC GGATCCCGGAAACCTCTCAGAACACA
 TATGAAGCCATGTGTGCATGGGGAAAAGAACATGGGCAAAGTGACTGTTGAATGCAAAGACACACCTGGA
 TTCATTGTCAACCGCTTGCTGGTGCCCTTATATGTTTGA

B.

TATGAAGCCATGTGTGCATGGGGAAAAGAACATGGGCAAAGTGACTGTTGAATGCAAAGACACACCTGGA
 TTCATTGTCAACCGCTTGCTGGTGCCCTTATATGTTTGAATCTGTTAGGATGCTAGAGAGAGGAGATGCA
 AGTGCCAGAGATATTGATGTAGCAATGAAGCTTGGTGCTGGCTACCCCATGGGACCTTTTGAGCTCATG
 GATTACGTTGGTCTTGACACTGGAAAATTCATTGTTGATGGTTGGGCTAAGGAATACCCAGATAACCCA
 CTCTTCCAGCCTTTTGAACCTTTGAACAAGATGGTTGCGGAGGGCAAGCTGGGTGTAAAGTCTGGAGAA
 GGTTTTTACTCTTACAAGAAGTAAAAAAGCAAGACTAGCCACACCCAGAAATTGTCAAACGAGTGATG
 TAAGGAGGCAAGATGAACACTCGTTTGAATTTGTCCATAATACTGAAGAAGGAATATTCTGTTATGAAA
 TTTTCATGCAATACTAATACTAGTCGTGAATCTGTACAGAAATATTATGTGTTTTTCTGTAAGATCTATATG
 CACATCAATGCAATATTGTTAATACTGTATTTGTACTTTTAAAAATTAAAAAGATATTTTTTAAAAAAA
 AAAAAAAAAAAAAAAAAA

Figure 3.34 Nucleotide sequence of EST (A) and 3' RACE-PCR (B) of *L-3-hydroxyacyl coenzyme A dehydrogenase* of *P. monodon*. A reverse primer for RT-PCR (L3HF and L3HR, underlined) was used for 3' RACE-PCR of this gene.

The calculated *pI* and MW of *L-3-hydroxyacyl coenzyme A dehydrogenase* of *P. monodon* was 6.86 and 33.68 kDa, respectively, The predicted signal peptidase site was located at positions 42-43 and three putative *N*-linked-glycosylation sites were found at positions 24-26, 96-98 and 142-144 of the deduced protein (Figure 3.35).

Five overlapped protein domains were found from sequence analysis using SMART. Nevertheless, the E-values of NAD binding 2, NAD Gly3P dh N, UDPGP MGDH dh N, and Pyr redox domain were quite low (Figure 3.36). Accordingly, these domains should be artifact from protein sequence analysis.

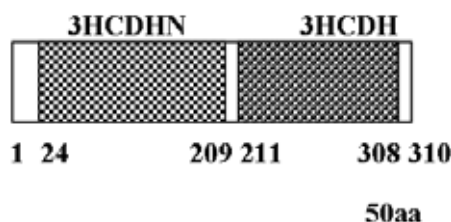
Two domains; 3HCDH_N and 3HCDH were bioinformatically found with high similarity (E-value = $1.30e-86$ and $1.60e-48$). Typically, 3-hydroxyacyl-CoA dehydrogenase (HCDH) is an enzyme functionally involved in fatty acid metabolism, it catalyzes the reduction of 3-hydroxyacyl-CoA to 3-oxoacyl-CoA. The 3HCD N and 3HCDH domains play an essential catalytic activity of this enzyme.

```

CGCCTGTTGGCAACACTTGACTCCTTTGCTCTCCTCGTTAAATAGCGCTAAAAAAAAATG 60
                                                                M 1
TCTTTCTTCACGGCTCTCACCCTAGGACTTTCTCCAGCTCGGCTAGGATGGCAGCTGCG 120
S F F T A L T T R T F S S S A R M A A A 21
ATTAAGAATGTTACCGTCATCGGGAGCGGGTTAATGGGCGCAGGTATTGCTCAGGTGGCA 180
I K N V T V I G S G L M G A G I A Q V A 41
GCCCAGACTGGCCACACAGTGACCATGGTTGATATTGACAAGGCAGCTGTGGAGAAGGCT 240
A Q T G H T V T M V D I D K A A V E K A 61
GAAAAGAGAATTGCTGCATCAATTCAAAGGGTTGCTAAGAAGAAATTTAGCAGCGATGAA 300
E K R I A A S I Q R V A K K K F S S D E 81
GGGGAGGCAACCAAGTTCATCTCGGAGGCACTTAGCCGCTGAACACTTCCACAGATGCA 360
G E A T K F I S E A L S R L N T S T D A 101
GTTGCCTCTGTGGGCTCGGCTGACTTGGTTGTGGAGGCTATTGTGGAGAACATTGGGGTC 420
V A S V G S A D L V V E A I V E N I G V 121
AAGCAGAAGTTGTTCAAGGAAGTAGATCAGGCTGCTCCAGAGCACACCATTTTTGCATCC 480
K Q K L F K E L D Q A A P E H T I F A S 141
AATACCTCATCCCTTCTTATTGGCAAGATTGCTGAGGTTACAGATAGGAAGGACAGGTTT 540
N T S S L P I G K I A E V T D R K D R F 161
GGAGGCCTGCATTTCTCAACCTGTGCCAGTGATGAAGCTTTAGAGGTGGTGC GGATC 600
G G L H F F N P V P V M K L L E V V R I 181
CCGGAAACCTCTCAGAACACATATGAAGCCATGTGTGCATGGGGAAAGAACATGGGCAA 660
P E T S Q N T Y E A M C A W G K N M G K 201
GTGACTGTTGAATGCAAAGACACACCTGGATTGATTGTTCAACCGCTTGGTGCCTTAT 720
V T V E C K D T P G F I V N R L L V P Y 221
ATGTTTGAATCTGTTAGGATGCTAGAGAGAGGAGATGCAAGTGCCAGAGATATTGATGTA 780
M F E S V R M L E R G D A S A R D I D V 241
GCAATGAAGCTTGGTGTGGCTACCCCATGGGACCTTTTGGAGCTCATGGATTACGTTGGT 840
A M K L G A G Y P M G P F E L M D Y V G 261
CTTGACACTGGAAAATTCATTGTTGATGGTTGGGCTAAGGAATACCCAGATAACCCACTC 900
L D T G K F I V D G W A K E Y P D N P L 281
TTCCAGCCTTTTGAACCTTTTGAACAAGATGGTTGCGGAGGGCAAGCTGGGTGTAAAGTCT 960
F Q P F E L L N K M V A E G K L G V K S 301
GGAGAAGGTTTTACTCTTACAAGAAGTAA*****AGCAAGACTAGCCACACCCAGAAATT 1020
G E G F Y S Y K K * 310
GTCAAACGAGTGATGTAAGGAGGCAAGATGAACACTCGTTTGAATTTGTCCATAATACTG 1080
AAGAAGGAATATTCTGTTATGAAATTTTCATGCAATACTAATAGTCGTGAATCTGTACAG 1120
AATATTATGTTTTTCTGTAAAGATCTATATGCACATCAATGCAATATTGTTAATACTG 1180
TATTTGTACTTTTAA*****AATTAA*****AGATATTTTTTAAAAAAAAAAAAAAAAAAAA 1238

```

Figure 3.35 The full length cDNA and deduced protein sequences of *L-3-hydroxyacyl coenzyme A dehydrogenase* of *P. monodon*. Start and stop codon are illustrated in boldfaced and underlined. The *N*-linked-glycosylation sites are highlighted. The poly A additional signal (AATTAA) is boldfaced.



Domain	Position	E-value
NAD_binding_2	22-150	4.60e-02
NAD_Gly3P_dh_N	23-148	1.20e-02
UDPG_MGDP_dh_N	23-160	8.90e-02
3HCDH_N	24-209	1.30e-86
:Pyr_redox	24-120	5.10e-02
3HCDH	211-308	1.60e-48

Figure 3.36 Diagram illustrating the full length cDNA of *L-3-hydroxyacyl coenzyme A dehydrogenase* of *P. monodon*. The 3HCDH_N and 3HCDH domains were found in this transcript. The scale bar is 200 bp in length.

3.4.5. Protein disulfide isomerase

The primary 5' and 3' RACE-PCR of *protein disulfide isomerase* generated fragments of 1000 and 1200 bp fragment were obtained from the primary primer (Figure 3.37). These fragments were further characterized by cloning and sequencing. Nucleotide sequences of the original EST and 5' and 3' RACE-PCR (Figure 3.38) were assembled.

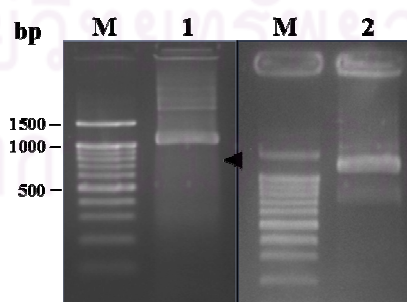


Figure 3.37 Repeating nested 5' (lane 1) and 3' (lane 2,) RACE-PCR product of *protein disulfide isomerase*. Arrowheads indicate RACE-PCR products that were cloned and sequenced. Lanes M are a 100 bp DNA ladder.

A.**I**

AAGCAGTGGTATCAACGCAGAGTACGCGGGAGCGTGACCTGCTTCGTCTGCTTTTGCGGTCACGAGACC
 TGGAGCGGAGCGGAGCGGCGGGACTTGGATTCTTTCTTTTATCTTTCTCCTTCTCTTTTTCTTTGG
 AGCTCTCTTCTGCCTTAGCTTCCCTCTTCTTCGCTCTTTACTCTCTTCTCCTTCTCCTTTTCGCTCGT
 TCTCGGTCTCCTTTATTGCTCCAGTTTCTTCTCCTCCCTCTTCTCTTTGTCTTTATCCTTTGATTTGT
 CCTTATCCCTGTCTTGTCCCTATCCTTATCCTTGTCTTGTCTTTGTCTTGTCTTTGCCTTTGCCAC
 GGCTGCTGCTGCTCGAGCCCTTGTCTCTCCTTGAAGGATGACGCCGTAGACTTCGACTTGGACCTTGACC
 TCTTTGAGCGGGATTTGGACCTTGATTTCTTCTGTGATGGAGACCTGGATCTGGACTTCTTGCAGACC
 TTGATCGCGATCTCTTTCTGCGCTGCGCTTCTAGAGCGTCCGTGTCGGTCTCTAGATCGGGTCTGG
 AACGTAACCTCCGGCGGGAGTGTGACCTTATTCCATCCAACCTTCCA

II

CGTGGCCTATGTCTCAGGGCCGATCTTAACGGGTGCGGAAGAACGAGCACGAGGTGAGGTAAATTTCT
 TTTTCAATGCTTCAAAGGCAATCCATTTCTGGTGACCAAAATCAGCCAGAATGAGATTTTTGTGCAATA
 GCATCC

Nested 5' RACE-PCR

TCATAATGGGTGGGAGTGCCAGGGATGTATTCTCCCTCTAGTGGCGTTGTGACCTTATTCCATCCAAC
TTCCAGGGAGAAGTTCTGAACAGTGATGCTGTGGGGATCATCGAGTTTATGCCCCATGGTGCGGTCCAC
TGTCAGCGATTGGTACCCGAGTACACAAAAGCAGCTCAAGCCCTTAGTGGAGTTGTTAAAGTTGGTGCT
 GTTAATGCTGATGAACACAGGAGTTTAGGAGGTCAGTATGGGGTTCAGGGATTTCCCAACTATTAAGTC
 TTTGGCCTAGATAAGAAGAAACCAGAAGATTTCAATGGACAAAGAACAGCACAAGGTATTGTTGATGCT
 GCAATGAGGGCTGCTAGAGAAAAGGTAAATGCACAACCTATCAGGAAAGAAGAGTGGTGGCAGCAGTGGAA
 AGCCAGATGACGTTATTGAGCTTACAGATTCAAACTTTGAAAAGATGGTACTTAAATCAGATGATTTTC
 TGGCTGGTAGAATTCTTTGCCCTTGGTGTGGACATTGCAAGAACCCTGCACCTCACTGGCAGAAGGCT
 GCCACAGAGCTGAAGGGCAAGATTAATAATGGGAGCCTTAGATGCCACTGTTACACTGTCATGGCGAGT
 CGTTATGGTGTACAGGGTTATCCGACTATCAAGTTCTTCCACAAGGGAGAGGTTGGAGATTATGATGGT
 GGGCGCACTGCTTACAGACATCGTTGCCTGGGCTGATGACAAAGCTGCTGCAAATTTGCCACCACCAGAA
 ATTGTACAGATCACAGACAATGCCATCTTGACATCAGCTTGTAAAGAGCATCCCATCTGTATCATTACA
 GTTCTCCACACATTCTTGAAGTCCAGAGC

B.

GTGGCAGCAGCGGCGGTGGTGGCAGCAGTGGAAAGCCAGATGACGTTATTGAGCTTACAGATTCAAAC
 TTGAAAAGATGGTACTTAAATCAGACGATTTCTGGCTGGTAGAATTCTTTGCCCTTGGTGTGGACATT
 GCAAGA

3' RACE-PCR

ACCTTGACCTCACTGGCAGAAGGCTGCCACAGAGCTGAAGGGCAAGATTAATAATGGGAGCCTTAGATG
CCACTGTTACACTGTCATGGCGAGTCGTTATGGTGTACAGGGTTATCCCACTATCAAGTTCTTCCACA
AGGGAGAGGTTGGAGATTATGATGGTGGGCGCACTGCTTACAGACATCGTTGCCTGGGCTGATGACAAAG
 CTGCTGCAAATTTGCCACCACCAGAAATGTACAGATCACAGACAATGCCATCTTGACATCAG

5' RACE-PCR

CTTGTAAGAGCATCCCATTTGTATCATTACAGTTCTCCACACATTCTTGAAGTCCAGAGCAAGTGCC
 GCAACAATTACATTGAGATTCTGAGCAGACTTGGTGACAAATACAAGCAGAAGATGTGGGGATGGGTTT

Nested 3' RACE-PCR

GGAGTGAAGCAATGGCCCAACCTGAACTTGAACAAGCTCTGGATATGGTGGATTGGATACCTTGCTC
TTGCTGCTCTCAATGCAAAGAAGATGCAGTTTGCCTCCTGAAGGGGTCTTTTAGTGAGAGCGGCATTA
ACGAGTTCTTGCAGACATTTCTGATGGAAGAGGACGCACAGCACCTGTGCGAGGAGCTGAATTGCCAG
 CCATACAGGAAGTAGAGGCTTGGGGTGGTCCAGGATGGTGTGTTTGGCAGAGGAGGAAGACATTGATTTAT
 CTGATGTTGATCTAGATGATCTTGTGGTGAAGCTCATGAGGAGCTGTAAGACTATCTTTATTTTACTT
 TGCTGTGAAAAGTAAAGACTTAAACATTGAAAAGTAAAAGGAAGCAAAGGAAAAGTTGTAATTTCTCTAA
 TTT

C.

TGGTGGATTTGGATAACCTGCTCTTGCTGCTCTCAATGCAAAGAAGATGCAGTTTGCCCTCCTGAAGGG
 GTCTTTTAGTGAGAGCGGCATTAACGAGTTCTTGCGAGACATTTTCGTATGGAAGAGGGCGCACAGCACC
 TGTGCGAGGAGCTGAATTGCCAGCCATACAGGAAGTAGAGGCTTGGGATGGTCAGGATGGTGTGTTTGGC
 AGAGGAGGAAGACATTGATTTATCTGATGTTGATCTAGATGATCTTGATGGTGAAGCTCATGAGGAGCT
 GTAAGACTATCTTTATTTTACTTTGCTGTGAAAAGTAAAGACTTAACATTGAAAAGTAAAAGGAAGCAAA
 GGAAAAGTTGTAGTTTCTCCTAATTTCTCATGTTGAGAATGGAATGCTGTGACACATGAGCTATTCTTC
 ATTTTGGACAAAGTCAGGCCTTTTAAAAGTGCTTCTTAGGCTCTGCTAACATTTGCCCATAGAGAATG
 GATAAGCCTTACAAGTTCAAATGTAGGCTTGAACATCCCAATTTTACGAACTTATATTTTACATTGAT
 ATTATCATAATTTTTATTGTACTGTGTACACCATCTTCATTGTATCATTGGGAAGTTCAAGCTGCTGAA
 TTTAGTATTTTTTATCATGTAATTTGACATAGGAAAATTACAATTTGTTTCAGGTTTCTTTTTGCTGTATA
 AAAGCTTCTGGGTTGGGCATGTTACTAGTCGTTAAATCTGAAAAGTAAATTTTCAACTGTGCTGAAAT
 GTTAAAAGAACTTAAAAAAAAAAAAAAAAAAAAAAAAAAAAAAAAA

Figure 3.38 The sequence of primary (I, A), repeat-nested (II, A) RACE-PCR, EST (B) and 3' RACE-PCR (C) of *protein disulfide isomerase* of *P. monodon*. RT-PCR primers (PDIF and PDIR, underlined) were initially used followed by nested 5' and 3' RACE-PCR primers for isolation of the full length cDNA of this gene.

The full length cDNA of *protein disulfide isomerase P. monodon* was 2088 bp in length consisting an ORF of 1293 bp corresponding to a polypeptide of 430 amino acids and 5' and 3' UTRs of 144 and 651 bp (excluding the poly A tail) (Fig. 3.39). The closest similarity of this transcript was *protein disulfide isomerase A6* of *Tribolium castaneum* (E-value = 3e-155).

Protein disulfide isomerase A6 (also called PDI P5) plays an important role in rearrangement of disulfide bonds. It may also control function of certain extracellular proteins by regulating their redox state.

AAGCAGTGGTATCAACGCAGAGTACGCGGGGAGAAGGGAACGAGAGACGAACGCGAGGTG 60
 ACGTCTTTTCAAACCTTCTCCTCTTCTCCAACCTCTGGCCTTCCAAAGCTCAATCTCCATTG 120
 TCTGGTGACCAAAAATCAGGCAGGATGAGATTATTTGTTGCAATATGCATCCTCATGATG 180
 M R L F V A I C I L M M 12
 GGTGGGAGTGCCACAGCGATGTACTCTCCCTCTAGTGGCGTTGTGGACCTTACTCCATCC 220
 G G S A T A M Y S P S S G V V D L T P S 32
 AACTTCCAGCGAGAGGTTCTGAACAGTGATGCTGTGTGGATCATCGAGTTCTATGCCCA 280
 N F Q R E V L N S D A V W I I E F Y A P 52
 TGGTGC GGTC ACTGT CAGCGATTGGTACCCGAGTACACAAAAGCAGCTCAAGCCCTTAGT 340
 W C G H C Q R L V P E Y T K A A Q A L S 72
 GGAGTTGTAAAGTTGGTGTGTTAATGCTGATGAACACAGGAGTTTAGGAGGTCAGTAT 400
 G V V K V G A V N A D E H R S L G G Q Y 92
 GGGGTT CAGG GATCCCAACTATTAAAGTCTTTGGCCTAGATAAGAAGAAACCAGAAGAT 460
 G V Q G F P T I K V F G L D K K K P E D 112
 TTCAATGGACAAAGAACAGCACAAAGTATTGTTGATGCTGCAATGAGGGCTGCTAGAGAA 520
 F N G Q R T A Q G I V D A A M R A A R E 132

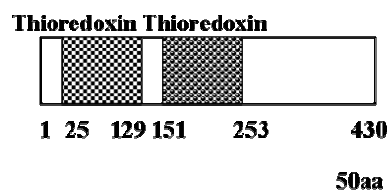
```

AAGGTAAATGCACAACATATCAGGAAAGAAGAGTGGTGGCAGCAGTGGAAGCCCAGATGAC 580
K V N A Q L S G K K S G G S S G S P D D 152
GTTATTGAGCTTACAGATTCAAACCTTTGAAAAGATGGTACTTAAATCAGATGATTTCTGG 640
V I E L T D S N F E K M V L K S D D F W 172
CTGGTAGAATTCTTTGCCCTTGGTGTGGACATTGCAAGAACCTTGCACCTCACTGGCAG 700
L V E F F A P W C G H C K N L A P H W Q 192
AAGGCTGCCACAGAGCTGAAGGGCAAGATTAATAATGGGAGCCTTAGATGCCACTGTTCAC 760
K A A T E L K G K I K M G A L D A T V H 212
ACTGTCATGGCGAGTCGTTATGGTGTACAGGGTTATCCGACTATCAAGTTCTTCCACAAG 820
T V M A S R Y G V Q G Y P T I K F H K 232
GGAGAGTTGGAAATTATGATGGTGGGCGCAGCTGCTCAGACATCGTTGCCTGGGCTGAT 880
G E V G N Y D G G R T A S D I V A W A D 252
GACAAAGCTGCTGCAAATTTGCCCCACCAGAAAATTGTACAGATCCCAGACAATGCCATC 940
D K A A A N L P P P E I V Q I P D N A I 272
CTGACATCAGCTTGTAAAAGAAGCATCCCATCTGTATCATTACAGTTCTTCCACACATT 1000
L T S A C K R S I P S V S L Q F L P H I 292
CTTGACTGCCAGAGCAAGTGCCGCAACAATTACATTGAGATTCTGAGCAGACTTGGTGAC 1060
L D C Q S K C R N N Y I E I L S R L G D 312
AAATACAAGCAGAAGATGTGGGGATGGGTTTGGAGTGAAGCAATGGCCCAACCTGAACTT 1120
K Y K Q K M W G W V W S E A M A Q P E L 332
GAACAAGCTCTGGATATTGGTGGATTGGATACCCCTGCTCTTGCTGCTCTCAATGCAAAG 1180
E Q A L D I G G F G Y P A L A A L N A K 352
AAGATGCAGTTTGGCCCTCCTGAAGGGGTCTTTTAGTGAGAGCGGCATTAACGAGTTCTTG 1240
K M Q F A L L K G S F S E S G I N E F L 372
CGAGACATTTTCGTATGGAAGAGGACGCACAGCACCTGTGCGAGGAGCTGAATTGCCAGCC 1300
R D I S Y G R G R T A P V R G A E L P A 392
ATACAGGAAGTAGGCTTGGGATGGTCAGGATGGTGTGTTTGGCCAGAGGAGGAAGACATT 1360
I Q G E V E A W D G Q D G V L P E E E D I 412
GATTIATCTGATGTTGATCTAGATGATCTTGTATGGTGAAGCTCATGAGGAGCTG T A AGAC 1420
D L S D V D L D D L D G E A H E E L * 430
TATCTTTATTTTACTTTGCTGTGAAAAAGTAAAAGACTTAAACATTGAAAAGTAAAAGGAAGCA 1480
AAGGAAAAGTTGTAATTTCTCCTAATTTCTCATGTTGAGAATGGAATGCTGTGACACATG 1540
AGCTATTCTTCATTTTGGACAAAAGTCAGGCCTTTTAAAAGTGCTTCTTAGGCTCTGCTAA 1600
CATTTGCCCATAGAGAATGGATAAGCCTTACAAGTTCAAATGTAGGCTTGAACATCCCA 1660
ATTTTACGAAACTTATATTTACATTGATATTATCATAATTTTTATTGTACTGTGTACAC 1720
CATCTTCATTGTATCATTGGGAAGTTCAAGCTGCTGAATTTAGTATTTTTTATCATGTAA 1780
TTTGACATAGGAAATTACAATTTGTTTCAGTTTCTTTTTGCTGTATAAAAAGCTTCCCTGGG 1840
TTGGGCATGTTACTAGTCGTTAAATCTGAAAAGTAAATTTTCAACTGTGCTGAAATGTTA 1900
AAAGAACTTGAAAAATAACACATTTTGTGAAAAAAAAAAAAAAAAAAAAAAAAAAAAAAAAA 1954

```

Figure 3.39 The full length cDNA and deduced protein sequences of *protein disulfide isomerase A6* of *P. monodon*. Start and stop codon are illustrated in boldfaced and underlined. The poly A additional signal (AATAA) is boldfaced.

The calculated *pI* and MW of the deduced protein disulfide isomerase protein was 5.55 and 52.65 kDa, respectively. The thioredoxin domains were found at the amino acid positions 25 - 129 (1.90e-37) and 151 - 253 (1.30e-50; Figure 3.40) of the deduced protein, respectively. The *N*-linked-glycosylation domain was not found.



Domain	Position	E-value
Thioredoxin	25-129	1.90e-37
Thioredoxin	151-253	1.30e-50

Figure 3.40 Diagram illustrating the full length cDNA of *protein disulfide isomerase A6* of *P. monodon*. The thioredoxin domains were found in this transcript. The scale bar is 50 amino acid in length.

3.4.6. Valosin-containing protein

An amplified fragment of approximately 1050 bp was obtained from the primary 5' RACE-PCR of *valosin-containing protein* (Figure 3.41). An amplification fragment was cloned and sequenced. Nucleotide sequences of the original EST and 5' RACE-PCR (Figure 3.42) were assembled.

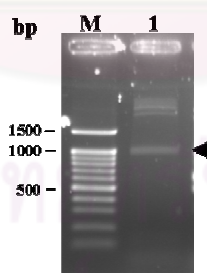


Figure 3.41 The primary 5' RACE-PCR product of *valosin-containing protein*. An arrowhead indicates a RACE-PCR product that was cloned and sequenced. Lanes M is a 100 bp DNA ladder.

A.

```
CTAATACGACTCACTATAGGGCAAGCAGTGGTATCAACGCAGAGTACGCGGGGAGTGTTCGAGGAGCCGT
CAGAGAGGAAGGAACGCTCGGGGGATTTCTTCGTCTTTTTATTAAAAAAAACACAATAATCCTTCGTTT
AATTTATCGAAGCCATGGCCGAACAGGACGACTTAGCTACTGCCATTCTTAAAGAGAAGAAGAAGCCCA
ACAGACTCATTGTGCGAGGATGCTGTCAACGACGACAATTCCGTGGTGGCACTCAGCCAGGCCAAGATGG
ATGAGCTGCAGCTCTTCCGCGGCGACACAGTCCTGTCTCAAGGGCAAGAAGCGCAAACAGACTGTGTGCA
TTGTGCTCTCAGACGACACCATGCAGGATGACAAGATTCGCATGAACCGTGTGGTCAGAAACAACCTTC
```

GCATCCGCTTGGGAGACATCGTGTCCATCCAGCCGTGTCCAGACGTCAAGTATGGCAAACGTATCCATG
 TCCTGCCGATTGATGACACTGTTGAAGGTCTCACGGGAAACATCTTTGAGGTATATTTGAAGCCCTACT
 TTCTGGAGGCATACAGGCCCATCCACAAGGGTGACCTGTTCCCTGGTGCAGGTGGTATGAGGGCTGTGG
 AGTTCAAGGTGGTGGAGACGGATCCTGCGCCTTATTGCATCGTCTCCAGGACACTGTTATCTACTGTG
 AAGGAGAGCCAGTTAAGCGAGAGAGGAGGAGGAAGAGCAGTTGAACGAGGTGGGCTACGATGACATCGGTG
 GCTGCCGCAAACAGTTGGCACAGATCAAGGAGATGGTGGAGCTGCCCTCCGCCACCCTTCACTCTTCA
 AGGCCATTGGTGTCAAGCCCCAAGAGGTATCCTTCTCTATGGTCCCTCGGTACTGGTAAGACCCTCA
 TTGCCCGTGGCAGTGGCCAACGAGACCGGAGCATTCTTCTTCCCTCATCAACGGGCTGAGATCATGTTT
 AAAGTTAGCTGGTGAATCCGAGAGGCAACCTTCGCAA

B.

CGGATCCTGCGCCTTATTGCATCGTCTCCAGGACACTGTTATCTACTGTGAAGGAGAGCCAGTTAAGC

5' RACE-PCR

GAGAGGAGGAGGAAGAGCAGTTGAACGAGGTGGGCTACGATGACATCGGTGGCTGCCGCAAACAGTTGG
 CACAGATCAAGGAGATGGTGGAGCTGCCTCTCCGCCACCCTTCACTCTTCAAGGCCATTGGTGTCAAGC
 CCCCAGAGGTATCCTTCTCTATGGTCCCTCGGTACTGGTAAGACCCTCATTGCCCGTGCAGTGGCCA
 ACGAGACCGGAGCATTCTTCTTCCCTCATCAACGGGCTGAGATCATGTCAAAGTTAGCTGGTGAATCCG
 AGAGCAACCTTCGCAAGGCCTTCGAAGAGGCTGAGAAGAATGCCCTGCCATCATCTTCATTGATGAGA
 TTGATGCCATTGCACCCAAGCGTGAAAAGACACATGGTGGAGGTGGAAAGACGTATAGTGTACAGCTGC
 TAACTCTTATGGATGGCCTCAAGCAACGAGCCATGTTATTGTTATGGCTGCCACAAACCGCCCCAACT
 CCATCGACCCGGCACTCAGGCGATTTGGACGCTTTGACAGGGAGGTTGACATCAGTATCCCAGACACTA
 CAGGTGCTCTGGAGATTTTGCATCCACACTAAGAACATGAAGCTGTCAGATGATGTGGACCTGGAAC
 AGATTGCAGCAGAAACCCATGGCCATGTTGGTGTGAC

Figure 3.42 Nucleotide sequence of 5' RACE-PCR (A) and EST (B) of *valosin containing protein* of *P. monodon*. A reverse RT-PCR primer (names of primers, underlined) was used for 5' RACE-PCR of this gene.

The partial cDNA sequence covering the 5' UTR and the N-terminus portion of *valosin-containing protein* were obtained. This transcript was significantly similar to *valosin-containing protein* of *Xenopus tropicalis* (E-value = 0.0).

Valosin-containing protein are highly similar to VCP/P97/Cdc48 cluster of genes within the superfamily of ATPase-Associated with diverse cellular Activity (AAA). Several reports have demonstrated VCPs crucial role in cell proliferation, reproductive functioning and spermatogenesis (Suzuki et al.,2005). VCP homologues in *Drosophila* have been shown to be associated with germ cell development, such as meiosis and oogenesis (Leon and McKearin, 1999; Ruden et al., 2000).


```

CTAATACGACTCACTATAGGGCAAGCAGTGGTATCAACGCAGAGTACGCGGGGAGTGTTCG 60
AGGAGCCGTCAGAGAGGAAGGAACGCTCGGGGATTTCTTCGTCTTTTTATTAIAAAAAA 120
CACAATAATCCTTCGTTTAATTTATCGAAGCCATGGCCGAACAGGACGACTTAGCTACTG 180
M A E Q D D L A T 9
CCATTCTTAAAGAGAAGAAGAAGCCCAACAGACTCATTGTCGAGGATGCTGTCAACGACG 240
A I L K E K K K P N R L I V E D A V N D 29
ACAATTCGGTGGTGGCACTCAGCCAGGCCAAGATGGATGAGCTGCAGCTCTTCCGCGGCG 300
D N S V V A L S Q A K M D E L Q L F R G 49
ACACAGTCCTGCTCAAGGGCAAGAAGCGCAAACAGACTGTGTGCATTGTGCTCAGAG 360
D T V L L K G K K R K Q T V C I V L S D 69
ACACCATGCAGGATGACAAGATTTCGCATGAACCGTGTGGTCAGAAACAACCTTCGCATCC 420
D T M Q D D K I R M N R V V R N N L R I 89
GCTTGGGAGACATCGTGTCCATCCAGCCGTGTCCAGACGTCAAGTATGGCAAACGTATCC 480
R L G D I V S I Q P C P D V K Y G K R I 09
ATGTCTGCCGATTGATGACACTGTTGAAGGTCTCACGGGAAACATCTTTGAGGTATATT 540
H V L P I D D T V E G L T G N I F E V Y 129
TGAAGCCCTACTTTCTGGAGGCATACAGGCCCATCCACAAGGGTGACCTGTTCCCTGGTGC 600
L K P Y F L E A Y R P I H K G D L F L V 149
GAGGTGGTATGAGGGCTGTGGAGTTCAAGGTGGTGGAGACGGATCCTGCGCCTTATTGCA 660
R G G M R A V E F K V V E T D P A P Y C 169
TCGTCTCCAGGACACTGTTATCTACTGTGAAGGAGAGCCAGTTAAGCGAGAGGAGGAGG 720
I V S Q D T V I Y C E G E P V K R E E E 189
AAGAGCAGTTGAACGAGGTGGGCTACGATGACATCGGTGGCTGCCGCAAACAGTTGGCAC 780
E E Q L N E V G Y D D I G G C R K Q L A 209
AGATCAAGGAGATGGTGGAGCTGCCTCTCCGCCACCCTTCACTCTTCAAGGCCATTGGTG 840
Q I K E M V E L P L R H P S L F K A I G 229
TCAAGCCCCCAAGAGGTATCCTTCTCTATGGTCTCCTGCTACTGGTAAGACCCTCATTG 900
V K P P R G I L L Y G P P G T G K T L I 249
CCCGTGCAGTGGCCAACGAGACCGGAGCATTCTTCTTCTCATCAACGGGCCTGAGATCA 960
A R A V A N E T G A F F F L I N G P E I 269
TGTCAAAGTTAGCTGGTGAATCCGAGAGCAACCTTCGCAAGGCCTTCGAAGAGGCTGAGA 1020
M S K L A G E S E S N L R K A F E E A E 289
AGAATGCCCTGCCATCATCTTCATTGATGAGATTGATGCCATTGCACCCAAGCGTGAAA 1080
K N A P A I I F I D E I D A I A P K R E 309
AGACACATGGTGGAGGTGAAAGACGTATAGTGTACAGCTGCTAACTCTTATGGATGGCC 1140
K T H G E V E R R I V S Q L L T L M D G 329
TCAAGCAACGAGCCCATGTTATTGTTATGGCTGCCACAAACCGCCCCAACTCCATCGACC 1200
L K Q R A H V I V M A A T N R P N S I D 349
CGGCACTCAGGCGATTTGGACGCTTTGACAGGGAGGTTGACATCAGTATCCAGACACTA 1260
P A L R R F G R F D R E V D I S I P D T 369
CAGGTGCTCTGGAGATTTTGCATCCACACTAAGAACATGAAGCTGTGAGATGATGTGG 1320
T G R L E I L R I H T K N M K L S D D V 389
ACCTGGAACAGATTGCAGCAGAAACCCATGGCCATGTTGGTGCTGAC 1367
D L E Q I A A E T H G H V G A D 405

```

Figure 3.43 Partial nucleotide and deduced amino sequences of *valosin containing protein* of *P. monodon*. The start codon and primer position are illustrated in boldfaced and underlined.

3.5 RT-PCR and tissue distribution analysis of gene homologues

Total RNA from ovaries revealed predominated discrete bands along with smeared high molecular weight RNA (Figure 3.44). The ratios of purified RNA were 1.7-2.0 implying that the quality of extracted DNA was acceptable for further applications. The first cDNA synthesized from those total RNA covered the large product sizes (Figure 3.45).

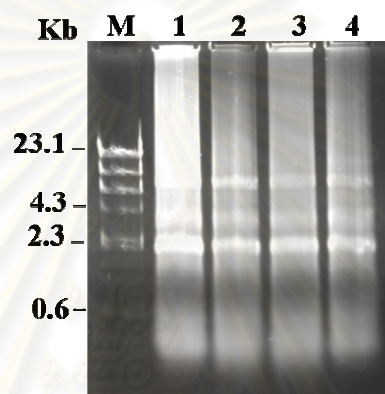


Figure 3.44 A 1.0% ethidium bromide-stained agarose gel showing the quality of total RNA extracted from female broodstock of *P. monodon*. Lane M = λ -Hind III. Lane 1-4 = total RNA from ovaries of each *P. monodon* broodstock.

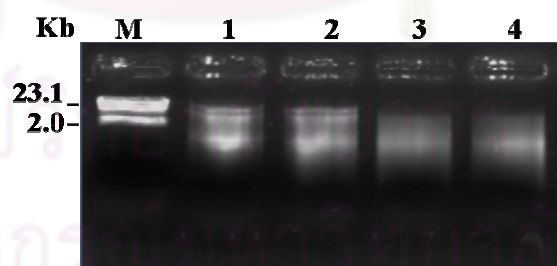


Figure 3.45 A 1.0% ethidium bromide-stained agarose gel showing the first strand cDNA synthesized from ovaries of *P. monodon*. Lane M = λ -Hind III. Lane 1-4 = the first strand cDNA from ovaries of each *P. monodon* broodstock.

Ten primer pairs were designed from nucleotide sequences of EST libraries previously established from ovaries (7 primer pairs), hemocyte (2 primer pairs) and gill (1 primer pair) of *P. monodon*. RT-PCR was carried out using an identical amplification condition for all primer pairs.

Initially, the first strand cDNA synthesized from ovaries were subjected to RT-PCR and electrophoretically analyzed. All genes were expressed in ovaries of female broodstock.

Subsequently, tissue distribution analysis was carried out to examine the expression of 8 gene homologues (*DEAD box 52*, *DEAD box ATP-dependent RNA helicase*, *ATP-dependent RNA helicase*, *heterogeneous nuclear ribonucleoprotein*, *protein disulfide isomerase*, *helicase lymphoid specific isoform 2*, *L-3-hydroxyacyl coenzyme A dehydrogenase* and *valosin containing protein*) in ovaries, testes, heart, hemocytes, lymphoid organs, intestine, gills, pleopods, thoracic ganglion, stomach, epicuticle, eyestalk and hepatopancrease of a single female broodstock of *P. monodon*.

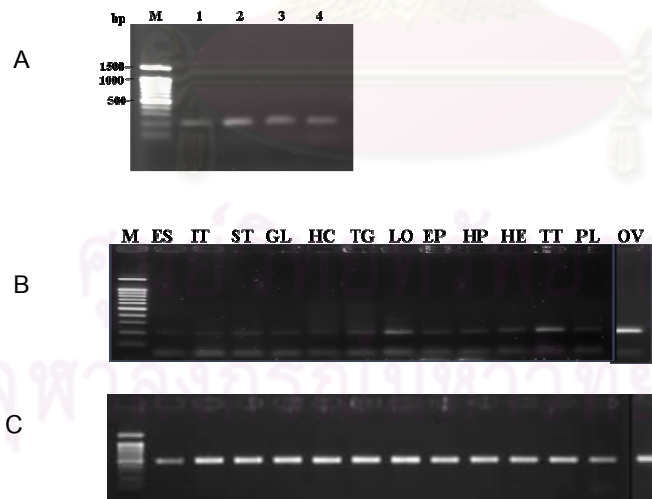


Figure 3.46 A 1.5% ethidium bromide-stained agarose gel showing results from RT-PCR (A) and tissue distribution analysis (B) *DEAD box 52* using the first strand cDNA of ovaries (lanes 1-4, A) and various tissues of broodstock sized *P. monodon* (B) and *EF-1 α* (C). Lane M is a 100 bp DNA ladder marker. ES = eyestalk, IT = intestine, ST = stomach, GL = gill, HC = hemocytes, TG = thoracic ganglion, LO = lymphoid organ, EP = epicuticle, HP = hepatopancrease, HE = heart, TT = testes, PL = pleopod and OV = ovaries.

DEAD box 52 and *DEAD box ATP-dependent RNA helicase* were abundantly expressed in ovaries and lower expression was observed in testes and lymphoid organ. Expression of these transcripts in heart, hemocytes, intestine, gills, pleopods, thoracic ganglion, stomach, epicuticle, eyestalk and hepatopancrease of a female broodstock of *P. monodon* was extremely low (Figures 3.46 and 3.47).

ATP-dependent RNA helicase were abundantly expressed in ovaries followed by intestine, lymphoid organ, epicuticle and hepatopancreas. Low abundant levels of *ATP-dependent RNA helicase* was observed in stomach, gills, hemocytes, thoracic ganglion, heart, testes and pleopod. This transcript was not expressed in eyestalk of a female broodstock (Figure 3.48).

Expression of *helicase lymphoid specific isoform 2* was observed in all examined tissues except thoracic ganglion. Slightly greater expression levels were observed in ovaries, intestine and lymphoid organ. Comparable lower levels were observed in the remaining tissues (Fig. 3.49).

Heterogeneous nuclear ribonucleoprotein was constitutively expressed in all examined tissues. Low expression of this transcript was observed in hemocytes and thoracic ganglion (Figure 3.50).

Protein disulfide isomerase was expressed at a low level in most examined tissues. This transcript was not expressed in thoracic ganglion and epicuticle (Fig. 3.51). In contrast, *valosin-containing protein* was abundantly expressed in all examined tissues (Fig. 3.52).

L-3-hydroxyacyl coenzyme A dehydrogenase was abundantly expressed in ovaries, testes, heart, hemocytes, lymphoid organs, gills, pleopods, thoracic ganglion, stomach, epicuticle and hepatopancrease. This transcript was not expressed in eyestalk and intestine of a female broodstock (Fig. 3.53).

A summary on expression of these genes in various tissues was illustrated in Table 3.7. Comparison of expression profiles of examined genes were shown in Table 3.8.

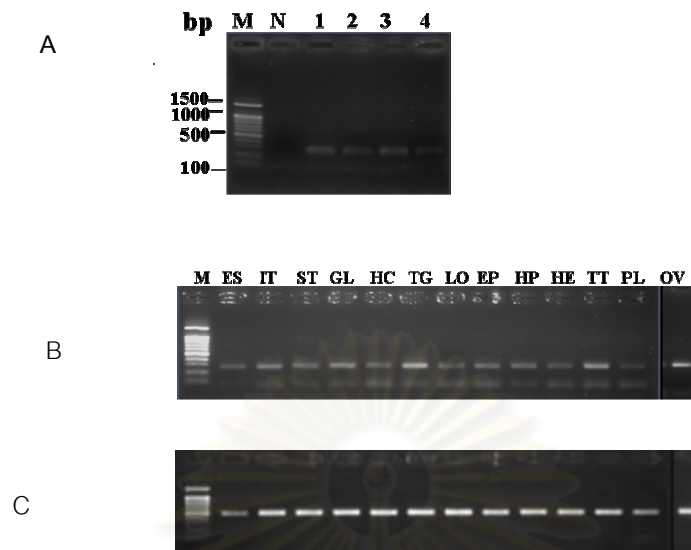


Figure 3.47 A 1.5% ethidium bromide-stained agarose gel showing results from RT-PCR (A) and tissue distribution analysis (B) of *DEAD box ATP-dependent RNA helicase* using the first strand cDNA of ovaries (lanes 1-4, A) and various tissues of broodstock sized *P. monodon* (B) and *EF-1 α* (C). Lane M is a 100 bp DNA ladder marker. ES = eyestalk, IT = intestine, ST = stomach, GL = gill, HC = hemocytes, TG = thoracic ganglion, LO = lymphoid organ, EP = epicuticle, HP = hepatopancrease, HE = heart, TT = testes, PL = pleopod and OV = ovaries.

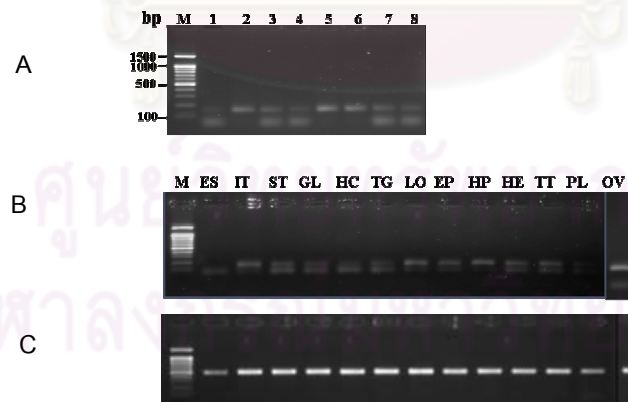


Figure 3.48 A 1.5% ethidium bromide-stained agarose gel showing results from RT-PCR (A) and tissue distribution analysis (B) of *ATP-dependent RNA helicase* using the first strand cDNA of ovaries (lanes 1-8, A) and various tissues of broodstock sized *P. monodon* (B) and *EF-1 α* (C). Lane M is a 100 bp DNA ladder marker. ES = eyestalk, IT = intestine, ST = stomach, GL = gill, HC = hemocytes, TG = thoracic ganglion, LO = lymphoid organ, EP = epicuticle, HP = hepatopancrease, HE = heart, TT = testes, PL = pleopod and OV = ovaries.

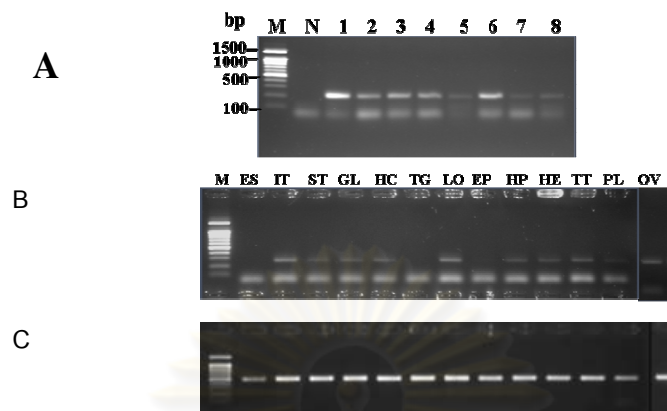


Figure 3.49 A 1.5% ethidium bromide-stained agarose gel showing results from RT-PCR (A) and tissue distribution analysis (B) of *helicase lymphoid specific isoform 2* using the first strand cDNA of ovaries (lanes 1-8, A) and various tissues of broodstock sized *P. monodon* (B) and *EF-1 α* (C). Lane M is a 100 bp DNA ladder marker. ES = eyestalk, IT = intestine, ST = stomach, GL = gill, HC = hemocytes, TG = thoracic ganglion, LO = lymphoid organ, EP = epicuticle, HP = hepatopancrease, HE = heart, TT = testes, PL = pleopod and OV = ovaries.

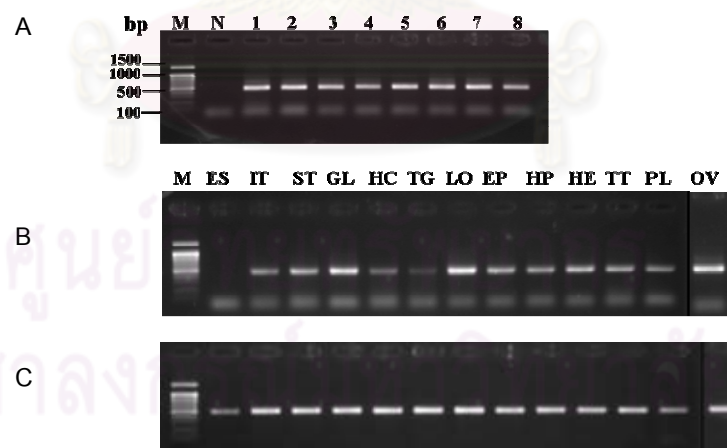


Figure 3.50 A 1.5% ethidium bromide-stained agarose gel showing results from RT-PCR (A) and tissue distribution analysis (B) of *heterogeneous nuclear ribonucleo protein* using the first strand cDNA of ovaries (lanes 1-8, A) and various tissues of broodstock sized *P. monodon* (B) and *EF-1 α* (C). Lane M is a 100 bp DNA ladder marker. ES = eyestalk, IT = intestine, ST = stomach, GL = gill, HC = hemocytes, TG = thoracic ganglion, LO = lymphoid

organ, EP = epicuticle, HP = hepatopancrease, HE = heart, TT = testes, PL = pleopod and OV = ovaries.

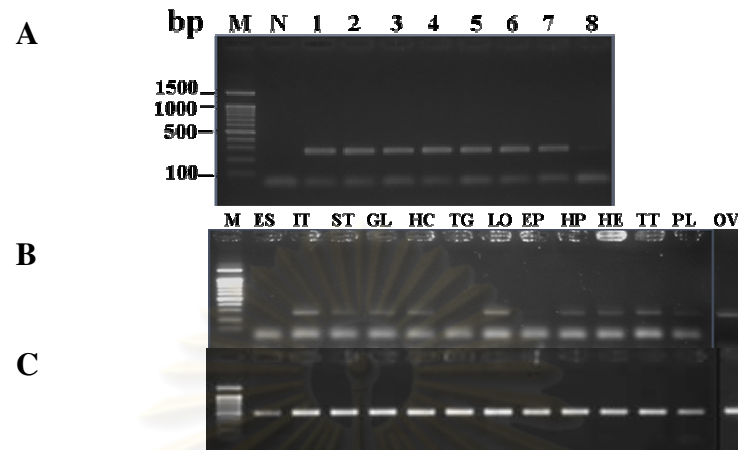


Figure 3.51 A 1.5% ethidium bromide-stained agarose gel showing results from RT-PCR (A) and tissue distribution analysis (B) of *protein disulfide isomerase* using the first strand cDNA of ovaries (lanes 1-8, A) and various tissues of broodstock sized *P. monodon* (B) and *EF-1 α* (C). Lane M is 100 bp DNA ladder marker. ES = eyestalk, IT = intestine, ST = stomach, GL = gill, HC = hemocytes, TG = thoracic ganglion, LO = lymphoid organ, EP = epicuticle, HP = hepatopancrease, HE = heart, TT = testes, PL = pleopod and OV = ovaries.

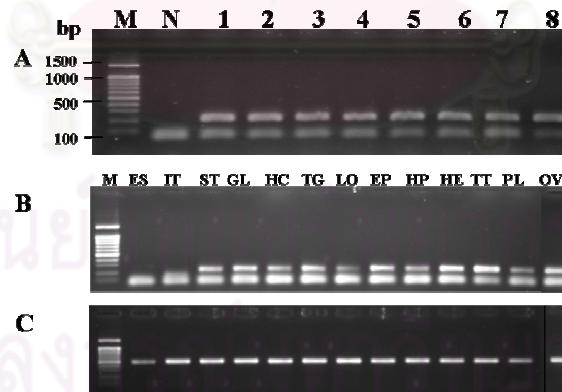


Figure 3.52 A 1.5% ethidium bromide-stained agarose gel showing results from RT-PCR (A) and tissue distribution analysis (B) of *valosin-containing protein* using the first strand cDNA of ovaries (lanes 1-8, A) and various tissues of broodstock sized *P. monodon* (B) and *EF-1 α* (C). Lane M and N are 100 bp DNA ladder marker and negative control respectively. ES = eyestalk, IT = intestine, ST = stomach, GL = gill, HC = hemocytes, TG = thoracic ganglion, LO = lymphoid organ, EP = epicuticle, HP = hepatopancrease, HE = heart, TT = testes, PL = pleopod and OV = ovaries.

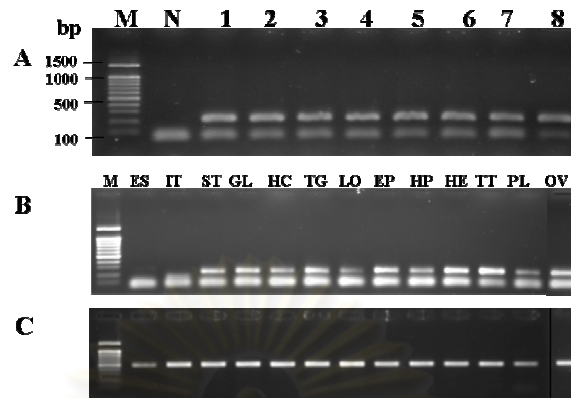


Figure 3.53 A 1.5% ethidium bromide-stained agarose gel showing results from RT-PCR (A) and tissue distribution analysis (B) of *L-3-hydroxyacyl coenzyme dehydrogenase* using the first strand cDNA of ovaries (lanes 1-8, A) and various tissues of broodstock sized *P. monodon* (B) and *EF-1 α* (C). Lane M and N are a 100 bp DNA ladder marker and the negative control, respectively. ES = eyestalk, IT = intestine, ST = stomach, GL = gill, HC = hemocytes, TG = thoracic ganglion, LO = lymphoid organ, EP = epicuticle, HP = hepatopancrease, HE = heart, TT = testes, PL = pleopod and OV = ovaries.

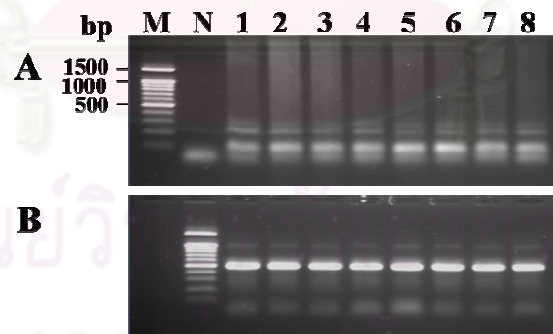


Figure 3.54 A 1.6% ethidium bromide-stained agarose gel showing results from RT-PCR (A) and *EF-1 α* (B) of *beta-thymosin* using the first strand cDNA of ovaries (lanes 1-4, A = normal shrimp) and (lane 5-6, A = eyestalk-ablated shrimp) of broodstock sized *P. monodon*. Lane M and N are a 100 bp ladder marker DNA and the negative control, respectively.

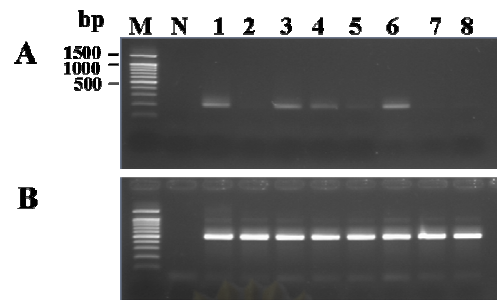


Figure 3.55 A 1.6% ethidium bromide-stained agarose gel showing results from RT-PCR (A) and *EF-1α* (B) of *p68 RNA helicase* using the first strand cDNA of ovaries (lanes 1-4, A = normal shrimp) and (lane 5-6, A = eyestalk-ablated shrimp) of broodstock sized *P. monodon*. Lane M and N are a 100 bp ladder marker DNA and the negative control, respectively.

ศูนย์วิทยทรัพยากร
จุฬาลงกรณ์มหาวิทยาลัย

Table 3.7 Expression of functionally important genes in different tissues of *P. monodon*

Gene homologues	Expected size (bp)	Tissue
1. <i>DEAD box 52</i>	204	ES, IT, ST, GL, HC, TG, LO,EP, HP, HE, TT, PL, OV
2. <i>DEAD box ATP-dependent RNA helicase</i>	269	ES, IT, ST, GL, HC, TG, LO,EP, HP, HE, TT, PL, OV
3. <i>ATP-dependent RNA helicase</i>	153	IT, ST, GL, HC, TG, LO,EP, HP, HE, TT, PL, OV
4. <i>Helicase lymphoid specific isoform 2</i>	216	IT, ST, GL, HC, TG, LO,EP, HP, HE, TT, PL, OV
5. <i>Heterogeneous nuclear ribonucleo protein</i>	482	IT, ST, GL, HC, TG, LO,EP, HP, HE, TT, PL, OV
6. <i>Protein disulfide isomerase</i>	275	IT, ST, GL, HC, LO,EP, HP, HE, TT, PL, OV
7. <i>Valosine containg protein</i>	276	ES, ST, LO,EP, HP, HE, TT, OV
8. <i>L-3-hydroxyacyl coenzyme A dehydrogenase</i>	217	ES, ST, GL, HC, TG, LO,EP, HP, HE, TT, PL, OV
9. <i>Beta-thymosin</i>	110	Not determined
10. <i>p68 RNA helicase</i>	201	Not determined

Table 3.8 Expression profiles of gene homologues in various tissues of a female and testes of a male *P. monodon* broodstock

Gene	Expression level													
	OV	ES	IT	ST	GL	HC	TG	LO	EP	HP	HE	TT	PL	
1. <i>DEAD box 52</i>	+++	+	+	+	+	+	+	++	+	+	+	++	+	
2. <i>DEAD box ATP-dependent RNA helicase</i>	+++	+	+	+	+	+	++	+	+	+	+	++	+	
3. <i>ATP-dependent RNA helicase</i>	+++	-	++	+	+	+	+	++	+	++	+	+	+	
4. <i>Helicase lymphoid specific isoform 2</i>	++	-	+++	+	+	+	-	+++	-	+	+	+	+	
5. <i>Heterogeneous nuclear ribonucleo protein</i>	++++	-	+++	+++	++++	+	+	++++	+++	+++	+++	+++	+++	
6. <i>Protein disulfide isomerase</i>	+++	-	+++	+	+	+		+++	+	++	++	++	+	
7. <i>Valosine containg protein</i>	++++	+	-	+	+++	+	+++	+	+++	+	++++	++++	+	
8. <i>L-3-hydroxyacyl coenzyme A dehydrogenase</i>	+++	+	-	+	+++	+	+++	+	+++	+	++++	++++	+	

3.6 Semiquantitative RT-PCR of functionally important gene during ovarian development of *P. monodon* broodstock

Expression levels of 5 genes (*DEAD box 52*, *DEAD box ATP-dependent RNA helicase*, *ATP-dependent RNA helicase*, *helicase lymphoid specific isoform 2* and *protein disulfide isomerase*) were determined by semiquantitative RT-PCR. *EF-1 α* was used as an internal control.

The first strand cDNA of ovaries from normal and eyestalk-ablated female broodstock were used as the template for semiquantitative RT-PCR analysis. This technique requires optimization of several parameters including concentration of primers, MgCl₂ and the number of PCR cycles.

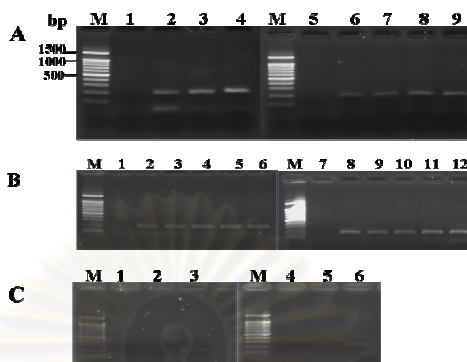
3.6.1 Optimization of the primer concentration, MgCl₂ concentration and cycle numbers

RT-PCR of each gene was initially carried out with fixed components except primer concentration. Lower concentration may result in non-quantitative amplification whereas higher concentration of primer may leave a large amount of unused primer which could give rise to non-specific amplification products. The suitable concentration of primers for each gene is shown by Figures 3.56A-3.60A and Table 3.9.

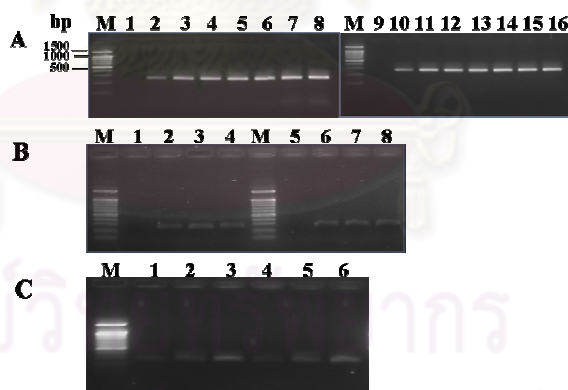
The optimal concentration of MgCl₂ for each primer pair was further examined using the amplification conditions with the optimized primer concentration. The concentration of MgCl₂ that gave the highest yield and specificity for each PCR product was chosen (Figures 3.56B-3.60B and Table 3.9).

The number of amplification cycles was important because the product reflecting the expression level should be measured quantitatively before reaching a plateau amplification phase. At the plateau stage, transcripts initially present at different levels may give equal intensity of amplification products. In this experiment, the cycles number of RT-PCR of each gene was performed using the condition that primer and MgCl₂ concentrations were optimized. The number of cycle that gave the

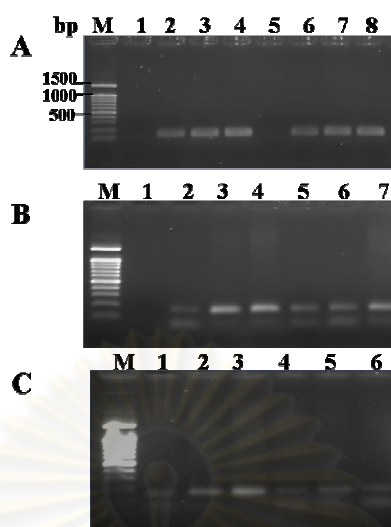
highest yield before the product reached plateau phase of amplification was chosen (Figures 3.56C-3.60C).



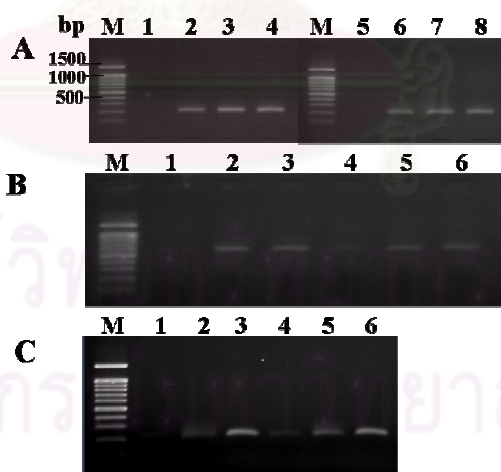
Figures 3.56 Optimization of primer concentration (A), $MgCl_2$ concentration (B) and number of cycles (C) of *P. monodon* DEAD box 52. Lanes 1-4, A; 1-6, B and lanes 1-3, C = normal broodstock. Lanes 5-9, A; 7-12, B and 4-6, C = eyestalk-ablated broodstock. (A). Lanes 1 & 5 = 0 μM , lanes 2 & 9 = 0.1 μM , lanes 3 & 6 = 0.02 μM , lanes 4 & 7 = 0.04 μM , lane 8 = 0.07 μM primer concentration (B) Lanes 1 & 7 = 0 mM, lanes 2 & 8 = 1.0 mM, lanes 3 & 9 = 1.5 mM, lanes 4 & 10 = 2.0 mM, lanes 5 & 11 = 2.5 mM, lane 6 & 12 = 3.0 mM $MgCl_2$ concentration. (C) Lane 1 & 4 = 23 cycles, lanes 2 & 5 = 25 cycles and lanes 3 & 6 = 28 cycles. Lane M = 100 bp ladder marker.



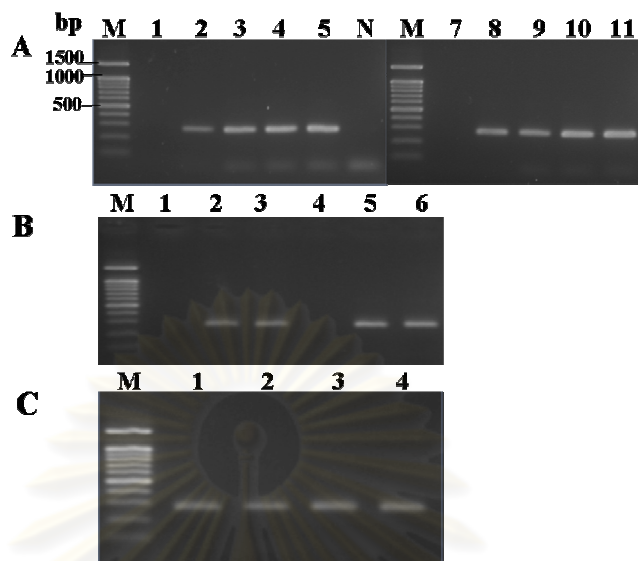
Figures 3.57 Optimization of primer concentration (A), $MgCl_2$ concentration (B) and number of cycles (C) of DEAD box ATP-dependent RNA helicase (*P. monodon*). Lanes 1-8, A; 1-4, B and 1-3, C = normal broodstock. Lanes 9-16, A; 5-8, B and 4-6, C = eyestalk-ablated shrimp. (A). Lanes 1 & 9 = 0 μM , lanes 2 & 10 = 0.02 μM , lanes 3 & 11 = 0.04 μM , lanes 4 & 12 = 0.05 μM , lanes 5 & 13 = 0.07 μM , lanes 6 & 14 = 0.08 μM , lanes 7 & 15 = 0.1 μM , lanes 8 & 16 = 0.15 μM primer concentration (B). Lanes 1 & 7 = 0 mM, lanes 2 & 8 = 1.0 mM, lanes 3 & 9 = 1.5 mM, lanes 4 & 10 = 2.0 mM, lanes 5 & 11 = 2.5 mM, lanes 6 & 12 = 3.0 mM $MgCl_2$ concentration. (C) Lanes 1 & 4 = 25 cycles, lanes 2 & 5 = 28 cycles, lanes 3 & 6 = 30 cycles. Lane M = 100 bp ladder marker.



Figures 3.58 Optimization of primer concentration (A), $MgCl_2$ concentration (B) and number of cycles (C) of *ATP-dependent RNA helicase (P. monodon)*. Lanes 1-4, A; 1-4, B and 1-3, C = normal broodstock. Lanes 5-8, A; 5-7, B and 4-6, C = eyestalk-ablated shrimp. (A). Lanes 1 & 5 = 0 μM , lanes 2 & 6 = 0.02 μM , lanes 3 & 7 = 0.04 μM , lanes 4 & 8 = 0.07 μM . primer concentration. (B). Lanes 1 = 0 mM, lanes 2 & 5 = 1.0 mM, lanes 3 & 6 = 1.5 mM, lanes 4 & 7 = 2.0 mM $MgCl_2$ concentration. (C) Lanes 1 & 4 = 25 cycles, lanes 2 & 5 = 28 cycles, lanes 3 & 6 = 30 cycles. Lane M = 100 bp ladder marker.



Figures 3.59 Optimization of primer concentration (A), $MgCl_2$ concentration (B) and number of cycles (C) of *helicase lymphoid specific isoform 2 (P. monodon)*. Lanes 1-4, A; 1-4, B and 1-3, C = normal broodstock. Lanes 5-8, A; 5-8, B and 4-6, C = eyestalk-ablated shrimp. (A). Lanes 1 & 5 = 0 μM , lanes 2 & 6 = 0.02 μM , lanes 3 & 7 = 0.04 μM , lanes 4 & 8 = 0.07 μM primer concentration. (B). Lanes 1, 4 = 0 mM, lanes 2 & 5 = 1.0 mM, lanes 3 & 6 = 1.5 mM $MgCl_2$ concentration. (C) Lanes 1 & 4 = 25 cycles, lanes 2 & 5 = 28 cycles, lanes 3 & 6 = 30 cycles. Lane M = 100 bp ladder marker.



Figures 3.60 Optimization of primer concentration (A), $MgCl_2$ concentration (B) and number of cycles (C) of *protein disulfide isomerase* (*P. monodon*). Lanes 1-6, A; 1-3, B and 1-2, C = normal broodstock. Lanes 7-11, A; 4-6, B and 3-4, C = eyestalk-ablated shrimp. (A). Lanes 1 & 7 = 0 μM , lanes 2 & 8 = 0.02 μM , lanes 3 & 9 = 0.04 μM , lanes 4 & 10 = 0.07 μM , lanes 5 & 11 = 0.07 μM primer concentration (B). Lanes 1 & 4 = 0 mM, lanes 2 & 5 = 1.0 mM, lanes 3 & 6 = 1.5 mM $MgCl_2$ concentration (C) Lanes 1 & 3 = 28 cycles, lanes 2 & 4 = 30 cycles. Lane M and N = 100 bp ladder marker and the negative control, respectively.

Table 3.9 Optimal primer and $MgCl_2$ concentration and the number of PCR cycles for semiquantitative RT-PCR analysis of gene homologues in *P. monodon*

Transcript	Expected size (bp)	Primer concentration (μM)	$MgCl_2$ concentration (mM)	PCR cycles
<i>DEAD box 52</i>	204	0.04	1	28
<i>DEAD box ATP-dependent RNA helicase</i>	269	0.02	1.5	30
<i>ATP-dependent RNA helicase</i>	153	0.04	1.5	30
<i>Helicase lymphoid specific isoform 2</i>	216	0.04	1.5	30
<i>Protein disulfide isomerase</i>	275	0.02	1.5	30

3.6.2 Semiquantitative RT-PCR analysis

DEAD box 52

The expression level of *DEAD box 52* during ovarian development of normal and eyestalk-ablated *P. monodon* broodstock were examined by semi-quantitative RT-PCR (Figures 3.61 and 3.62). Expression level of this gene was not significantly different in both normal and eyestalk-ablated broodstock ($P > 0.05$). In normal shrimp, the expression level in stages II (1.0649 ± 0.1623) and IV (1.0643 ± 0.1584) was slightly greater but not significant to that of stages I (0.9175 ± 0.1482) and III (0.9687 ± 0.0630). Expression of this gene in eyestalk-ablated shrimp was steadily comparable in all ovarian stages (0.7337 ± 0.1564 , 0.7363 ± 0.0777 , 0.7209 ± 0.0790 and 0.7304 ± 0.1313 for stages I, II, III and IV, respectively) (Table 3. 10).

DEAD box ATP-dependent RNA helicase

The expression level of *DEAD box ATP-dependent RNA helicase* in stages I (1.1942 ± 0.0574) and II (1.3132 ± 0.14513) ovaries was significantly greater than that of stage III (1.1795 ± 0.0492) and IV (1.0901 ± 0.1080) ovaries of *P. monodon* broodstock ($P < 0.05$, Figure 3.63). However, expression levels of *DEAD box ATP-dependent RNA helicase* in eyestalk-ablated broodstock were not significantly different throughout ovarian development (0.8126 ± 0.0071 , 0.8185 ± 0.0040 , 0.8212 ± 0.0420 and 0.7928 ± 0.0222 , respectively) (Figure 3.64, Table 10).

ATP-dependent RNA helicase

Unlike *DEAD box ATP-dependent RNA helicase*, the expression level of *ATP-dependent RNA helicase* at stages I (0.8547 ± 0.0787) and II (0.8604 ± 0.0492) were significantly lower than at stages III (0.9279 ± 0.0676) and IV (0.9660 ± 0.0968) ovaries of normal broodstock (Figure 3.65). However, expression levels of *ATP-dependent RNA helicase* in eyestalk-ablated broodstock were not significantly different throughout ovarian development (0.6076 ± 0.1686 , 0.7093 ± 0.0808 , 0.6814 ± 0.1072 and 0.6451 ± 0.0711 , respectively) (Figure 3.66, Table 10).

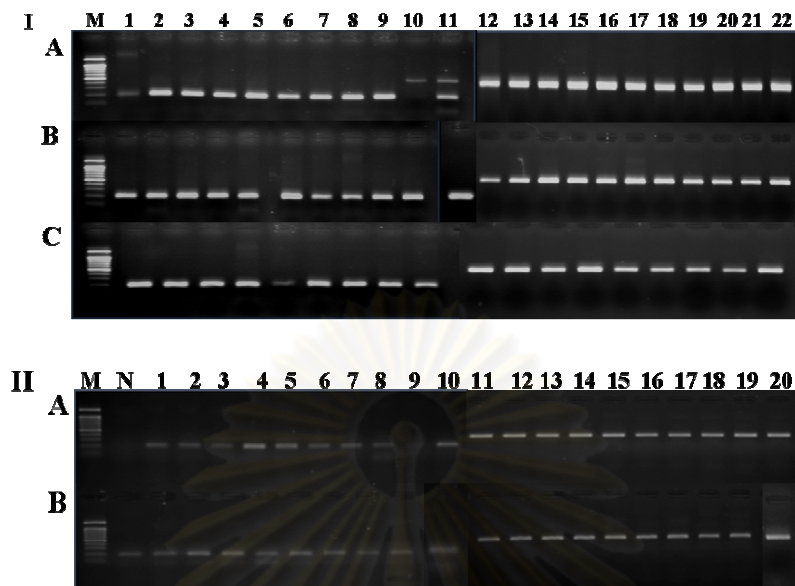


Figure 3.61 A 1.6% ethidium bromide-stained agarose gel showing the expression level of *DEAD box 52* (lanes 1-11, A-C of panel I and lanes 1-10, A-B of panel II) and *EF-1α* ((lanes 12-22, A-C of panel A and lanes 11-20, A-B of panel B) of normal (panel I) broodstock exhibiting stage I (lanes 1-7, A and 12-18, A; panel I for *DEAD box 52* and *EF-1α*, respectively), stage II (lanes 8-9, A and 12-13, B; panel I), stages III, (lanes 3-11, B and 14-22, B; panel I), stages IV (lanes 1-9, C and lanes 12-19, C; panel I) and eyestalk-ablated (panel II) broodstock exhibiting stage I (lanes 1-4, A and lanes 11-14, A; panel II), stage II (lane 5-7, A and 15-17, B; panel II), stage III (lanes 8-9, A and 1 & 3-5, B for *DEAD box 52* and 18-19, A and 12 & 14-16, B; panel II for *EF-1α*) and stage IV (lane 10, A, N, B, 2 & 9-10, B; panel II for *DEAD box 52* and lane 20, A, 11, 13, 19-20, B; panel II for *EF-1α*). Lane M = 100 bp DNA ladder.

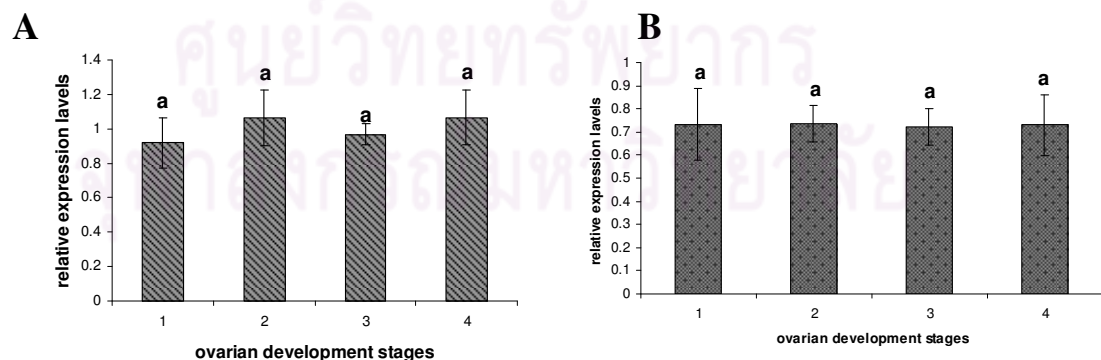


Figure.3.62 Histograms showing relative expression levels of *DEAD box protein 52* during ovarian development of normal (A) and unilateral eyestalk-ablated (B) *P. monodon* broodstock. The same letters indicate non-significant differences between relative expression level of different groups of samples.

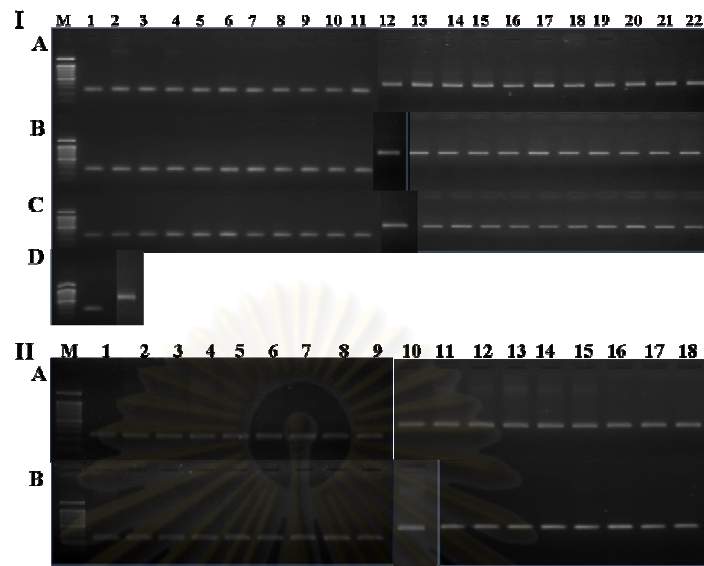


Figure 3.63 A 1.6% ethidium bromide-stained agarose gel showing the expression level of *DEAD box ATP-dependent RNA helicase* (lanes 1-11, A-C of panel I and lanes 1-9, A-B, of panel II) and *EF-1 α* ((lanes 12-22, A-C of panel A and lanes 11-18, A-B of panel B) of normal (panel I) broodstock exhibiting stage I (lanes 1-7, A and 12-18, A; panel I for *DEAD box 52* and *EF-1 α* , respectively), stage II (lanes 8-11, A and 1-2, B; panel I for the target gene and lanes 19-22A and 12-13, B; panel I for *EF-1 α*), stages III, (lanes 3-10, B and 14-21, B; panel I), stages IV (lanes 11, B- 1, D for the target gene and lanes 22, B, 12-22, C & 2, D; panel I for *EF-1 α*) and eyestalk-ablated (panel II) broodstock exhibiting stage I (lanes 1-3, A and lanes 11-13, A; panel II), stage II (lane 4-6, A and 14-16, A; panel II), stage III (lanes 7-9, A, 2, 4-5 & 7, B, panel II for the target gene and lanes 16-18, A, 11, 13-14 & 16, B; panel II for *EF-1 α*) and stage IV (lanes 1, 3, 6 & 8-9, B; panel II for the target gene and lanes 10, 12, 15 & 17-28, B; panel II for *EF-1 α*). Lane M = 100 bp DNA ladder.

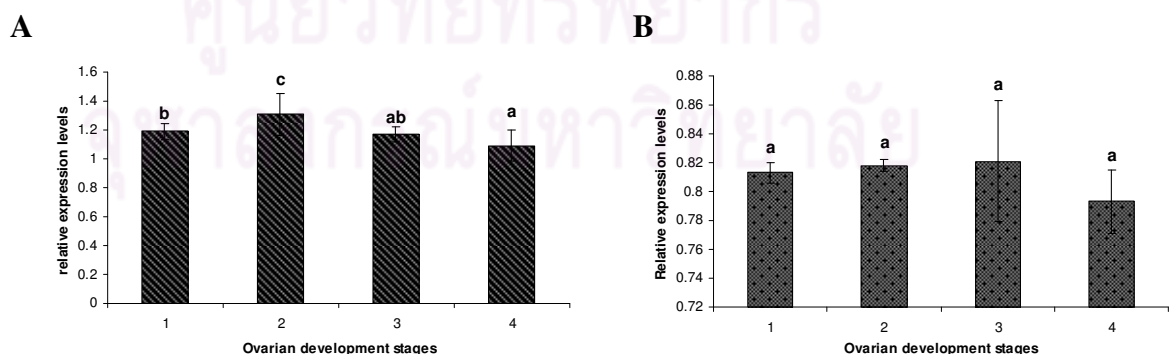


Figure.3.64 Histograms showing relative expression level of *DEAD box ATP-dependent RNA helicase* during ovarian development of normal (A) and unilateral eyestalk-ablated (B) *P. monodon* broodstock. The same letters indicate non-significant differences between relative expression levels of different groups of samples.

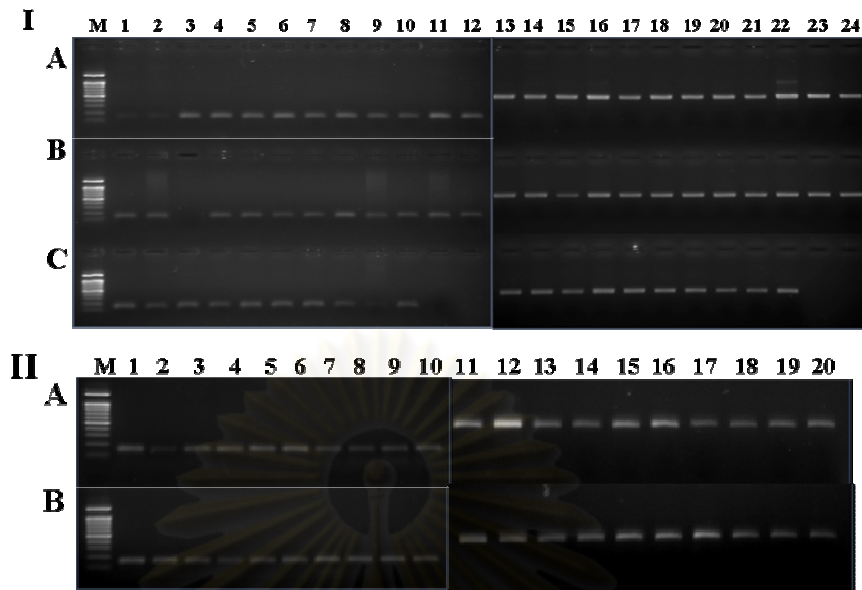


Figure 3.65 A 1.6% ethidium bromide-stained agarose gel showing the expression level of *ATP-dependent RNA helicase* (lanes 1-12, A-C of panel I and lanes 1-10, A-B of panel II) and *EF-1 α* (lanes 13-24, A-C of panel I and lanes 11-20, A-B of panel II) of normal (panel I) broodstock exhibiting stage I (lanes 1-7, A and 12-18, B; panel I for the target gene and *EF-1 α* , respectively), stage II (lanes 8-11, A & 1-2, B; panel I for the target gene and lanes 19-22, A & 12-13, B, panel I for *EF-1 α*), stages III, (lanes 19-22, A and 12-13, B; panel I), stages IV (lanes 11, B – 1,D, panel I for the target gene and lanes 22, B, 12-22, C & 2, D; panel I for *EF-1 α*) and eyestalk-ablated (panel II) broodstock exhibiting stage I (lanes 1-4, A and lanes 11-14, A; panel II), stage II (lane 5-7, A and 15-17, A; panel II), stage III (lanes 8-10, A and 3, 5-6 & 8, B for the target gene and lanes 18-20, A, 13, 14-16 & 18, B; panel II for *EF-1 α*) and stage IV (lane 1-2, 4, 7, 9 & 10, B, panel II for the target gene and lanes 11-12, 14, 17 & 19-20, B; panel II for *EF-1 α*). Lane M = 100 bp DNA ladder.

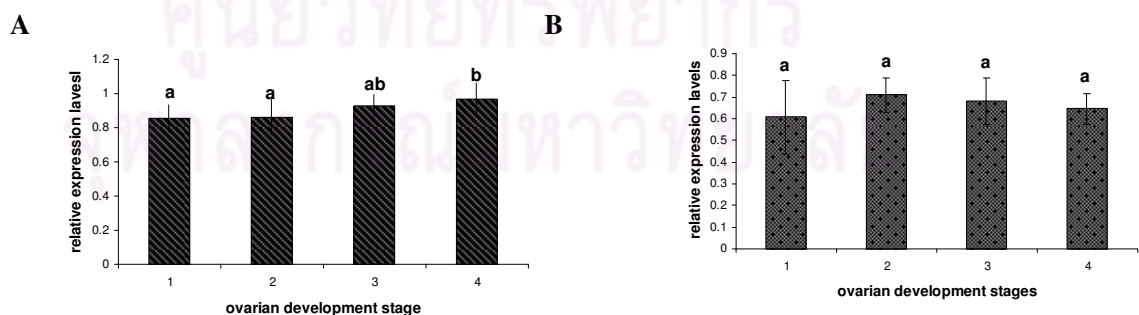


Figure.3.66 Histograms showing relative expression level of *ATP-dependent RNA helicase* during ovarian development of normal (A) and unilateral eyestalk-ablated (B) *P. monodon* broodstock. The same letters indicate non-significant differences between relative expression levels of different groups of samples.

Helicase lymphoid specific isoform 2

In normal broodstock, the expression level of *helicase lymphoid specific isoform 2* in stage II ovaries (0.8388 ± 0.0863) was down-regulated from stage I ovaries (1.0141 ± 0.0698) ($P < 0.05$). Subsequently, its expression level was significant increased at stages III (1.0800 ± 0.0958) and IV (1.0890 ± 0.1052) ovaries ($P < 0.05$, Figure 3.67). In contrast, this transcripts in stages II (0.8333 ± 0.0586), III (0.8436 ± 0.0845) and IV (0.8696 ± 0.0975) was significantly greater than that of stage I (0.6589 ± 0.1106) ovaries ($P < 0.05$, Figure 3.68, Table 10)

Protein disulfide isomerase

Expression profiles of *protein disulfide isomerase* in normal and eyestalk-ablated broodstock were different (Figures 3.69 and 3.70). Relatively high expression levels of this gene were observed in stages I (1.2956 ± 0.0809) and II (1.3577 ± 0.1590) ovaries of normal broodstock. Significant reduction of its expression level were observed in stages III (1.1054 ± 0.0624) and IV (1.1314 ± 0.1098) ovaries ($P < 0.05$). In contrast, expression level of *protein disulfide isomerase* in ovaries of eyestalk-ablated broodstock was not significantly different (0.9169 ± 0.0358 , 0.8978 ± 0.0102 , 0.9383 ± 0.0478 and 0.9719 ± 0.0601 , respectively ($P < 0.05$, Table 10).



Figure 3.67 A 1.6% ethidium bromide-stained agarose gel showing the expression level of *helicase lymphoid specific isoform 2* (lanes 1-12, A-C of panel I and lanes 1-10, A-B of panel II) and *EF-1α* (lanes 13-24, A-C of panel I and lanes 11-20, A-B of panel II) of normal (panel I) broodstock exhibiting stage I (lanes 1-7, A and 12-18, A; panel I for the target gene and *EF-1α*, respectively), stage II (lanes 8-11, A & 1-2, B; panel I for the target gene and lanes 19-22, A and 12-13, B, panel I for *EF-1α*), stages III, (lanes 3-10, B and 14-21, B; panel I), stages IV (lanes 11, B – 1, D, panel I for the target gene and lanes 22, B, 12-22, C & 2, D; panel I for *EF-1α*) and eyestalk-ablated (panel II) broodstock exhibiting stage I (lanes 1-4, A and lanes 11-14, A; panel II), stage II (lane 5-7, A and 15-17, A; panel II), stage III (lanes 8-10, A and 3, 5-6 & 8, B for the target gene and lanes 18-20, A, 13, 15-16 & 18, B; panel II for *EF-1α*) and stage IV (lane 1-2, 4, 7, & 9-10, B, panel II for the target gene and lanes 11-12, 14, 17 & 19-20, B; panel II for *EF-1α*). Lane M = 100 bp DNA ladder.

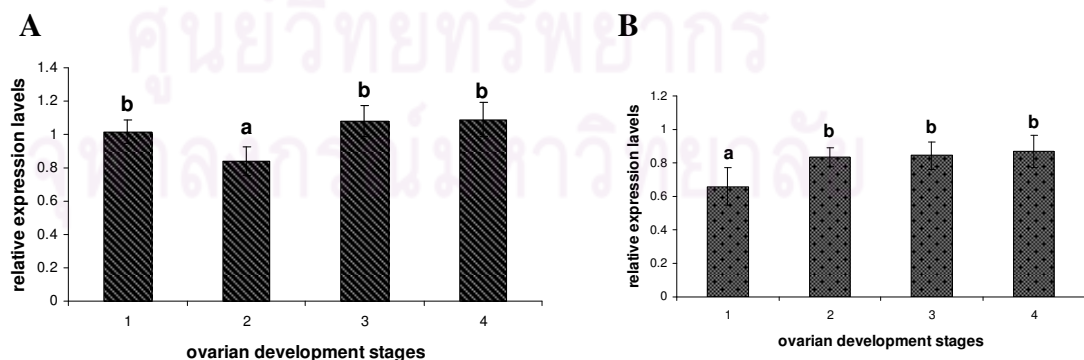


Figure 3.68 Histograms showing relative expression levels of *helicase lymphoid specific isoform 2* during ovarian development of normal (A) and unilateral eyestalk-ablated (B) *P. monodon* broodstock. The same letters indicate non-significant differences between relative expression level of different groups of samples.

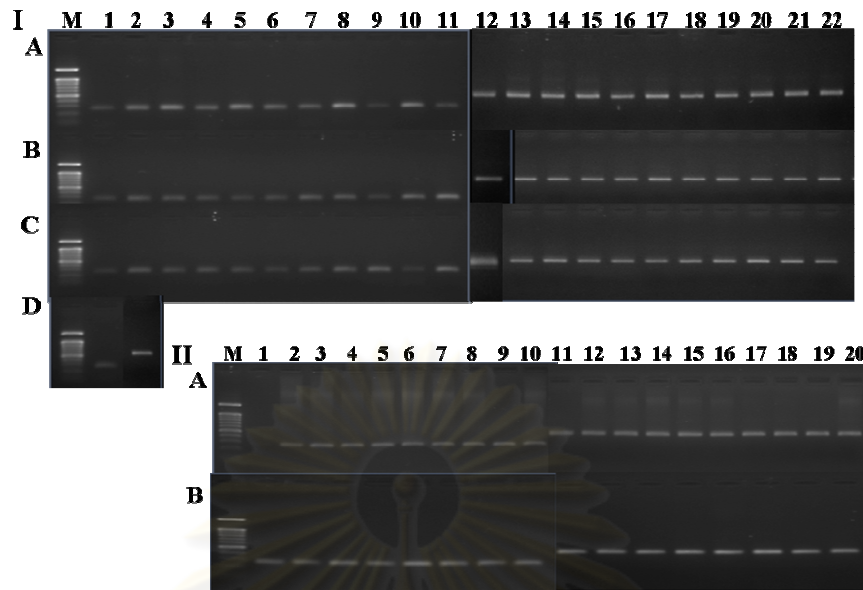
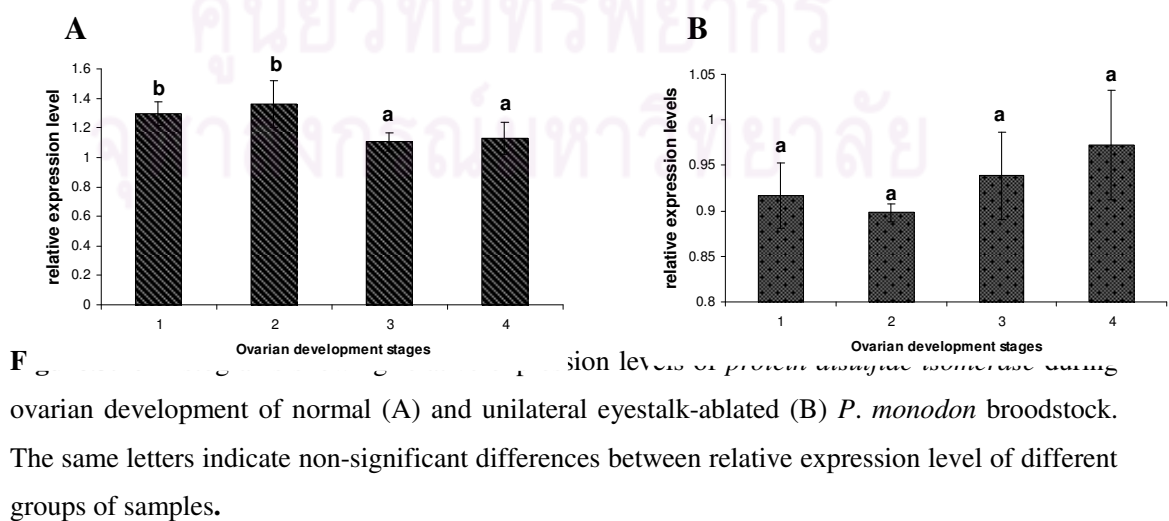


Figure 3.69 A 1.6% ethidium bromide-stained agarose gel showing the expression level of *protein disulfide isomerase* (lanes 1-11, A-C of panel I and lanes 1-10, A-B of panel II) and *EF-1α* (lanes 12-22, A-C of panel I and lanes 11-20, A-B of panel II) of normal (panel I) broodstock exhibiting stage I (lanes 1-7, A and 12-18, A; panel I for the target gene and *EF-1α*, respectively), stage II (lanes 8-11, A & 1-2, B; panel I for the target gene and lanes 19-22, A & 12-13, B, panel I for *EF-1α*), stages III, (lanes 3-10, B and 14-21, B; panel I), stages IV (lanes 11, B – 1, D, panel I for the target gene and lanes 22, B, 12-22, C & 2, D; panel I for *EF-1α*) and eyestalk-ablated (panel II) broodstock exhibiting stage I (lanes 1-4, A and lanes 11-14, A; panel II), stage II (lane 5-7, A and 15-17, A; panel II), stage III (lanes 8-10, A and 3, 5-6 & 8, B for the target gene and lanes 18-20, A and 13, 15-16 & 18, B; panel II for *EF-1α*) and stage IV (lane 1-2, 4, 7, & 9-10, B, panel II for the target gene and lanes 11-12, 14, 17 & 19-20, B; panel II for *EF-1α*). Lane M = 100 bp DNA ladder.



F Relative expression levels of *protein disulfide isomerase* during ovarian development of normal (A) and unilateral eyestalk-ablated (B) *P. monodon* broodstock. The same letters indicate non-significant differences between relative expression level of different groups of samples.

Table 3.10 Analysis of relative expression levels of various genes during ovarian development of normal and eyestalk-ablated *P. monodon* broodstock using semiquantitative RT-PCR. The same superscript indicates non-significant differences between relative expression level of different groups of samples.

Genes	Mean relative expression level							
	Normal shrimp				Eyestalk-ablated shrimp			
	Stage I	Stage II	Stage III	Stage IV	Stage I	Stage II	Stage III	Stage IV
<i>DEAD box 52</i>	0.917 ± 0.148 ^a	1.064 ± 0.162 ^a	0.968 ± 0.063 ^a	1.064 ± 0.158 ^a	0.733 ± 0.156 ^a	0.736 ± 0.077 ^a	0.721 ± 0.079 ^a	0.730 ± 0.131 ^a
<i>DEAD box ATP-dependent RNA helicase</i>	1.194 ± 0.057 ^b	1.313 ± 0.145 ^c	1.179 ± 0.049 ^{ab}	1.090 ± 0.108 ^a	0.813 ± 0.007 ^a	0.818 ± 0.004 ^a	0.822 ± 0.042 ^a	0.792 ± 0.022 ^a
<i>ATP-dependent RNA helicase</i>	0.855 ± 0.078 ^a	0.860 ± 0.106 ^a	0.927 ± 0.067 ^{ab}	0.966 ± 0.096 ^b	0.607 ± 0.168 ^a	0.709 ± 0.080 ^a	0.681 ± 0.107 ^a	0.645 ± 0.071 ^a
<i>Helicase lymphoid specific isoform 2</i>	1.014 ± 0.069 ^b	0.839 ± 0.086 ^a	1.080 ± 0.095 ^b	1.089 ± 0.105 ^b	0.659 ± 0.110 ^a	0.833 ± 0.058 ^b	0.843 ± 0.084 ^b	0.869 ± 0.097 ^b
<i>Protein disulfide isomerase</i>	1.295 ± 0.081 ^b	1.357 ± 0.159 ^b	1.105 ± 0.062 ^a	1.131 ± 0.109 ^a	0.917 ± 0.036 ^a	0.897 ± 0.010 ^a	0.938 ± 0.047 ^a	0.972 ± 0.060 ^a

3.7 Quantitative analysis of *DEAD box ATP-dependent RNA helicase*, *protein disulfide isomerase* and *valosin containing protein* in ovaries of female *P. monodon* broodstock analyzed by real-time PCR

3.7.1 *DEAD box ATP-dependent RNA helicase*

The standard curve of *DEAD box ATP-dependent RNA helicase* was constructed (Figure 3.71A). Results from real-time PCR revealed that the expression level of *DEAD box ATP-dependent RNA helicase* in ovaries of juveniles was not significantly different from stage I ovaries ($P > 0.05$) but significantly lower than that of subsequent ovarian stages of normal shrimp ($P < 0.05$). In normal broodstock, this transcript was up-regulated at stages III and IV ovaries ($P < 0.05$). The expression level was then decreased at the post-spawning stage ($P < 0.05$) (Figure 3.72A). In eyestalk-ablated broodstock, *DEAD box ATP-dependent RNA helicase* was up-regulated at stages IV ovaries ($P < 0.05$) (Figure 3.72B).

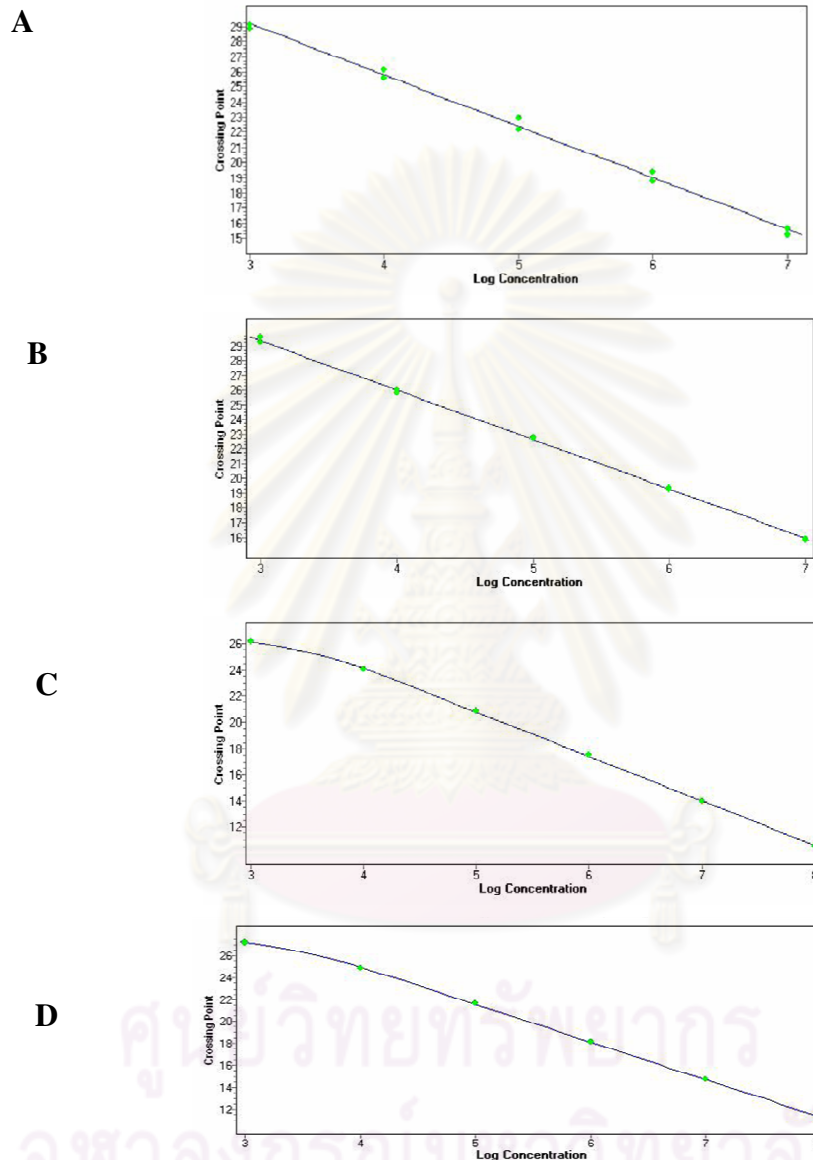
Results were concordant when expression levels of *DEAD box ATP-dependent RNA helicase* in both normal and eyestalk-ablated *P. monodon* were considered simultaneously.

Notably, expression profiles of *DEAD box ATP-dependent RNA helicase* examined by semiquantitative PCR were contradictory to those examined by real-time PCR. Although the same sample set was used for both approaches, the number of individuals in semiquantitative RT-PCR was smaller than that used in quantitative real-time PCR analysis.

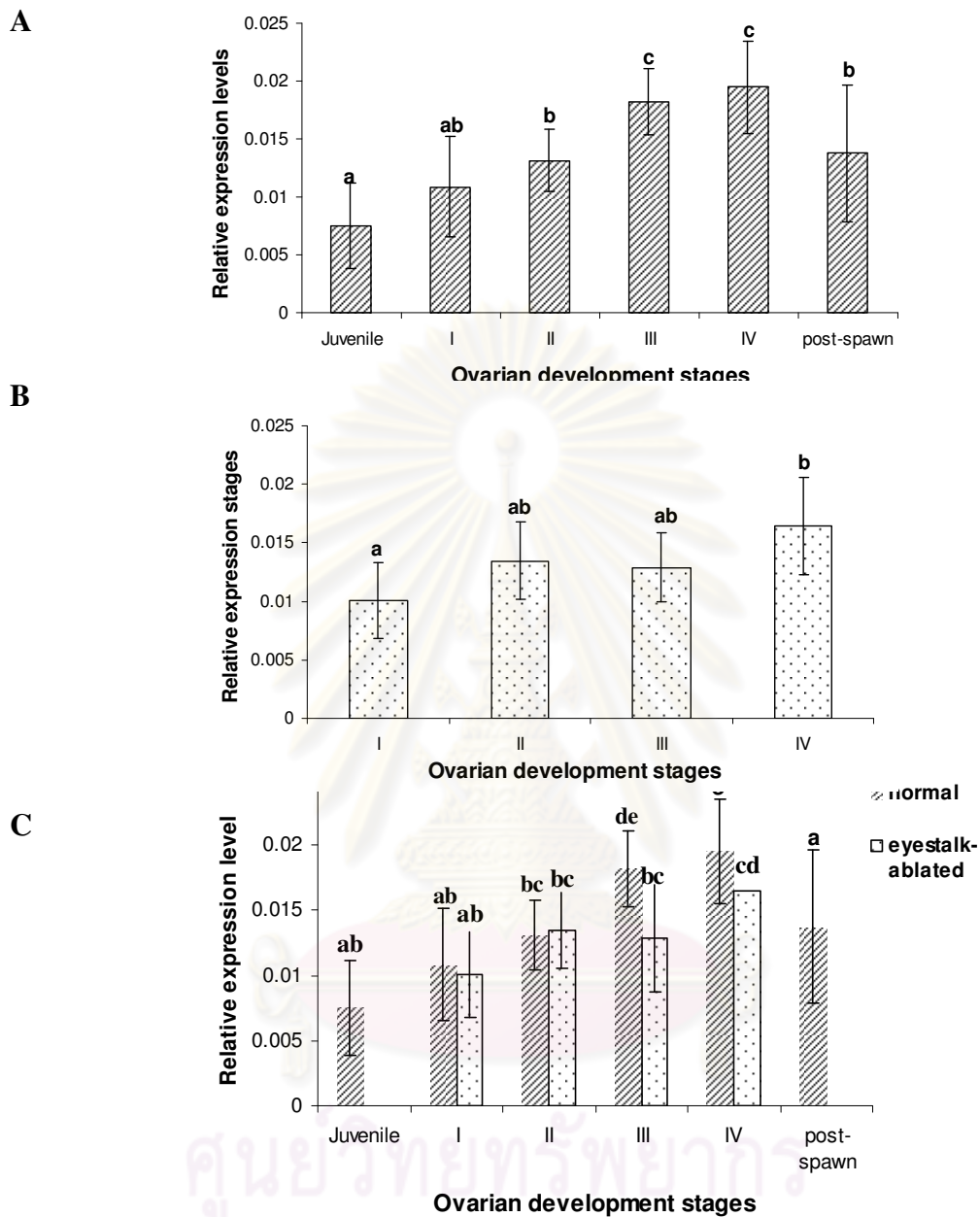
3.7.2 *Valosin containing protein*

The standard curve of *valosin containing protein* was constructed (Figure 3.71B). Results from quantitative real-time PCR revealed that the expression level of *valosin containing protein* in ovaries of juveniles was significantly lower than that of normal broodstock ($P < 0.05$). However, expression levels of *valosin containing protein* were not significant different throughout ovarian development of normal broodstock ($P > 0.05$) (Figure 3.73A). The expression level of *valosin containing*

protein was significantly increased at stage IV of ovaries of eyestalk-ablated broodstock ($P < 0.05$) (Figures 3.73B).



Figures 3.71 The standard amplification curve of various genes examine by real-time PCR. The standard curve of *DEAD box ATP-dependent RNA helicase* (A; r^2 for standard curve = 0.9850, efficiency for the amplification = 1.970), *PmVCP* (B; r^2 for standard curve = 0.993, efficiency for the amplification = 1.986), *PmPDI* (C; r^2 for standard curve = 0.9870, efficiency for the amplification = 1.974) and *EF-1 α* (D; r^2 for standard curve = 0.9805, efficiency for the amplification = 1.961). The abscissa reveals log copy number concentrations of each gene (10^3 to 10^8 copy, respectively).



Figures 3.72 Histograms showing relative expression levels of *DEAD box ATP-dependent RNA helicase* during ovarian development of normal (A), unilateral eyestalk-ablated (B) and both groups (C) of *P. monodon* broodstock. The same letters indicate non-significant differences between relative expression levels of different groups of samples.

Results were concordant when expression levels of *valosin containing protein* in both normal and eyestalk-ablated *P. monodon* were considered simultaneously. Nevertheless, the mRNA levels of *valosin containing protein* in ovaries of eyestalk-ablated broodstock were significantly greater than those of normal broodstock at all stages of ovarian development ($P < 0.05$) (Figures 3.73C).

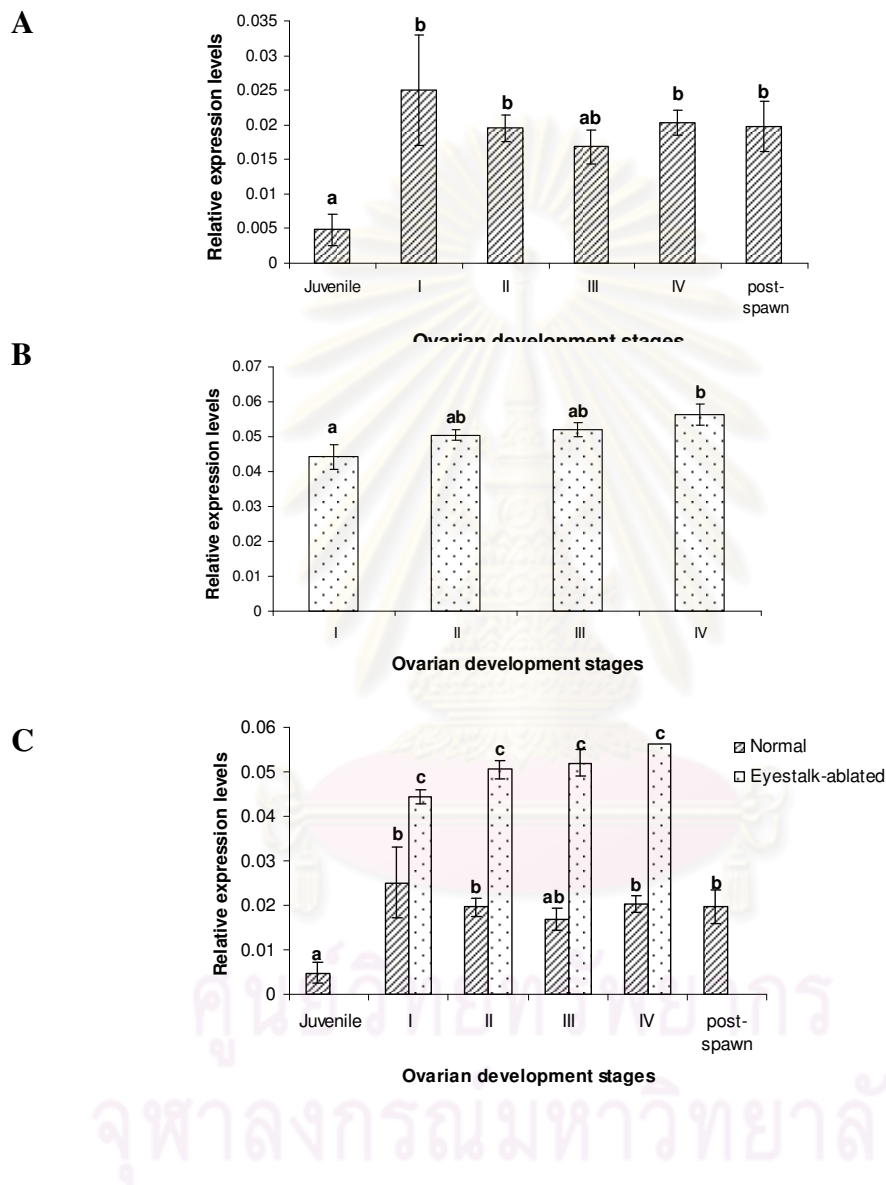
3.7.3 Protein disulfide isomerase

The standard curve of *protein disulfide isomerase* was constructed (Figure 3.71C). Results from real-time PCR revealed that the expression level of *protein disulfide isomerase* in stages II, III and IV ovaries was significantly greater than that in ovaries of juveniles ($P < 0.05$). In normal broodstock, *protein disulfide isomerase* levels between different stages of ovarian development were not significantly different ($P < 0.05$) (Figures 3.74A). The expression level of this transcript was significantly increased in stage IV ovaries of eyestalk-ablated broodstock ($P < 0.05$) (Figure 3.734B).

Considering expression levels of *PDI* in both normal and eyestalk-ablated *P. monodon* simultaneously, *PDI* was up-regulated at stage III ovaries of normal shrimp ($P < 0.05$) but its levels were not significant different during ovarian development of eyestalk-ablated broodstock ($P > 0.05$) as shown in Figure 3.74C. Importantly, the mRNA levels of *PDI* in ovaries of normal broodstock (including that in juveniles) were significantly greater than those in ovaries of eyestalk-ablated broodstock ($P < 0.05$).

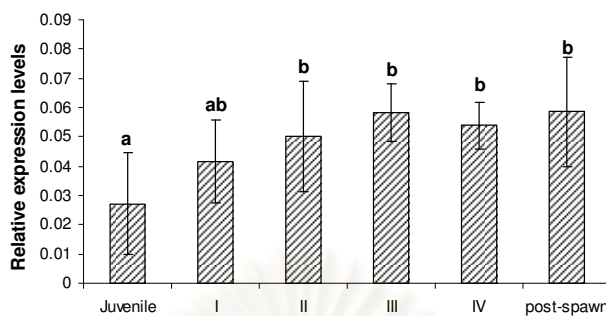
Notably expression profiles of *PDI* examined by semiquantitative RT-PCR were contradictory to those examined by real-time PCR. This transcript seemed to be downregulated in more mature ovaries when analyzed by semiquantitative RT-PCR but results from real-time PCR showed a decreasing level of *PDI* at stage III ovaries but the reduction was not significant ($P > 0.05$). This possible due to large standard deviation of data obtained from real-time PCR analysis. In contrast, real-time PCR illustrated a significant greater level of *PDI* in stage IV ovaries of eyestalk-ablated *P. monodon* broodstock ($P < 0.05$). This data was not significant when analyzed by

semiquantitative RT-PCR ($P > 0.05$). Results suggested greater sensitivity of real-time PCR than semiquantitative PCR when the marginal differences of gene expression levels are examined.

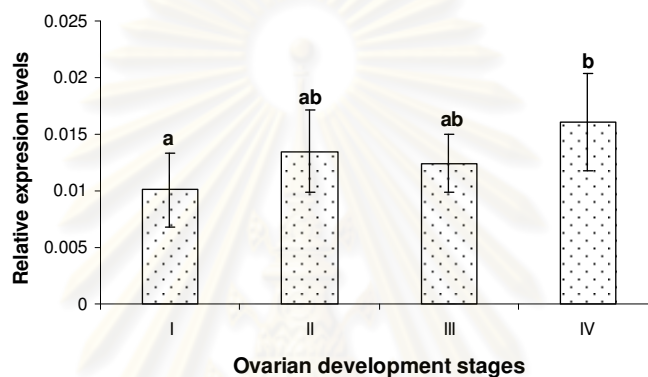


Figures 3.73 Histograms showing relative expression levels of *valosin containing protein* during ovarian development of normal (A), unilateral eyestalk-ablated (B) and both groups (C) of *P. monodon* broodstock. The same letters indicate non-significant differences between relative expression levels of different groups of samples.

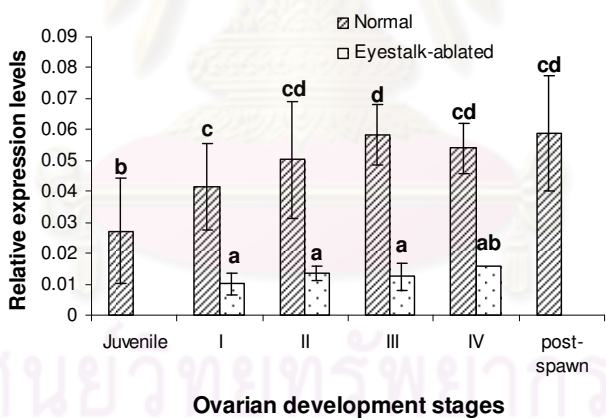
A



B



C



Figures 3.74 Histograms showing relative expression levels of *protein disulfide isomerase* during ovarian development of normal (A), unilateral eyestalk-ablated (B) and both groups (C) of *P. monodon* broodstock. The same letters indicate non-significant differences between relative expression levels of different groups of samples.

CHAPTER IV

DISCUSSION

Proteomic studies of proteins in ovaries of *P. monodon*

Isolation and characterization of reproduction-related genes in ovaries of *P. monodon* have been reported based on EST analysis (Leelatanawit et al., 2004; Preechaphol et al., 2007). Nevertheless, identification of the gene products at the protein levels provided more direct information of molecule functionally involving ovarian development of this species.

Proteomic studies on alteration of protein expression profiles in *P. monodon* upon WSSV and YHV infection have been reported (Rattanaojpong et al., 2007; Bourchokarn et al., 2008). However, expression profiles of proteins in different stages of ovarian development of *P. monodon* have not been studied.

Bulau et al. (2004) characterized neuropeptides from the X-Organ-sinus gland neurosecretory system of the crayfish, *Orconectes limosus* using a nanoflow liquid chromatography system coupled to quadrupole time-of-flight tandem mass spectrometry (nanoLC-QTOF MS/MS). The existence and structural identity of four crustacean hyperglycemic hormone precursor-related peptide variants and two new genetic variants of the pigment-dispersing hormone, not detected by conventional chromatographic systems, molecular cloning, or immunochemical methods before, was revealed. This indicates the usefulness of proteomic approaches for identification of novel uncharacterized proteins.

Initially, the residual proteins from RNA extraction by TRI-REAGENT were extracted and used for 2-DE. More acidic proteins were observed in ovaries of *P. monodon*. Therefore, a narrower pH gradient, pH 4-7, was used for finer separation of acidic proteins in ovaries of *P. monodon*.

Sheoran et al. (2009) evaluated four protein extraction methods, i.e., trichloroacetic acid (TCA)-acetone, phenol, direct iso-electric focusing (IEF) buffer,

and Tris-HCl buffer, using tomato pollen for proteome analysis. The data showed that the TCA-acetone and phenol protein extraction methods are superior to the other two tested methods for tomato pollen proteome analysis, in terms of two-dimensional gel electrophoresis (2-DE) gel separation, mass spectrometric analysis, and identification of proteins by peptide mass fingerprinting (PMF).

In addition, Lee et al., (2008) reported that the quality of proteins from Trizol (a monophasic solution of phenol and guanidine isothiocyanate) extracted from dinoflagellate was high in terms of resolution, spot number and spot intensity when analyzed by 2-DE.

Although the quality of phenol-extracted proteins was reported to be the same as total proteins extracted from the TCA-acetone method, the number of ovarian protein spots of the same shrimp from the TCA-acetone method was slightly greater (635, 647, 467 and 357 spots for stages I-IV of normal shrimp and 617, 469, 374 and 312 spots from stages I-IV ovaries of eyestalk-ablated shrimp, respectively) than those from Trizol (537, 378, 363 and 300 spots for stages I-IV of normal shrimp and 543, 421, 434 and 642 spots from stages I-IV ovaries of eyestalk-ablated shrimp, respectively) after electrophoresis. In addition, total proteins extracted from the TCA-acetone method gave clearer electrophoresed patterns. Accordingly, the former extraction method was chosen for preparation of protein samples.

Initially, 35 trypsin-digested protein spots were selected to analyze by PMF using MALDI-TOF and all characterized proteins were unknown. The use of a more sensitive technique, peptide fragmentation by MALDI-TOF/TOF for characterization of 90 spots revealed only 4 matched deduced proteins derived from EST of the local *P. monodon* database (<http://pmonodon.biotec.or.th/libraries.jsp>). This may be explained that the number of ESTs in the local *P. monodon* database was not large enough (40001 ESTs) and additional numbers of ESTs should be sequenced.

Subsequently, nanoLC-MS/MS was applied for characterization of stages II and IV proteins in ovaries of normal and eyestalk-ablated broodstock of *P. monodon*. Data were searched against both the local and nr databases. In total, 192 (75.20%)

from 375 examined protein spots from ovaries of normal broodstock and 126 (42.00%) from 300 protein spots from ovaries of eyestalk-ablated broodstock were identified. This indicating that the peptide fragmentation resulted obtained from nanoLC-MS/MS exhibited higher are many than those of peptide fragmentation results from MALDI-TOF/TOF on characterization of proteins in ovaries of *P. monodon*.

From mass spectrometry analysis, the molecular mass of several proteins in different stages of ovaries was decreased (e.g. beta actin, PDI, trios-phosphate isomerase) or increased (arginine kinase, , PDI and F1-ATP-synthase) due to posttranslational modifications; for example, phosphorylation and dephosphorylation. In eukaryotes, signal transduction pathways that activate cyclin/cdc2 complex (maturation promoting factor, MPF) and related processes are the key pathways in oocyte maturation.

Proteomic profiles from different stages of ovaries of female *P. monodon* broodstock

One difficulty in identifying compounds that stimulate crustacean reproduction is the lack of adequate biological markers for reproduction. Vitellogenin is a female-specifically expressed protein and can easily be purified and characterized. As a result, it was popularly applied to follow reproductive maturation of various animals. However, a problem with using the presence of the vitellogenin proteins as indicators of reproduction is that it was synthesized from both ovaries and hepatopancreas. Accordingly, biological markers at both translational (protein) and transcriptional (cDNA) levels of other genes may be used as markers for reproductive maturation of *P. monodon*.

When the presence/absence and expression levels of known proteins in ovaries were considered simultaneously, several interesting proteins were identified. Interestingly, many proteins were down-regulated during ovarian development of normal *P. monodon*. These included cyclic AMP-regulated protein-like protein (0.13 fold), cofilin/actin-depolymerizing factor (0.07 fold), CG10527-like methyltransferase

(0.1 fold), glutathione *s*-transferase (0.1 fold), glutathione peroxidase (0.01 fold), 2-cys thioredoxin peroxidase (0.01 fold), proteasome subunit α type 5 (0.05 fold), cytosolic manganese superoxide dismutase (0.1 fold), alcohol dehydrogenase (0.15 fold), β -actin (0.13), chaperonin containing TCP1 subunit 2, tubulin beta-1 chain.(0.07 fold) Results indicated that high level of these proteins may not be required for ovarian maturation of *P. monodon*.

Several proteins were found in stage IV but not in stage II ovaries of normal broodstock of *P. monodon*. Proteins categorized in this group were protein disulfide isomerase (MW/pI = 55000/5.5), mitochondrial aldehyde dehydrogenase, L-3-hydroxyacyl coenzyme A dehydrogenase, trios-phosphate isomerase, secreted inorganic pyrophosphatase, HAD family hydrolase, vitellogenin and putative conjugal transfer protein. The proteins in this group are candidate for further studies on their involvement in ovarian maturation of *P. monodon*.

In eyestalk-ablated broodstock, several proteins displayed differential expression (upregulation or downregulation during ovarian development. The first subgroup was candidate proteins possibly necessary for late ovarian development. These included glutathione peroxidase (5.40 fold), protein disulfide isomerase (60000/5.70), histidine-rich glycoprotein precursor, PDI (60000/4.8), hypothetical protein (28.55 fold), unnamed protein product (3.11 fold) and two unknown proteins (4.28 fold and 1.57 fold). The second group was proteins that may functionally suppress ovarian development. They were, for example, nucleoplasmin isoform 1-like protein, eukaryotic initiation factor 5A, CG10527-like methyltransferase (0.1 fold), Rab3 GTPase-activating protein, hydroxyacyl glutathione hydrolase, beta thymosin (22000/5.4), arginine kinase, 26s proteasome regulatory subunit 7, isocitrate dehydrogenase 2 (NADP⁺), peroxiredoxin 4, es1 protien, proteasome subunit α type, unknown protein, D-lactate dehydrogenase, rab gdp-dissociation inhibitor and PDI (60000/5.75).

Proteins found in stage IV but not in stage II ovaries of eyestalk-ablated shrimp were glyoxylase 1, transaldolase, RAN binding protein, phosphoglycerase kinase, cytosolic NADP-dependent isocitrate dehydrogenase, Tat- binding protein 7,

Fah-prov protein, Rab3 GTPase-activating protein, heat shock protein 70 and vitellogenin. The expression of these proteins should be influenced by eyestalk ablation.

Stage-specific protein biomarkers for indicating reproductive maturation of *P. monodon* could be further developed using the basic information in this study. It is also important to identify proteins directly affected by eyestalk ablation because these proteins may be applied as bioindicators to illustrate effects of hormones, neurotransmitters or nutrition on inducing ovarian maturation of *P. monodon*.

Mitochondrial aldehyde dehydrogenase and pyrroline-5-carboxylate dehydrogenase were found in stage IV ovaries of normal broodstock. These transcripts were expressed earlier in stage II ovaries as a result of eyestalk ablation. Eyestalk ablation also causes increasing expression levels of CG10527-like methyltransferase from stage IV ovaries of normal brood stock for 4.37 time.

O-methyltransferase (OMT) is ubiquitously present in diverse organisms and plays an important regulatory role in growth, development, reproduction and defense mechanisms in plants and animals (Ruddell et al., 2003). Two kinds of OMT; farnesoic acid-*O*-methyltransferase (FAMeT) and catechol-*O*-methyltransferase (COMT) were identified according to their selectivity to methyl acceptors. Crustacean FAMeT catalyses methylation of farnesoic acid (FA) to produce isoprenoid methyl farnesoate (MF) at the final step of the MF biosynthetic pathway whereas COMT catalyses the transfer of the methyl group from *S*-adenosyl-methionine (SAM) to the hydroxyl group of catechol compounds. Thus, COMT plays an important role in the catabolism and *O*-methylation of endogenous catecholamines, such as dopamine and noradrenaline, in brains of animals.

Isolation of the full length cDNA and expression analysis of functionally important genes

The full length cDNA of *DEAD box 52*, *DEAD box ATP-dependent RNA helicase*, *ATP-dependent RNA helicase*, *L-3-hydroxyacyl coenzyme A dehydrogenase*, *PDI* and *valosin containing protein* were successfully characterized and reported for

the first time in *P. monodon*. In addition, the full length transcripts of gene encoding PDI and valosin containing protein identified by 2-DE were also characterized by RACE-PCR but the larger portion of an ORF of each gene was obtained.

DEAD box proteins are putative ATP-dependent RNA unwinding proteins whose primary biochemical function is the alteration of RNA secondary structure. These proteins have been implicated in translation initiation, ribosome assembly, RNA splicing, and RNA stability (Goldbout et al., 2002). DEAD-box RNA helicases required for germ cell function. The deduced DEAD box ATP-dependent RNA helicase of *P. monodon* contained the conserved motif, (V/I)-L-D-E-AD- X-(M/L)-L-X-X-G-F, observed in all members of the DEAD box protein family (Linder et al., 1989; Tanner and Linder, 2001).

However, *P. monodon* DEAD box 52 did not contain that conserved motif suggesting that this transcript should be regarded as an *ATP-dependent RNA helicase* (molecular mass of 69.15 kDa) rather than a novel member of the DEAD box protein family. In addition, DEAD box 52 (ATP-dependent RNA helicase 69), DEAD box ATP-dependent RNA helicase and ATP-dependent RNA helicase proteins contained DEXDc and HELICc domains suggesting that the functions of these proteins should be similar.

Gene expression and tissue distribution analysis are important and provide the basic information to set up the priority for further analysis of functional genes. Based on the fact that a particular genes may express in several tissues and possesses a different function in different tissues.

Tissues distribution analysis of *DEAD box 52*, *DEAD box ATP-dependent RNA helicase*, *ATP-dependent RNA helicase*, *helicase lymphoid specific isoform 2*, *heterogeneous nuclear ribonucleoprotein*, *L-3-hydroxyacyl coenzyme A dehydrogenase*, *PDI* and *valosin containing protein* were examined in various tissues of a female broodstock and testes of a male broodstock. No transcript exhibited a gonad-specific expression pattern. This suggested that these gene products may play multifunctional properties in different tissues. More importantly, these transcripts

were abundantly expressed in ovaries suggesting that they should be functionally important for ovarian (and oocyte) development.

The transcripts preferentially expressed in different stages of ovarian development can be used as the responsive indicators for reproductive maturation of *P. monodon*. Expression analysis based on quantitative real-time PCR indicated that *DEAD box ATP-dependent RNA helicase*, *valosin containing protein* and *PDI* were differentially expressed during ovarian development of *P. monodon* ($P < 0.05$). Results also indicated that eyestalk ablation positively affected expression levels of *valosin containing protein*, negatively affected expression levels of *PDI* ($P < 0.05$), but had no direct effects on *DEAD box ATP-dependent RNA helicase* ($P > 0.05$).

Semiquantitative RT-PCR illustrated that expression levels of *DEAD box 52 (ATP-dependent RNA helicase 69)* was not significantly different in both normal and eyestalk-ablated broodstock ($P > 0.05$). *ATP-dependent RNA helicase* and *helicase lymphoid specific isoform 2* were differentially expressed in ovaries of normal but not in eyestalk-ablated broodstock of *P. monodon*. In contrast, *helicase lymphoid specific isoform 2* was down-regulated at stage II ovaries of normal broodstock but up-regulated since stage II ovaries in eyestalk-ablated broodstock.

Taken results together, eyestalk ablation does not strongly influence expression of RNA helicases. Therefore, promotion of *P. monodon* ovarian development may not directly relate with this pathway.

Yamano *et al.* (2004) illustrated that in most cases ovaries of *M. japonicus* start to develop in the reproductive season but fail to reach full grown requisite for the formation of cortical rods (CRs). Ovaries degenerate without spawning. This is also the major constraint in *P. monodon*. In the present study, a large number of proteins in ovaries of *P. monodon* were identified and characterized. Molecular mechanisms and functional involvement of these proteins in ovarian development of *P. monodon* should be further studied for better understanding the reproductive maturation of *P. monodon* in captivity.

CHAPTER V

CONCLUSIONS

1. Two dimensional gel electrophoresis of TRI-REAGENT-extracted proteins from different ovarian stages of normal and eyestalk-ablated broodstock was performed at pH 3-10 and pH 4-7 was carried out.
2. Two dimensional gel electrophoresis of total protein from stages I-IV of normal and eyestalk-ablated broodstock were performed at pH 4-7 was carried out.
3. In total, 35 proteins spots from all ovarian stages were analyzed by MALDI-TOF but all of them did not match known proteins in the database. In addition, 90 protein spots representing stages I-IV ovaries were analyzed by MALDI-TOF/TOF and only 4 protein spots matched PDI, transketolase, careticulin and allergen pen m2.
4. A total of 675 protein spots including 215 and 160 spots from stages II and IV ovaries of normal broodstock and 180 and 120 spots from those of eyestalk-ablated broodstock were analyzed by nanoESI-LC-MS/MS, respectively.
5. For proteins from ovaries of normal broodstock, 90 and 102 protein spots accounting for 41.86 and 63.75% of the respective ovarian stages significantly matched previously deposited sequences in the databases. For those in ovaries of the eyestalk-ablated broodstock, 85 and 41 protein spots accounting for 47.22 and 34.16% of examined proteins were regarded as homologues of known proteins.
6. Expression profiles of proteins in ovaries of *P. monodon* can be divided into four groups; 1) proteins found in stage II ovaries of normal broodstock, 2) proteins found in stages IV ovaries of normal broodstock, 3) proteins found both stage II and IV ovaries of normal broodstock and 4) proteins found only in ovaries of eyestalk-ablated broodstock.
7. The full length cDNAs of a *DEAD box 52* homologue (2043 bp long with an ORF of 1824 bp corresponding to 607 amino acids), *DEAD box ATP-dependent RNA helicase* (1680 bp long with an ORF of 1029 bp corresponding to 402 amino acids),

ATP-dependent RNA helicase (1404 bp long with an ORF of 1206 bp corresponding to 401 amino acids), *L-3-hydroxyacyl coenzyme A dehydrogenase helicase* (1238 bp long with an ORF of 933 bp corresponding to 310 amino acids) were successfully characterized by RACE-PCR.

8. Several forms of protein disulfide isomerase (*PDI*) were found from proteomic analysis. In addition, valosin containing protein was found only in stage II ovaries of normal broodstock. RACE-PCR of these genes was carried out. However, partial nucleotide sequences of this transcript (1947 and 1367 bp, respectively) were obtained.

9. Semiquantitative RT-PCR of several genes was carried out. Expression levels of *DEAD box 52* were not significantly different during ovarian development of normal and eyestalk-ablated *P. monodon* broodstock ($P > 0.05$). *ATP-dependent RNA helicase* was up-regulated whereas *DEAD box ATP-dependent RNA helicase* and *protein disulfide isomerase* was down-regulated during ovarian development of *P. monodon* ($P < 0.05$). However, expression levels of these genes in different ovarian stages of eyestalk-ablated broodstock were not significantly different ($P > 0.05$). *Helicase lymphoid specific isoform 2* was down-regulated in stage II ovaries ($P < 0.05$). In contrast, this transcripts in stages II, III and IV was significantly greater than that of stage I ovaries ($P < 0.05$).

10. Quantitative real-time PCR indicated that *DEAD box ATP-dependent RNA helicase* was up-regulated at stages III and IV ovaries of normal broodstock and at stage IV ovaries of eyestalk-ablated broodstock ($P < 0.05$). Expression levels of *valosin containing protein* were not significant different throughout ovarian development of normal broodstock ($P > 0.05$) but significantly increased at stage IV ovaries of eyestalk-ablated broodstock ($P < 0.05$). The expression levels of *protein disulfide isomerase* between different stages of ovarian development were not significantly different ($P < 0.05$). This transcript was upregulated at stage IV ovaries of eyestalk-ablated broodstock ($P < 0.05$). Generally, the expression levels of these genes in ovaries of juveniles were significantly lower than that of normal broodstock ($P < 0.05$).

REFERENCES

- Aktas, M., Kumlu, M., and Eroldogan, O.T. 2003. Off-season maturation and spawning of *Penaeus semisulcatus* by eyestalk ablation and/or temperature–photoperiod regimes. Aquaculture. 228: 361-370.
- Aligianis, I.A., Morgan, N.V., Mione, M., Johnson, C.A., Rosser, E., Hennekam, R.C., Adams, G., Trembath, R.C., Pilz, D.T. Stoodley, N., Moore, A.T., Wilson, S. and Maher, E.R.. 2006. Mutation in Rab3 GTPase-Activating protein (RAB3GAP) noncatalytic subunit in a Kindred with Martsolf syndrome. Human Gene 78 .
- Baksh, S., Burns, K., Andrin, C., and Michalak, M. 1995a. Interaction of calreticulin with protein disulfide isomerase. The Journal of Biological Chemistry 270: 31338-31344.
- Benzie, J.A.H..1998. Penaeid genetics and biotechnology. Aquaculture 164 : 23–47.
- Brouwer, M., Brouwer, T.H., Grater, W. and Brown-Peterson, N. 2003. Replacement of a cytosolic copper/zinc superoxide dismutase by a novel cytosolic manganese superoxide dismutase in crustaceans that use copper (haemocyanin) for oxygen transport. Biochemistry Journal. 374 : 219-228.
- Bulau, P., Meisen, I., Schmitz, T., Keller, R., and Katalinic, J.P. 2004. Identification of neuropeptides from the sinus gland of the crayfish *Orconectes limosus* using nanoscale on-line liquid chromatography tandem mass spectrometry. Molecular & Cellular Proteomics 3.6 : 588-564.
- Bohren, K.M., Bullock, B., Wermuth, B. and Gabbay, K.H. 1989. The Aldo-Keto Reductase superfamily cDNAs and deduced amino acid sequence of human aldehyde and aldose reductase. The Journal of Biology Chemistry 264 : 9547-9651.

- Bradford, M.M.. 1976. A rapid and sensitive method for the quantitation of microgram quantities of protein utilizing the principle of protein-dye binding, *Anal. Biochemistry*. 72 : 248-254.
- Calvert, M.E., Digilio, L.C., Herr, J.C., Coonrod, S.A., 2003. Oolemmal proteomics- identification of highly abundant heat shock proteins and molecular chaperones in the mature mouse egg and their localization on the plasma membrane. *Reproductive. Biological. Endocrinology* 1 : 27.
- Cesar Lopez, C., Garcia-Hernandez, M.L., Marchat, L.M., Luna-Arias, J.P., Hernandez de la Cruz, O., Mendoza, L. and Orozco, E.. 2008. *Entamoeba histolytica* EhDEAD1 is a conserved DEAD-box RNA helicase with ATPase and ATP-dependent RNA unwinding activities. *Gene* 414 : 19-31.
- Clifford, H. C. and Preston, N. P.. 2006. Genetic improvement; in *Operating Procedures for Shrimp Farming: Global Shrimp OP Survey Results and Recommendations*,. *Global Aquaculture Alliance*, St. Louis, USA. : 73-77,.
- Coonrod, S.A.,Wright, P.W., Herr, J.C., 2002. Oolemmal proteomics. *Journal of. Reproductive Immunology*. 53: 55–65.
- Dym, O., Pratt, E.A., Ho, C. and Eisenberg, D.. 2000. The crystal structure of D-lactate dehydrogenase, a peripheral membrane respiratory enzyme. *PNAS* 97 : 9413–9418.
- Goplen, D. Wang, J. P., Berit, E., Tysnes, A.J.A., Ole D, T., Laerum, R.B.. 2006. Protein disulfide isomerase expression is related to the invasive properties of malignant glioma. *Cancer Res* : 66. 20.
- Gigue, P., Turcottea, M.E., Hamelina, E. Parenta, A., Brissona, J., Larochea, G., Labrecquea, P., Dupuisb, G. and Parenta, J.L.. 2007. Peroxiredoxin-4 interacts with and regulates the thromboxane A2 receptor. *FEBS* 581 : 3863–3868.

- Horling, P., Lamkemeyer, P., Konig, J., Finkemeier, I., Kandlbinder, A., Baier, M. and Dietz, K.J.. 2003. Divergent light-, ascorbate-, and oxidative stress-dependent regulation of expression of the peroxiredoxin gene family in *Arabidopsis*. Plant Physiology 131: 317–325.
- Husain, M and Steenkamp, D.J..1983. Electron transfer flavoprotein from pig liver mitochondria. Biochemistry Journal 209 : 541-545.
- Huberman, A., Aguilar, M.B. and Quackenbush, L.S..1995. A neuropeptide family from the sinus gland of the Mexican crayfish, *Procambarus bouvieri* (Ortmann). Aquaculture 135 : 149-160.
- Hynes, G., Sutton, C.W., U, S. and Willin, K. 1996. Peptide mass fingerprinting of chaperonin-containing TCP-1 (CCT) and copurifying proteins. FASEBJ 10 ;137-147 .
- Khalifah, R.G. 1970. The Carbon dioxide hydration activity of carbonic anhydrase. The Journal of Biology Chemistry. 246 :256-2573.
- Keyvanshokoh, S., Kalbassi, M.R., Hosseinkhani, S. and Vaziri, B.. 2008. Comparative proteomics analysis of male and female Persian sturgeon (*Acipenser persicus*) gonads. Animal Reproduction Science.
- Kleijn de, D. P. V., Janssen, K.P.C., Waddy, S.L., Hegeman, R., Lai, W.Y., Martens, G. J.M., and Herp F.V. 1998. Expression of the crustacean hyperglycaemic hormones and the gonad-inhibiting hormone during the reproductive cycle of the female American lobster *Homarus americanus*. Journal of Endocrinology. 156: 291–298.
- Klinbunga, S., Penman, D.J., McAndrew, B.J. and Tassanakajon, A.. 1999. Mitochondrial DNA diversity in three populations of the giant tiger shrimp *Penaeus monodon*. Marine. Biotechnology 1: 113–121.

- Kwok, R., Zhang, J.R., and Tobe, S.S. 2005. Regulation of methyl farnesoate production by mandibular organs in the crayfish, *Procambarus clarkia* : A possible role for allatostatins. Journal of Insect Physiology. 51: 367-378
- Laufer, H., Ahl 1, J., Rotllant, G. and Baclaski, B. 2002. Evidence that ecdysteroids and methyl farnesoate control allometric growth and differentiation in a crustacean. Insect Biochemistry and Molecular Biology 32: 205-210.
- Lam Hui , J. H., Tobe, S. S., Chan, S. M.. 2008. Characterization of the putative farnesoic acid O-methyltransferase (LvFAMeT) cDNA from white shrimp, *Litopenaeus vannamei* : Evidence for its role in molting. Peptide 2 9 : 2 52 – 2 60.
- Langbein, S., Zerilli, M., Hausen, A.Z. Staiger, W., Rensch-Boschert, K., Lukan, N. Popa, J., Ternullo, MP. Steidler, A. Weiss, C. Grobholz, R. Willeke, F., Alken, P., Stassi, G., Schuber, P. and Coy , JF. 2006. Expression of transketolase TKTL1 predicts colon and urothelial cancer patient survival: Warburg effect reinterpreted. British Journal of Cancer : 94. 578-585.
- Lee, F.W.F. and Chun-Lap-Lo, S..2008. The use of Trizol reagent (phenol/guanidine isothiocyanate) for producing high quality two-dimensional gel electrophoretograms (2-DE) of dinoflagellates. Journal of Microbiological Methods 73 : 26–32.
- Lounsbury, K.M. and Macara, I.G..1997. Ran-binding protein 1 (RanBP1) forms a ternary complex with Ran and Karyopherin b and reduces Ran GTPase-activating Protein (RanGAP) inhibition by Karyopherin β . The Journal of Biology Chemistry 272 : 551–555.
- Meusy, J.J., Payen, G.G., 1988. Female reproduction in malacostracan Crustacea. Zoology. Science. 5: 217–265
- Nagao, M., Parimoo, B., and Tanaka, K. 1993. Developmental, Nutritional, and

Hormonal regulation of tissue-specific expression of the genes encoding various Acyl-CoA Dehydrogenases and α -subunit of electron transfer flavoprotein in rat. The Journal of Biological Chemistry : 268. 24114-24124.

Okumura, T., Kim, Y. K., Kawazoe, I., Yamano, K., Tsutsui, N. and Aida, K. 2006. Expression of vitellogenin and cortical rod proteins during induced ovarian development by eyestalk ablation in the kuruma prawn, *Marsupenaeus japonicus*. Comparative Biochemistry. Physiology. 143: 246-253.

Okumura, T. 2004. Review Perspectives on hormonal manipulation of shrimp reproduction. JARQ 38 (1): 49 – 54.

Pajonk, F., Riess, K., Sommer, A. and McBride, W.. 2000. N-acetyl-L-cysteine inhibits 26 s proteasome function : Implication for effect on NF-kB activation. Free Radical Biology & Medicine 32 : 536–543.

Preechaphol, R., Leelatanawit1, R., Sittikankeaw1, K., Klinbunga, S., Khamnamtong, B., Puanglarp, N. and Menasveta, P.. 2007. Expressed sequence tag analysis for identification and characterization of sex-Related genes in the giant tiger shrimp *Penaeus monodon*, JBMB 40: 501-510.

Qiu, G-F. and Yamano, K.. 2005. Three forms of cyclin B transcripts in the ovary of the kuruma prawn *Marsupenaeus japonicus*: Their molecular characterizations and expression profiles during oogenesis. Comparative. Biochemistry. Physiology B 141: 186-195.

Ruddell, C.J., Wainwright, G., Geffen, A., White, M.R.H., Webster, S.G., and Rees, H.H., 2003. Cloning, characterization, and developmental expression of a putative farnesoic acid O-methyl transferase in the female edible crab. Cancer pagurus. Bio. Bull. 205: 308-318.

- Salamon, C., Chervenak, M., Piatigorsky, J. and Sax, C.M. 1998. Mouse transketolase (TKT) gene: cloning, characterization, and functional promoter analysis, GENOMICS : 48. 209–220.
- Sheoran, I. S., Ross, A.R.S., Douglas J.H. Olson, D.J.H. and Sawhney, V.K.. 2009. Compatibility of plant protein extraction methods with mass spectrometry for proteome analysis. Plant Science 176 : 99–104.
- Storch, J. and Thumser, A.E.A..2000. The fatty acid transport function of fatty acid-binding proteins. Biochimica et Biophysica Acta 1486 : 28-44.
- Suzuki, T., Honda , M., Matsumoto, S., Sturzenbaum, S.R. and Gamou, S..2005. Valosine-containing proteins (VCP) in an annelid: Identification of a novel spermatogenesis related factor. Gene 362 : 11–18.
- Tsutsui, N., Katayama, H., Ohira, T., Nagasawa, H., Wilder, M.N. and Aida, K. 2005. The effects of crustacean hyperglycemic hormone-family peptides on vitellogenin gene expression in the kuruma prawn, *Marsupenaeus japonicus* . General and Comparative Endocrinology 144: 232–239.
- Tsukimura, B., Nelson , W.K. and Linder , C.J..2006. Inhibition of ovarian development by methyl farnesoate in the tadpole shrimp, *Triops longicaudatus*. Comparative Biochemistry and Physiology Part A 144 : 135–144.
- Tokuda, C., Ishikura, Y., Shigematsu, M., Mutoh, H., Tsuzuki, S., Nakahira, Y., Tamura, Y., Shinoda, T., Arai, K., Takahashi, O. and Taguchi, H. 2003. Conversion of *Lactobacillus pentosus* D-lactate dehydrogenase to a D-Hydroxyisocaproate dehydrogenase through a single amino acid replacement. Journal of Bacteriology 185 : 5023–5026.

- Udomkit, A., Chooluck, S., Sonthayanon, B., and Panyim, S. 2000. Molecular cloning of a cDNA encoding a member of CHH/MIH/GIH family from *Penaeus monodon* and analysis of its gene structure. Journal of Experimental Marine Biology and Ecology. 244: 145–156.
- Udomkit, A., Treerattrakool, S. and Panyim, S. 2004. Crustacean hyperglycemic hormones of *Penaeus monodon*: cloning, production of active recombinant hormones and their expression in various shrimp tissues. Journal of Experimental Marine Biology and Ecology. 298: 79– 91.
- Withyachumnarnkul, B., Boonsaeng, V., Flegel, T. W., Panyim, S. and Wongteerasupaya C..1998. Domestication and selective breeding of *Penaeus monodon* in Thailand, in: Proceedings to the Special Session on Advances in Shrimp Biotechnology, Felgel, T.(ed.) :73-77,. The Fifth Asian Fisheries Forum: International Conference on Fisheries and Food Security Beyond the Year 2000. 11-14 November 1998. Chiangmai, Thailand.
- Yano, I. 1995. Final oocyte maturation, spawning and mating in penaeid shrimp. Journal of Experimental Marine Biology and Ecology. 193: 113 -118.
- Yamano, K., Qiu, G.-F., Unuma, T., 2004. Molecular cloning and ovarian expression profiles of thrombospondin, a major component of cortical rods in mature oocytes of penaeid shrimp, *Marsupenaeus japonicus*. Biological Reproductive 70 : 1670–1678.
- Yamaguchi, K., Hidema, S. and Mizuno, S.. 1998. Chicken chromobox proteins: cDNA cloning of CHCB1, -2, -3 and their relation to W-Heterochromatin. Experimental Cell Research 242 : 303–314.
- Ziv, T., Gattegno, T., Chapovetsky, V., Wolf, H., Barnea, E., Lubzens, E., Admon, A. 2008. Comparative proteomics of the developing fish (zebrafish and gilthead seabream) oocytes. Comparative Biochemistry and Physiology. D3 : 12-35.

Zhao, R., Du, L., Huang, Y., Wu, Y. and Gunst, S.J..2008. Actin depolymerization factor/cofilin activation regulates actin polymerization and tension development in canine tracheal smooth muscle. The Journal of Biological Chemistry 283 : 6522–36531.

Zhao, W.N. and McAlister-Henn, L. 1996. Assembly and function of a cytosolic form of NADH-specific isocitrate dehydrogenase in Yeast. The Journal of Biological Chemistry 271:10347–10352.



ศูนย์วิทยทรัพยากร
จุฬาลงกรณ์มหาวิทยาลัย



ศูนย์วิทยทรัพยากร
จุฬาลงกรณ์มหาวิทยาลัย

Appendix A

Table A1 Protein spot analyzed by MALDI-TOF MS

Stage	Spot ID	Protein name	Accession number	Theoretical Mr (Da)/pI	Observed Mr (Da)/pI	% coverage	Score
1	171	unknown					
	172	unknown					
	170	unknown					
	169	unknown					
	89	unknown					
	173	unknown					
	53	unknown					
	44	unknown					
	61	unknown					
	60	unknown					
	59	unknown					
	58	unknown					
	38	unknown					
	39	unknown					
	40	unknown					
	30	unknown					
	37	unknown					
	1	unknown					
	2	unknown					
	3	unknown					
4	unknown						
5	unknown						
6	unknown						
2	1	unknown					
	7	unknown					
	8	unknown					
	9	unknown					
	10	unknown					
	11	unknown					
	12	unknown					
3	81	unknown					
	13	unknown					
	36	unknown					
4	123	unknown					
	63	unknown					

Table A2 Protein spot analyzed by MALDI-TOF/TOF MS

Stage	Spot ID	Protein name	Accession number	Theoretical Mr (Da)/pI	Observed Mr (Da)/pI	% coverage	Score
1EA	17	unknown					
	18	unknown					
	19	unknown					
	20	unknown					
	78	unknown					
	79	unknown					
	95	unknown					
	96	unknown					
	113	unknown					
	114	unknown					
	115	unknown					
	130	unknown					
	159	unknown					
	174	unknown					
	175	unknown					
	176	unknown					
	177	unknown					
	178	unknown					
	179	unknown					
1N	28	unknown					
	49	unknown					
	50	unknown					
	51	unknown					
	68	unknown					
	70	unknown					
	121	unknown					
	122	unknown					
2EA	123	unknown					
	1	unknown					
	2	Calreticurin	11977	60000/4.5	16288/5.5	9	69
	42	unknown					
	73	unknown					
	74	unknown					
	75	unknown					
	76	Transketolase	29503	60000/5.8	26662/5.4 7	7	77
	77	unknown					
	78	unknown					
	79	Protein disulfide isomerase	23253	49000/5.3	23929/4.5 2	6	62
	80	unknown					
	82	unknown					
	83	unknown					
84	unknown						

Table A2 Protein spot analyzed by MALDI-TOF/TOF MS (cont).

Stage	Spot ID	Protein name	Acc. No.	Theoretical Mr (Da)/pI	Observed Mr (Da)/pI	% coverage	Score
3EA	52	unknown					
	62	unknown					
	65	unknown					
	66	unknown					
	67	unknown					
	68	unknown					
	69	unknown					
	70	unknown					
	71	Allergen Pen m2	139652	40000/6.5	27877/7.84	57	73
	72	unknown					
	73	unknown					
	74	unknown					
	75	unknown					
	76	unknown					
	79	unknown					
	81	unknown					
	83	unknown					
	85	unknown					
	86	unknown					
	87	unknown					
	88	unknown					
	95	unknown					
	96	unknown					
	97	unknown					
	120	unknown					
	121	unknown					
	122	unknown					
	124	unknown					
	125	unknown					
126	unknown						
127	unknown						
128	unknown						
129	unknown						
4EA	31	unknown					
	32	unknown					
	33	unknown					
	62	unknown					
	116	unknown					
	117	unknown					
	118	unknown					
	119	unknown					
	120	unknown					
	121	unknown					
122	unknown						

Table A2 Protein spot analyzed by MALDI-TOF/TOF MS (cont)

Stage	Spot ID	Protein name	Acc. No.	Theoretical Mr (Da)/pI	Observed Mr (Da)/pI	% coverage	Score
4EA	123	unknown					
	124	unknown					
	125	unknown					
	126	unknown					
	127	unknown					
4N	26	unknown					
	27	unknown					
	28	unknown					
	29	unknown					
	30	unknown					
	34	unknown					
	35	unknown					
	36	unknown					
	37	unknown					



ศูนย์วิทยทรัพยากร
จุฬาลงกรณ์มหาวิทยาลัย

Appendix B

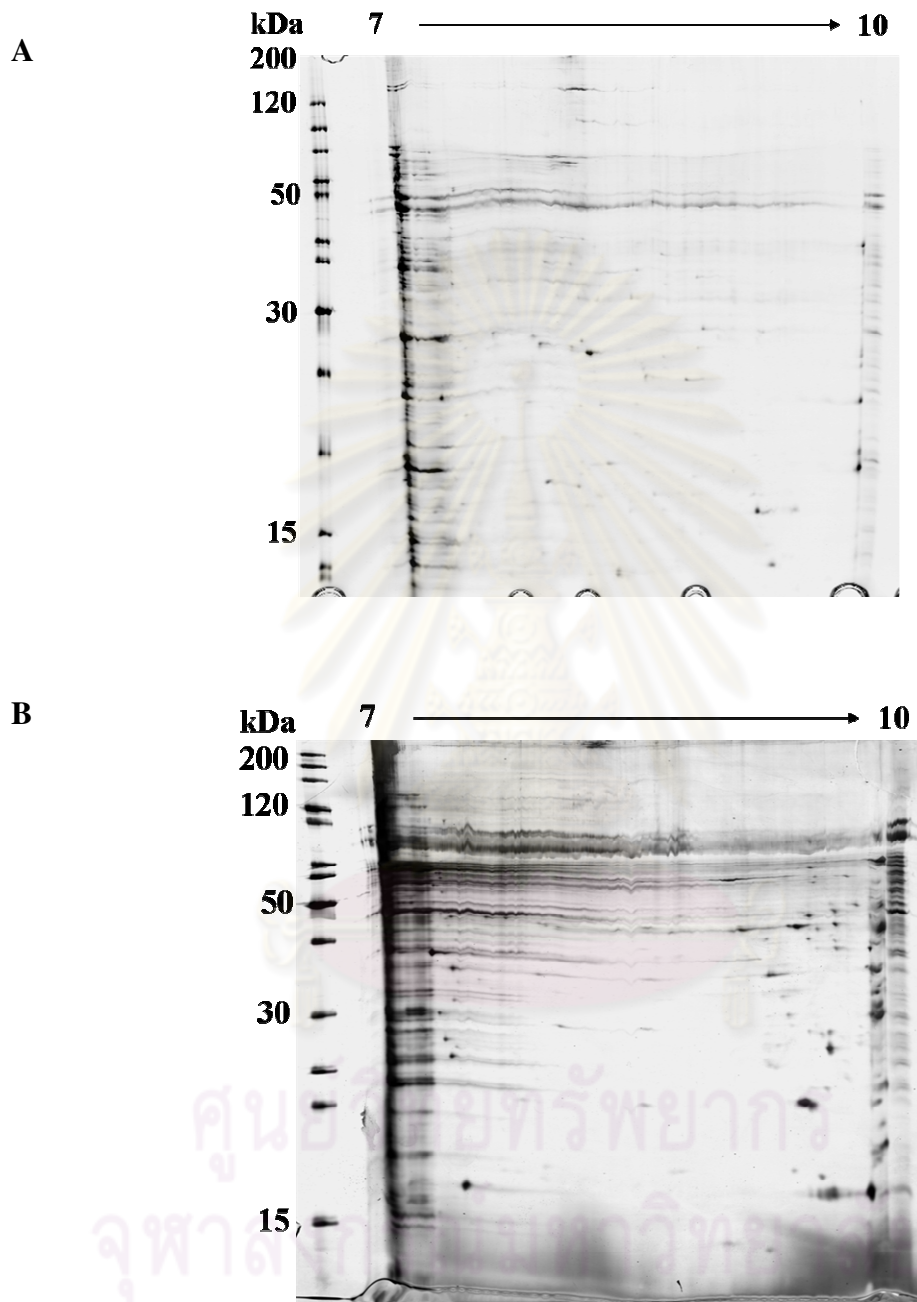


Figure B1 Protein profiles of stage I(A) and II(B) ovaries of wild *P. monodon* broodstock analyzed by 2D gel electrophoresis. Total proteins from two individuals (panels A and B, GSI = 0.57%, GSI = 1.33%) were electrophoretically analyzed in Immobiline Drystrip gels (pH 7-10) and silver-stained stained.

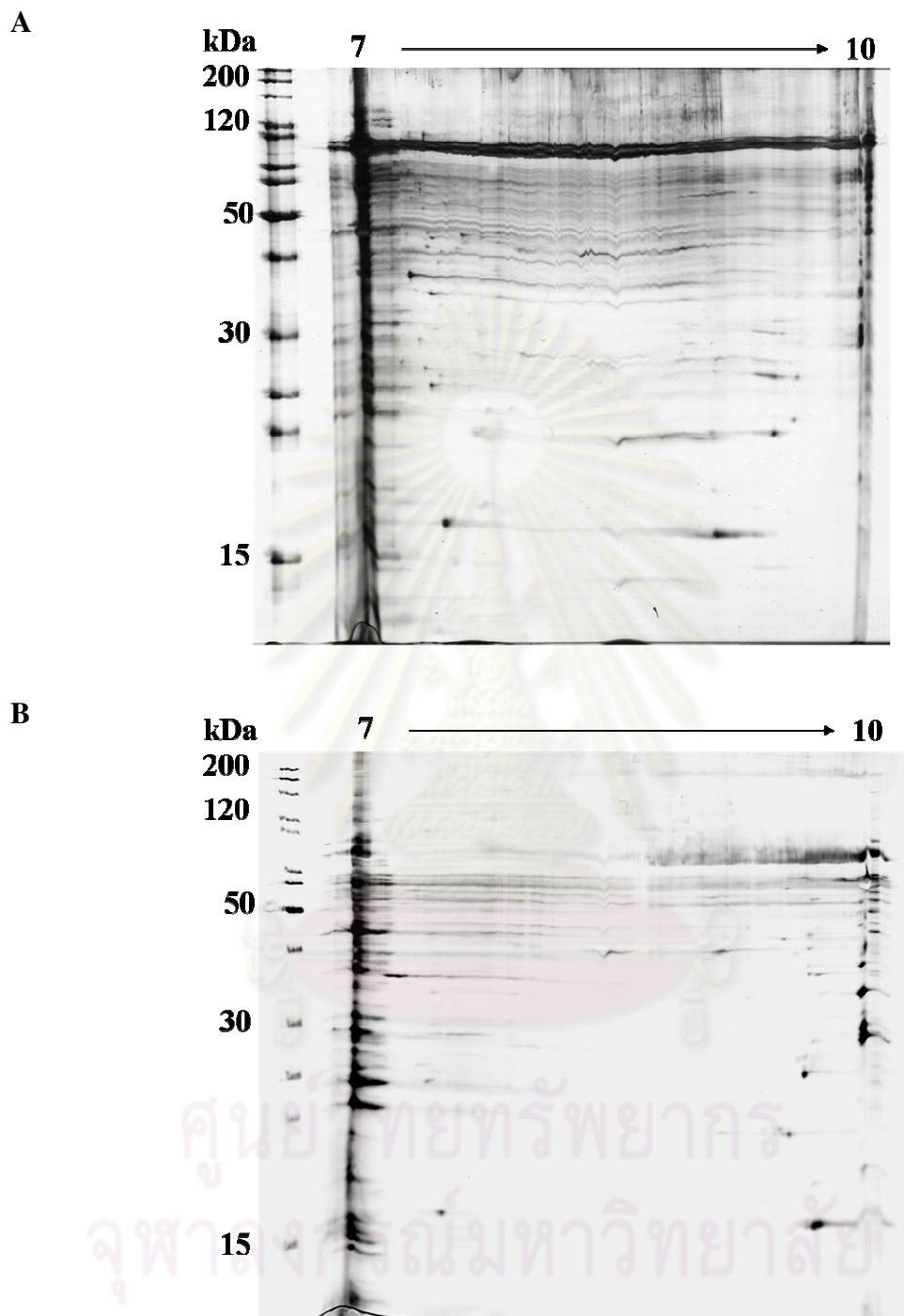


Figure B2 Protein profiles of stage I(A) and II(B) ovaries of eyestalk-ablated wild *P. monodon* broodstock analyzed by 2D gel electrophoresis. Total proteins from two individuals (panels A and B, GSI = 0.76%, GSI = 1.23%) were electrophoretically analyzed in Immobiline Drystrip gels (pH 7-10) and silver-stained.

Appendix C

Table. C1 Raw materials and relative expression level data of *DEAD box 52* of normal broodstock *P. monodon* using semi-quantitative RT-PCR.

Sample Group	Densities of band			Average	STD	
	<i>DEAD box 52</i>	EF-1 α	Ratio of gene/EF-1 α			
1	BUF3	20921087	35066889	0.596605	5.588445	0.1482767
	BUF2	34593162	37982602	0.910763		
	BUF1	34095534	37098891	0.919045		
	BUF6	35337052	35646500	0.991319		
	BUF4	37024873	35675425	1.037826		
	AGYL3	32974495	33180056	0.993805		
	BUF7	35390008	36350484	0.973577		
2	BUF5	36644570	35414408	1.034736	2.368051	0.1623690
	AGYL1	33939671	36896357	0.919865		
	BFN22	32431469	26147047	1.240349		
3	BFN4/1	35877867	34411783	1.042604	6.841443	0.0630670
	BFN7	36331891	36317513	1.000396		
	BFN18	34511025	35924678	0.96065		
	BFN3	34551482	35715485	0.967409		
	BFN4	34581383	36317479	0.952197		
	BFN5	31253088	37040258	0.84376		
	BFN23	32837704	34762270	0.944636		
	BFN1	35714774	34396488	1.038326		
4	BFN19	37146987	33785613	1.099491	10.81012	0.1584675
	BFN9	35045722	33054521	1.06024		
	BFN8	34253383	33612412	1.019069		
	BFN2	35017263	33487683	1.045676		
	BFN10	34142376	31767420	1.074761		
	BFN12	35304243	34854437	1.012905		
	BFN21	21589562	30822449	0.700449		
	BFN15	32853835	28687362	1.145237		
	BFN20	36436989	27294275	1.334968		
	BFN16	33070795	26940728	1.227539		
	BFN13	31547354	31941733	0.987653		

Table. C2 Raw materials and relative expression level data of *DEAD box 52* of eyestalk-ablated broodstock *P. monodon* using semi-quantitative RT-PCR.

Sample Group	Densities of band			Ratio of gene/EF-1 α	Average	STD
	<i>DEAD box 52</i>	EF-1 α				
1	YLB1	29495772	35974116	0.819917	2.254848	0.1564742
	YLB6	23655170	37015903	0.639054		
	YLB5	21091910	37058002	0.569159		
	YLB8	34371574	37901326	0.90687		
2	YLB7	31205710	37778735	0.826013	1.750475	0.077711
	YLB4	25908058	37270459	0.695137		
	YLB3	25837579	37555959	0.687975		
3	BFEA8	27155944	36912874	0.735677	3.552834	0.0790516
	BFEA5	30171095	36269376	0.831861		
	BFEA2	28302565	36932134	0.76634		
	BFEA4	22300484	36974807	0.603126		
	BFEA7	23305581	36033714	0.646772		
	BFEA6	25004857	36206151	0.690625		
	BFEA13	28715300	37193219	0.772057		
4	BFEA3	23413863	36033714	0.655937	2.953688	0.1313156
	BFEA1	24388783	35824998	0.680776		
	BFEA12	31826377	36867056	0.863274		
	BFEA9	0.579051	35824998	0.579051		
	BFEA4	0.873249	35824998	0.873249		

Table. C3 Raw materials and relative expression level data of *ATP-dependentRNA helicase* of normal broodstock *P. monodon* using semi-quantitative RT-PCR.

Sample Group	Densities of band			Average	STD	
	<i>ATP-dependentRNA helicase</i>	EF-1 α	Ratio of gene/EF-1 α			
1	BUF3	11600419	15067155	0.769914	0.854739	0.0787002
	BUF2	11704504	16185461	0.723149		
	BUF1	14362618	15410832	0.931982		
	BUF6	14794497	17300087	0.855169		
	BUF4	14169944	15637751	0.906137		
	AGYL3	15171002	16688053	0.909094		
	BUF7	14045169	15821432	0.887731		
2	BUF5	14258037	15533798	0.917872	0.8604686	0.1066546
	AGYL1	13113262	14193925	0.923864		
	AGYL4	12384106	18450220	0.671217		
	AGYL2	14740682	16407487	0.898412		
	BFN22	12577667	14116696	0.890978		
3	BFN4/1	13219093	14055876	0.940467	6.670663	0.0676379
	BFN7	13616949	13689105	0.994729		
	BFN3	13138168	14719684	0.892558		
	BFN4	13843781	13676469	1.012234		
	BFN5	12467956	13724142	0.908469		
	BFN23	12683083	15358119	0.825823		
	BFN24	14774499	14941689	0.98881		
	BFN1	12633752	14680454	0.860583		
4	BFN19	12524412	14916537	0.839633	11.76249	0.0968652
	BFN9	12626755	12776302	0.988295		
	BFN8	10832731	12323582	0.879025		
	BFN6	12345702	10547381	1.170499		
	BFN2	11332053	12052022	0.940262		
	BFN10	12250707	11438524	1.071004		
	BFN12	12263171	13495956	0.908655		
	BFN21	13058865	13219734	0.987831		
	BFN15	12823409	12815843	1.00059		
	BFN20	12848949	12202779	1.052953		
	BFN16	11690799	11743192	0.995538		
	BFN16	10269650	11915061	0.861905		
	BFN13	11190693	12982891	0.861957		

Table. C4 Raw materials and relative expression level data of *ATP-dependentRNA helicase* of eyestalk-ablated broodstock *P. monodon* using semi-quantitative RT-PCR.

Sample Group	Densities of band			Average	STD
	<i>ATP-dependentRNA helicase</i>	EF-1 α	Ratio of gene/EF-1 α		
1	YLB1	13925743	22298825	1.86119	0.1686860
	YLB6	11096014	30108613		
	YLB5	12673155	18680694		
	YLB8	13462444	17737843		
2	YLB7	13615042	21027406	1.594293	0.0808331
	YLB4	14411630	21198100		
	YLB3	12489843	15595823		
3	BFEA8	11726256	16649736	4.180244	0.1072234
	BFEA5	12370118	15819825		
	BFEA2	12871080	15361216		
	BFEA4	11977870	18380211		
	BFEA7	11822355	21343406		
	BFEA6	12197030	22085874		
	BFEA13	12311822	17895766		
4	BFEA11	12893817	20745142	3.255916	0.0711225
	BFEA3	12936488	19385047		
	BFEA1	10769887	20231557		
	BFEA12	13472606	21752268		
	BFEA9	11705693	16907446		
	BFEA4	10804951	14640758		

Table. C5 Raw materials and relative expression level data of *DEAD boxATP-dependentRNA helicase* of normal broodstock *P. monodon* using semi-quantitative RT-PCR

Sample Group	Densities of band			Average	STD	
	<i>DEAD box ATP-dependentRNA helicase</i>	EF-1 α	Ratio of gene/EF-1 α			
1	BUF3	104272.1	86429.95	1.206434	7.257892	0.0574971
	BUF2	111404.8	96491.53	1.154556		
	BUF1	111163.3	96977.73	1.146276		
	BUF6	110124.7	98216.66	1.121242		
	BUF4	113690.5	91787.76	1.238624		
	AGYL3	116803.2	96763.28	1.207102		
	BUF7	115210.4	89615.75	1.285604		
2	BUF5	110227.4	90097.13	1.223429	5.369847	0.1451370
	AGYL1	103489.5	88433.59	1.170251		
	AGYL4	103823.7	84036.2	1.235463		
	AGYL2	113476.5	78715.49	1.441603		
	BFN22	101086.3	67593.36	1.495506		
3	BFN4/1	109981	99773.3	1.102309	9.554812	0.0492238
	BFN7	113219.8	98094.14	1.154195		
	BFN18	114099.2	98732.81	1.155636		
	BFN3	116519.8	98489.32	1.18307		
	BFN4	123531.6	105247.1	1.173729		
	BFN5	126557.3	100558.7	1.258542		
	BFN23	114683.9	99990.23	1.146951		
	BFN24	117255.8	93975.91	1.247721		
	BFN1	109032.2	91321.87	1.193933		
4	BFN19	109347.1	91718.49	1.192204	13.36731	0.1080079
	BFN9	81843.39	83605.08	0.978928		
	BFN8	87154.59	78606.9	1.10874		
	BFN6	93969.97	94108.59	0.998527		
	BFN2	106255.8	98926.82	1.074085		
	BFN14	113790	94680.86	1.201826		
	BFN10	119022.2	92953.12	1.280454		
	BFN12	105156.4	91464.84	1.149692		
	BFN15	110180.4	95679.16	1.151561		
	BFN20	104775.2	97868.88	1.070567		
	BFN16	103929.4	100687.1	1.032202		
	BFN16	100352.9	94542.45	1.061459		
	BFN13	74794.89	85784.5	0.871893		

Table. C6 Raw materials and relative expression level data of *DEAD box* ATP-dependent RNA helicase of eyestalk-ablated broodstock *P. monodon* using semi-quantitative RT-PCR.

Sample Group	Densities of band			Average	STD
	<i>DEAD box</i> ATP- dependent RNA <i>helicase</i>	EF-1 α	Ratio of gene/EF-1 α		
1	YLB6	90579.24	111567.4	1.891292	0.0071215
	YLB8	93832.11	116414.6		
	YLB5	95302.14	116195.3		
2	YLB7	95609.04	116913.9	1.907119	0.0041116
	YLB4	96276.34	118125		
	YLB3	96204.98	116906.3		
3	BFEA8	97011.71	111118.8	4.268288	0.0420973
	BFEA5	92261.16	108971.3		
	BFEA2	90447.24	104498		
	BFEA4	89607.3	1173.501		
	BFEA6	92293.62	1171.935		
	BFEA13	94360.63	1192.087		
4	BFEA11	92447.36	1125.868	4.153177	0.0222561
	BFEA3	88953.27	1111.316		
	BFEA1	90417.33	1128.223		
	BFEA12	93294.14	1186.747		
	BFEA9	91903.42	1123.948		
	BFEA4	87303.88	1151.201		

Table. C7 Raw materials and relative expression level data of *helicase lymphoid specific isoform 2* of normal broodstock *P. monodon* using semi-quantitative RT-PCR.

Sample Group	Densities of band			Average	STD	
	<i>helicase lymphoid specific isoform 2</i>	EF-1 α	Ratio of gene/EF-1 α			
1	BUF3	16633231	464.7918	1.10394	6.293104	0.0698671
	BUF2	15191322	422.684	0.938578		
	BUF1	16616351	487.6234	1.078225		
	BUF6	16939552	641.5077	0.97916		
	BUF4	15375597	436.6294	0.983236		
	AGYL3	17950203	552.3377	1.075632		
	BUF7	14877357	500.2036	0.940329		
2	BUF5	14798502	503.799	0.952665	2.801355	0.0863600
	AGYL4	13717409	643.2234	0.743482		
	AGYL2	14777457	672.3553	0.900653		
	BFN22	11550569	494.418	0.81822		
3	BFN4/1	13407757	285.4812	0.95389	7.680898	0.0958701
	BFN7	16433691	321.7046	1.200494		
	BFN3	15964205	412.9591	1.084548		
	BFN4	16117629	356.1916	1.178493		
	BFN5	15380063	402.2595	1.120657		
	BFN23	16774563	411.2188	1.092228		
	BFN24	13781754	427.5859	0.922369		
	BFN1	15058512	395.1718	1.025752		
4	BFN19	14658018	471.6474	0.982669	13.20643	0.1052650
	BFN9	13945417	424.2792	1.091507		
	BFN8	11589338	409.611	0.94042		
	BFN6	11580371	268.6658	1.097938		
	BFN2	12834603	299.1038	1.064934		
	BFN14	14804874	254.9173	1.294299		
	BFN10	15529381	413.0516	1.150669		
	BFN12	14663773	381.3501	1.109234		
	BFN15	14377558	375.9023	1.121858		
	BFN20	15499450	345.6199	1.270157		
	BFN16	11695515	287.7028	0.99594		
	BFN16	12004370	259.9534	1.007495		
	BFN13	13385821	377.748	1.031036		

Table. C8 Raw materials and relative expression level data of *helicase lymphoid specific isoform 2* of eyestalk-ablated broodstock *P. monodon* using semi-quantitative RT-PCR.

Sample Group	Densities of band			Average	STD
	<i>helicase lymphoid specific isoform 2</i>	EF-1 α	Ratio of gene/EF-1 α		
1	YLB1	12035093	22298825	2.12337	0.1106310
	YLB6	12175354	30108613		
	YLB5	14117942	18680694		
	YLB8	14979907	17737843		
2	YLB7	15744296	21027406	1.774009	0.586354
	YLB4	13217639	21198100		
	YLB3	15787557	15595823		
3	BFEA8	14842444	16649736	5.117597	0.843694
	BFEA5	14274247	15819825		
	BFEA2	13116379	15361216		
	BFEA4	12419345	18380211		
	BFEA7	12520392	21343406		
	BFEA6	13049646	22085874		
	BFEA13	12319088	17895766		
4	BFEA11	13437646	20745142	4.71837	0.0975662
	BFEA3	13748131	19385047		
	BFEA1	11787877	20231557		
	BFEA12	15858987	21752268		
	BFEA9	1.092184	16907446		
	BFEA4	1.079583	14640758		

Table. C9 Raw materials and relative expression level data of *protein disulfide isomerase (PDI)* of normal broodstock *P. monodon* using semi-quantitative RT-PCR.

Sample Group	Densities of band			Average	STD	
	<i>PDI</i>	EF-1 α	Ratio of gene/EF-1 α			
1	BUF3	105908.7	86429.95	1.22537	7.953115	0.0809109
	BUF2	122049.9	96491.53	1.264876		
	BUF1	132829.2	96977.73	1.369687		
	BUF6	120764.1	98216.66	1.229569		
	BUF4	132008.3	91787.76	1.438191		
	AGYL3	119918.8	96763.28	1.239301		
	BUF7	116755.7	89615.75	1.302848		
2	BUF5	133889.4	90097.13	1.486056	5.591078	0.1590236
	AGYL1	100008.2	88433.59	1.130885		
	AGYL4	119143.5	84036.2	1.417765		
	AGYL2	98939.46	78715.49	1.256925		
	BFN22	101203.2	67593.36	1.497236		
3	BFN4/1	110680.9	99773.3	1.109324	8.843278	0.0624667
	BFN7	110098.4	98094.14	1.122375		
	BFN18	107741.4	98732.81	1.091243		
	BFN3	104786.7	98489.32	1.06394		
	BFN4	107293.3	105247.1	1.019441		
	BFN5	113626.5	100558.7	1.129952		
	BFN23	110627.2	99990.23	1.10638		
	BFN24	99842.2	93975.91	1.062423		
	BFN1	113586	91321.87	1.243799		
4	BFN19	121833.5	91718.49	1.328342	13.80776	0.1098169
	BFN9	93019.47	83605.08	1.112605		
	BFN8	105598.5	78606.9	1.343375		
	BFN6	103307.1	94108.59	1.097744		
	BFN2	106365.3	98926.82	1.075192		
	BFN14	104157.9	94680.86	1.100095		
	BFN10	100385.6	92953.12	1.07996		
	BFN12	104124.2	91464.84	1.138407		
	BFN15	110528.2	95679.16	1.155196		
	BFN20	113387.4	97868.88	1.158565		
	BFN16	97831.62	100687.1	0.97164		
	BFN16	110764.2	94542.45	1.171582		
	BFN13	83701.99	85784.5	0.975724		

Table. C10 Raw materials and relative expression level data of *protein disulfide isomerase (PDI)* of eyestalk-ablated broodstock *P. monodon* using semi-quantitative RT-PCR.

Sample Group	Densities of band			Ratio of gene/EF-1 α	Average	STD
	PDI	EF-1 α				
1	YLB8	108858.4	116414.6	0.891569	1.362708	0.0358567
	YLB5	118911.1	116195.3	0.942278		
2	YLB7	116780.9	116913.9	0.890139	2.087248	0.0102300
	YLB4	120329.3	118125	0.893957		
	YLB3	119877.5	116906.3	0.909455		
3	BFEA8	115344.3	111118.8	0.886811	4.846375	0.0478193
	BFEA5	114958.8	108971.3	0.900331		
	BFEA2	114553	104498	0.904689		
	BFEA4	126372.1	1173.501	0.975424		
	BFEA6	138284.4	1171.935	1.022658		
	BFEA13	135266.4	1192.087	0.938771		
4	BFEA11	141571.5	1125.868	0.94003	4.972095	0.0601049
	BFEA3	111719.3	1111.316	0.88568		
	BFEA1	126300.2	1128.223	0.959751		
	BFEA12	152113.7	1186.747	1.051884		
	BFEA9	134421.3	1123.948	0.969176		
	BFEA4	135027.3	1151.201	0.993442		

Appendix D

Table. D1 Relative expression level data of *DEAD box ATP-dependent RNA helicase* in ovaries of normal broodstock *P. monodon* using real-time PCR.

Sample Group	concentration		Ratio of gene/ <i>EF-1α</i>	Average	STD				
	<i>DEAD box ATP- dependent RNA helicase</i>	<i>EF-1α</i>							
1	BUF3	2.31E5	2.21E7	0.00755	0.09695	0.0043529			
	BUF6	6.41E4	1.61E7	0.00281					
	BUF4	2.75E5	1.78E7	0.0112					
	AGYL3	2.31E5	1.78E7	0.0094					
	BUF7	9.56E4	4.09E6	0.0174					
	BUF5	8.49E4	3.77E6	0.0167					
	AGYL1	2.73E5	1.81E7	0.011					
	AGYL4	2.38E5	2.26E7	0.00761					
	AGYL2	2.89E5	1.75E7	0.012					
	BFN32	2.05E5	1.18E7	0.0128					
	2	BFN38	1.61E5	8.59E6			0.0138	0.07784	0.0026907
		BFN33	1.14E5	5.76E6			0.0146		
ASP10		2.02E5	1.55E7	0.00949					
BFN35		1.61E5	8.35E6	0.0141					
ASP6		2.46E5	1.94E7	0.00918					
BFN31		1.86E5	9.51E6	0.0144					
BFN4/1		1.06E5	4.84E6	0.0162					
3		BFN18	5.55E4	1.96E6	0.0212	0.018185	0.0028731		
	BFN3	8.82E4	5.06E6	0.0128					
	BFN4	1.01E5	4.31E6	0.0173					
	BFN23	1.75E5	6.82E6	0.019					
	BFN24	9.91E4	3.52E6	0.021					
	BFN5	1.06E5	4.65E6	0.017					
	BFN1	1.08E5	4.25E6	0.019					
4	BFN2	6.25E4	2.64E6	0.0176	0.0194				
	BFN14	7.96E4	3.06E6	0.0194					

Table. D1 Relative expression level data of *DEAD box ATP-dependent RNA helicase* in ovaries of normal broodstock *P. monodon* using real-time PCR (cont).

Sample Group	concentration		Ratio of gene/ <i>EF-1α</i>	Average	STD
	<i>DEAD box ATP- dependent RNA helicase</i>	<i>EF-1α</i>			
4	BFN10	7.27E4	3.94E6	0.0136	0.158356 0.0039886
	BFN12	5.90E4	3.12E6	0.014	
	BFN21	9.77E4	3.20E6	0.0228	
	BFN15	4.84E4	1.91E6	0.019	
	BFN20	5.43E4	1.89E6	0.0214	
	BFN17	4.63E4	1.55E6	0.0223	
	BFN13	7.38E4	2.17E6	0.0255	
5	BFN30	1.15E5	7.12E6	0.0119	0.080098 0.0058564
	BFN36	1.95E5	9.17E6	0.0156	
	BFN34	1.74E5	8.58E6	0.0149	
	BFN37	1.89E5	7.35E6	0.0191	
	BFN39	1.47E5	6.02E6	0.0181	
	BFN40	1.30E5	3.06E7	0.00299	
	6	JNOV5	1.01E5	1.06E7	
JNOV6		2.64E5	2.02E7	0.00945	
JNOV7		2.54E5	1.35E7	0.0138	
JNOV8		4.40E4	6.95E6	0.00454	
JNOV9		7.62E4	8.89E6	0.00619	
JNOV10		1.14E5	1.98E7	0.00409	

Table. D2 Relative expression level data of *DEAD box ATP-dependent RNA helicase* in ovaries of eyestalk-ablated broodstock *P. monodon* using real-time PCR.

Sample Group	concentration		Ratio of gene/ <i>EF-1α</i>	Average	STD	
	<i>DEAD box ATP- dependent RNA helicase</i>	<i>EF-1α</i>				
1	BFEA18	2.81E5	1.07E7	0.0137	0.02417	0.032547
	YLB1	5.51E5	3.78E7	0.00743		
	YLB6	1.70E5	9.61E6	0.00905		
2	YLB8	4.00E5	2.41E7	0.0108	0.069713	0.032591
	BFEA19	1.86E5	5.81E6	0.0161		
	BFEA17	2.05E5	7.96E6	0.0154		
	YLB7	1.55E5	7.41E6	0.00848		
	BFEA16	2.14E5	6.91E6	0.0167		
	YLB4	2.45E5	8.30E6	0.0134		
3	BFEA21	2.01E5	9.79E6	0.0107	0.11779	0.029161
	YLB2	1.88E5	9.24E6	0.0107		
	YLB3	1.52E5	6.98E6	0.0106		
	BFEA8	3.16E5	1.63E7	0.0144		
	BFEA5	3.05E5	1.28E7	0.0105		
	BFEA2	1.82E5	8.71E6	0.012		
	BFEA11	1.48E5	7.11E6	0.0187		
	BFEA3	3.07E5	9.94E6	0.0161		
	BFEA20	1.14E5	4.11E6	0.0123		
	BFEA4	1.46E5	4.57E6	0.0179		
	BFEA1	1.53E5	5.14E6	0.0114		
4	BFEA7	2.73E5	1.26E7	0.012	0.1489	0.041574
	BFEA6	1.92E5	6.26E6	0.0159		
	BFEA24	1.81E5	5.28E6	0.0167		
	BFEA10	2.03E5	9.21E6	0.0187		
	BFEA12	1.64E5	7.08E6	0.0155		
	BFEA13	2.62E5	8.55E6	0.0211		
	BFEA22	1.25E5	3.50E6	0.0112		
	BFEA23	8.73E4	2.18E6	0.0248		
BFEA9	8.74E4	1.86E6	0.016			

Table. D3 Relative expression level data of *protein disulfide isomerase (PDI)* in ovaries of normal broodstock *P. monodon* using real-time PCR.

Sample Group	concentration		Ratio of gene/ <i>EF-1α</i>	Average	STD				
	<i>PDI</i>	<i>EF-1α</i>							
1	BUF3	5.90E5	2.21E7	0.0337	0.37277	0.044525			
	BUF6	5.76E4	1.61E7	0.03495					
	BUF4	5.94E5	1.78E7	0.00736					
	AGYL3	4.68E5	1.78E7	0.0467					
	BUF7	1.22E5	4.09E6	0.0507					
	BUF5	1.18E5	3.77E6	0.0379					
	AGYL1	6.39E5	1.81E7	0.0555					
	AGYL4	7.40E5	2.26E7	0.0513					
	AGYL2	5.64E5	1.75E7	0.05					
	BFN32	3.68E5	1.18E7	0.0466					
	2	BFN38	2.17E5	8.59E6			0.09	0.305286	0.0188277
		BFN33	1.89E5	5.76E6			0.039		
ASP10		3.44E5	1.55E7	0.0507					
BFN35		2.73E5	8.35E6	0.0341					
ASP6		5.70E5	1.94E7	0.04					
BFN31		3.34E5	9.51E6	0.0438					
BFN4/1		1.97E5	4.84E6	0.0538					
3		BFN18	4.81E4	1.96E6	0.0582	0.349586	0.0098251		
	BFN3	1.36E5	5.06E6	0.0428					
	BFN4	1.74E5	4.31E6	0.0669					
	BFN23	2.20E5	6.82E6	0.0528					
	BFN24	1.42E5	3.52E6	0.068					
	BFN5	1.46E5	4.65E6	0.0512					
	BFN1	1.89E5	4.25E6	0.0678					
4	BFN2	5.47E4	2.64E6	0.0464	0.0554				
	BFN14	9.92E4	3.06E6						

Table. D3 Relative expression level data of *protein disulfide isomerase (PDI)* in ovaries of normal broodstock *P. monodon* using real-time PCR (cont).

Sample Group	concentration		Ratio of gene/ <i>EF-1α</i>	Average	STD	
	<i>PDI</i>	<i>EF-1α</i>				
4	BFN10	8.63E4	3.94E6	0.0606	0.435656	0.0079915
	BFN12	8.10E4	3.12E6	0.0656		
	BFN21	1.07E5	3.20E6	0.0394		
	BFN15	4.83E4	1.91E6	0.0477		
	BFN20	4.78E4	1.89E6	0.0564		
	BFN17	3.98E4	1.55E6	0.0566		
	BFN13	7.76E4	2.17E6	0.0568		
5	BFN30	1.71E5	7.12E6	0.0398	0.297483	0.0185585
	BFN36	3.31E5	9.17E6	0.0524		
	BFN34	2.81E5	8.58E6	0.0503		
	BFN37	2.99E5	7.35E6	0.0619		
	BFN39	2.33E5	6.02E6	0.0887		
	BFN40	1.80E5	3.06E7	0.0263		
6	JNOV5	1.74E5	1.06E7	0.0432	0.12682	0.0171657
	JNOV6	4.77E5	2.02E7	0.0525		
	JNOV7	4.88E5	1.35E7	0.0104		
	JNOV8	2.92E4	6.95E6	0.0182		
	JNOV9	9.12E4	8.89E6	0.0126		

Table. D4 Relative expression level data of *protein disulfide isomerase* in ovaries of eyestalk-ablated broodstock *P. monodon* using real-time PCR.

Sample Group	concentration		Ratio of gene/ <i>EF-1α</i>	Average	STD				
	<i>PDI</i>	<i>EF-1α</i>							
1	BFEA18	4.94E5	1.07E7	0.0137	0.024147	0.0018791			
	YLB1	1.41E6	3.78E7	0.00743					
	YLB6	4.21E5	9.61E6	0.00905					
2	YLB8	1.06E6	2.41E7	0.0108	0.069263	0.0036435			
	BFEA19	2.75E5	5.81E6	0.0161					
	BFEA17	3.16E5	7.96E6	0.0154					
	YLB7	3.54E5	7.41E6	0.00848					
	BFEA16	3.68E5	6.91E6	0.0167					
	YLB4	4.51E5	8.30E6	0.0107					
	BFEA21	3.89E5	9.79E6	0.0107					
3	YLB2	4.06E5	9.24E6	0.0106	0.11539	0.0025166			
	YLB3	3.54E5	6.98E6	0.0161					
	BFEA8	7.48E5	1.63E7	0.0144					
	BFEA5	6.19E5	1.28E7	0.0105					
	BFEA2	3.61E5	8.71E6	0.0167					
	BFEA11	3.12E5	7.11E6	0.0112					
	BFEA3	5.63E5	9.94E6	0.01					
	BFEA20	1.91E5	4.11E6	0.0134					
	BFEA4	2.50E5	4.57E6	0.0179					
	4	BFEA1	2.42E5	5.14E6			0.0114	0.1445	0.0043410
		BFEA7	5.16E5	1.26E7			0.012		
BFEA6		3.24E5	6.26E6	0.0159					
BFEA24		2.73E5	5.28E6	0.0187					
BFEA10		4.49E5	9.21E6	0.0155					
BFEA12		3.55E5	7.08E6	0.0211					
BFEA13		5.14E5	8.55E6	0.0112					
BFEA22		1.84E5	3.50E6	0.0248					
BFEA23		1.23E5	2.18E6	0.0123					
BFEA9		9.86E4	1.86E6	0.016					

Table. D5 Relative expression level data of *valosin containing protein(VCP)* in ovaries of normal broodstock *P. monodon* using real-time PCR.

Sample Group	concentration		Ratio of gene/ <i>EF-1α</i>	Average	STD	
	<i>VCP</i>	<i>EF-1α</i>				
1	BUF3	4.55E4	2.21E7	0.00775	0.18742	0.0241562
	BUF6	9.78E4	1.61E7	0.0232		
	BUF4	7.07E4	1.78E7	0.015		
	AGYL3	2.44E4	1.78E7	0.00515		
	BUF7	1.95E4	4.09E6	0.0186		
	BUF5	8.27E4	3.77E6	0.0872		
	AGYL1	4.84E4	1.81E7	0.0101		
	AGYL4	5.71E4	2.26E7	0.00951		
	AGYL2	4.20E4	1.75E7	0.00904		
	BFN32	5.75E4	1.18E7	0.0187		
2	BFN38	3.65E4	8.59E6	0.0163	0.126271	0.0050744
	BFN33	3.19E4	5.76E6	0.0215		
	ASP10	6.64E4	1.55E7	0.0163		
	BFN35	5.88E4	8.35E6	0.0272		
	ASP6	9.85E4	1.94E7	0.0192		
	BFN31	5.92E4	9.51E6	0.024		
	BFN4/1	1.55E4	4.84E6	0.0124		
3	BFN18	1.40E4	1.96E6	0.0284	0.109886	0.0064542
	BFN3	1.87E4	5.06E6	0.0144		
	BFN4	1.49E4	4.31E6	0.0134		
	BFN23	2.24E4	6.82E6	0.0127		
	BFN24	1.70E4	3.52E6	0.0189		
	BFN5	2.47E4	4.65E6	0.0208		
	BFN1	9.87E3	4.25E6	0.009		
	4	BFN2	1.56E4	2.64E6		
BFN14		1.47E4	3.06E6	0.0189		

Table. D5 Relative expression level data of *valosin containing protein* in ovaries of normal broodstock *P. monodon* using real-time PCR (cont).

Sample Group	concentration		Ratio of gene/ <i>EF-1α</i>	Average	STD
	<i>VCP</i>	<i>EF-1α</i>			
4	BFN10	1.08E4	3.94E6	0.0107	0.19017 0.0058733
	BFN12	1.48E4	3.12E6	0.0186	
	BFN21	1.12E4	3.20E6	0.0137	
	BFN15	1.22E4	1.91E6	0.0254	
	BFN20	1.21E4	1.89E6	0.0255	
	BFN16	9.84E3	1.42E6	0.0278	
	BFN17	9.64E3	1.55E6	0.0248	
	BFN13	8.12E3	2.17E6	0.0147	
5	BFN30	2.95E4	7.12E6	0.016	0.102383 0.0036674
	BFN36	3.99E4	9.17E6	0.0167	
	BFN34	4.12E4	8.58E6	0.0185	
	BFN37	4.23E4	7.35E6	0.0223	
	BFN39	3.99E4	6.02E6	0.0257	
	BFN40	1.55E5	3.06E7	0.0191	
6	JNOV6	4.45E4	2.02E7	0.00829	0.019494 0.0022902
	JNOV7	8.70E3	1.35E7	0.00242	
	JNOV8	7.75E3	6.95E6	0.00425	
	JNOV9	7.96E3	8.89E6	0.00339	
	JNOV10	3.03E4	1.98E7	0.00572	

Table. D6 Relative expression level data of *valosin containing protein(VCP)* in ovaries of eyestalk-ablated broodstock *P. monodon* using real-time PCR.

Sample Group	concentration		Ratio of gene/ <i>EF-1α</i>	Average	STD				
	<i>VCP</i>	<i>EF-1α</i>							
1	YLB1	1.16E7	3.78E7	0.0373	0.101067	0.006035			
	YLB6	3.69E6	9.61E6	0.0479					
	BFEA15	5.78E6	1.78E7	0.0476					
2	YLB8	1.01E7	2.41E7	0.0523	0.26205	0.0040746			
	BFEA19	9.59E6	5.81E6	0.056					
	BFEA17	2.48E6	7.96E6	0.0515					
	YLB7	2.96E6	7.41E6	0.0445					
	BFEA16	3.08E6	6.91E6	0.0488					
	YLB4	2.96E6	8.30E6	0.0537					
	BFEA21	4.04E6	9.79E6	0.0465					
3	YLB2	3.72E6	9.24E6	0.0449	0.47045	0.0063878			
	YLB3	3.09E6	6.98E6	0.0523					
	BFEA8	6.26E6	1.63E7	0.0604					
	BFEA5	5.48E6	1.28E7	0.0486					
	BFEA2	3.14E6	8.71E6	0.0503					
	BFEA11	2.96E6	7.11E6	0.0633					
	BFEA3	4.81E6	9.94E6	0.0557					
	BFEA20	1.58E6	4.11E6	0.0437					
	BFEA4	2.29E6	4.57E6	0.0475					
	4	BFEA1	1.82E6	5.14E6			0.0531	0.577509	0.0094795
		BFEA7	4.48E6	1.26E7			0.0564		
		BFEA6	2.63E6	6.26E6			0.056		
		BFEA24	2.36E6	5.28E6			0.0592		
BFEA10		4.13E6	9.21E6	0.0591					
BFEA12		3.34E6	7.08E6	0.0584					
BFEA13		4.04E6	8.55E6	0.0766					
BFEA22		1.61E6	3.50E6	0.0439					
BFEA23		1.31E6	2.18E6	0.0581					
BFEA9		8.39E5	1.86E6	0.0529					
BFEA14		4.76E5	1.42E6	0.0419					

APPENDIX E

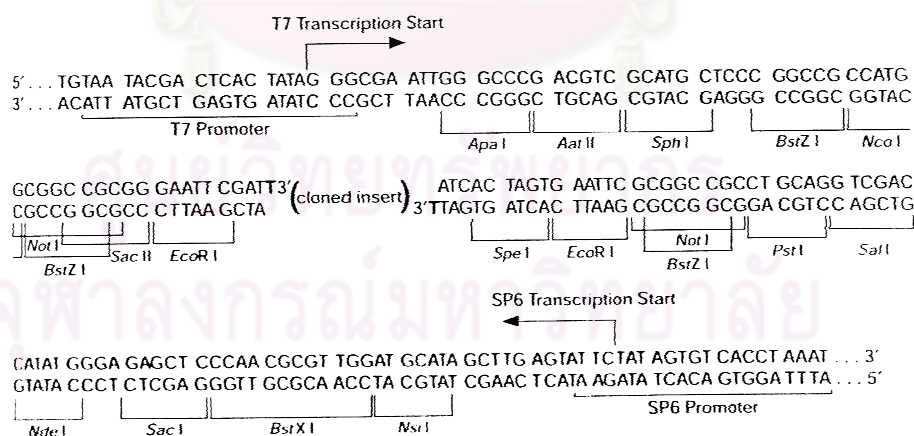
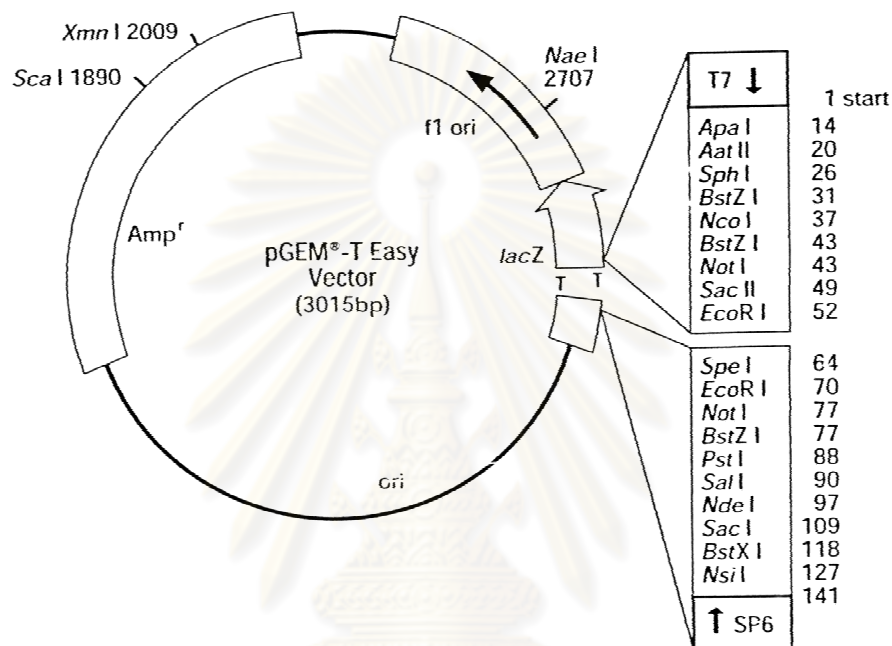
Table E1 The percentage of GSI and another data of *p. monodon* using in this thesis

No.	Body weight (g.)	Gonad weight (g.)	GSI (%)	Total length (cm.)	Original codes	Gonad colour	Remark
1	115.28	0.32	0.27	23.5	BUFOV03	light white	Stage I
2	76.37	0.47	0.61	23.0	BUFOV06	light white	Stage I
3	105.70	0.70	0.66	24.5	BUFOV04	light white	Stage I
4	99.96	0.77	0.77	23.5	AGYLOV03	white	Stage I
5	170.28	1.46	0.86	-	PMBF2	white	Stage I
6	112.35	1.00	0.89	23.0	BUFOV07	light yellow	Stage I
7	82.71	0.90	1.08	21.5	BUFOV05	turbid white	Stage I
8	157.33	1.73	1.10	27.0	AGYLOV01	white + light pink	Stage I
9	104.97	1.18	1.12	23.0	AGYLOV04	white	Stage I
10	120.58	1.60	1.33	23.5	AGYLOV02	white	Stage I
11	186.69	2.69	1.44	26.0	BFNOV32	yellow	Stage I
12	188.30	2.76	1.47	-	PMBF1	light yellow	Stage I
13	218.71	4.70	2.15	28.0	BFNOV38	light green + yellow	Stage II
14	205.67	4.61	2.24	27.5	BFNOV33	light yellow	Stage II
15	128.74	2.25	2.25	24.5	ASPOV10	light yellow	Stage II
16	205.05	5.29	2.58	28.0	BFNOV35	light yellow	Stage II
17	149.64	2.68	2.68	26.7	ASPOV06	light yellow	Stage II
18	208.54	6.16	2.95	26.0	BFNOV31	light green	Stage II
19	181.30	6.00	3.31	28.5	BFNOV04/1	yellow + green	Stage II
20	159.80	6.40	4.01	27.7	BFNOV07	light green	Stage III
21	187.10	8.27	4.42	30.0	BFNOV18	green + yellow	Stage III
22	173.40	8.00	4.61	28.0	BFNOV03	green	Stage III
23	164.50	7.60	4.64	27.5	BFNOV04	green	Stage III
24	230.93	12.12	5.28	32.0	BFNOV23	green + yellow	Stage III
25	235.98	12.69	5.37	33.0	BFNOV24	green	Stage III
26	172.30	9.90	5.75	28.0	BFNOV05	green	Stage III
27	172.60	10.20	5.91	28.0	BFNOV01	green	Stage III
28	136.40	8.40	6.16	26.5	BFNOV09	dark green	Stage IV
29	133.20	8.30	6.23	26.0	BFNOV08	green	Stage IV
30	176.20	12.90	7.32	29.0	BFNOV06	dark green	Stage IV
31	272.20	20.30	7.46	32.0	BFNOV02	green	Stage IV
32	152.20	12.80	8.42	27.0	BFNOV14	green	Stage IV
33	139.90	13.10	9.36	25.5	BFNOV10	dark green	Stage IV
34	162.20	16.20	9.99	28.0	BFNOV12	dark green	Stage IV
35	166.90	16.70	10.01	27.5	BFNOV11	light green	Stage IV
36	239.86	24.98	10.41	33.0	BFNOV21	green	Stage IV
37	207.40	23.20	11.19	30.5	BFNOV15	dark green	Stage IV
38	232.57	26.08	11.21	30.0	BFNOV20	green	Stage IV
39	156.10	18.20	11.66	27.0	BFNOV16	dark green	Stage IV
40	252.11	31.30	12.41	30.0	BFNOV17	green	Stage IV
41	158.60	19.90	12.55	27.5	BFNOV13	dark green	Stage IV
42	300.12	10.47	3.49	32.5	BFNOV30	light green + yellow	post-spawn

Table F1 (cont.)

No.	Body weight (g.)	Gonad weight (g.)	GSI (%)	Total length (cm.)	Original codes	Gonad colour	Remark
43	194.49	3.61	1.86	27.5	BFNOV36	light yellow + little green	post-spawn
44	256.40	8.39	3.27	29.5	BFNOV34	light yellow	post-spawn
45	264.70	7.66	2.89	30.0	BFNOV37	light yellow	post-spawn
46	285.97	8.30	2.90	32.0	BFNOV39	yellow	post-spawn
47	200.79	5.18	2.58	28.0	BFNOV40	light yellow	post-spawn
48	236.51	1.79	0.76	27.50	BFEOV18	white	Eyestalk-ablated; Stg I
49	111.00	1.00	0.90	24.50	YLBOV01	white + light yellow	Eyestalk-ablated; Stg I
50	163.00	2.00	1.22	25.00	YLBOV06	white	Eyestalk-ablated; Stg I
51	272.20	3.71	1.36	30.00	BFEOV15	yellow	Eyestalk-ablated; Stg I
52	125.00	2.00	1.60	24.50	YLBOV05	white + light yellow	Eyestalk-ablated; Stg II
53	118.00	2.00	1.69	24.50	YLBOV08	white	Eyestalk-ablated; StgII
54	173.37	4.72	2.72	25.50	BFEOV19	light green + yellow	Eyestalk-ablated;Stg II
55	252.03	7.16	2.84	29.50	BFEOV17	green + yellow	Eyestalk-ablated;Stg II
56	151.00	5.00	3.31	25.00	YLBOV07	light green	Eyestalk-ablated;Stg II
57	291.39	10.31	3.54	30.50	BFEOV16	green	Eyestalk-ablated;Stg II
58	164.00	6.00	3.66	26.00	YLBOV04	light green	Eyestalk-ablated;Stg II
59	193.65	8.82	4.55	27.00	BFEOV21	dark green	Eyestalk-ablated;Stg III
60	153.00	7.00	4.57	25.50	YLBOV02	light green	Eyestalk-ablated;Stg III
61	125.00	6.00	4.80	25.00	YLBOV03	light green	Eyestalk-ablated;Stg III
62	118.80	5.90	4.97	24.50	BFEOV08	green	Eyestalk-ablated;Stg III; BIOTEC shrimp
63	186.50	9.40	5.04	27.50	BFEOV05	light green	Eyestalk-ablated;Stg III
64	196.90	10.00	5.08	29.50	BFEOV02	light green + yellow	Eyestalk-ablated;Stg III
65	96.20	4.90	5.09	23.30	BFEOV11	green	Eyestalk-ablated;Stg III; BIOTEC shrimp
66	182.70	9.40	5.15	28.00	BFEOV03	yellow + little green	Eyestalk-ablated;Stg III
67	278.23	14.37	5.16	29.50	BFEOV20	dark green + little yellow	Eyestalk-ablated;Stg III
68	197.40	10.80	5.47	29.50	BFEOV04	light green + yellow	Eyestalk-ablated;Stg III
69	229.60	14.60	6.36	30.00	BFEOV01	green + yellow	Eyestalk-ablated; StgIV
70	220.10	14.00	6.36	28.50	BFEOV07	light green + yellow	Eyestalk-ablated; StgIV
71	170.20	11.60	6.82	27.00	BFEOV06	light green + yellow	Eyestalk-ablated; StgIV
72	365.38	25.08	6.86	33.00	BFEOV24	green	Eyestalk-ablated; StgIV
73	116.40	8.00	6.87	25.50	BFEOV10	dark green	Eyestalk-ablated; StgIV; BIOTEC shrimp
74	128.70	8.90	6.92	25.20	BFEOV12	dark green	Eyestalk-ablated; StgIV; BIOTEC shrimp
75	188.20	13.80	7.35	27.50	BFEOV13	dark green	Eyestalk-ablated; StgIV
76	167.54	14.33	8.55	25.00	BFEOV22	dark green	Eyestalk-ablated; StgIV
77	256.34	22.41	8.74	29.50	BFEOV23	dark green	Eyestalk-ablated; StgIV
78	249.50	22.30	8.94	31.50	BFEOV09	light green	Eyestalk-ablated; StgIV
79	115.60	12.80	11.07	23.50	BFEOV14	dark green	Eyestalk-ablated; StgIV; BIOTEC shrimp

Appendix F

Restriction mapping of pGEM[®]-T Easy Vector

BIOGRAPHY

Miss. Witchulada Talakhun was born on September 10, 1983 in Sakonnakhon. She graduated with the degree of Bachelor of Science from the Department of Science (Biotechnology), Ramkhumhang University in 2005. She has enrolled a Master degree program at the Program in Biotechnology, Chulalongkorn University since 2008.

Publications related with this thesis

1. **Talakhun, W.**, Kittisenachai, S., Roytrakul, S., Klinbunga, S. and Menasveta, P. (2008). Identification of proteins related to ovarian development of the giant tiger shrimp *Penaeus monodon* using two dimensional gel electrophoresis. 34th Congress on Science and Technology of Thailand, 31 October-2 November 2008, Queen Sirikit National Convention Hall, Bangkok, Thailand (Oral presentation).
2. **Talakhun, W.**, Kittisenachai, S., Roytrakul, S., Klinbunga, S. and Menasveta, P. (2008). Identification and characterization of proteins related to ovarian development of the giant tiger shrimp *Penaeus monodon*. The 20th Annual Meeting and International conference of the Thai Society for Biotechnology, 14–17 October 2008, Maha Sarakham, Thailand (Poster presentation).

ศูนย์วิทยทรัพยากร
จุฬาลงกรณ์มหาวิทยาลัย